Interactions between nuclear lamins and their binding partners in EDMD fibroblasts

Mauricio Alvarez-Reyes

Interactions between nuclear lamins and their binding partners in EDMD fibroblasts.

Mauricio Alvarez-Reyes

School of Biological and Biomedical Sciences
University of Durham, December, 2003

Interactions between nuclear lamins and their binding partners in EDMD fibroblasts.

Mauricio Alvarez-Reyes

Thesis Abstract

Lamins are components of the nuclear lamina and are divided in A and B-types, which interact with proteins of the inner nuclear membrane like emerin. Mutations in emerin (X-linked) and A-type lamins (Autosomal Dominant) has been linked to the Emery-Dreifuss Muscular Dystrophy (EDMD), which conduced to the hypothesis that these two proteins might interact in the nucleus. I examined the interaction between A and B-type lamins with emerin using a panel of deletion mutants of lamin B1 and full-length lamins A, C and B1 in a yeast two-hybrid assay, where emerin interacted with all lamins and the preferred region of interaction was the globular tail domain of lamin B1. Ectopic expression of tagged proteins in human dermal fibroblasts confirmed that emerin remains attached to the inner nuclear envelope through its association with lamin B1, as aggregation of tagged A-type lamins did not miss localize endogenous emerin or lamin B1. In addition, methanol-acetone fixation showed higher number of cells presenting characteristic morphological abnormalities called "honeycombs". A-type lamins and their associated protein emerin co-localized in these structures. Lamin B1 depletion from the honeycombs was accompanied by depletion of nuclear pore complexes. In the honeycombs, A-type lamins segregated from the B-type lamins, forming homo-filaments.

On the other hand, AD-EDMD cell lines showed a characteristic pattern as a high sub-population of cells presented nesprin 1 (amino-terminal) in stress fibres co-localizing with α-S-Actin fibres, which was enhanced by growth inhibition induced by serum starvation. Re-stimulation of fibroblasts by normal serum concentrations increased the appearance of honeycombs by up to 2.5 fold in the AD-EDMD cell lines. Late passage cultures of AD-EDMD entered a senescence state reminiscent of the induced quiescence state induced by serum starvation. Finally, differential allelic expression was evidenced using a specific set of ARMS-primers in the cell lines studied, indicative of transcript imbalance, and bioinformatics analysis demonstrated the presence of SNPs in the coding region of the wild type LMNA gene. The results of these study confirm that lamins interact with emerin and suggest that the interacting region is the tail domain of lamins; honeycomb structures might have a biological meaning in patient cells; other proteins might be involved in EDMD, like nesprins; and heterozygosis is presented with transcript imbalance, which might have a negative impact in the correct assembly of the nuclear lamina.

Declaration

I declare that myself carried out the experiments described in this thesis at the School of Biological and Biomedical Sciences, University of Durham, under the supervision of Prof. Chris J. Hutchison. This thesis has been composed by myself and has not been submitted previously for a higher degree.

Mauricio Alvarez-Reyes

Abbreviations:

3AT: 3-amino-1,2,4-triazole

ACTC: Actin

AD-EDMD: Autosomal Dominant Emery Dreifuss Muscular Dystrophy

AGPAT2: alpha acylglycerol 3 phosphate o acyltransferase 2

ALS: Amyotrophic Lateral Sclerosis

AR-CMT2: Autosomal Recessive Charcot-Marie-Tooth type 2

B4GALT3: Beta-1,4-Galactosyltransferase polypeptide 3

BAF: Barrier Autointegration Factor

BPAG1: Bullous Pemphigoid Antigen 1

CDC2: Cell Division Cycle 2 kinase

cM: centiMorgan = One map unit = 1 % of recombinant phenotypes

CSRP3: Cysteine and Glycine Rich Protein

DES: Desmin

DMD: Dystrophin gene

DNA: Deoxy-ribonucleic Acid

EDMD: Emery Dreifuss Muscular Dystrophy

EMG: Electromyography

ER: Endoplasmic Reticulum

FISH: Fluorescence In-Situ Hybridization

FPLD: Familial Partial Lipodystrophy

GFAP: Glial Fibrillary Acidic Protein

GFP: Green Fluorescent Protein

HDL: High Density Lipoprotein

HLA: Human Leukocyte Antigen

HSP: Heat Shock Protein

IF: Intermediate Filament

IFAP: Intermediate Filament Associated Protein

INM: Inner Nuclear Membrane

KCNQ1: Potassium Channel, Voltage-Gated

kDa: Kilo Daltons

LAP: Lamin Associated Protein

LBR: Lamin B Receptor

LEM: protein motif called after the initials of **L**AP2β , **E**merin and **M**an

LGMD: Limb-Girdle Muscular Dystrophy

LMNA: Lamin A gene

LMNB1: Lamin B1 gene

LMNB2: Lamin B2 gene

MAD: Mandibuloacral Dysplasia

mDa: Mega Daltons

MRI: Magnetic Resonance Imaging

MYBPC3: Cardiac Myosin-Binding Protein C

MYH7: Cardiac Beta-Myosin Heavy Chain

NE: Nuclear Envelope

NES: Nuclear Export Signal

NF-H: neurofilament heavy

NF-L: neurofilament light

NLS: Nuclear Localization Signal

nm: nanometres

NPC: Nuclear Pore Complex

NUANCE: Nuclear Anchorage Envelope

ONM: Outer Nuclear Membrane

PFA: Para-Formaldehyde

PKA: Protein Kinase cAMP-dependent

PKC-α: Protein kinase C-α

PP1: Protein Phosphatase 1

PPARG: Peroxisome Proliferator Activated Receptor □

PRELP: proline/arginine-rich end leucine rich repeat protein gene

PTACs: Protein Transport Associated Complexes

RECQL2: DNA Helicase–like

RNA: Ribonucleic Acid

RSS: Rigid Spine Syndrome

RT-PCR: Reverse Transcriptase Polymerase Chain Reaction

STR: Short Tandem Repeat

TCAP: Titin

TM: Transmembrane Domain

TNNT2: Troponin T

XL-EDMD: X-Linked Emery Dreifuss Muscular Dystrophy

YTHS: yeast two hybrid system

Acknowledgments

I would like to acknowledge all colleagues and friends who supported me during the course of my Ph. D studies.

... special thanks to Professor Chris J. Hutchison, who gave me the opportunity to come to his lab to do my Ph. D, and for all his support that extended from the application process for my ORS scholarship to the tedious corrections (especially my written English!) of the final draft of this thesis.

... to all the patients who supplied biopsies for the establishment of cell lines with the purpose of research in muscular dystrophies.

... to all the former and current colleagues in Chris' lab: Dr. Tony Vaughan, Dr. Ewa Markiewicz, Dr. Martin Goldberg, Dr. Rekha Rao, Dr. Rachel Venables, Miss Georgia Salpingidou, Miss Naomi Willis, Mrs. Pamela Ritchie (special thanks for all the technical support and efficient lab organization) and Mrs. Vanja Pekovic.

... to Professor Roy A. Quinlan and Dr. Ming Der Perng for the valuable discussions and kind provision of materials regarding heat shock proteins and chaperons. Thanks to other members of Roy's lab for help provided, especially to Mr. Terry Gibbon.

... to Dr. Colin Jahoda for his initial suggestions about α-S-Actin positive flattened cells in chapter 4 and kind provision of rat dermal fibroblasts and α-S-Actin antibody.

... to Dr. Adam Benham for close collaboration and kind provision of PDI antibody.

... to Dr. Artoo Maatta for help with cell biology techniques and scientific discussions about my data, and Miss Heather Long for the help regarding intermediate filaments references.

... to Dr. Rumaisa Bashir for all her valuable help and scientific discussions, and her patience with my Bioinformatics dyslexia.

... to Dr. Steve Chivasa for precise advices on protein biochemistry.

... to Mr. Manuel Weber and Mr. Carlos Lopez de Luna for statistical support.

... to Mrs. Christine Richardson and Dr. Tijs Ketelaar for their brilliant support with confocal microscopy and their patience during the "crisis" with the confocal microscopes.

... to all the technical and secretarial staff at the School of Biological and Biomedical Sciences, University of Durham, for their invaluable help.

... to Dr. Manfred Wehnert for the kind provision of the EDMD patient cell lines.

... to Dr. Catherine M. Shanahan and Dr. Qiuping Zhang for kind provision of nesprin antibodies and valuable discussions about nesprins data.

... to Dr. Irina Hausmanowa-Petrucewicz for the kind provision of EDMD cell lines.

Table of Contents

Table of Figures

1 Chapter One: Introduction.

1.1 Eukaryotic nuclei

In Nature, two major groups form life's kingdom: the prokaryotes, comprising exclusively unicellular organisms, and the eukaryotes, which include uni and multicellular organisms, from fungi to plants. In the animal kingdom, eukaryotes include two major groups: protozoan and metazoan. Evolution of the latter involves cellular entities that are more specialized. Prokaryotes and Eukaryotes are very similar in that they contain the basic components that characterize self-sufficient living units. However, there are few major differences between them, mainly based on the presence or not of an organized nucleus. Eukaryotes contain membrane-bound nuclei and other organelles, while prokaryotes lack this level of organization.

The nucleus, being one of the largest sub-cellular compartments, varies in diameter from 10 to 20 micrometers under normal conditions, but can be larger in disease. Eukaryotic nuclei evolved as a very specialized organelle with a high level of compartmentalization. Up to 16 different entities have been described inside the eukaryotic nuclei so far including: Nucleoli (**Carmo-Fonseca et al., 2000**), SAM68/SLM body (**Chen et al., 1999**), Perinucleolar Compartment (PNC) (**Ghetti et al., 1992**), OPT Domain (**Grande et al., 1997; Spector, 2001**), Cleavage Body (**Spector, 2001**), Cajal Body (**Gall, 2000**), Gem (**Hebert et al., 2001**), Nuclear Diffuse Body (**Sutherland et al., 2001a**), Nuclear Speckles (**Monneron and Bernhard, 1969**), Promyelocitic Leukaemia Body (PML) (**Maul et al., 2000**), Polycomb Body (PcG Body) (**Alkema et al., 1997**), RNA II Transcription Sites (**Iborra et al., 1996**), Chromatin, Heterochromatin, Nuclear Pore Complexes (NPC) (**Aaronson and Blobel, 1975**), and the Nuclear Lamina (**Gerace et al.,**

1978)(Figure 1.1). The growing number of proteins the nucleus contains evidences its complexity, as visual gene trap screening revealed more than 100 new nuclear proteins (**Sutherland et al., 2001b**).

The plant nuclear envelope (NE) is very similar to its animal equivalent in that it completely dissolves and reassembles during open mitosis, but contains obvious differences as for example, the lack of centrosomes (**Stoppin et al., 1994**) and the absence, so far, of lamin polypeptides (**Irons et al., 2003**).

1.2 The Nuclear Envelope

A double membrane forming the nuclear envelope, about 30 nm wide, surrounds the cell nucleus (Figure 1.2). This selectively allows molecules to enter and leave the nucleus, and physically separates chemical reactions taking place in the cytoplasm from reactions happening within the nucleus. The inner and outer membranes fuse at regular spaces, forming the nuclear pores. A luminal space separates the two membranes, which is continuous to the endoplasmic reticulum (ER) and can contain newly synthesized proteins as in the ER. It has been suggested that the luminal space provides the aqueous environment that allows signal transduction in both directions: to and from the cytoplasm (**Sullivan et al., 1993**). A growing number of nuclear membrane proteins are been discovered as new proteomics approaches allow the study of complex protein mixtures in sub-cellular organelles (**Dreger et al., 2001**).

Higher eukaryotes exhibit the most intriguing characteristic of the NE: its ability to disassemble and re-assemble during open mitosis, mediated by a wide variety of membrane components and their interaction with other binding partners. Proteins of the nuclear envelope play important roles in

development and disease, by mediating a variety of fundamental processes including DNA replication, gene expression and silencing, chromatin organization cell division, apoptosis, sperm nuclear remodelling, cell fate determination, nuclear migration and cell polarity (**Wolfner and Wilson, 2001**).

1.3 Outer Nuclear Membrane

Is the outer nuclear membrane (ONM) an extension of the ER, or vice versa? Answer 1 would be, yes, it is; the interphase outer envelope is continuous with the rough ER, so it contains ribosomes. Answer 2 would be, yes, it is; the interphase ER comprises a continuous network of cisternae and tubular membranes extending from the ONM into the cytoplasm. During mitosis, the ER undergoes disassembly to vesicles and membrane tubules/cisternaes to allow the partitioning of ER membranes to daughter cells (**Warren and Wickner, 1996**). In higher eukaryotes, the NE breaks down during mitotic prophase into a form that cannot be distinguished from disassembled elements of the peripheral ER (**Porter and Machado, 1960; Zeligs and Wollman, 1979**). Association of membrane vesicles and cisternaes during late anaphase reassembles the ER and the NE (**Porter and Machado, 1960; Robbins and Gonatas, 1964**). Then NE proteins diffuse from the ER trough the ONM until they reach their anchoring sites at the INM by means of their interaction with the lamina and/or other nucleoplasmic proteins (**Yang et al., 1997**). A special subset of proteins can be located specifically at the ONM, including a new giant protein connecting the nucleus with the actin cytoskeleton called NUANCE (**Zhen et al., 2002**).

1.4 Inner Nuclear Membrane

Proteins located at the inner nuclear membrane (INM) belong predominantly to the type II integral membrane protein family, and they contain a general structure with a long N-terminal nucleoplasmic domain and a transmembrane domain (TM) close to the C-terminus (**Hartmann et al., 1989**). Protein-protein interactions between members of the INM and lamins, chromatin and other nucleoplasmic proteins show the dynamic state of this structure. The discovery that human diseases are associated with mutations in some type II integral membrane proteins and/or interacting partners has brought more attention into the biological role of this family of proteins.

During interphase, INM proteins are embedded into the lipid bi-layer through their TM domain, exposing their C-terminus to the luminal space, and the long N-terminus to the nucleoplasm. During mitosis, when the NE is disassembled, integral membrane proteins of the INM are dispersed throughout all ER membranes and the NE loses its identity as an ER sub-compartment. At late anaphase, when membrane vesicles re-organize around the surface of the chromosomes, INM proteins diffuse through a functionally continuous ER to their localization into the INM (**Yang et al., 1997**). Other authors consider INM proteins contain specific targeting and retention signals, following a so-called diffusion-retention model (**Furukawa et al., 1995; Soullam and Worman, 1993; Tsuchiya et al., 1999**). This model claims INM proteins diffuse freely in the interconnected membranes of the rough ER and the NE after synthesis, move along the lateral channels of the Nuclear Pore Complex (NPC) and arrive at the INM. Binding to their interacting partners like lamins and/or chromatin, they achieve their functional localization. Evidence for this model comes from chimerical studies where putative targeting signals in the Lamin B Receptor (LBR)

mediated targeting of non-nuclear membrane proteins to the INM (**Ellenberg et al., 1997; Soullam and Worman, 1993**). On the other hand, movement through the lateral channels of the NPC is limited to the protein size of ~67 kDa (**Soullam and Worman, 1993**). In agreement with this fact, most INM proteins have a mass less than 60 kDa, with the exception of Nesprin 1.

In plants, transfection of N-terminal domains of INM proteins from mammalian cells, like LBR, fused to Green Fluorescent Protein (GFP), can localize them exclusively at the INM (**Irons et al., 2003**). LBR nucleoplasmic domain (contains a nuclear localization signal (NLS), the lamin-binding and chromatin-binding domains, and ends in the first of eight transmembrane domains) have shown previously to be sufficient for INM targeting in mammalian cells (**Ellenberg et al., 1997; Soullam and Worman, 1993**). The finding in plants suggest that a targeting and/or retaining mechanism of transmembrane proteins is conserved in animals and plants, as proposed by the current model for targeting INM proteins (**Ellenberg et al., 1997**).

1.5 Nuclear Pore Complex

The Nuclear Pore Complex (NPC) has a molecular mass of ~125 mDa in vertebrates and contains about 50 or more proteins that are different (**Lyman and Gerace, 2001; Nakielny and Dreyfuss, 1999**). NPC spans the dual membrane of the NE and acts as a gateway for macromolecular traffic between the cytoplasm and the nucleus. The basic framework of NPC consists of a central core with a ring-spoke structure exhibiting 8-fold radial symmetry. From this central ring, 50 – 100 nm fibres extend into the nucleoplasm and the cytoplasm. The NPC is in turn anchored in the NE by the interaction of Nup153 with B-type lamins at the nuclear lamina (**Smythe**

et al., 2000). A number of proteins (nucleoporins, Nups) have been localized to discrete regions of the NPC and are often used as markers for this compartment, e.g. Nup153 (**Stoffler et al., 1999**). Approximately half of the Nups contain a phenylalanine-glycine repeat motif (FG repeat), which may be diagnostic for proteins playing a role in nuclear transport. Protein cargo identifies itself to the nuclei-cytoplasmic transport machinery by NLSs or nuclear export signals (NESs), which can be protein, RNA or consist of a composite of both (**Nakielny and Dreyfuss, 1999**). A number of nuclear transport receptors exist that recognize these signals, variously called karyopherins, Protein Transport Associated Complexes (PTACs), importins or transportins. These receptors are generally large acidic proteins that share the ability to bind components of the NPC and contain both an N-terminal RanGTP-binding domain and a C-terminal cargo-binding domain. Cargo (protein, RNA or both) can bind its cognate nuclear transport receptor directly through NLS and NES signals or via adaptor proteins. In particular, proteins with simple or bipartite NLSs are imported via the β-importin receptor indirectly by association with the α-importin family of adaptors.

The progress made in identifying yeast and mammalian nucleoporins by proteomic approaches (**Allen et al., 2001; Cronshaw et al., 2002**) is currently used to search putative homologues in plants, especially in Arabidopsis thaliana genome, where some candidates are suggested (**Altschul et al., 1997; Hodel et al., 2002; Schwacke et al., 2003**).

1.6 Intermediate Filaments

The cytoskeleton of all metazoan cells contains three major filaments systems: 1) microtubules (MTs), with a diameter of 25 nm, 2) intermediate filaments (IFs), with a diameter of 10-12 nm, and 3) actin microfilaments

(MFs) with a diameter of 7-10 nm. Apart from the physical appearance of the three different filament systems, structural features distinguishing MFs and MTs from IFs in that the building blocks of the first two are globular proteins, while the third ones are assembled from elongated and thin filaments. On the other hand, MFs and MTs form polar fibres; IFs have no polarity, as individual dimers are orientated in an anti-parallel fashion (**Strelkov et al., 2003**). The integrated network formed by the three filament systems is responsible for the mechanical integrity of the cell, and it is involved in critical cellular functions ranging from the cell membrane to the nucleoplasm (**Goldman et al., 1996**). Therefore, once affected, it results in several types of disorders.

Intermediate filaments are differentially expressed in most tissues, and are expressed from at least 65 different genes in humans (**Hesse et al., 2001**). All IFs share a characteristic tripartite structure: Head, Coiled-coil and tail domain (**Fuchs and Weber, 1994**), and are grouped in 6 categories according to their primary sequence and structural features (Table 1.1).

Intermediate Filaments can assemble into homodimers or heterodimers with each other, even those belonging to different sequence homology types. According to these characteristics, there are three assembly groups: Keratins form assembly Group 1, forming obligatory heterodimers. Group 2 is composed by IFs type III and IV, and the last one, Group 3, includes the lamins, which are only capable of assembling into homodimers due to their long coil B fragment.

Type	Protein	Tissue	KDa	Reference
	Acidic Keratins K9 – K20	Epithelia	40-64	(**Fuchs and Green,**
	Hal 1-4	Trichocytes	42-54	(**Fuchs and Green,**
	Basic Keratins K1-K8	Epithelia	52-68	(**Fuchs and Green,**
	Hb 1-4	Trichocytes	58-64	(**Fuchs and Green,**
	Vimentin	Messenchyme	55	(**Ramaekers et al.,**
	Glial Fibrillary Acidic Prot.	Astroglia	51	(**Osborn et al., 1981**)
	Desmin	Muscle	53	(**Gard and Lazarides,**
	Peripherin	Neuronal	58	(**Portier et al., 1983**)
	Syncoilin	Muscle	54	(**Newey et al., 2001**)
	Neurofilament Heavy	Neurons	220	(**Hoffman and Lasek,**
	Neurofilament Medium	Neurons	110	(**Hoffman and Lasek,**
	Neurofilament Light	Neurons	68	(**Hoffman and Lasek,**
	α-internexin	Neurons	66	(**Pachter and Liem,**
	A and B-type lamins	Nucleated cells	40-69	(**Benavente et al.,**
	Nestin	Neuro-Epithelia	200	(**Niki et al., 1999**)
	Filensin/CP49	Eye lens	95	(**Merdes et al., 1991**)
	Phakinin	Eye lens	47	(**Merdes et al., 1993**)
	Synemin	Avian Muscle	230	(**Lazarides, 1982**)
	Paranemin	Muscle	280	(**Lazarides, 1982**)
	Septins	Nucleated cells	50-60	(**Walikonis et al., 2000**)
	Minor lens IFPs	Lens	50-60	(**Ramaekers et al.,**

Table 1.1

1.6.1 Structure

All IFs exhibit a characteristic structure that includes a highly α-helical central domain, flanked by the non-helical head towards the N-terminus and globular tail domain at the C-terminus of the protein (**Fuchs, 1994**).

The central rod domain displays a seven-residue periodicity $(abcdefg)_n$ in the distribution of apolar residues. Within these repeat positions, a and d are preferentially small hydrophobic residues like Leu, Ile, Met or Val; positions e and g are usually charged, and polar residues are located elsewhere (**McLachlan, 1978**). There is a charge periodicity of approximately 9.5 residue interval in this region, which might contribute to the lateral electrostatic interactions between coiled coils, thereby helping in the formation of higer-order oligomers (**Stuurman et al., 1998**). This heptad organization is characteristic of coiled-coil structures, where two or more α-helices twist on each other in parallel, unstaggered fashion with the hydrophobic chains of one α-helice interacting with those of the other one, and the hydrophilic residues exposed to the aqueous environment, forming a super-helix (**Burkhard P, 2001**). The rod domain is interrupted in several places by variable non-helical linkers, not containing proline in lamins but conserved between them. Linkers are responsible for dividing the central domain in consecutive short α-helical fragments: 1A and 1B (forming coil 1), and 2A and 2B (forming coil 2) (**Stuurman et al., 1998**). The length of the α-helical segments is conserved in vertebrate cytoplasmic IFs, but nuclear lamins rod domain differs from cytoplasmic IFs by six additional heptads (**Parry et al., 1986**). A 26 amino acids long segment at the N-terminal end and 32 residues situated at the very end of the coil 2B of the rod domain play a critical role for the association of IFs into higher order complexes, where mutations appear to be related to human disorders (**Coulombe,**

1993). Another highly conserved feature, structurally and positionally, in the rod domain among IFs is a discontinuity in the heptad repeat pattern within coil 2B, called stutter, due to an insertion of four amino acids (**Strelkov SV et al., 2002**).

The head domain of IFs is mainly composed of basic residues, and analysis of its primary sequence shows a highly flexible conformation with low content of secondary structure. Although there is not enough crystallographic data to make further analysis as in the rod domain, functional studies have demonstrated its essential role in a tetramer state, as mutant vimentins with deletions in the head domain only form dimers (**Herrmann, 1996**). It is likely that the head domain interacts with specific sites on the coiled-coil rod domain and the tail domain, considering the basic nature of the head and the acidic properties of the others, promoting lateral association of tetrameric protofilaments into octameric protofibrils, and ultimately into 10 nm filaments.

The lack of crystallographic data of the tail domain of IFs forced the use of functional approaches to unravel its role. In lamins, tailless lamin B2 associated into long filaments resembling the head-to-tail filaments formed by full-length lamins. This tail-domain deletion mutant did not inhibit filament formation but produced increase in filament width. Not until recently, the crystal structure of the tail domain of IFs was partially revealed. A region of the tail domain of lamins (amino acids 436 – 552 of Lamin A) forms a compact, globular, well-defined domain composed entirely of β-strands, where two large β-sheets form a β-sandwich, an Ig-like structure (**Dhe-Paganon et al., 2002**), which might control lateral assembly of protofilaments and mediate IF network formation (**Stuurman et al., 1998**).

Apart from size, another feature that differentiates the tail domain of IFs is the unique presence of a NLS in lamins, which contains an invariant lysine, followed by three other basic residues (lysine or arginine), a hydrophobic residue (Isoleucine or Leucine), and an acidic residue (Aspartic or Glutamic) (**Stuurman et al., 1998**).

1.6.2 Intermediate Filaments Associated Proteins

Intermediate Filament Associated Proteins (IFAPs) are a growing group of proteins which mainly function to cross-link intermediate filaments to other cytoskeletal filament systems, structuring the cytoplasm by forming flexible, reversible arrays that provide essential resistance to environmental stress (**Houseweart and Cleveland, 1998**). They are grouped in families of proteins with specific binding partners and most of them are at least bivalent with regards the type of cytoskeletal elements they interact with. Keratin-specific bundling IFAP include Filaggrin and Trichohyalin, which are highly charged (**Lee et al., 1993; Mack et al., 1993**). Cytolinkers, the Plakins, are large multi-domain proteins and include Plectin, Desmoplakin and Bullous Pemphigoid Antigen 1 (BPAG1). Actin-binding proteins include Fimbrin/Plastin and Calponin, and a fourth group is formed by αβ-crystalins, Heat Shock Protein 27 (HSP27) and 14-3-3 proteins (**Coulombe et al., 2000**), which are specific for different intermediate filaments. Mutations in the gene for Plectin are the cause for a kind of muscular dystrophy with Epidermolysis Bullosa, due to the failure to link IF cytoskeleton with the plasma membrane (**McLean et al., 1996**).

1.6.3 Cytoplasmic Intermediate Filaments and disease

Disorders related to IFs have been described since the 19th century, but it was not until 1991 when mutations in the keratins were first linked to

Epidermolysis Bullosa Simplex (**Ryynanen et al., 1991**). Since then, several inherited mutations affecting the primary structure of cytoplasmic IF proteins have been reported, and found responsible for a vast number of rare, usually dominant inherited diseases. The majority of the mutations are missense variations affecting highly conserved residues in the head and rod domains of the filament (**Irvine and McLean, 1999**). A hot-spot mutation has been identified in type I keratin sequences affecting the beginning of α-helix 1A, co-related with a high severity of the disease (**Lane et al., 1992; Ma et al., 2001**). In milder forms, mutations in this group of keratins are located outside the highly conserved region, do not form hot-spots, and the structure of the filaments appear to be normal (**McLean and Lane, 1995**).

Other IF proteins have shown structural impairment in several human diseases. Many cardiomyopathies are due to myosin defects, but some others with no myosin defects show ultra-structural abnormalities in desmin filaments (**Pellissier et al., 1989**). Desmin mutations affecting conserved residues cause a form of skeletal myopathy that frequently has cardiac abnormalities associated with it. Although Desmin-null-mice develop normally, it is only after birth when degenerative muscular processes begin, leading to aberrant muscle fibres and cardiovascular lesions (**Li et al., 1997**).

Similarly, massive accumulation of neurofilaments in cell bodies and proximal axons in neurons are sufficient to trigger a neurodegenerative disorder as is the case in some motor-neuron diseases (**Xu et al., 1993**). A number of mutations in Glial Fibrillary Acidic Protein (GFAP) have been found to be associated with Alexander disease, a severe-fatal neurodegenerative disorder (**Brenner et al., 2001**). Mutations appear in highly conserved regions of the filament, although there is no linkage

between mutations and severity of the disease as in keratins. GFAP null mice develop and grow normally, but some late-onset abnormalities have been described (**Gomi et al., 1995; Liedtke et al., 1996**).

To date no human disease has been linked to mutations in vimentin. Vimentin-null mice developed and grew normally, although later produced deficiencies in vascular toning, mechanotransduction and wound healing (**Eckes et al., 2000; Henrion et al., 1997; Terzi et al., 1997**). In other cases, vimentin over-expression produced tissue specific alterations, as occurs when vimentin is ectopically expressed in transgenic mice, producing cataract (**Capetanaki et al., 1989**).

A group of human genetic disorders is associated with defects in neurofilaments (NF), like Amyotrophic Lateral Sclerosis (ALS), Infantile Spinal Muscular Atrophy and some other forms of Charcot-Marie-Tooth Neuropathy. Mutations occurring in the head and rod domains of the protein appear to be responsible for the disruption of self-assembly of human neurofilament light (NF-L) (**Perez-Olle et al., 2002**). Mutations in the neurofilament heavy (NF-H) have been found in ALS (**Al-Chalabi et al., 1999**). NF-L and NF-H null-mice have shown reduced axonal diameter (**Jacomy et al., 1999; Rao et al., 1998**).

An emerging group of human genetic diseases involving intermediate filament proteins is the laminopathies, where mutations in the LMNA gene can be associated with 6 clearly different phenotypes up to date. A more detailed description is given in section 1.10.

1.7 The Nuclear Lamina

The lamina is a flattened, discontinuous, open cage-like structure (**Capco et al., 1982; Hutchison, 2002; Paddy et al., 1990**) subjacent to the inner

nuclear membrane and is composed of a well-organized meshwork of filaments called lamins (**Aebi et al., 1986**). This highly physically and chemically resistant association of polymers interacts directly (B-type lamins) or indirectly (A and B-type lamins) with the INM, and contributes to maintain the shape and size of the metazoan nucleus (**Schirmer et al., 2001**). Its thickness varies at different areas (**Belmont et al., 1993**) and lamins can be found forming intranuclear foci during G1 (**Bridger et al., 1993; Goldman et al., 1992**), reinforcing the idea of multiple lamina complexes and its functional versatility.

Lamins are members of the type V intermediate filament family (**Fisher et al., 1986; McKeon et al., 1986; Parry et al., 1986**). Phylogenetic analysis of lamins and cytoplasmic IF sequences from invertebrates suggest that the nuclear lamins were the progenitor IF and cytoplasmic polypeptides arose through gene duplication of the lamin sequence (**Riemer et al., 2000; Stick, 1992**). The rod domain (~ 360 amino acids) of the lamins consists of a heptad repeat that is characteristic of proteins forming α-helices and contains six heptads that are absent from the cytoplasmic IF. Lamins and cytoplasmic IF have linker regions with no heptads, but unlike the latter ones, linker sequences of lamins do not have proline residues, giving a continuous rod domain (**Parry et al., 1986; Parry and Steinert, 1999**). Functional studies demonstrated that the rod domain drives the dimerization of lamin protein chains and higher order interactions between dimers (**Stuurman et al., 1998**).

A non-helical (head) N-terminal (30 - 40 amino acids) and a globular (tail) C-terminal (170 – 265 amino acids) domains flank the lamin's central rod domain. Here reside the main differences between the lamins and their

cytoplasmic relatives. Both, the head and tail domains in lamins contain specific phosphorylation sites, which play a key role in the dynamic regulation of these proteins during the cell cycle. Mitotic Cell Division Cycle 2 kinase (CDC2) phosphorylates residues in the head domain which mediate lamina assembly-diassembly (**Haas and Jost, 1993; Peter et al., 1990; Thompson et al., 1997**), while Protein kinase C-α (PKC-α) phosphorylates residues near the NLS and regulates its nuclear import (**Hennekes et al., 1993; Shimizu et al., 1998**). PKC-δ is required to hyperphosphorylate lamins during apoptotic breakdown to facilitate access of Caspase 6 to the nuclear lamina (**Cross et al., 2000**). Lamins C-terminus domain mediates targeting to the nucleus through the NLS (**Frangioni and Neel, 1993**), and as the rod domain (**Glass et al., 1993**), contains chromatin-binding sites (**Taniura et al., 1995**) . The very end of the C-terminal region of lamins contains a CaaX motif that undergoes post-translational modifications by iso-prenylation, farnesylation and/or proteolitic cleavage (**Holtz et al., 1989; Krohne et al., 1989**).

1.7.1 B-type Lamins

B-type lamins are differentially expressed in human tissues (**Broers et al., 1997**) and RNA interference of lamin B1 has shown to produce cell death (**Harborth et al., 2001**). Taken together, these experimental evidences suggest a relevant role of B-type lamins during embryogenesis and development. There are three B-type lamins in vertebrates: B1, B2 and B3. Lamin B1 is encoded by the LMNB1 gene (**Hoger et al., 1988**), situated on the chromosome 5q (**Wydner et al., 1996**), while lamins B2 (**Hoger et al., 1990**) and B3 (**Furukawa and Hotta, 1993**) are splicing variants of the LMNB2 gene, situated on chromosome 19p13.3 (**Biamonti et al., 1992**). In human tissues, every cell type expresses lamin B2, while lamin B1 is

expressed preferentially in proliferating cells, and is absent from skeletal muscle and heart (**Broers et al., 1997**), while lamin B3 is expressed only in sperm cells (**Furukawa and Hotta, 1993**). In other vertebrates, a similar pattern of expression is seen. In chicken for example, there appear to be differences between lamin B1 and B2 expression. Lamin B2 expression appears relatively constant, while Lamin B1 expression is high in embryonic tissues but drops in adult tissues (**Lehner et al., 1986**). In lamin B3, the rod domain is very short and the N-terminal 208 amino acids of lamin B2 are replaced by a unique 85 amino acid sequence, giving a molecular structure apparently responsible for the nuclear shape in sperm cells (**Furukawa and Hotta, 1993**).

All B-type lamins are permanently farnesylated at a sequence motif CaaX (**C**ysteine, any **a**liphatic **a**mino acid, **X** any amino acid) at the very N-terminus of the molecule. This motif is target for farnesyl-modification of the cysteine in the motif and appears to anchor B-type lamins to the inner nuclear membrane (**Farnsworth et al., 1989; Krohne et al., 1989**). Splicing variants in other species show different modifications. For example, a new splicing variant of the *Xenopus laevis* lamin B3 (not homologous to mammalian B3), where the last 12 amino acids are replaced by 12 new ones, includes a second cysteine targeted for palmitoyl-modification, which confers stronger association with membrane vesicles during nuclear breakdown (**Hofemeister et al., 2000**). These modifications may be responsible for the behaviour of B-type lamins during open mitosis, when the nuclear envelope breaks down but B-type lamins remain associated with ER vesicles (**Gerace and Blobel, 1980**), together with the interaction with specific integral membrane proteins like LBR. Other modifications like

phosphorylation occur during the S phase (**Kill and Hutchison, 1995**), when B-type lamins are synthesized (**Foisy and Bibor-Hardy, 1988**).

There is no report in the literature which links LMNB1 or LMNB2 genes to any known disease phenotype. Only one study in FPLD patients with no mutations in the LMNA gene have found novel Single Nucleotide Polymorphisms (SNPs) in LMNB1, four intronics and one in the coding sequence of lamin B1 (A501V), but they were not linked to the disease phenotype. No genetic variation was found in the LMNB2 (**Hegele et al., 2001**), supporting the observations made by Broers et al 1997 and Lehner et al 1986.

A large number of genomic clones for vertebrate lamins have been characterized, and analysis of the sequences show that intronic positions are very well conserved among A and B-type lamins of different species. Since B-type lamins are expressed in all tissues, it has been suggested that they are the progenitor ancestor of lamins by exon shuffling (**Stick, 1992**).

1.7.2 A-type Lamins

A-type lamins are expressed exclusively in differentiated tissues (**Stick and Hausen, 1985**). In mouse embryos, lamins A and C do not appear until 8 – 11 days post-fertilization, initially in developing muscle (**Rober et al., 1989; Stewart and Burke, 1987**). Hemopoietic and intestinal epithelial cells do not express Lamin A/C even in the adult (**Rober et al., 1989**). The induction of A-type lamins coincides with major changes in tissue structure, but occurs well after cells have committed to form a particular tissue, suggesting that A-type lamins are involved in maintaining a differentiated phenotype rather than determining the fate of cells during embryogenesis.

There are four different A-type lamins; all transcribed as different splicing variants from the LMNA gene, which is located on the chromosome 1q21.2. Lamins A and C (**Fisher et al., 1986**) are somatic lamins expressed in almost all differentiated cells (**Benavente et al., 1985**), lamin C2 is the specific A-type lamin of sperm cells (**Furukawa et al., 1994**), while Lamin AΔ10 was found in somatic cells and tumours (**Machiels et al., 1996**). Lamin A and C are identical in sequence up to the C-terminus, where splicing of exon 10 produces a unique 98 amino acids C-terminus for Lamin A and a specific 6 amino acids C-terminus for lamin C (**Fisher et al., 1986; Lin and Worman, 1993**). Lamin AΔ10 lacks 30 amino acids from the C-terminus specific for Lamin A. Lamins A and AΔ10 contain the specific CaaX motif at the very end of the globular domain (**Holtz et al., 1989**), where the cysteine of the motif undergoes a series of modification by farnesylation, subsequent cleavage of the three N-terminal residues and carboxy-methylation.

Other modifications of lamins are phosphorylation of residues in the head and tail domain, which are responsible for the dynamics of A-type lamins during interphase and mitosis (**Ottaviano and Gerace, 1985**). Early in mitosis, A-type lamins are hyper-phosphorylated by PKC and CDK2 (**Dessev et al., 1988**) and become dispersed throughout the cytoplasm, most probably into oligomeric complexes (**Hutchison et al., 2001**), where they are more easily extractable (**Gerace and Blobel, 1980**). But the phosphorylation and disassembly of A-type lamins is not enough for the NE diassembly (**Newport and Spann, 1987**). At the end of telophase, the rate of dephosphorylation by Protein Phosphatase 1 (PP1) at CDK2 sites modulates the initial rate of lamin filament assembly (**Thompson et al., 1997**). During interphase, lamins are phosphorylated as well, but to a different extent, which plays different roles than the phosphorylation event during mitosis

(**Moir et al., 1995**). Phosphorylation at sites adjacent to the NLS by PKC can influence nuclear import of lamins, limiting the availability of lamin subunits (**Hennekes et al., 1993**). On the other hand, phosphorylation by Protein Kinase cAMP-dependent (PKA) facilitates the incorporation of new lamin subunits into the assembled lamina as the nucleus grows (**Peter et al., 1990**).

The role of A-type lamins in differentiated tissues gained more significance following the findings, first, that lamin binding partner Emerin, when mutated or absent (**Bione et al., 1994**), produces a muscular dystrophy disorder, and secondly, when mutations in the LMNA gene were linked to similar phenotypes (**Bonne et al., 1999**). Currently near 60 different mutations in the LMNA gene have been reported, related to six/seven different phenotypes so far, but no hot-spots have been observed. Rather mutations are clustered for some phenotypes. For example, Dilated Cardiomyopathy with Cardiac Conduction Defects is associated with mutations in the rod domain; while Familial Partial Lipodystrophy associated mutations are mainly in the globular tail domain. Werner Syndrome, where LMNA is involved, seems to cluster the DNA changes in the rod domain of the protein. In the case of Autosomal Dominant Emery-Dreifuss Muscular Dystrophy, mutations are dispersed along the gene. Progeria disorder Hutchison-Gilford presents a deletion in the specific tail domain of Lamin A.

1.7.3 Lamina Associated Proteins

As with their cytoplasmic relatives, nuclear intermediate filaments, the lamins, have their associated proteins (LAP). Most of them are type II integral membrane proteins with a characteristic protein structure of C-terminal transmembrane domain (except LAP2α) and a long nucleoplasmic

N-terminal domain, which are considered to be responsible for the association of the nuclear lamina with the INM. LAP1 proteins (LAP1A, LAP1B and LAP1C) are monovalent due to their apparent unique interaction with lamins. LAP2 proteins (LAP2α, β, δ, ε, γ and ξ) appear to be bivalent as they interact with lamins and chromatin (**Foisner and Gerace, 1993; Hutchison et al., 2001**).

Specific for B-type lamins is the LBR, the best characterized Lamin Associated Protein (**Moir et al., 1995**). Another LAP is emerin, an INM protein that interacts with A and B-type lamins (**Vaughan et al., 2001**), posses a LEM motif (**L**AP2β , **E**merin and **M**an) at the very end of the N-terminal domain that interact with other nucleoplasmic proteins. Unlike the cytoplasmic intermediate filaments, no human diseases have been described to involve mutations in LAPs, except emerin (see section 1.10).

1.7.4 Assembly Models

Nuclear lamins form 10 nm filaments in vivo (**Fuchs and Weber, 1994**), but the stepwise study of Lamin assembly in vitro results in paracrystal formation (> 13nm), through enhanced lateral associations (**Quinlan et al., 1995**). Most of the models for intermediate filament assembly in vitro have been developed using cytoplasmic intermediate filaments, particularly vimentin and keratins, although it has been suggested that the filament assembly pathways may differ between IF types and even between individual IF proteins (**Strelkov et al., 2003**). It has been proposed that the basic structure of intermediate filaments is two monomers associated in parallel via their rod domains in a coiled-coil super helical configuration. Dimers associate laterally through three distinct interaction models called A_{11}, A_{22} and A_{12} (**Steinert et al., 1993**). The A_{11} mode corresponds to an

antiparallel, half-staggered association of two dimers with their coil 1B segments almost aligned (**Herrmann and Aebi, 1998**). The A_{22} mode corresponds to a half-staggered anti-parallel association of dimers with the coil2B segments aligned (**Strelkov SV et al., 2002**). The A_{12} mode is an unstaggered anti-parallel association. Mature IFs associate in an A_{CN} mode, where the N and C-terminal domains of longitudinally aligned dimers overlap (**Parry and Steinert, 1999**). A linear arrangement of tetramers within a mature intermediate filament corresponds to a protofilament, and the lateral association of protofilaments assembles protofibrils (**Strelkov et al., 2003**).

In vitro studies have demonstrated that, as in cytoplasmic IFs, the elementary building block of lamins is a parallel, unstaggered two-stranded α-helical coiled-coil dimer involving the central rod domain (**Heitlinger et al., 1991**). In contrast with the lateral mode of association of cytoplasmic intermediate filaments, nuclear lamins associate longitudinally to form polar head-to-tail polymers (**Gieffers and Krohne, 1991**), which associate laterally in an anti-parallel, half-staggered fashion to form IF-like assemblies with a periodical 25 nm beading repeat, and eventually forming paracrystals (**Heitlinger et al., 1991**). These lamin specific structures can be disassembled in vitro by incubation either in cell-free extracts of mitotic cells (**Ward and Kirschner, 1990**) or with highly purified fractions of $p34^{CDC2}$ (**Peter et al., 1991**), suggesting the predominant role of phosphorylation processes in the diassembly of the nuclear lamina in vivo (**Moir et al., 1995**).

Accordingly, several models have been developed to explain the steps of the lamina assembly in vivo. Because of the basic nuclear lamina must be formed around B-type lamins, and, like their cytoplasmic relatives (IFAPs),

LAPs influence the formation of a primary nuclear lamina (B-type lamins based), lamin dimers are forced to associate with the INM and further form a 10 – 13 nm flattened array. At mitosis, the NE disassembles and phosphorylation of lamins dissociates the flattened meshwork, keeping B-type lamins at the mitotic vesicles and A-type lamins into a soluble pool (**Bridger et al., 1993**). B-type lamin subunits retain A-type lamins constraining elements (like emerin, LAP1C and others) that recruit lamins A and C heterotetramers only after an evident NE is re-assembled (**Broers et al., 1999**). During interphase, phosphorylation of lamins at sites adjacent to the NLS regulates the rate of incorporation of new lamins as the nucleus grows in preparation for the next M-phase. For more details of this model, see (**Hutchison et al., 2001**).

1.7.5 Functional Theories

After the discovery that mutations in the LMNA gene are involved in several human diseases, "laminologists" have divided their opinions regarding the role of lamins in the cell, in order to explain the tissue-specific effect of the mutations. Some support the structural hypothesis, which proposes that mutations give rise to weakness of the lamina and lead to fragility of the nuclear envelope and its consequent breakage (**Hutchison et al., 2001; Sullivan et al., 1999**). The other group supports the gene expression hypothesis which proposes that A-type lamins are involved in the tissue-specific changes in patterns of gene expression (**Cohen et al., 2001**).

As with cytoplasmic intermediate filaments, lamins play a structural role maintaining the integrity of the nucleus. Physical depletion of lamins does not prevent nuclear assembly, but produces a weak nucleus (**Newport et al., 1990**), and lamin deletion mutants alter nuclear morphology (**Schirmer et**

al., 2001). Cultured cells from EDMD patients with different mutations in the LMNA gene have an increased number of defective nuclei compared to respective controls (**Favreau et al., 2003; Novelli et al., 2002; Vigouroux et al., 2001**). Similarly, nuclei from EDMD patients with mutations in the LMNA gene are less resistant to external, artificial stress (Broers et al., (**SEB-Symposia, 2003**)).

It has been long suggested that lamins should be involved in gene expression by early observations that lamins A and C are expressed only in differentiated cells (**Lehner et al., 1987**). A series of experimental evidence demonstrated the role of lamins in DNA synthesis. B-type lamins are specifically synthesized (**Foisy and Bibor-Hardy, 1988**), phosphorylated (**Kill and Hutchison, 1995**) and distributed to active sites of DNA replication during S phase (**Moir et al., 1994**). B-type lamins, but not A-type, are involved in a lamin-dependent DNA synthesis in *Xenopus* egg extracts (**Meier et al., 1991**). Nuclei lacking lamins are able to import karyolitic proteins involved in DNA replication (Proliferating Cell Nuclear Antigen, PCNA), but do not form a resistant nuclear matrix that retains its protein composition (**Jenkins et al., 1993**). B-type lamins interact with cytoplasmic intermediate filaments during telophase (**Djabali et al., 1991**) and a model has been developed for the role of an intermediate filament polymer and/or the cooperation between cytoplasmic and nucleoplasmic intermediate filaments in transporting karyolitic proteins in telophase to the DNA replication/elongation/transcription initiation sites (**Traub and Shoeman, 1994**). But still the role of A-type lamins in any pathway involving control of gene expression has to be demonstrated.

1.8 Lamins and Emerin in disease

1.8.1 X-Linked Emery Dreifuss Muscular Dystrophy (XL-EDMD)

A typical pattern was first described by (**Dreifuss and Hogan, 1961; Emery and Dreifuss, 1966**) who studied Virginia kindred in which there were 8 affected males in three generations. Onset of muscle weakness, first affecting the lower extremities with a tendency to walk on the toes, was noted around the age of 4 or 5 years. In general, the disease was characterized by the triad of 1) slowly progressive muscle wasting and weakness with humero-peroneal distribution in the early stages; 2) early contractures of the elbows, Achilles tendons, and post-cervical muscles; and 3) cardiomyopathy. The cardiac conduction defect in EDMD patients is the most serious and life threatening clinical manifestation of the disease. Cardiac defects have been described in female carriers (**Emery, 1989**) in the absence of any skeletal muscle abnormality, suggesting a prominent role of emerin in the cardiac conduction system. Studies of the cardiac status in three patients with EDMD revealed the effect on the heart in teenage years and it was characterized by cardiac conduction defects and infiltration of the myocardium by fibrous and adipose tissue (**Buckley et al., 1999**). It first affected the atria, which resulted in atrial paralysis; treatment with ventricular pacing was usually needed. Female carriers developed heart problems and were at risk of sudden death, in agreement with Emery's work (**Emery, 1989**).

The name Rigid Spine Syndrome (RSS) was given to a disorder found in a 17 years old boy, with a myopathy and stiffness of the back and neck at an early age, and progressive scoliosis in his teens (**Dubowitz, 1973**). For several years, the patient had difficulties in extending his elbows. It was then suggested that this may be a X-linked disorder and may be related to

the EDMD with contractures (**Wettstein, 1983**). RSS is distinguished from EDMD by lack of cardiac involvement and autosomal recessive inheritance. Under the designation Scapulo-Peroneal Syndrome, kindred were described with typical X-linked inheritance of a myopathy manifesting as muscular weakness and wasting, affecting predominantly the proximal muscles of the legs. Accompanying features were contractures of the elbows, pes cavus, and, in adulthood, cardiomyopathy (**Thomas et al., 1972**). The authors pointed out similarities to the Emery benign type of muscular dystrophy with contractures but thought that the distribution of muscular involvement distinguished the two. Later revised opinions concluded that the disorder was in fact EDMD (**Thomas, 1985**). Many studies reached the conclusion that X-linked Scapulo-Peroneal Syndrome was the same condition as EDMD (**Mawatari and Katayama, 1973; Merlini et al., 1986; Rotthauwe et al., 1972; Rowland et al., 1979; Sulaiman et al., 1981; Thomas, 1985**).

XL-EDMD gene is inherited as a recessive character, with 100% penetrance by the second/third decade of life. Heterozygous females show no indication of skeletal muscle disorder, but arrhythmia and bradycardia are observed with risk of sudden death (**Bialer et al., 1991; Emery, 1987; Fishbein et al., 1993; Merlini et al., 1986; Pinelli et al., 1987**). Molecular analysis of the XL-EDMD began with the construction of a transcriptional map of the 2 Mb region of chromosome Xq28 (**Bione et al., 1993**). Within this region, the STA gene was identified, which encodes a 254 amino acids protein termed Emerin. This protein lacks a signal peptide, contains a long N-terminal domain, and is hydrophilic, except for a highly hydrophobic 20 amino acids sequence at the C-terminal region. In addition, it has several putative phosphorylation sites and one potential glycosylation site. Northern blot analysis demonstrated ubiquitous expression of a major transcript of

approximately 1 kb, with the highest expression in skeletal muscle and heart, and abundant expression in other tissues including colon, testis, ovary, and placenta. It was then suggested that Emerin belongs to a class of tail-anchored proteins of the secretory pathway involved in vesicular transport.

Among the many genes located in the special part of Xq28, eight transcripts expressed at high levels in skeletal muscle, heart and/or brain were selected as the best candidates for the site of the mutation causing XL-EDMD (**Bione et al., 1994**). Each of the five patients investigated had a unique mutation in one of the genes. These mutations resulted in the loss of all or part of the protein. In addition, heteroduplex analysis of emerin gene exons in 30 unrelated XL- EDMD patients revealed abnormal patterns of single exons in seven patients. Direct sequencing of the respective exons revealed six novel mutations distributed in the promoter region and exons 3 – 6. This study identified the first mutations in the promoter region and exon 5. With the mutations here described, a total of 25 mutations were then known. All of the mutation abolished the synthesis of functional Emerin (**Wulff et al., 1997**). Several mutations have been found in the STA gene, and have been classified as: non-sense (34), frame-shift (31, splice-donor (7), splice acceptor (5) gene deletions (5), missense (3), in-frame (3) promoter (1) and large deletions (1) (**Yates, 1998**).

Biochemical analysis involving mutations affecting Proline-183 (P183) had had demonstrated that the mobility and expression levels of the mutant form of Emerin is indistinguishable from those of the wild type form, but have weakened interaction with nuclear lamina components (**Ellis et al., 1999**). In comparison with the usual XL-EDMD phenotype, patients with

P183 missense mutation had a later age at onset of first symptoms (elbow contractures, ankle contractures, and upper and lower limb weakness), but there was no difference for the age at onset of cardiac involvement. A TCTAC deletion was identified in two brothers with XL-EDMD, spanning nucleotides 631 – 635 of the Emerin gene. Both showed an unusual severe disease phenotype (**Hoeltzenbein et al., 1999**). The same mutation had been found previously in two brothers with significantly milder phenotype in an unrelated family (**Manilal et al., 1998**).

A panel of 12 monoclonal antibodies to a large fragment of emerin cDNA was prepared by PCR and expressed as a recombinant protein *E. coli* (**Manilal et al., 1996**). These antibodies detected 4 different epitopes on Emerin. All monoclonal antibodies recognized a 34 kDa protein in all tissues tested. Immunofluorescence and cell fractionation studies confirmed that Emerin is located at the nuclear membrane. Amino acid sequence similarities and cellular localization suggested that Emerin is a member of the nuclear lamina-associated protein family.

Monoclonal antibodies showed that Western blotting and immuno-histology of a biopsy from an XL-EDMD patient could be simple diagnostic test for this disorder (**Manilal et al., 1996**). Studies in three families with XL-EDMD that showed different mutations in the STA gene emphasized the usefulness of early diagnosis because insertion of a peacemaker may be life saving (**Nevo et al., 1999**). For example, a case of XL-EDMD in 3 years old boy was described with contractures of the Achilles tendons, but without characteristic contractures of the elbows and cardiac involvement. Immunofluorescence analysis of a muscle biopsy showed no Emerin presence at the nuclear membrane. RT-PCR and PCR-based genomic

analysis of the STA gene revealed no amplification products in the patient's samples (**Fujimoto et al., 1999**). The authors stressed that Emerin staining should be part of the work-up of every unexplained muscular dystrophy, in agreement with (**Manilal et al., 1996; Nevo et al., 1999**).

Emerin localizes to the INM via its hydrophobic C-terminal domain, but in heart and cultured cardiomyocytes it is also associated with the intercalated discs. A general role for Emerin was then proposed as a membrane anchorage element to the cytoskeleton (**Cartegni et al., 1997**). In the nuclear membrane, Emerin plays a ubiquitous and indispensable role in associating the nuclear membrane with the lamina. In heart, it is specifically located to desmosomes and fasciae adherents. The role of this complex assortment of protein is best demonstrated by the existence of many genetic diseases that perturb adhesion, and in the heart, by the dramatic consequences of plakoglobin (gamma catenin) knockout (**Ruiz et al., 1996**): plakoglobin -/- mice die at mid-gestation due to rupture of the ventricles. In heart, the specific localization of Emerin to desmosomes and fasciae adherents could account for the characteristic conduction defects described in patients with XL-EDMD.

Using two antisera against a synthetic peptide predicted form Emerin cDNA, a positive nuclear membrane staining was found in skeletal, cardiac and smooth muscle in normal controls and in patients with neuromuscular diseases other than XL-EDMD (**Nagano et al., 1996**). In contrast, a deficiency in immunofluorescence staining of skeletal and cardiac muscle from XL-EDMD patients was observed. In heart, the specific localization of Emerin to desmosomes and fasciae adherents could account for the characteristic conduction defects described in patients with XL-EDMD

(**Cartegni et al., 1997**). In contrast, other studies found that affinity purified antibodies against Emerin gave immuno-staining only in the nuclear membrane, casting doubt on the hypothesis that cardiac defects in XL-EDMD are caused by absence of Emerin from intercalated discs. Although Emerin was abundant in the membranes of cardiomyocyte nuclei, it was absent from non-myocyte cells in the heart. This distribution of Emerin was similar to that of Lamin A, which is mutated in the Autosomal Dominant – EDMD (AD-EDMD) syndrome. In contrast, Lamin B1 was absent from cardiomyocyte nuclei, suggesting that Lamin B1 is not essential for localization of Emerin to the nuclear lamina. Lamin B1 was also almost completely absent from skeletal muscle nuclei, suggesting that in XL-EDMD the additional absence of lamin B1 from heart and skeletal muscle that already lack Emerin might explain why these tissues are particularly affected (**Manilal et al., 1999**). Studies of ultra-structural localization of Emerin in human skeletal muscle and HeLa cells, using ultra-thin cryo-sections, showed that immune-labelled-colloidal gold particles were localized on the nucleoplasmic surface of the INM, but not on the nuclear pore likewise demonstrating that Emerin is localized at the INM (**Yorifuji et al., 1997**).

Other mutation analysis determined that several, but not all disease mutations in the STA gene mapped to a central Lamin A-binding domain, and that mutations in this region disrupt Emerin-Lamin A interaction. Emerin binds directly to Barrier Autointegration Factor (BAF), a DNA-binding protein, and this binding requires conserved residues in the N-terminal LEM domain of Emerin (**Lee et al., 2001**). In addition, Emerin co-localized with BAF at the core region of chromosomes during telophase in HeLa cells. An Emerin mutant deficient in BAF-binding-region mislocalized in vivo to the

core of chromosomes and subsequently, failed to localize to the reformed nuclear envelope. In HeLa cells expressing a BAF mutant that did not show core localization, endogenous Emerin failed to localize to the core region during telophase and did not assemble into the nuclear envelope during the subsequent interphase (**Haraguchi et al., 2001**). This BAF mutant also dominantly mislocalized LAP2β and Lamin A from the nuclear envelope. This finding suggested that BAF is required for the assembly of Emerin and A-type lamins at the reforming nuclear envelope during telophase and may mediate their stability in the subsequent G1.

Using Fluorescence In-Situ Hybridization (FISH) and immunofluorescence, the nuclear organization of every human chromosome was analyzed in diploid lymphoblasts and primary fibroblasts. Most gene-rich chromosomes were concentrated at the centre of the nucleus, whereas the gene-poor chromosomes were located towards the nuclear periphery. There was no significant relationship between chromosome size and position within the nucleus. The intranuclear organization of chromosomes of a patient with XL-EDMD was not altered, suggesting that Emerin may not be necessary for localizing chromosomes at the nuclear periphery, and that the muscular dystrophy phenotype in such individuals may not be due to grossly altered chromatin organization (**Boyle et al., 2001**).

1.8.2 Autosomal Dominant EDMD

Studies in two Dutch families, with a seemingly unique form of myopathy, revealed features intermediate between Limb-Girdle Muscular Dystrophy and Scapulo-Peroneal Atrophy. Onset occurred between 17 and 42 years of age and cardiomyopathy was a late feature, with several instances of male-to-male transmission (**Jennekens et al., 1975**). Another disorder was

described that might be labelled EDMD but was inherited as autosomal dominant (**Miller et al., 1985**). The father and daughter had muscle contractures, especially of posterior cervical muscles but also affecting elbows and ankles, cardiac involvement with atrial rhythm disturbance and slow ventricular rate, slowly progressive weakness mainly of humeral and peroneal muscles with some pelvic girdle involvement and tendon areflexia, and Electromyography (EMG) and histological evidence of myopathy. Hauptmann-Thannhauser eponym was then suggested (**Becker, 1972**) to be attached to autosomal muscular dystrophy with early contractures and cardiomyopathy, as Hauptmann reported in 1941 the disorder in a family of French-Canadian descent in which nine persons in three generations were affected by a form of muscular dystrophy "*not heretofore described in the literature*" (**Hauptmann, 1941**). The disorder was manifested by inability to flex the neck and slight webbing due to shortened muscle as well as limitation on spinal flexion and elbow extension from the same cause. A German family was also described with an autosomal dominant form of EDMD. Several affected members died in middle age of sudden cardiac death and at least two had a pacemaker implanted. One patient had heart transplant and four instances of male-to-male transmission were observed (**Witt et al., 1988**).

XL-EDMD genetic defects reside in the STA gene. In the AD form, Emerin is normal. Distribution of Emerin was found to closely resemble that of Lamins A and C (**Manilal et al., 1999**). A functional interaction between Emerin and Lamin A in the nucleus could explain the identical phenotype in the different forms of EDMD. Using genetic linkage analysis, the locus for AD-EDMD was mapped to an 8cM interval on 1q11-q23 in a large French pedigree, and the AD-EDMD phenotype in other four small families was potentially linked to

this locus (**Bonne et al., 1999**). This region contains the LMNA gene, which encodes four proteins of the nuclear lamina, lamins A, AΔ10, C and C_2, by alternative splicing. Mutations in the LMNA gene co-segregated with the disease phenotype in five families: one nonsense and three missense mutations. These results represented the first identification of mutations in a component of the nuclear lamina as a cause of and inherited muscle disorder.

1.8.3 Autosomal Recessive EDMD

A mutation in the LMNA gene in a 40 years old man with severe EDMD was identified. Both parents, who were first cousins, were heterozygous for the mutation. The patient had experienced difficulties when he started walking at age 14 months. At age of 5 years, he could not stand because of contractures. At age of 40 years, he presented severe and diffuse muscle wasting and was confined to a wheelchair. His intelligence was normal; careful cardiological examination of the patient and his parents showed that they did not present cardiac problems. None of them showed cardiac or skeletal muscle abnormities. This study showed that heterozygous mutations in LMNA could cause diverse phenotypes ranging from typical EDMD to no phenotypic effects. The distribution of mutations in autosomal dominant patients suggested that the unique interactions between Lamin A/C with other nuclear components exist that have an important role in cardiac and skeletal function (**Raffaele Di Barletta et al., 2000**).

1.8.4 Familial Partial Lipodystrophy (FPLD)

Patients with partial lipodystrophy have a normal fat distribution in early childhood, but with the onset of puberty, almost all subcutaneous adipose tissue from the upper and lower extremities and gluteal and truncal areas

gradually disappears, causing prominence of muscles and superficial veins in these areas. Simultaneously, adipose tissue accumulates on the face and neck, causing a double chin and fat neck. Adipose tissue may also accumulate in the axillae, back, labia majora, and intra-abdominal region. Affected patients are insulin-resistant and may develop glucose intolerance and diabetes mellitus after the age of 20 years, with hypertriglycideridemia, and low levels of high density lipoprotein (HDL). The phenotype is readily discernible in females. Affected males, however, are more difficult to recognize due to relative muscularity and reduced body fat in normal individuals, accounting for the past suggestion of X-Linked dominant inheritance of this disorder.

A dominantly inherited disorder in six females in four generations was described, where clinical features were symmetric lipoatrophy of the trunk and limbs with rounded, full face, tuberoeruptive xanthomata, acanthosis nigricans and insulin-resistant hyperinsulinism (**Dunnigan et al., 1974**). In a second family, six females in three generations were affected. This syndrome was distinct from congenital lipodystrophy, a recessive form with progressive partial lipodystrophy. It was then concluded that there are two types of familial lipodystrophies: type 1, with loss of subcutaneous fat confined to the limbs; and type 2, in which the trunk is also affected with the exception of the vulva, giving an appearance of labial hypertrophy (**Kobberling and Dunnigan, 1986**). Diabetes mellitus, hyperlipoproteinemia, and acanthosis nigricans were present to a variable degree in some but not all patients. Both types, occurring either as a familial disorder or sporadically, had been observed only in females. The pedigrees suggested to the authors X-linked dominant inheritance with lethality in the hemizygous XY conceptus. It was suggested as a one possibility that the

two types were allelic. Other pedigrees showed clear autosomal dominant inheritance (**Jackson et al., 1997; Peters et al., 1998; Robbins et al., 1982**). It was uncertain whether there was a distinct Kobberling variety of familial lipodystrophy, which had been characterized as having loss of subcutaneous adipose tissue limited to the limbs without involvement of the trunk and with normal facial fat (**Kobberling and Dunnigan, 1986; Kobberling et al., 1975**).

To investigate whether there was a unique pattern of fat distribution in men and women with FPLD, whole-body magnetic resonance imaging in one male and three female patients from two pedigrees confirmed the clinical findings of near-total absence of subcutaneous fat from all extremities. Reduction in subcutaneous adipose tissue from the truncal area was more prominent anteriorly than posteriorly. Increased fat stores were observed in the neck and face. It was then concluded that FPLD results in a characteristic absence of subcutaneous fat from the extremities, with preservation of intermuscular fat stores (**Garg et al., 1999**). Anthropometric variables and prevalence of diabetes mellitus, dyslipidemia, hypertension, and atherosclerotic vascular disease were assessed among 17 post-pubertal males and 22 females with FPLD from eight pedigrees. All individuals were analyzed for glucose, insulin and lipoprotein concentrations and presented similar patterns of fat loss. Compared with the affected men, women had a higher prevalence of diabetes (50% women vs. 18% men) and atherosclerotic vascular disease (45% women vs. 12% men), and had higher serum triglycerides and lower HDL cholesterol concentrations. The prevalence of hypertension and fasting serum insulin concentrations were similar, suggesting that females with FPLD are more severely affected with metabolic complications of insulin resistance than males (**Garg, 2000**).

Genomewide scan studies with a set of highly polymorphic short tandem repeats (STRs) in individuals from five well-characterized pedigrees mapped the genetic locus to 1q21-q22, with no evidence for genetic heterogeneity (**Peters et al., 1998**). Linkage and haplotype analysis with highly polymorphic microsatellite markers on large, multigenerational Caucasian kindred of German ancestry with the Dunnigan's form of FPLD linked FPLD gene near marker D1S2721 (**Anderson et al., 1999**), supporting the minimal region previously reported (**Jackson et al., 1998; Peters et al., 1998**). A genomewide linkage search using microsatellite markers provided conclusive evidence of linkage to 1a21 (D1S498), with no evidence of heterogeneity. Additional haplotype and multipoint analysis supported the location of the FPLD locus within a 21.2 cM chromosomal region that is flanked by markers D1S2881 and D1S484. The LMNA gene was considered to be a candidate for FPLD for several reasons: FPLD maps to the same region of chromosome 1 as the LMNA gene; mutations in LMNA gene cause muscle wasting in AD-EDMD; and regional muscle wasting in AD-EDMD is analogous to the regional adipocyte degeneration in FPLD. DNA sequencing of the LMNA gene in five Canadian families affected by FPLD showed an R482G missense mutation (**Cao and Hegele, 2000**).

In a three generation Canadian kindred, in whom four members had autosomal dominant familial lipodystrophy and normal LMNA gene sequence, a mutation was identified in the Peroxisome Proliferator Activated Receptor γ (PPARG) gene. All four affected members were heterozygous for an 1164 T-A transversion in exon 5, predicting a F388L substitution. The mutation altered a highly conserved residue within helix 8 of the predicted ligand-binding pocket of PPARG, and was not found in normal family members or normal unrelated subjects. The mutant receptor had significantly decreased

basal transcriptional levels, and impaired stimulation by a synthetic ligand. Clinically, the patient phenotype was similar to that seen in the Canadian FPLD probands with missense mutations in LMNA gene (**Hegele et al., 2002**).

In another form of FPLD, lipoatrophy with diabetes was described by in a 27 years old male patient whose phenotype was characterized by acquired generalized lipoatrophy with metabolic alterations, massive liver steatosis, distinctive subcutaneous manifestations, and cardiac abnormalities involving both endocardium and myocardium. Generalized atrophy of subcutaneous fat resulted in sunken cheeks and muscular pseudo-hypertrophy of the four limbs. Multiple whitish papules on pigmented skin were present on the neck, trunk, and upper limbs and to a lesser extent on the lower limbs. Muscular strength was normal, and no neurological defects were detected. Cardiac involvement included concentric hypertrophy of the left ventricle without cavity dilatation associated with thickness and regurgitant valves, aortic fibrotic nodules, and calcification of the posterior annulus. Doppler echocardiographical findings were similar to dose described in aged patients. Abdominal Magnetic Resonance Imaging (MRI) revealed an absence of body at both, the subcutaneous and visceral levels. Family members were unaffected, and no consanguinity was reported. Mutation analysis of the LMNA gene found a heterozygous 398 G-T transversion in exon 2. This mutation resulted in amino acid change R133L in the rod domain of lamins A and C. Arginine 133 is located in a charged peptide stretch, which is highly conserved in A and B-type lamins in vertebrates. The switch from positively charged Arginine to hydrophobic Leucine in the Lamin A/C dimerization domain may severely impair its polymerization and further filament assembly. Accordingly, nuclear abnormalities in primary cultures of patient fibroblasts were observed (**Caux et al., 2003**).

1.8.5 Dilated Cardiomyopathy with Conduction Defects (DCM-CD)

In a family where 10 members were suffering or had died from cardiomyopathy, and six others were probably affected, transmission seemed to occur only through the female, although both males and females were affected (**Whitfield, 1961**). In a different family, two sisters presented with Familial Idiopathic Cardiomegaly (**Schrader et al., 1961**). Based on similar clinical phenotypes, cardiomyopathies were classified in: type 1, with predominant fibrosis; type 2, with predominant ventricular hypertrophy, hereditary; and type 3, with deposits of a nonmetachromatic polysaccharide (**Boyd et al., 1965**).

Studies in kindred in which 12 members had Cardiomegaly with poor ventricular function and/or dysrhythmia, the disorder was evident by echocardiogram in a 6 month old infant. Skeletal muscle biopsies showed subtle myopathic alterations. The pedigree, spanning 5 generations, was consistent with autosomal dominant inheritance (**Gardner et al., 1985**). In a different family, multiple members in three generations had dilated cardiomyopathy with overt clinical onset between the fourth and seventh decades. It was then concluded that there may be an associated skeletal myopathy manifested by very mild proximal weakness or detectable only on biopsy (**Gardner et al., 1987**). Further studies found in eight individuals, four of whom were males in three generations, showed variation in muscle fibre size and interstitial fibrosis. Average time to death from onset of symptoms suggestive of cardiomyopathy was 16 months. One member died suddenly after being asymptomatic (**MacLennan et al., 1987**).

Linkage studies demonstrated the disease locus was near the centromere of chromosome 1, between D1S305 and D1S176 (**Kass et al., 1994**). Based on

the disease phenotype and the map location, it was speculated that the gap-junction protein connexin-40 was a candidate for mutations that result in conduction system disease and dilated cardiomyopathy. PCR-based studies and Southern blot analysis of the dystrophin gene (DMD) in 27 males with idiopathic dilated cardiomyopathy showed no defects. None of the patients had clinical evidence of skeletal muscle disease or any systemic illness that could cause heart disease (**Michels, 1993**). Genetic studies excluded linkage between the disease phenotype and a 21 cM region spanning the Human Leukocyte Antigen (HLA) cluster in at least 60% of the families studied (**Olson et al., 1995**). Another study compared 31 familial and 209 non-familial cases of dilated cardiomyopathy, concluding that familial form was more malignant: it occurred at an earlier age and progresses more rapidly than the non-familial form (**Csanady et al., 1995**).

Dilated cardiomyopathy, a disorder characterized by cardiac dilation and reduced systolic function, represents an outcome of heterogeneous group of inherited and acquired disorders. Causes include myocarditis, coronary artery disease, systemic diseases, and myocardial toxins; idiopathic dilated cardiomyopathy in which these causes are excluded, represents approximately one-half of the cases (**Olson and Keating, 1996**). Among patients with idiopathic dilated cardiomyopathy, familial occurrence accounts for 20-25%, with the exception of rare cases resulting from mutations in dystrophin of mitochondrial genes. Familial dilated cardiomyopathy is characterized by an autosomal dominant pattern of inheritance with age-related penetrance. It presents with development of ventricular dilation and systolic dysfunction usually in the second or third decade of life.

Several loci for familial dilated cardiomyopathy have been mapped. In addition to the CMD1A locus on chromosome 1p11-q11, these include CMD1B on 9q13; CMD1C on 10q21; CMD1D on 1q32; CMD1E on 3p; CMD1F on 6q; CMD1G on 2q31; CMD1H on 2q14-q22; CMD1I, which results from mutations in Desmin (DES) on 2q35; CMD1J on 6q23-q24; CMD1K on 6q12-q16; CMD1L, which results from mutations in the Sarcoglycan (SGCD) gene on 5q33; CMD1M, from mutations in Cysteine and Glycine Rich Protein (CSRP3) gene on 11p15.1; and CMD1N from mutation in Titin (TCAP) on 17q12. Another form of CMD is caused by mutation in actin (ACTC). Mutation in the cardiac beta-myosin-binding protein C (MYBPC3) can cause CMD or hypertrophic cardiomyopathy. Another form of autosomal dominant dilated cardiomyopathy and heart failure is caused by missense mutations in the phospholamban gene. For a review of the genetic and clinical heterogeneity of familial dilated cardiomyopathy see (**Semsarian and Seidman, 2001**).

The region to which the CMD1A locus had been mapped, namely 1p1-q21, overlaps with the region where the nuclear lamins A and C are encoded by the LMNA gene. Mutations in the head, rod and tail domain of this gene are known to cause autosomal dominant Emery-Dreifuss muscular dystrophy. A study of eleven families with autosomal dominant cardiomyopathy and conduction system defects showed five novel mutations in the heterozygous state: four in the α-helical rod domain of the LMNA gene, and one in the lamin C specific tail domain. Each mutation caused heritable, progressive conduction system disease (sinus bradycardia, atroventricular conduction block, or atrial arrhythmias) and dilated cardiomyopathy. Heart failure and sudden death occurred frequently within these families. No family members with mutations had either join contractures or skeletal muscle myopathy.

Furthermore, serum creatine kinase levels were normal in family members with mutations in the lamin rod domain, but mildly elevated in some family members with a defect in the tail domain of lamin C. The findings indicated that the Lamin A/C intermediate filament protein plays an important role in cardiac conduction and contractility (**Fatkin et al., 1999**). In a different study, a large family presented a severe autosomal dominant dilated cardiomyopathy with atroventricular conduction defect in some affected members. In addition, some affected family members had skeletal muscle symptoms varying from minimal weakness to a mild limb-girdle muscular dystrophy. Affected individuals were heterozygous for a single nucleotide deletion in the LMNA gene, increasing the range of phenotype arising from this mutation (**Brodsky et al., 2000**). For a review of the chromosomal locations of the known loci responsible for inherited forms of dilated cardiomyopathy see (**Fatkin et al., 1999**).

Another form of dilated cardiomyopathy presented quadriceps myopathy in a large family (**Charniot et al., 2003**). Cardiac involvement preceded neuromuscular disease in all affected patients, whereas in previously reported cases with both cardiac and neuromuscular involvement, the neuromuscular disorders had preceded cardiac abnormalities. Twenty-nine members of the family were examined, of whom eleven classified as affected, and four had both cardiac and peripheral muscle symptoms. Average age at onset of cardiac symptoms was 40 years. Bilateral motor deficit of the quadriceps deteriorated progressively, without involvement of other muscles. A mutation in the LMNA gene (R377H) was found, similar to a mutation found in a French family causing limb-girdle muscular dystrophy with age-related atroventricular cardiac conduction disturbances and the absence of early contractures (**Muchir et al., 2000**), and it was suggested

the presence of factors other than the R377H mutation influencing the phenotypic expression in their family.

Another genetic cardiac disorder is Atrial Fibrillation, characterized by rapid and irregular activation of the atrium. The prevalence of Atrial Fibrillation in the general population rises with increasing age, ranging from less than 1% in young adults to greater than 5% in those older than 65 years. Atrial Fibrillation causes thromboembolism, tachycardia-mediated cardiomyopathy, heart failure and ventricular arrhythmia. Within a critical region on chromosome 11p15.5, mutation S140G was found in a Potassium Channel, Voltage-Gated (KCNQ1) gene in all affected members of a four generation Chinese family with autosomal dominant hereditary atrial fibrillation (**Chen et al., 2003**). Screening of the coding region of the LMNA gene in DNA samples from 66 cases of dilated cardiomyopathy with or without associated features identified a mutation E161K in one family with early onset of Atrial Fibrillation (**Sebillon et al., 2003**).

1.8.6 Limb-Girdle Muscular Dystrophy 1B (LGMD1B)

The clinical picture of three families with autosomal dominant Limb-Girdle Muscular Dystrophy (LGMD) associated with cardiac involvement showed affected individuals with symmetric weakness in the proximal lower-limb muscles before the age of 20 years (**van der Kooi et al., 1996; van der Kooi et al., 1997**). In the third and fourth decades, upper-limb muscles gradually became affected as well. Early contractures of the spine were absent, and contractures of elbows and Achilles tendons were either minimal or late, distinguishing this disorder from EDMD. Electromyography (EMG) and muscle biopsy were consistent with mild muscular dystrophy. Cardiological abnormalities were found in 62.5% of the patients, including atroventricular

conduction disturbances and dysrhythmias, presenting as bradycardia; syncopal attacks needed pacemaker implantation, and sudden cardiac death occurred at age of approximately 50 years. Linkage studies found association with chromosome 1q11-q21, and suggested connexin 40 as a potential candidate gene (**van der Kooi et al., 1997**). Although the clinical description of the LGMD1B patients differed from those with AD-EDMD by the absence of significant contractures, predominance of proximal limb weakness, and occasional presence of calf hypertrophy, the two phenotypes could result from different alleles of the same locus.

In three LGMD1B families linked to markers on chromosome 1q11-q21, mutations in the LMNA gene were identified: a missense mutation, a deletion of a codon, and a splice-donor site variant (**Muchir et al., 2000**). The three mutations were identified in all affected members of the corresponding families and were absent in 100 unrelated control subjects, demonstrating that LGMD1B and AD-EDMD are allelic disorders. Although the report by Bonne 1999 was the first linking a specific disease to a mutation in the lamin family, they found that the gene encoding lamin B1 mapped to the same region, 5q23.3-q31.3, in another dominantly inherited myopathy, LGMD1A.

1.8.7 Autosomal Recessive Charcot-Marie-Tooth type 2 (AR-CMT2) (CMT2B1)

Charcot-Marie-Tooth disease constitutes a clinically and genetically heterogeneous group of hereditary motor and sensory neuropathies. On the basis of electrophysiological criteria, CMT is divided into two major types: type 1, the demyelinating form, characterized by a motor median nerve conduction velocity less than 38m/s; and type 2, the axonal form, with a

normal or slightly reduced nerve conduction velocity. CMT2B2 is clinically similar to CMT2B1 but maps to 19q.

In a large consanguineous Moroccan family with autosomal recessive CMT2, nine affected sibs presented the onset of the clinical features in the second decade of life. All affected individuals had weakness and wasting of the distal lower limb muscles and lower limb areflexia; pes cavus was present in seven patients, and there was a proximal muscle involvement in six. Motor nerve conduction velocities were normal or slightly reduced in all patients, reflecting an axonal process (**Bouhouche et al., 1999; Leal et al., 2001**). A genome-wide search showed linkage of the disorder to marker on chromosome 1q, specifically 1q21.2-q21.3. Myelin protein zero gene (MPZ) was excluded as a candidate for mutations by physical mapping and direct sequencing (**Bouhouche et al., 1999**).

In a separate study, three consanguineous Algerian families with autosomal recessive CMT2 were linked to chromosome 1q21. A homozygous mutation was found in the LMNA gene (R298C). An animal model has revealed that LMNA null mice presented with axonal clinical and pathological phenotype highly similar to patients with autosomal recessive CMT2 (**De Sandre-Giovannoli et al., 2002**).

1.8.8 Mandibuloacral Dysplasia (MAD)

Two teenaged males with hypoplastic mandible producing severe dental crowding, acroosteolysis, stiff joins, and atrophy of the skin over hands and feet were described. The clavicles were hypoplastic and persistently wide cranial sutures and multiwormian bones were noted. Alopecia and short stature were other features of this progeria-like syndrome (**Young et al., 1971**). The differential diagnosis also included pycnodysostosis, Hajdu-

Cheney syndrome, cleidocranial dysplasia, and acrogeria. Patients with MAD have been mistakenly diagnosed as having Werner syndrome (**Cohen et al., 1973**).

Partial lipodystrophy, extreme insulin resistance and marked hypermetabolism have been observed in MAD patients. Studies of body fat distribution in two male and two female patients with MAD by anthropometry, dual energy X-ray absorptiometry, and magnetic resonance imaging found that three of the four subjects had loss of subcutaneous fat from the extremities with normal or slight excess in the neck and truncal regions (Pattern A). In contrast, one patient had generalized loss of subcutaneous fat involving the face, trunk, and extremities (Pattern B). All of the patients had normal glucose tolerance but fasting and postprandial hyperinsulinemia were suggestive of insulin resistance. Therefore, there are two types of body fat distribution patterns, both of which are associated with insulin resistance and its metabolic complications (**Cutler et al., 1991; Freidenberg et al., 1992; Simha and Garg, 2002**).

By analysis of five consanguineous Italian families, a linkage of MAD to 1q21 was found. DNA sequencing of the LMNA gene identified a homozygous mutation (R527H) in the families (**Novelli et al., 2002**). Mutational analysis of the LMNA gene in patients with MAD from six pedigrees found that patients from two pedigrees with type A lipodystrophy had the homozygous R527H mutation, whereas the other four affected subjects, who had type B lipodystrophy, did not have any mutation in the exons or splice junctions of the LMNA gene. RNA extracted from lymphoblasts of two of the patients also revealed normal sequence. In these four subjects, sequencing of other genes implicated in lipodystrophies, i.e.

alpha acylglycerol 3 phosphate o acyltransferase 2 (AGPAT2), seipin and PPARG revealed no substantial alterations (**Simha et al., 2003**). These authors noted that patients reported by (**Novelli et al., 2002**) had type A lipodystrophy, and concluded that MAD is a genetically heterogeneous disorder, with defects at locus other than LMNA being responsible for the MAD with type B lipodystrophy phenotype. According to the latter, a study described a 13 years old girl with mandibuloacral dysplasia who had absent breast development, although pubic and axillary hair was normal. Hormone studies revealed no abnormalities (**Cogulu, 2003**).

1.8.9 Others

1.8.9.1 Hutchinson-Gilford Progeria Syndrome

Hutchinson-Gilford Progeria Syndrome (HGPS) is an exceedingly rare disorder characterized by precocious senility of a striking degree. Death from coronary artery disease is frequent and may occur before 10 years of age. The name Progeria was given to this disorder in an article where the term ateleiosis was assigned to a pituitary growth hormone deficiency (**Gilford, 1904**). Earlier reports about this disorder had been written (**Hutchinson, 1886**) and recorded cases of two possible affected brothers whose parents were first cousins were described as: "A boy, aged 8 years. Condition has been present since birth. There are four children in the family: the girls are unaffected; both boys are affected. The senile condition of the skin and facies should be noted. The vessels show arteriosclerosis. There is almost complete absence of subcutaneous fat" (**Paterson, 1922**).

A Japanese patient with Progeria survived the age of 45 years and died of myocardial infarction. Clinically he seemed typical except for the unusual long survival (**Ogihara et al., 1986**). According to reviews of the literature,

the age at death ranges between 7 and 27.5 years, with a median age of 13.4 years. Identical twins with Progeria, who developed heart failure at the age of 8, died within one month of each other. Cytogenetical analysis showed an inverted insertion in the long arm of chromosome 1 in 70% of the cells, suggesting that a gene for Progeria might be located on chromosome 1 (**Brown, 1990**). In a 9 years old patient with a classic picture of Hutchinson-Gilford Progeria, an interstitial deletion on region 1q23 was found. It was then suggested that the genetic defect might reside in the β-1,4-Galactosyltransferase polypeptide 3 (B4GALT3) gene, which maps to 1q23, as perturbation of glycosylation in connective tissue had been demonstrated in patients with this condition (**Delgado Luengo et al., 2002**). A later study suggested that the defect causing Progeria might reside in the proline/arginine-rich end leucine-rich repeat protein gene (PRELP), which maps to region 1q32 and is a small leucine-rich proteoglycan that binds type I collagen to basement membrane and type II collagen to cartilage (**Lewis, 2003**).

A recent study reported de novo point mutations in Lamin A causing Hutchinson-Gilford Progeria Syndrome. The HGPS gene was initially localized on chromosome 1q by observing two cases of uniparental isodisomy of 1q, and one case with a 6 Mb paternal interstitial deletion. Eighteen out of twenty classic cases of HGPS harboured the identical de novo single-base substitution, a C-T transition (C-T 2036) resulting in a silent G-G change at codon 608 within exon 11 (G608G). One additional case was identified with a different substitution within the same codon. Both of these mutations were shown to result in activation of a cryptic splice site within exon 11 of the LMNA gene, resulting in the production of a protein product that deletes 50 amino acids near the C-terminus. This pre-Lamin A

still retains the CaaX box but lacks the site for endoproteolytic cleavage. Immunofluorescence of HGPS fibroblasts with antibodies directed against Lamin A revealed that many cells showed visible abnormalities of the nuclear membrane (**Eriksson et al., 2003**).

Other studies with cells lines from HPGS probands showed that five carried the common mutation within exon 11 of the LMNA gene (C-T 2036) (**Cao and Hegele, 2003**); one of the seven patients carried the mutations G608S, and confirmed the findings made by (**Eriksson et al., 2003**) using the same cell lines. One of the patients with an apparently typical HGPS, who was 28 years old at the time of DNA analysis, presented compound heterozygosity for two missense mutations, R471C in exon 8 and R527C in exon 9. Unfortunately, parental DNA samples were not available for analysis. In a separate study, the exon cryptic splice-site activation mutation (1824C-T = 1819-1968del) in two HGPS patients was found. Immunocytochemical analysis of lymphoblasts from one patient using specific antibodies against Lamin A/C, Lamin A and Lamin B1 showed that most cells had strikingly altered nuclear sizes and shapes, with nuclear envelope interruptions accompanied by chromatin extrusion. Lamin A was detected in 10-20% of HPGS cells. Only Lamin C was present in most cells, and Lamin B1 was found in the nucleoplasm, suggesting that it had dissociated from the nuclear envelope. Western blot analysis showed 25% of normal Lamin A levels and no truncated form was detected (**De Sandre-Giovannoli et al., 2003**).

1.8.9.2 Werner Syndrome

The clinical features of Werner Syndrome are scleroderma-like skin changes, especially in the extremities, cataract, subcutaneous calcification,

premature arteriosclerosis, diabetes mellitus, and wizened-prematurely aged faces. A particular instructive pedigree was reported were the habitus was characteristic: short stature, slender limbs, and stocky trunk (**McKusick, 1963**). Werner Syndrome has been found to be caused by mutations in the DNA Helicase-like (RECQL2) gene, which encodes a homolog of the *E. coli* RecQ helicase. Patients whose phenotype was classified as "atypical Werner Syndrome", with a more severe phenotype than that observed with mutations in the RECQL2 gene, were found to have mutations in the LMNA gene.

An extended study of 129 indexed patients referred to the international registry for molecular diagnosis of Werner Syndrome, 26 (20%) had wild type WRN protein coding regions and were categorized as having atypical Werner Syndrome on the basis of molecular criteria. In these individuals, DNA sequencing of all exons of the LMNA gene revealed that four patients (15%) were heterozygous for novel missense mutations in this gene, specifically A57P, R133L and L140R. These mutations altered relatively conserved residues within Lamin A/C. Fibroblasts from the patient with mutation L140R had a substantially enhanced proportion of nuclei with altered morphology and mislocalized lamins. Individuals with atypical Werner Syndrome with mutations in the LMNA gene had a more severe phenotype than did those with the disorder due to mutant RECQL2.

Typical Werner Syndrome is autosomal recessive; atypical Werner Syndrome due to mutations in the LMNA gene is a heterozygous disorder (Autosomal Dominant). A report by Hegele et al 2003 states that the clinical designation of Werner Syndrome for each of the four patients described by Chen et al 2003, appeared somewhat insecure. The author noted that the

comparatively young ages of onset in the patients with mutant LMNA would be just as consistent with late onset HGPS as with early onset Werner Syndrome. Patients with so-called atypical Werner Syndrome and mutant LMNA also expressed component typical of non-progeroid laminopathies. It was then suggested that DNA analysis could help draw a diagnostic line that clarifies potential overlap between older patients with Hutchinson-Gilford Progeria Syndrome and younger patients with Werner Syndrome, and that therapies may depend on a precise molecular classification.

1.9 The yeast two-hybrid system (YTHS)

The yeast two hybrid system (YTHS) has probed to be one of the most popular methods in biochemistry to test for protein-protein interaction, which combined with other biochemical approaches, produces a powerful tool for biochemists and cell biologists.

In yeast, the genes required for galactose metabolism are controlled by two regulatory proteins, GAL4 and GAL80, as well as by the carbon source in the medium. When galactose is present, the GAL4 protein binds to GAL4-responsive elements within the UAS upstream of several genes involved in galactose metabolism and activates transcription. In the absence of galactose, GAL80 binds to GAL4 and blocks transcriptional activation. Furthermore, in the presence of glucose, transcription of the galactose genes is immediately repressed. The tight regulation of the GAL UASs by GAL4 makes it a valuable tool for manipulating expression of reporter genes in two-hybrid systems that are dependent on the GAL4 DNA-Binding Domain (BD). However, in such systems, the yeast host strains must carry deletions of the GAL4 and GAL80 genes to avoid interference by endogenous gal4 and gal80 proteins. If this is the case, no significant

glucose repression is observed in these strains and no induction is produced unless a two-hybrid interaction is occurring. Therefore, nutritional regulation of GAL4 UASs is not a feature of the GAL4 based two-hybrid systems.

The native yeast HIS3 promoter contains a UAS site recognized by the transcriptional activator GCN4, and two TATA boxes. GCN4 regulates one of the TATA boxes (TR), while the other TATA box (TC) drives low-level constitutive expression of HIS3. TC is not regulated by the native GCN4-binding UAS, the GAL1 UAS, or the artificial UASG constructs. HIS3 reporter gene in the yeast strain Y190 is unusually strong among the GAL4 two-hybrid reporter genes in that it is under the control of the GAL1 UAS and a minimal promoter containing both HIS3 TATA boxes. The result is high level of expression (due to GAL1 UAS) when induced by a positive two-hybrid interaction; this strain also exhibits a significant level of constitutive leaky expression (due to HIS3 TC). In contrast, in other yeast strains (HF7c, PJ69-2A or AH109) the entire HIS3 promoter (including both TATA boxes) is replaced by the entire GAL1 promoter, leading to a tight regulation of the HIS3 reporter in these strains.

Recently, systematic two-hybrid system approaches have been used in bacteria, yeast and nematodes to construct impressive large-scale protein-protein interaction maps involving complex processes from DNA-damaging responses to vulval development. Yeast two-hybrid assays have proven to be very useful when coupled to other protein-protein interaction tests, allowing the assignment of putative function categories to novel proteins. But on its own, as any experimental approach, it has disadvantages. First, the volume of experimental work required and contradictory results. For example, in yeast, a genome-wide protein-protein interaction map gave

around 4500 putative interactions. Even the well-characterized proteins interacted with 5-7 other proteins. So, considering the amount of potential coding sequences derived from the yeast genome, the number of interactions is estimated in 30 – 40 000, compared to the actual 4500 interactions found. Secondly, approximately 50 % of the interactions are false, due to spurious interactions between proteins that do not interact in vivo. Third, a conventional two-hybrid interaction occurs in the nucleus, and uses a transcriptional system, limiting the study of interaction of cell membrane proteins and transcription factors.

1.10 Aim of this thesis.

The emergence of new clinical diagnosis of old-rare human diseases involving nuclear membrane filaments has revolutionized the Laminology field and has provided a powerful tool to address the unresolved issue of the role of lamins A and C in nuclear metabolism. More importantly, the existence of similar disorders (AD and XL-linked EDMD) involving nuclear lamins (A-type) and their associated proteins (emerin) has given key clues of the importance of the interaction between lamins and their interacting partners.

Chapter 3 of this thesis addressed the question whether lamins interact with emerin, a type II integral membrane protein of the nuclear membrane. Using a YTHS approach, not only demonstrated that all lamins interact with emerin, but a further step proved that the interaction occurs preferentially with the globular tail domain. Transfection experiments supported the protein-protein interactions *in vitro*, confirming that emerin and lamin B remain attached to the nuclear when A-type lamins are expressed ectopically and form nucleoplasmic aggregates.

In Chapter 4, these studies show that mutations in the AD-EDMD are not involved in any molecular cross-linking, even in the case when a new cysteine appears in the A-type filaments. In vivo analysis confirmed that a nuclear check-point in G0→G1 exist, where the re-arrangement of nuclear proteins occurs with a higher frequency in cells lines with mutations in the LMNA gene. This event occurs independently of the location of the mutations. In addition, this study provided an in vitro model to assess the behaviour of mutant lamins in laminopathies, as typical honeycomb structures were induced by serum starvation. In parallel, it has been

demonstrated the role of Nesprins in the cell cycle and in senescence, and their possible involvement in muscular dystrophies.

Finally, chapter 5 compiles sufficient evidence to justify further studies to first, describe a possible common haplotype that explains the different laminopathies based on SNPs patterns; second, the possible differential allelic expression of lamins in AD-EDMD; third, to study regulatory mechanisms of lamins at different levels (transcription and translation); and last but not least, the possible role of subtle stoichiometric changes in the composition of the nuclear lamina.

Figures Chapter 1.

Figure 1.1.

Diagram showing the structure of the nucleus with all the sub-compartments described up to date, with special emphasis on the nuclear lamina.

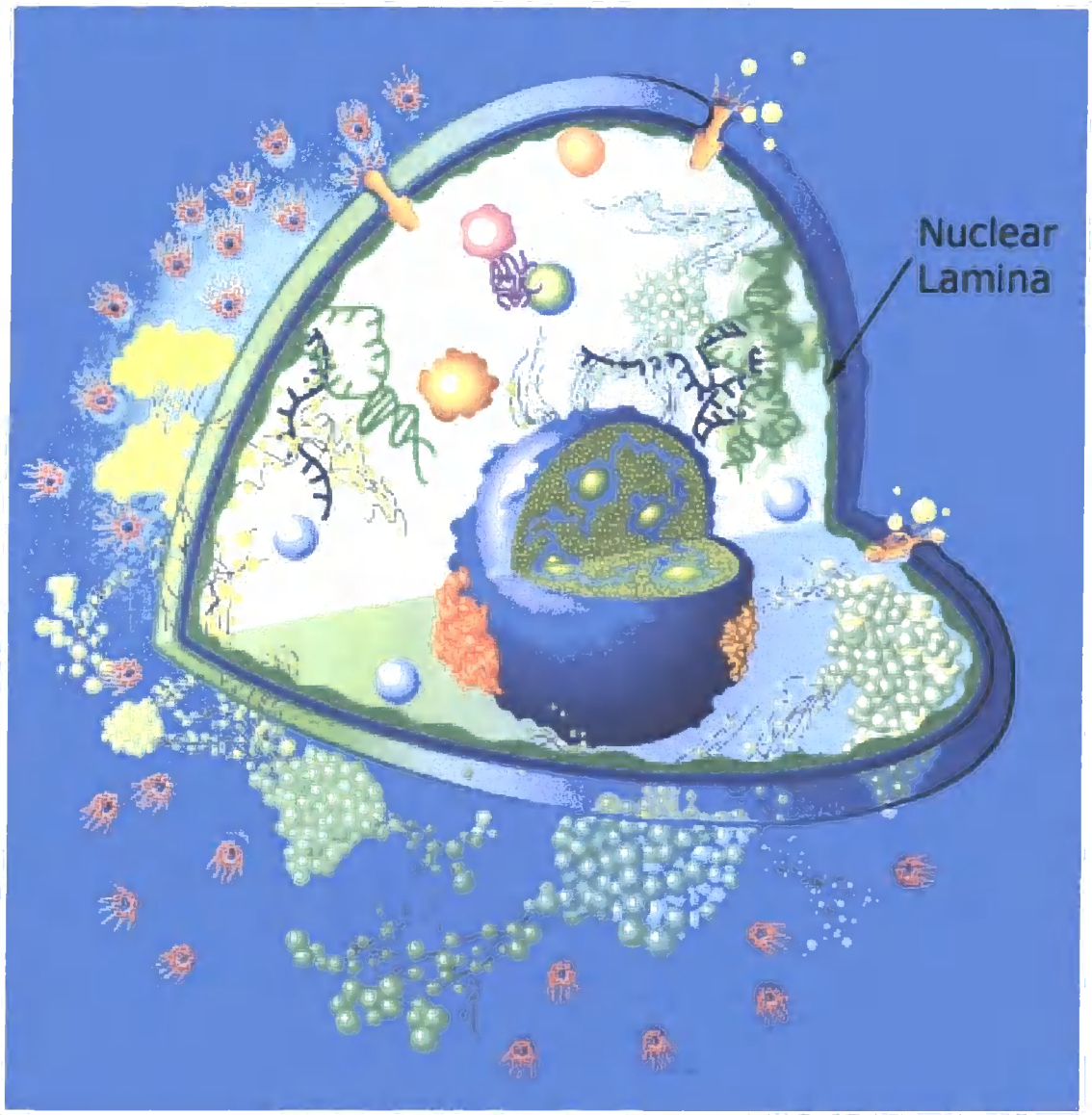
Nuclear
Lamina

Figure 1.2

Electron micrograph showing the ultrastructure of the nucleus. Arrows show: NE (nuclear envelope), Mit (mitocondria), ER (endoplasmic reticulum), Nu, (nucleoli).

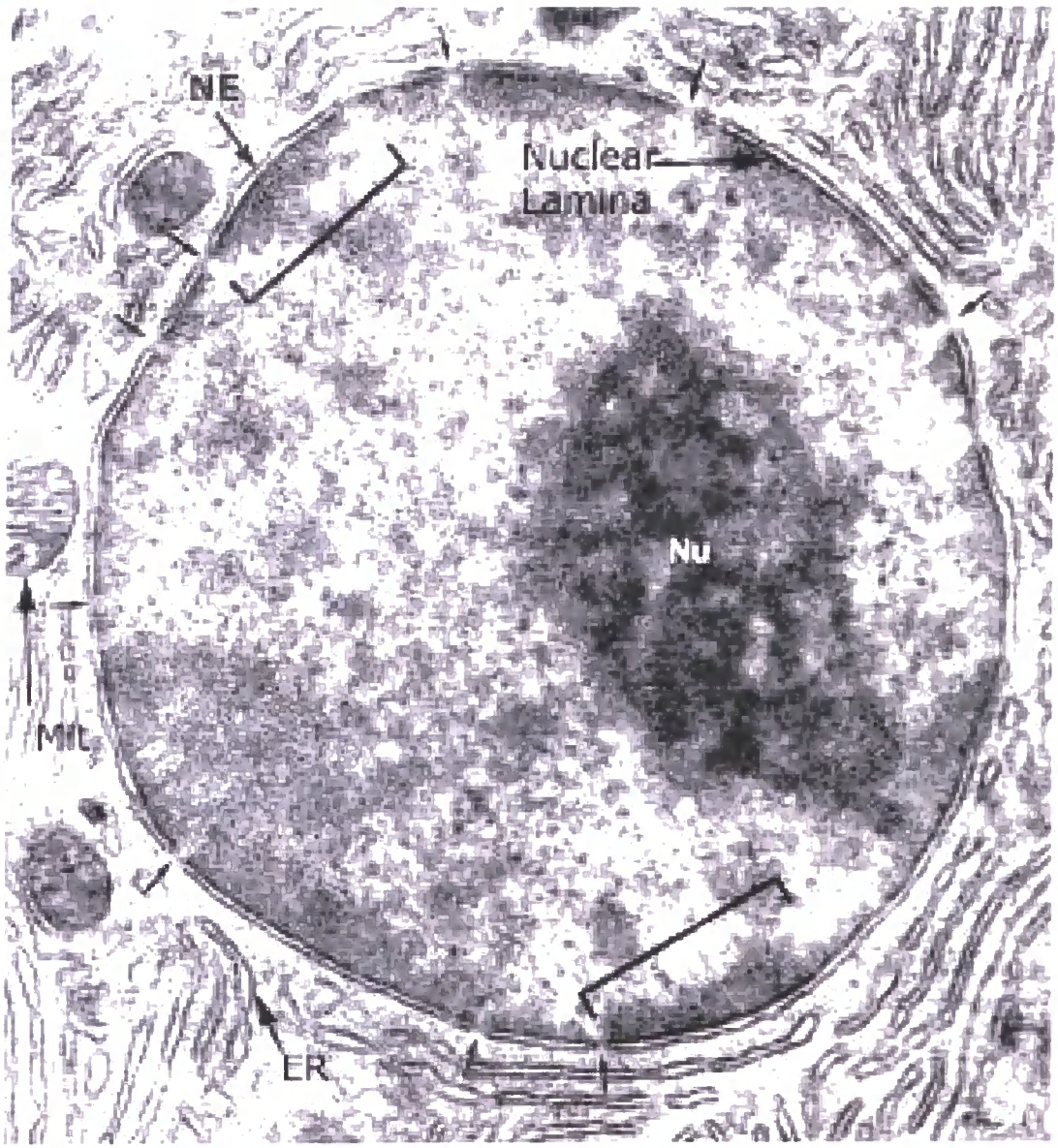
NE
Nuclear
Lamina
Nu
Mit
ER

2. Chapter Two- Materials and Methods

2.1. Cloning

2.1.1. Media

For drug selection of transformed *E. coli*, LB-agar plates (10 g/L Triptone, 5 g/L Yeast Extract, 10 g/L NaCl, pH 7.2) were supplemented with 100 μg/ml Ampicillin or 50 μg/ml Kanamicin where it corresponded (**J. Sambrook, 1989**).

2.1.2. Bacterial strains

E. coli strain DH5-α [F-, recA1, endA1, hsdR17, supE44, thi1, gyrA, recA1] and JM109 [e14-(McrA-) recA1 endA1 gyrA96 thi-1 hsdR17 (rK- mK+) supE44 relA1 D(lac-proAB)[F'traD36proABlacI^{q}ZDM15]] was used as the bacterial transformation recipient for all plasmid constructs.

2.1.3. Sub-cloning the emerin gene into pAS1-CYH2

For cloning Emerin into plasmid pAS1-CYH2 (GAL4 Binding Domain), a full length cDNA of human Emerin in pEGFP-C1 was provided by Dr. Will Whitfield. This plasmid was digested with 30 units of HindIII (A▼AGCTT) (in Buffer E, Promega) per 1 μg of plasmid DNA for 2 hours at 37°C, and purified with the Promega's DNA Clean-up System. The HindIII ends were treated with 1 unit of DNA Polymerase Large Fragment (Klenow) per 1 μg of plasmid DNA in Klenow buffer (50mM Tris-HCl (pH 7.2 at 25°C), 10mM $MgSO_4$, 0.1 mM DTT) at 25°C for 10 minutes and purified with Clean-Up System, following digestion with 30 units of BamHI (G▼GATCC) (in buffer E, Promega) per 1 μg of plasmid DNA for 2 hours at 37°C. The fragment generated was treated with 1 unit of DNA Polymerase Large Fragment (Klenow) per 1 μg of plasmid DNA in Klenow buffer at 25°C for 10 minutes, and purified by the Clean-Up System. The DNA products were separated by electrophoresis on 1% Low Melting Point Agarose Gel in TAE buffer. The band of around 700 bp was excised from the gel and purified by using the Wizard® SV Gel and PCR Clean-Up System.

The pAS1-CYH2 vector was digested with 40 units of SmaI (CCC▼GGG) (in Buffer J, Promega) per μg of plasmid DNA for 2 hours at 25°C, purified by the DNA clean-up system (Promega) and then digested with 30 units of BamHI (G▼GATCC) (in buffer E, Promega) per 1 μg of plasmid DNA for 2 hours at 37°C (Figure 1a). Once the linear vector (SmaI - BamHI) was purified with the Clean-Up System, the emerin fragment was ligated using 1 unit of T4 DNA Ligase (in T4 DNA Ligase buffer [30mM Tris-HCL (pH 7.8 at 25°C), 10mM $MgCl_2$, 10mM DTT and 1mM ATP] per ligation reaction and incubated at 22°C for 16 hours (optimal temperature for blunt end cloning) (**J. Sambrook, 1989**). Two vector-insert ratios where used, 1:3 and 1:6, to increase the probability of cloning the insert at the blunt end.

Transformation reactions where set up using 2.5 μl of the ligation reactions and 80 μl of JM109 competent cells prepared by Rubidium Chloride method (**Ano and Shoda, 1992**). The mixtures were incubated on ice for 30 minutes; heat shocked at 42°C for 1 minute and cooled down on ice for 2 minutes. Growing media (800 μl LB medium without antibiotics) was added and bacteria were allowed to recover by gentle shaking at 37°C for 1 hour. The whole culture was centrifuged at 5000 x g for 5 minutes and resuspended in 200 μl of LB medium. Two 90 mm LB/Agar plates (containing 25 μl of X-Gal (50mg/ml) and 50 μ of IPTG 0.1M, freshly plated, but dry) were plated with 100 μl of the bacteria suspension, air dried and incubated at 37°C until colonies appeared (14-18 hours).

Ten colonies where picked up for each transformation reaction, and were inoculated in LB medium containing 100 μg/ml ampicillin. Bacteria were incubated at 37°C and shacked at 250 rpm for 16 hours. Glycerol stocks were prepared using 0.2 ml of the culture, and the rest of the cultures were used to purify plasmid DNA using Promega's Wizard® Plus Minipreps DNA Purification System.

2.1.4. Confirmation of the insert cloned.

Plasmid DNAs were analyzed by restriction enzymes to confirm that the insert with the expected size was cloned. Plasmid DNA recovered from pAS1 + emerin ligation reactions was digested with 20 units NcoI (C▼CATG G) and BamHI (in Multicore Reaction Buffer, Promega) per 0.5 μg of plasmid DNA at 37°C for 2 hours and the products were analyzed by electrophoresis on 1% agarose gel in TAE buffer. A band around 700 bp was considered as a positive clone. The construct was called pAS1-Emerin.

2.1.5. Other DNA constructs

All lamin constructs for yeast experiments were kindly provided by Dr. Howard J. Worman University of Columbia, USA) (**Ye and Worman, 1995**) (Table 3.2). EGFP-Lamin A full length was a gift from Dr. Masako Ozumi (Institute of Physical and Chemical Research, Saitama, Japan). EGFP-Emerin was a gift from Dr. Will Whitfield. DS-Red2-Lamin C was produced in our laboratory by Maria Choleza.

2.1.6. Sequence analysis

The pAS1-Emerin DNA plasmid was purified using the Promega's Wizard® Plus Minipreps DNA Purification System. Prior to DNA sequencing, 100 μl of plasmid DNA was precipitated with 50 μl of 7.5M Ammonium Acetate and 375 μl of Absolute Ethanol, mixed by vortex and centrifuged at 14000 x g for 15 minutes at room temperature. The pellet was washed with 70% cold Ethanol and centrifuged again. Supernatant was removed carefully, pellet air dried, and resuspended in 50 μl of ddH_2O. Samples were quantified by reading OD_{260} and 2 μl checked by electrophoresis on 1% agarose gel compared to a DNA standard.

Samples were sequenced twice by the cycle sequencing method using dye-terminator chemistry (**Rosenblum et al., 1997**) (Applied Biosystems) at the DNA Sequencing Service, Department of Biochemistry, University of Dundee, using an ABI 377 Automatic DNA Sequencer (Applied Biosystems).

2.2. Allelic specific RT-PCR

2.2.1. RNA isolation

Cells were grown on 90mm dishes until 80 % confluence, and total RNA was isolated using 1 ml of TRI reagent (Sigma) per dish and incubated for 5 minutes at room temperature. Dishes were scraped, the lysates transferred to a 1.5 ml centrifuge tube and 200 µl of Chloroform was added. Samples were mixed by vortex for 15 seconds, incubated 3 minutes at room temperature and centrifuged at 12000 x g for 15 minutes at 4°C. The supernatants were collected (total RNA), transferred to a fresh centrifuge tube and 500 µl of Isopropanol was added. Samples were then vortexed for 15 seconds, incubated for 10 minutes at room temperature and then centrifuged for 10 minutes at 4°C. Supernatant was removed and the RNA pellets were washed with 1 ml of 75% Ethanol (diluted with DEPC-treated water). The tubes were briefly vortexed and centrifuged for 5 minutes at 12000 x g at 4°C. Pellets were air dried for 10 minutes, resuspended in 20 µl of DEPC-treated ddH_2O and heated at 50°C for 5 minutes. An aliquot was taken to read absorbance at 260nm to assess RNA concentration.

2.2.2. DNase treatment of RNA samples

Twenty µg of total RNA were treated with 0.075 units of RQ1 RNase-Free DNase (**Moore, 1981**) (Promega) per µg of RNA for 30 minutes at room temperature in 1X reaction buffer (40mM Tris-HCl [pH 8.0 at 25°C], 10mM $MgSO_4$, 1mM $CaCl_2$). The reaction was stopped by adding 1 µl of 20mM EGTA, pH 8.0, and incubating the samples at 65°C for 10 minutes. The RNA was precipitated with 1/10 of the reaction volume of 3M NaOAC, pH 5.2 and 2 volumes of 100% Ethanol and incubated overnight at -20°C. To recover the RNA, tubes were centrifuged at 12000 x g at 4°C for 15 minutes, the supernatant removed, pellets washed with 300 µl of 70% Ethanol (in DEPC treated ddH_2O) and vacuum dried for 5 minutes at

room temperature. Finally, total RNA was diluted in 20 μl of DEPC-treated ddH_2O and RNA concentration assessed by reading the absorbance at 260 nm.

2.2.3. Primer design

Allele-specific RT-PCR depends on the synthesis of a PCR oligonucleotide primer that precisely matches with one of the alleles but mismatches with the other (**Newton et al., 1989; Wu et al., 1989**). When the mismatch occurs near the 3' end of the PCR primer, amplification is inefficient (**Sommer et al., 1989**). Based on this evidence, specific primers were designed for the wild type and mutant alleles of the LMNA gene differing in only one base.

Primers were designed using NetPrimer PCR online software which combines the latest primer design algorithms with a web-based interface allowing analysis of primers over the Internet. All primers were analyzed for melting temperature using the nearest neighbour thermodynamic theory to ensure accurate Tm prediction. Primers were analyzed for secondary structures including hairpins, self-dimers, and cross-dimers in primer pairs. This ensured the optimum primer for the RT-PCR reactions, minimizing the formation of unspecific products. To facilitate the selection of an optimal oligonucleotide, each primer was given a rating based on the stability of its secondary structures. Only the best primers are tabulated here (See Table 5.1)

2.2.4. RT-PCR reactions

All reactions were downscaled from the original volumes (50 μl) considered by the Access- Quick RT-PCR System (**Promega**) to a final volume of 25 μl.

The reactions contained:

	Final Concentration in RT-PCR (25 ul)
Access Quick RT-PCR Master Mix	1X
Total RNA	0.004 µg/µl
Forward Primer	0.1875 pmol/µl
Reverse Primer	0.1875 pmol/µl
Avian Myeloblastosis Virus Reverse Transcriptase (AMV-RT)	0.125 u/µl

For all the reactions, Access Quick RT-PCR Master Mix (Tfl DNA polymerase, dNTPs, and magnesium chloride and reaction buffer), reverse primers, Total RNA, and DEPC-treated ddH_2O were mixed in a general Master Mix. Equal volumes were distributed in thin wall PCR tubes containing forward primers specific for each allele and heated up at 70°C for 5 minutes to denature the mRNA secondary structures. Samples were cooled down on ice, the AMV-RT was added, and after mixing gently, the tubes were spun down to collect the contents of the tubes before setting up the thermocycler. Different annealing temperature gradients were designed to establish the optimal conditions for the set of primers used. All steps were carried out in a Safety Cabinet pre-treated with UV light.

2.2.5. Fragment analysis

All amplified fragments were separated on 2% agarose gels in 1X TAE buffer at 70 Volts. 100 bp DNA ladder (Promega) was used to assess the size of the RT-PCR products. DNA products were stained with Ethidium Bromide and visualized on an UV transiluminator.

A pilot trial was set up in the Automatic DNA Sequencer CEQ-8000 (Beckman-

Coulter) to analyze the RT-PCR fragments using the light emitted by the fluorescence probes attached to the 5' end of the primers. CEQ-8000 was in the setting up process, so we did not manage to use the size standards in the trial run. My aim was basically to assess whether the ARMS-PCR primers were able to work in a one step multiplex RT-PCR reaction. Two μl of cleaned up products were mixed with 40 μl of di-methylformamide, vortexed for 1 minute and centrifuged. This mixture was injected into the capillary system and analyzed.

2.3. Bioinformatics

I analyzed all the regulatory elements contained in the genomic sequence of LMNA gene and its flanking regions, and compiled all the SNPs reported until the 20th November 2003 in the NCBI Database. The position of each regulatory element and SNP was related to its actual base pair on Chromosome 1, which contains 7864945 base pairs in total.

First, to allocate the regulatory elements, a LMNA gene sequence including 32kb upstream from the ATG and 14.5 Kb downstream from the TAA (57.5 Kb in total) was obtained using the OMIM Database at the National Centre for Biotechnology Information website (NCBI, USA, www.ncbi.nlm.nih.gov). The DNA sequence was sent on-line to the Human Genome Mapping Project (HGMP) computational facilities in Cambridge, UK, for NIX analysis, which searched for different regulatory elements like CpG islands, promoters and transcriptional sites using different algorithms (Table 5.5). After 2 days, a notice was given by email that the results were ready. A summary of the predicted regulatory elements was given in a chart that can only be analyzed by logging in the HGMP's website. By clicking on each feature on the computer's screen (Figure 5.9), details of the specific regulatory elements are tabulated, including the position related to the sequence provided, statistical scoring and quality of prediction (Table 5.4). But the number given to the region where the regulatory elements are in the NIX analysis is

related to the LMNA gene sequence provided, so it does not correspond to the actual position on chromosome 1. This inconvenience makes it almost impossible to find the regulatory elements in the Chromosome 1 sequence (7864945 bp) and overlap them with the SNPs by hand or any known software. A way to avoid this problem is to send the whole chromosome 1 sequence for NIX analysis, but this proved to be impossible to do on-line because of the size of the electronic file.

Chromosome 1 full sequence (NT079487) was searched in the OMIM database and used to assign the actual position for each base of the genomic sequence of the LMNA gene analyzed, including its regulatory elements. The whole chromosome 1 sequence was saved in Fasta format, and imported into BioEdit Sequence Alignment Editor, version 5.0.9 (**Hall, 1999**), which automatically assigned a number to each base from 1 to 7864945. But BioEdit does not give page numbers for the array, so it is very difficult to keep track of the position of several SNPs in the 7864945 bases of chromosome 1. The array was then saved in text format in Microsoft Word® and paginated, giving a map where each bp of chromosome 1 can be assigned to a page number. This approach demanded the maximum power of the computer used (DELL Pentium 4, 2.00 GHz, 512 MB RAM) and the maximum processing capacity of Microsoft Word® since the file generated contained 11001 pages of bases arranged in groups of 10 with the corresponding numbering. This gave the right coordinates to find any base pair on the chromosome 1 sequence in future analysis.

Having now both sequences in BioEdit format (the genomic sequence for LMNA gene plus its flanking regions, and Chromosome 1), the first step was to locate the actual positioning of the genomic sequence of the LMNA gene on chromosome 1. To do this, both files were opened simultaneously. The first 100 bp of the LMNA genomic sequence were copied and pasted in the BioEdit's searching engine to

look for this region on chromosome 1, finding the actual starting position (2502182). Then the same methodology was followed to find the end of LMNA genomic sequence (2559742). Both regions were easily found in the chromosome 1 file (text format) in Microsoft Word® on pages 3513 and 3594 respectively. Following the same methodology (cut, paste and BioEdit search engine), each regulatory element predicted in the NIX analysis can be mapped accurately.

Once the actual boundaries of the genomic sequence of the LMNA gene on chromosome 1 were defined and the regulatory elements allocated on it, then the compilation of SNPs from the NCBI website can be mapped onto the LMNA genomic sequence and its flanking regions to find whether they overlap or not with the areas of interest. To do this, two complementary approaches were used. First, the chromosome 1 file in Microsoft Word® was opened and the genomic sequence for LMNA gene was printed in hard copy (pages 3513 to 3594). All regulatory elements and SNPs were precisely located in the text. The second approach was to draw a diagram to scale in Microsoft PowerPoint®, where genomic regions containing all the features located in the text could be graphically represented (Figures 5.10 and 5.11).

2.4. Yeast Two-Hybrid Experiments

2.4.1. Media

For yeast culture, YPD (20 g/L Difco Peptone, 10g/L Yeast Extract, 20 g/L Glucose, 20 g/L Agar [for plates], pH 5.8) and SC (6.7 g/L Yeast Nitrogen Base Without Amino acids, 20 g/L glucose, 20 g/L Agar [for plates]) were used with 0.003% Adenine Hemisulfate supplement. Dropout supplements where added as required: 0.69 g/L -Leu, 0.74 g/L -Trp, 0.64 g/L -Leu/Trp, 0.62 g/L -Leu/-Trp/-His, 0.60 g/L -Leu/-Trp/-His/-Leu (**Parchaliuk, 1999b; Parchaliuk, 1999a**).

2.4.2. Yeast Strains

Yeast strain Y190 [MATa, ade2-101, ga!80, his3-200, leu2-3, 112 trp1-901, ura3-52, URA3::GAL1-lacZ, lys2::GAL1-HIS3] was obtained from Dr. Emma Warbrick (Department of Biochemistry, University of Dundee, UK), and was used as the recipient for all yeast transformations.

2.4.3. Yeast Transformation using the Lithium Acetate Method

S. cerevisiae strain Y190 was inoculated into 5 ml of YPD + Adenine medium and incubated overnight at 30°C on a shaker at 250 rpm. The titre of the overnight culture was determined by measuring the OD_{600} of a 1:10 dilution in YPD medium. 2.5 x 10^8 cells were added to pre-warmed (30°C) YPAD medium, to give a total volume of 50 ml in a 250 ml flask, giving a starting cell titre of about 5 x 10^6 cells / ml (For most yeast strains an OD_{600} of 0.1 corresponds to approximately 1 x 10^6 cells/ml). The culture was incubated at 30°C on a shaker at 250 rpm until the cells went through two divisions (2 x 10^7 cells/ml, approximately 3 - 4 hours).

Cells were harvested in a sterile 50 ml disposable centrifuge tube by centrifugation at 3000 x g for 5 min, the supernatant removed, and cells washed in 25 ml of sterile ddH_2O, centrifuged, and the supernatant removed. The cell pellet was resuspended in approximately 900 µl of sterile dH_2O and transferred to a 1.5 ml microcentrifuge tube. Cells were centrifuged at 14000 x g for 1 minute, resuspended in 0.1 M LiAc to a final volume of 1 ml, and incubated at 30°C for 10 minutes. For each 1 X transformation reaction, 100 µl aliquot of the LiAc cell suspension was transferred to a new 1.5 ml microcentrifuge tube. Cells were pelleted at top speed in a microcentrifuge for 1 minute and the supernatant removed.

Transformation mix was prepared by adding the following reagents:

50 % polyethylenglycol	240 µl
1.0 M LiAc	36 µl
ss-DNA (2 mg/ml)	50 µl
Plasmid DNA (0.5 µg)	X µl
Sterile H_2O	X µl
Total volume	360 µl

Transformation mix was added to the cell pellet, vortexed vigorously until the pellet was fully resuspended and the transformation mixture incubated at 30°C for 30 minutes with no shaking. Cells were heat shocked at 42°C in a water bath for 30 minutes, and then pelleted at top speed in a microcentrifuge for 1 minute and then the transformation mix was removed carefully.

Cells were washed with 1.0 ml of sterile ddH_2O by gently pipetting the suspension up and down (to much pipetting washes away transformants), and 100 µl of each sample was plated onto the appropriate SC-dropout medium. Plates were incubated at 30°C for 2-4 days until colonies appeared.

2.4.4. Testing the DNA-BD/bait protein for transcriptional activation

S. cerevisiae Y190 was transformed with 0.5 µg of the pAS1-Emerin (BD) construct using the small-scale yeast transformation protocol (**Agatep, 1998**). Transformants were plated on SD/-Leu/X-α-Gal, SD/-Trp/X-α-Gal, SD/-His/-Trp X-α-Gal, SD/-Ade/-Trp/ X-α-Gal and SD/-Trip/-His/40mM 3AT, and grown for 2 - 4 days at 30°C until colonies appeared. A negative control including the "empty" DNA-BD vector (pAS1) was used under the same growth conditions.

2.4.5. β-Galactosidase lift assay

The yeast two-hybrid system was prepared as described (**Fields and Song, 1989**). *S. cerevisiae* Y190 was grown in YPAD (20g/L peptone, 10 g/L Yeast Extract, 2% Glucose and 0.003% Adenine Hemisulfate, and 40 mM 3AT, pH 5.8) to mid log phase at 30°C in liquid cultures agitated at 250 rpm and then transformed with plasmid DNA using the modified lithium acetate procedure (**Agatep, 1998**). After transformation, yeasts were plated on SDA medium (6.7 g/L Yeast Nitrogen Base without Amino acids, 2% Agar and 0.003% Adenine Hemisulfate, and 40 mM 3AT, pH 5.8) and incubated at 30°C for 2 - 4 days (colonies 1-3 mm in diameter). Once colonies appeared, they were streaked in a "radial fashion" onto 90 mm master plates containing SD medium (6.7 g/L Yeast Nitrogen Base without Amino acids, 2% Agar and 0.003% Adenine Hemisulfate, and 40 mM 3AT, pH 5.8) and grown for another 2 days at 30°C.

For each plate of transformants, a sterile Whatman filter was pre-soaked in 2ml of Z-buffer (16.1 g/L $Na_2HPO_4x7H_2O$, 5.50 g/L $NaH_2PO_4xH_2O$, 0.75 g/L KCl and 0.246 g/L $MgSO_4x7H_2O$, pH 7.00, plus 0.039 M (3-mercaptoethanol and 0.33 mg/ml X-gal) (fresh solution) in a 90mm plate. Using forceps, a clean and sterile nitrocellulose filter was placed carefully over the surface of the plate of the colonies to be assayed, and gently rubbed to help colonies cling to the filter. After the nitrocellulose filter was properly marked for orientation on the original plate, and left to get properly wetted, it was carefully lifted off the agar plate and transferred, with the colonies facing up, to a pool of liquid nitrogen and completely submerged for 30 seconds. After the filter was completely frozen, it was removed from the liquid nitrogen and allowed to thaw at room temperature, then placed carefully, colonies side up, on the pre-soaked filter, avoiding any air bubbles under or between the filters. Finally, the filters were incubated at 30°C and checked periodically for the appearance of the blue colour.

2.4.6. Liquid Culture Assay

Transformants were grown at 30°C with shaking (250 rpm) overnight in 5 ml SD medium supplemented with -Ade/-Trp/-His and 40 mM 3-AT. Cultures were vortexed vigorously for 1 minute to disperse the yeast clumps and 2 ml were immediately transferred to 8 ml of YPDA medium. The cultures were incubated at 30°C for 3 - 5 hours, until the OD_{600} of 1 ml (culture vortexed for 1 minute to disperse the clumps) was 0.5 - 0.8 (mid-log phase). The culture was divided into 3 replicate aliquots of 1.5 ml each and centrifuged at 14000 x g for 30 seconds to pellet the cells. After the supernatant was removed, 1.0 ml of Buffer 1 (0.01 M HEPES, 0.154 M NaCl, 0.0045 M L-Aspartate [hemi-Mg salt], 10g/L BSA and 0.05 % Tween 20, pH 7.25) was added, vortexed until cells were thoroughly resuspended and centrifuged 14000 x g for 30 seconds. Supernatant was carefully removed, 0.3 ml of Buffer 1 was added (concentration factor 1.5/0.3 = 5 fold) and 0.1 ml (in triplicate) of the yeast suspension was transferred to fresh micro-centrifuge tubes. Samples were frozen in liquid nitrogen for 2 minutes and thawed in a water bath at 37°C for 1 minute. This freeze/thaw cycle was repeated 3 times to ensure that the cells were completely broken open. 0.7 ml of Buffer 2 (2.23 mM chlorophenol red-p-D-galactopyranoside, CPRG) was then added to the samples and mixed thoroughly by vortexing (very critical step for the assay). Time was recorded as soon as Buffer 2 was added to the samples. A blank consisted of 1 ml of Buffer 2, and a positive control consisted of 0.1 units of a commercial β-galactosidase enzyme in Buffer 2. Once the colour of the samples was yellow/grey to red, 0.5 ml of 0.003 M $ZnCl_2$ was added to each sample and vortexed vigorously to stop colour development. Time was recorded as reaction time. Samples were centrifuged at 14000 x g for 1 minute at room temperature to pellet the cell debris and the clear supernatant was transferred to a fresh cuvette. The spectrophotometer was set up to zero using the blank at $O.D_{578}$ and the O.D of the samples recorded (an OD_{578} between 0.25 - 1.8 is in the linear range of the

assay).

One unit of (β-galactosidase is defined as the amount of enzyme that hydrolyzes 1 μmol of CPRG to chlorophenol red and D-galactose per minute per cell (**Miller, 1972; Miller, 1992**). The units of β-galactosidases were calculated using the following formula:

β-galactosidase units = $100 \times OD_{578} / (t \times V \times OD_{600})$

Where:

t = Elapsed time (in minutes)

V = 0.1 x concentration factor

OD_{600} = Absorbance of 1 ml of culture

2.5. Mammalian Cell Culture and Transfection

2.5.1. Media

Dulbecco's modified Eagle's medium (DMEM) supplemented with 10 units/ml penicillin, 50 μg/ml streptomycin and 10% newborn calf serum (NCS, v/v) was used to routinely maintain the cell cultures. For transfection experiments, DMEM without phenol red (supplemented as above) was used to reduce the toxic effects of this chemical in the transfected cells.

2.5.2. Cell Lines

Human Dermal Fibroblasts (HDF) from a control and EDMD patients were established by needle biopsy from the inner forearm. The cultures were routinely maintained at 37°C in a humidified atmosphere containing 5% CO_2 until 70 - 80 % confluence. Serial passage was performed in the presence of Trypsin and 0.5% EDTA.

For the experiments including transfection and nuclear deformities studies, cultures were used between passage 4 and 12 and seeded at $0.02x10^6$cell/ml in 90 mm dishes containing 13 mm glass coverslips. For experiments involving nesprins and HSPs, cultures were used at later passages. Old cell cultures (up to passage 45) were used to assess the behaviour of fibroblasts from normal donors and from patients.

Cells were made quiescent by serum starvation. Primary cultures were seeded at $0.02x10^6$cell/ml in 90 mm dishes containing 13mm glass coverslips. After 24 hours in culture, the medium was removed, cells washed 1X with 10 ml of DMEM medium containing 0.5 % NCS. Cultures were maintained at 37°C in a humidified atmosphere containing 5% CO_2 for 5 days in DMEM supplemented with 0.5 % NCS, and coverslips collected and treated for indirect immunofluorescence. Re-stimulated cultures were obtained by removing the starvation medium at day five, washing cells 1X with 10 ml of DMEM supplemented with 10 % NCS and adding fresh medium containing the standard concentration of serum (10% NCS).

Rat dermal fibroblasts were a kind gift from Dr. Colin Jahoda (School of Biological and Biomedical Sciences, University of Durham, UK) and were maintained in DMEM supplemented with 10 % FBS.

2.5.3. Transfection of Human Fibroblasts by electroporation

Cells were grown until 90 % confluence, harvested by Trypsin treatment and washed 1X in DMEM (Gibco) without phenol red. Cells were resuspended in Hyposmolar buffer (Eppendorf, 0.025 M KCl, 0.003 M KH_2PO_4, 0.085 M K_2HPO_4, 90 mOsmol/kg myo-inositol, pH 7.2, conductivity at 25°C 3.5 mC/cm ± 10%), and the concentration assessed by counting in a haemocytometer. Cells were collected at 300 x g for 5 min at room temperature, and resuspended to $1x10^6$cell/ml. Four hundred µl of the $1x10^6$ cells/ml cell suspension was added to

an electroporation cuvette (Eppendorf) (gap width 2 mm) containing 20 μg/ml of each construct (GFP-LamA, DSRed2-LamC or GFP-Emerin) and pulsed in a Multiporator ® (Eppendorf, Soft Pulse™ Technology) at 400 V for 200 μS, 1 pulse, at room temperature. Cells were allowed to recover for 7 minutes after pulse, washed 1X in 5ml of outgrowth medium (DMEM without Phenol Red/10% NCS) at room temperature and collected at 250 x g for 10 min. Finally, cells were resuspended in 1ml outgrowth medium and grown on 13mm coverslips at 37°C in 5% CO_2 for 36 - 60 hours.

2.6. *Biochemistry*

2.6.1. Antibody reagents

A list of the primary antibodies used in this study is given below:

Antibody	Target	Assay	Source	Dil
Jol2	Lamin A and C tail	Immunofluoresc. Western Blot	Prof.C.J. Hutchison	1:25 1:600
Jol4	Lamin A tail	Immunofluoresc.	Prof.C.J. Hutchison	1:10
Lamin C1	Lamin C tail	Immunofluoresc. Western Blot	Prof.C.J. Hutchison	1:25 1:800
Emerin	Emerin	Immunofluoresc.	Novocastra	1:30
414	Nucleoporins	Immunofluoresc.	Boehringer	1:75
Lamin B1	Lamin B1	Immunofluoresc.	Santa Cruz	1:20
Lamin B2	Lamin B2	Immunofluoresc.	Dr. B Lane	1:1 0
PDI	PDI	Western Blot	Dr. A. Benham	1:800
Nesprin 1 C1	Nesprin 1 C terminus	Immunofluoresc.	Dr. C. Shanahan	1:75
Nesprin 1 N5	Nesprin 1 N terminus	Immunofluoresc.	Dr. C. Shanahan	1:75
Nesprin 2 N2	Nesprin 2 N terminus	Immunofluoresc.	Dr. C. Shanahan	1:1 00
Nesprin 2 CH3	Nesprin 2 C terminus	Immunofluoresc.	Dr. C. Shanahan	1: 100
HSP27	HSP27	Immunofluoresc.	Prof Roy Quinlan	1:200
HSP70	HSP70	Immunofluoresc. Western Blot	Prof Roy Quinlan	1:100 1:1000
α-S-actin	α-S-actin	Immunofluoresc.	Sigma	1:400
β-Actin	β-actin	Western Blot	Sigma	1:1600

A list of the secondary antibodies used in this study is given below:

Antibody	Assay	Dilution
FITC-Donkey-anti-mouse	Immunofluoresc.	1:50
TRITC-Donkey anti-mouse	Immunofluoresc.	1:50
TRITC-Donkey anti-goat	Immunofluoresc.	1:50
TRITC-Donkey anti-rabbit	Immunofluoresc.	1:50
Donkey-anti-mouse HRP	Western Blot	1:8000
Donkey-anti-rabbit HRP	Western Blot	1:8000

2.6.2. Cell fractionation

Cells were grown on 75 cm^3 flasks and were washed twice with Versene Buffer (137 mM NaCl, 2.7 mM KCl, 8 mM Na_2HPO_4, 1.5 mM KH_2PO_4) EDTA, pH 7.4) and then treated with Trypsin for 1 minute at 37°C in a humidified atmosphere containing 5% CO_2 and collected in DMEM plus 10 % NCS. Cells were transferred to a centrifuge tube and recovered by centrifugation at 300 x g for 5 minutes in a Sigma centrifuge. After centrifugation, cell pellets were washed 1X with DMEM + 10 % NCS and centrifuged to recover the cells. Cell concentration was assessed by counting in a haemocytometer, and $5x10^6$ cells were collected per tube. Finally, cells were washed with 1X PBS. After centrifugation at 300 x g for 5 minutes, cell lysis occurred after incubation in Ripa Buffer (50 mM Tris, pH 8.00, 150 mM NaCl, 1 % NP-40, 0.5 % Deoxycholic Acid (DOC) and 0.1 % SDS) containing 20 mM N-ethylmaleimide (NEM) to trap disulphide bonds and 1X Protein Inhibitor Cocktail (Sigma) for 10 minutes on ice. Protein concentration was assessed by the Bradford method.

2.6.3. Gel electrophoresis and immunoblotting

Five μg of total protein were loaded per well in the SDS-PAGE. Samples were mixed with the same volume of 2X Sample Buffer Reducing (125 mM Tris-HCL, pH 6.8, 2% SDS, 100mM DTT, 5% Glycerol and traces of BromoPhenolBlue) or Non-Reducing (125 mM Tris-HCL, pH 6.8, 2% SDS, 5% Glycerol and traces of BromoPhenolBlue). Proteins samples were incubated at 95°C for 3 minutes and pelleted at 15,000 g for 1min. Samples were resolved on SDS-PAGE at 70V in Tank Buffer (25 mM Tris, 192 mM Glycine and 0.1 % SDS) and transferred to nitrocellulose membrane (Protean) overnight at 4°C in Transfer Buffer (25 mM Tris, 192 mM Glycine, pH 9.2 plus 20 % Methanol). Nitrocellulose membranes were washed 1X in blot rinse buffer (BRB) (10 mM Tris, pH 7.4, 150mM NaCl and 1 mM EDTA) containing 0.1 % Tween 20 and incubated in blocking buffer (4% milk powder (w/v), 0.1% Tween-20 in BRB) for 16 hour at 4°C with constant shaking. Cell culture supernatant containing mAb Jol2 (1:600) was used to detect lamins A/C. Primary antibodies were incubated with membranes for 1 hour with constant agitation at room temperature. Membranes were rinsed with BRB-0.1 % Tween 20 3X for 5 minutes at room temperature and then incubated with appropriate HRP-conjugated secondary antibodies for 1 hour at room temperature. ECL reagents (1:1 v/v) (Amersham Life Science) were used for the immunological detection of proteins using ECL films (Amersham Life Science).

2.7. Immunofluorescence

2.7.1. Cell staining

Control and EDMD fibroblasts were grown on 13 mm glass coverslips until 70 - 80 % confluence, or until the time lapse pre-determined. Para-formaldehyde fixation was performed after 5 minutes incubation in hypotonic buffer (10 mM Tris, pH 7.4, 10 mM KCl and 3mM $MgCl_2$). Cells were fixed in 3.5 % Para-formaldehyde for 10 minutes, permeabilized by incubation in 0.5 % Triton X-100

in PBS for 5 minutes at 4°C and washed twice in 1X PBS for five minutes at room temperature. Methanol : Acetone (1:1) fixation was performed by incubating cells with methanol: acetone (1:1 v/v chilled to - 20°C) at 4°C for 10 minutes, without permeabilization, and washed twice in 1X PBS for 5 minutes at room temperature.

A blocking step was performed with 1X PBS/1 % NCS for 30 minutes, and then coverslips were washed twice with 1X PBS and allowed to air dry for 10 minutes. Primary antibodies were incubated at room temperature for 1 hour in a wet chamber, and coverslips washed 5 times in 1X PBS. Secondary antibodies were incubated 1 hour at room temperature in wet chamber, and then coverslips were washed five times in 1X PBS. After washes in PBS, coverslips were mounted face down on Mowiol (12% Mowiol (Calbiochem), 30 % glycerol, 120mM Tris-HCl, pH 8.5, 2.5 % DABCO, 1 ng/ml DAPI).

2.8. Microscopy

A BioRad Radiance 2000 confocal laser scanning system fitted to a Zeiss Axiovert microscope and equipped with a 40X and a 63X/1.40 oil immersion lens was used for imaging the cells. For imaging the honeycombs, a dynamic range adjustment was used to optimize the signal of the fluorophores, and Z-series were collected in Sequential Mode through individual nuclei using Kalman (4 times) averaging program at a scan speed of 500 lines per minute and a resolution of 1024 x 768 pixels.

For imaging the cells prepared for proliferating studies, a confocal microscope LMS 510 META (Zeiss) equipped with 40X and 63X/1.10 lens was used. A dynamic range adjustment was set up to optimize the signal, and images were collected in Multi-track Mode (similar to Sequential Mode in BioRad's software) averaging the background 4 times (similar to Kalman in the BioRad system) at a scan speed of

500 lines per minute and a resolution of 1024 x 1024.

3. Chapter Three- Protein-Protein interactions in vitro: emerin and lamins.

3.1. Introduction

The aim of this chapter was to assess the interaction in vitro between emerin and lamins, and to map the domain of Lamins involved in their interaction with emerin using the yeast two-hybrid assay.

EDMD is a rare neuromuscular disorder, characterized by slowly progressive skeletal muscle wasting of the shoulder girdle and distal leg muscles, early contractures of the joints (Achilles tendons, neck and elbows) and cardiomyopathy with conduction defects which often is presented as atrial ventricular block requiring a cardiac pacemaker implant. This disease is inherited as an autosomal dominant (Fenichel et al., 1982; Miller et al., 1985), autosomal recessive (Takamoto et al., 1984; Taylor et al., 1998) or an X-linked disorder (Hodgson et al., 1986; Thomas et al., 1986).

The disease gene for the X-linked form of Emery-Dreifuss Muscular Dystrophy (XL - EDMD) has been identified and it was mapped to distal Xq28. The STA gene, coding for emerin, a serine-rich inner nuclear membrane protein (Manilal et al., 1996; Yorifuji et al., 1997) consisting of 254 amino acids and with a carboxy-terminus transmembrane domain, was first described to contain mutations in all five patients studied (Bione et al., 1994).

Genetic studies in five French families with AD-EDMD linked locus 1q11-q23 to the disease phenotype, identifying four mutations in the LMNA gene that co-segregated with the disease phenotype (Bonne et al., 1999). Other studies have shown that mutations in the same gene are present in the Autosomal Recessive form of the disease, or have no phenotypic effect (Raffaele Di Barletta et al., 2000). The LMNA gene encodes for the A-type lamins, key components of the nuclear

lamina, by alternative splicing mechanisms at the 3'end of the mRNA (Lin and Worman, 1993).

Several studies have addressed the question of whether emerin and lamins interact at the protein level. Using bio-molecular interaction analysis (BIA) combined with the use of monoclonal antibodies, direct interaction between recombinant emerin and Lamin A molecules was demonstrated (Clements et al., 2000). By immuno-precipitation assay, it has been reported that emerin interacts specifically with Lamin A (Sakaki et al., 2001). The functional domain in A-type lamins that binds emerin has been localized in the globular tail domain, between amino acids 384 and 566 (Clements et al., 2000; Sakaki et al., 2001). Other studies in our laboratory have shown that using competition assays and immuno-precipitation with specific antibodies, emerin interacts preferentially with Lamin C (Vaughan et al., 2001). Not many studies have been undertaken using Lamin B1, probably because of the technical obstacles in producing high amounts of the recombinant protein for in vitro assays (Clements et al., 2000). The yeast two-hybrid system has been used to demonstrate that the tail domain of Lamin A and C is essential for the interaction with emerin. Evidence for the interaction between inner nuclear membrane proteins and the members of the lamins family has been established previously using similar approaches to the study by (Sakaki et al., 2001) mine. The α-helical rod domain of lamins B1 and B2, but not lamin B3 was shown to be involved in the interaction with LAP2β, an inner nuclear membrane protein, by biochemical assays and yeast two-hybrid system (Furukawa and Kondo, 1998).

The functional domains of emerin have been defined (Lee et al., 2001). The product of the STA gene interacts with the Barrier Auto-Integration Factor (BAF) throughout its amino acids 1 - 56, which includes the LEM domain (a conserved region between LAP-2β, Emerin and Man1 (Laguri et al., 2001; Wolff et

al., 2001), W01G7.5 (Laguri et al., 2001; Wolff et al., 2001), otefin and M01D7.6 (Wolff et al., 2001) and F42H11.2 (Laguri et al., 2001). Emerin domain extending from amino acids 70 and 178 is responsible for the interaction with A-type lamins, and a third domain not required to bind either BAF or Lamin A extends from amino acids 179–222 (Lee et al., 2001). Recently, new binding partners for emerin have been discovered by using different experimental approaches. Transcriptional repressor germ line-less (Holaska et al., 2003), YT521-B (Wilkinson et al., 2003), nuclear and cytoplasmic actin (Lattanzi et al., 2003), and Nesprin 1α interact with emerin (Mislow et al., 2002).

The yeast two-hybrid system offers a number of advantages over many biochemical methods historically used in protein biochemistry to test for putative protein-protein interactions. It is relatively inexpensive; cDNA libraries can be easily screened, putative new-interacting partner subcloned and further features of novel interactions described; the system is often more sensitive than in vitro techniques to test for weak or transient interactions and post-translational modifications and correct folding of many proteins is not a practical problem. Other two-hybrid technologies have been developed to study other complex protein-protein interactions. This is the case of the hSos/Ras recruitment system (cytoplasm-based yeast two-hybrid system using Ras signalling and rescue of a CDC25 temperature sensitive mutant) (Broder et al., 1998), Split-ubiquitin system (to study protein-protein interaction in transcription factors) (Johnsson and Varshavsky, 1994), three-protein system (study of ternary protein complexes, uses the classical two-hybrid approach plus the third protein fused to a nuclear localisation signal (Zhang and Lautar, 1996), Small ligand-dependent system, (original two-hybrid approach modified in the case of interactions dependent on non-protein ligands (Brent and Finley, 1997), dual bait system (based on two sets of reporter genes bound to different DNA-

binding domains (Serebriiskii et al., 1999), reverse-two-hybrid system (uses toxic reporter genes to dissect protein-protein interactions) (Vidal et al., 1996) and the mammalian and bacterial two-hybrid systems (Joung et al., 2000; Luo et al., 1997).

Applying the information above, a classical yeast two-hybrid experiment was set up using a series of deletion mutants of Lamin B1 constructs, including full length, and lamins A and C full length. In this chapter I confirm that emerin interacts with A and B-type lamins in the yeast two-hybrid system, and that the preferential domain in this interaction is the tail domain. A transfection assay in primary cultures of human skin fibroblasts (HDF) from healthy donor and from XL-EDMD patients (emerin null by indirect immuno-fluorescence) was used to confirm this result. GFP-Lamin A and DSRed2-Lamin C were individually transfected in these cells. Lamin C tagged with DSRed2 was excluded from the emerin defective nuclear envelope in a higher proportion of the transfected cells.

3.2. Results

3.2.1. Emerin is cloned in pAS1.

After cloning emerin in pAS1, colonies were picked and plasmid DNA was purified using Promega's Wizard® Plus Minipreps DNA Purification System. Restriction enzyme analysis was set up using Nco I and BamH I with Multicore buffer. The presence of a band of around 700 base pairs was used as criteria to consider positive clones for DNA sequencing (Figure 3.1A).

Positive clones were sequenced twice (forward and reverse) (Figure 3.1 B) and the sequence obtained was analyzed. BLAST® (Basic Local Alignment Search Tool, (http://www.ncbi.nlm.nih.gov/BLAST) algorithm confirmed the results, showing that the sequence submitted belonged to the STA gene (Figure 3.1 C). This analysis showed that the emerin gene was successfully cloned. The fusion protein contained the respective domains of GAL4 fused in-frame to full length human Emerin.

3.2.2. Emerin-BD construct does not auto-activate RNA polymerase in yeast.

The first step in setting up any yeast two-hybrid experiment consists of assessing the transcriptional activation risk conferred by the bait protein cloned downstream of the GAL4 Binding Domain (BD) as a fusion polypeptide. To determine whether pAS1-emerin construct was able to auto-activate RNA polymerase in the Yeast Two-Hybrid System (Y2HS), Y190 yeast strain was transformed with 0.5 μg of the "empty" pAS1 vector and the pAS1-BD-emerin using the Lithium Acetate method described in Chapter 2. Water was used in the transformation mix instead of the plasmid DNA as a negative control. Plates containing selective media SD/-leu, SD/-Trp plates, SD/-Trp/-His, SD/-Trp/-His/3AT 40mM, and SD/-Ade/-Trp/-His were plated with 100 μl of transformed cells by duplicate and incubated at 30°C for 2 - 4 days (Figure 3.2). Y190 yeast strain did not grow on any of the selective

medium, but grew on SD/-Trp when transformed either with pAS1 vector or with pAS1-emerin. 3-AT, a competitive inhibitor of the yeast HIS3 protein (His3p), was used to inhibit low levels of His3p expressed in a leaky manner in some reporter strains like in Y190 yeast strain, where the basal levels are relatively high. With this result, I confirmed that the emerin construct in pAS1 does not exhibit any auto-activation properties, showing that this construct it is suitable to set up the lift and liquid assays to assess (β-galactosidase activity upon any putative interaction in the Yeast Two-Hybrid assays.

3.2.3. Lift assay A: Emerin interacts with full length A and B-type lamins in the Yeast Two-Hybrid System.

To determine whether emerin interacts with lamins in a yeast two-hybrid system assay, the BD-emerin (in pAS1) construct was co-transformed with the AD-lamin constructs (in pGAD424) in the Y190 yeast strain. In the first instance, β-galactosidase lift assay, a qualitative assay to assess the strength of interaction between two proteins, was used. All the full length Lamin AD-constructs interacted with emerin, but Lamin B1 was the strongest one. A summary of the strength of the interactions is given in Table 3.1.

3.2.4. Lift assay B: Emerin interacts with lamin's tail domain in the Yeast Two-Hybrid System.

Using other fragments of Lamin B1, the region of interaction of lamins with emerin was determined. Five additional Lamin B1 fragments were used. Fragment 5 (region HC1a1b2), fragment 6 (region HC1a1b), fragment 7 (region C1a1b), and fragment 8 (region C1b2) (Table 3.2). None of the constructs gave a very strong interaction, as the time of appearance of the colour on the plates was around 1 hour. Strong interactions in β-galactosidase lift assay usually develops colour in 20 - 30 minutes (Clontech, 2000). The strongest interaction of pAS1BD-emerin was with the Lamin B1 full length and fragment 4, which consisted of the tail domain of

Lamin B1. The high levels of β-galactosidase activity suggested that emerin interacts preferentially with the tail domain of lamins in the yeast two-hybrid assay (Figure 3.4).

3.2.5. Emerin interaction with the tail domain of lamins is confirmed by the semi-quantitative liquid Yeast Two-Hybrid assay.

In order to semi-quantify the interaction between emerin and lamins, a Liquid Culture Assay was set up using chlorophenol red-β-D-galactopyranoside (CPRG) as substrate to assess the activity of β-galactosidase enzyme released by the interacting partners (Figure 3.5). The same constructs as in the lift assay A (see above) were used, plus the Lamin B1-a1b, Lamin B1-C2 and Lamin B1-tail deletion mutants. The strongest values for β-galactosidase activity were obtained for the constructs containing the tail domain and full length of Lamin B1. The interaction with Lamin C produced higher activity than with Lamin A, supporting the former results published by our laboratory (Vaughan et al., 2001).

Combining these results with the lift assays A and B (see above), the Y2H data suggests that emerin interacts preferentially with Lamin B1 through its tail domain. These results suggest that emerin interacts with A and B-type lamins in the yeast two-hybrid assay, and confirm that the functional domain for this interaction is through the tail domain of lamins (Clements et al., 2000; Sakaki et al., 2001).

3.2.6. Transfection efficiency

In order to confirm that emerin interacts with lamins, and to assess the distribution of the different lamin subtypes in emerin deficient cell lines, I set up in vivo experiments using human dermal fibroblasts from a healthy donor and from XL-EDMD patients. Cells were transfected with 20 μg/ml of GFP-Lamin A (wild type), GFP-Emerin (wild type) and DSRed2-Lamin C (wild type), and after 48

hours in culture, 300 cells were counted to assess the efficiency of transfection of the assay. A consistent efficiency transfection rate of 6 - 9 % was achieved. The percentage of cells transfected with the DSRed2-Lamin C construct was always higher than with the GFP-Lamin A construct, but it is not clear whether the differences in the transfection efficiency can be related to any preference in the rate of transfection of the different constructs due to differences in the DNA sequences (between the tag proteins, the tail domain of lamins A and C, or both) or just to the variability intrinsic to the transfection method.

3.2.7. GFP-Lamin A and DSRed2-Lamin C form aggregates in human primary cultures.

Human Skin Dermal Fibroblasts (from a healthy donor and from a patient with XL-EDMD) were used at early passages. After 48 hours of transfection with 20 μg/ml of DNA fusion constructs, confocal images showed different patterns of distribution of the endogenous tagged proteins: 1) normal nuclear rim and 2) intra-nuclear aggregates for both fusion proteins.

Replicate experiments were set up and three hundred cells were counted for each cell line per each fusion construct transfected. In the normal fibroblasts, 4.76% and 11.33 % of the cells presented aggregates after transfection with the GFP-Lamin A or DSRed2-laminC, respectively. The patient fibroblasts showed 14.33 % and 26% of the cells with intranuclear aggregates when transfected with the same constructs (Figure 3.6).

In the case of GFP-Lamin A, an increase of 3.1 fold ($Z= -5.657$; $p=0.0001$) in the amount of aggregates in the X-linked cell line as compared to the control may indicate that the absence of emerin in these cells causes less GFP-Lamin A to be targeted to the nuclear lamina. DSRed2-Lamin C produces an increase of 2.3 fold ($Z= -6.782$; $p=0.0001$) in the amount of aggregates in the patient cell line when

compared to the control. The overall increase of A-type lamin's aggregates in the X-linked fibroblasts was 2.5 fold (Z= -6.455; p=0.0001) compared to the control.

3.2.8. GFP-Lamin A transfection and staining with anti-Emerin, anti-Lamin C and anti-Lamin B1 antibodies in control and XL- EDMD cell lines.

In GFP-Lamin A transfected cells stained with anti-emerin antibody (Figure 3.7), when the exogenous protein was localized to the nuclear rim (GFP-Lamin A i), endogenous emerin showed normal rim localisation in control fibroblasts (Emerin i). Aggregation of the reporter protein (GFP-Lamin A ii) did not cause significant miss-localisation of endogenous emerin (Emerin ii) into aggregates. GFP-Lamin A wild type formed "honeycomb"-like structures in the patient fibroblasts (GFP-Lamin A v). The lack of emerin in these cell lines is shown in the red channel (Figure 3.7 panel iii -vi).

GFP-Lamin A transfected cells stained with anti-Lamin C antibody (Figure 3.8) showed different patterns of distribution of the exogenous protein. In control and X-L EDMD fibroblasts, when GFP-Lamin A was localized to the nuclear rim (GFP-Lamin A i, iii and v), endogenous Lamin C had a normal distribution (Lamin C i, iii and v). Aggregation of the reporter protein (GFP-Lamin A ii, iv and vi) caused mis-localisation of the endogenous Lamin C into aggregates in control fibroblasts (Lamin C ii), but only partial mis-localisation in the patient cell lines (Lamin C iv and vi).

Cells transfected with GFP-Lamin A and stained with anti-Lamin B1 antibody (Figure 3.9), both in control and X-L EDMD fibroblasts, presented GFP-Lamin A localized to the nuclear rim (GFP-Lamin A i, iii and v), and into aggregates (GFP-Lamin A ii, iv and vi). Endogenous Lamin B1 localisation at the nuclear rim was never affected by the distribution adopted by the reporter protein (Lamin B1 i - vi). Absence of Lamin B1 from one pole of the nucleus corresponded with the

absence of GFP-Lamin A aggregates from the same area.

3.2.9. DSRed2-Lamin C transfection and staining with anti-Emerin, anti-Lamin A and anti-Lamin B1 antibodies in control and XL- EDMD cell lines.

Fibroblasts from a healthy donor and X-L EDMD cell lines were transfected with DSRed2-LaminC (wild type) and stained with anti-emerin antibody (Figure 3.10). In control fibroblasts, DSRed2-LaminC was localized to the nuclear rim (DSRed2-LaminC i, iii and v), and into aggregates (DSRed2-LaminC ii, iv and vi). Endogenous emerin localisation at the nuclear rim was not affected by the distribution adopted by the reporter protein in the control fibroblasts (Emerin i - ii). As expected, emerin was not expressed in the patient cell lines (Figure 3.10 iii - vi).

All cell lines were transfected with DSRed2-LaminC (wild type) and stained with anti-lamin A antibody (Figure 3.11). In control and X-L EDMD fibroblasts, DSRed2-LaminC localized to the nuclear rim (DSRed2-LaminC i, iii and v), and into aggregates (DSRed2-LaminC ii, iv and vi). Endogenous lamin A localisation at the nuclear rim was not affected by the distribution adopted by the reporter protein (Lamin A i -vi).

Transfections with DSRed2-LaminC (wild type) were followed by staining with anti-laminB1 antibody (Figure 3.12). Different patterns of distribution of the exogenous protein were observed. In control and X-L EDMD fibroblasts, DSRed2-LaminC was localized to the nuclear rim (DSRed2-LaminC i, iii and v), and into aggregates (DSRed2-LaminC ii, iv and vi). Endogenous lamin B1 localisation at the nuclear rim was not affected by the distribution adopted by the reporter protein neither in the control nor the patient fibroblasts (lamin B1 i - vi).

3.2.10. GFP-Emerin transfection and staining with anti-Lamin A, anti-Lamin C and anti-Lamin B1 antibodies in control and XL- EDMD cell lines.

After GFP-Emerin (wild type) DNA transfection, cells were stained with anti-lamin A antibody (Figure 3.13). In control and X-L EDMD fibroblasts, when GFP-Emerin was localized to the nuclear rim (GFP-Emerin i, iii and v), endogenous lamin A showed a normal distribution (lamin A i, iii and v). GFP-Emerin was often localized in the cytoplasm, either in a smooth distribution (GFP-Emerin ii, iii and vi) or into aggregates (GFP-Emerin iii and iv). Aggregation of the reporter protein in control and patient fibroblasts did not cause mis-localisation of endogenous lamin A (lamin A ii, iv and vi) into aggregates.

Fibroblasts from a healthy donor and X-L EDMD cell lines were transfected with GFP-Emerin (wild type) and stained with anti-lamin C antibody (Figure 3.14). Different distribution patterns of the exogenous protein were observed. In control fibroblasts, when GFP-Emerin was localized to the nuclear rim (GFP-Emerin i, iii and v), endogenous lamin C showed a normal distribution (lamin C i, iii and v). Aggregation of the reporter protein in control cells caused mis-localisation of endogenous lamin C (lamin C ii) into the nucleoplasm. In the patient's cell lines, aggregation of the GFP-Emerin did not cause mis-localisation of the endogenous lamin C, but in this case, GFP-Emerin aggregates were localized mainly to the perinuclear space (GFP-Emerin iv and vi, lamin C iv and vi).

Cell lines were transfected with GFP-Emerin (wild type) and stained with anti-lamin B1 antibody (Figure 3.15). The exogenous protein assumed different distribution patterns. In control and X-L EDMD fibroblasts, GFP-Emerin was localized to the nuclear rim (GFP-Emerin i, iii and v), and into aggregates (GFP-Emerin ii, iv and vi). Endogenous lamin B1 localisation at the nuclear rim was never affected by the distribution adopted by the reporter protein (LaminB1 i - vi).

3.3. Discussion

3.3.1. The tail domain of lamins as a target for the interaction with emerin.

Understanding the biochemical nature of the interaction between emerin and lamins became an important objective after it was confirmed by genetic studies that the protein involved in XL- EDMD was emerin (Bione et al., 1994), and AD-EDMD was linked to locus 1q11-q23 (Bonne et al., 1999), where the LMNA gene was mutated. Since these initial reports, additional disease causing mutations have been characterized in the STA gene (68 reported until 1998) (Yates, 1998) and in LMNA gene (58 reported until 2003).

At the time I established the yeast two -hybrid experiments in February 2000, there was no data available regarding the interaction of emerin and lamins using this approach. Using different deletions mutants of Lamins B1 (a kind gift of Dr. Howard Worman), I have demonstrated that emerin interacts with lamins in the yeast two-hybrid system, and that the region of interaction is mainly through the tail domain.

The interaction of emerin with the head and rod domains of Lamin B1 appeared to be weak, but not absent. The growth of yeast transformed with the deletion mutants lacking the tail domain could be due to the "leak" of His3 protein characteristic of Y190 yeast strain which was not inhibited by the concentration of 3-AT used (0.040 M). But considering that the reporter gene (β-galactosidase) was weakly expressed in both, the lift and the liquid assays (the linear range of the assay is between 0.25 and 1.8 O.D 578); I conclude that these interactions were not relevant to the experiment. Alternatively, weak interactions between the mutant constructs lacking the tail domain of Lamin B1 and emerin could be produced by the "sticky" biochemical nature of the rod domain (α-helical structure), allowing the assembly of the GAL4 transcription factor in the yeast

system.

In contrast, a strong β-galactosidase activity was generated by the interaction between emerin and lamins (A and B-type) constructs containing the tail domain (globular domain, Ig-like structure in the case of Lamin A (Krimm et al., 2002)) in both of the Y2HS approaches used (β-galactosidase lift and liquid assays). In the qualitative lift β-galactosidase assay, the constructs containing the tail domain of Lamin B1 produced a blue colour which developed within the first 30 minutes of reaction, with the strongest point at 2 - 3 hours, after which the colour did not develop any further. The semi-quantitative liquid assay (using CPRG as substrate) with the same mutant and the full length protein rendered values of $O.D_{578}$ = 0.265 for the full length Lamin B1 and 0.292 for the tail domain (395-586 amino acids) (linear range for this assay is between 0.25 and 1.8 (Clontech, 2000).

Considering the Y2HS is an in vitro assay (some researchers consider it an in vivo assay) under "ideal" physiological conditions in the yeast, artefacts generated by other in vitro assays (overlay, immuno-precipitation, column binding) may be minimized. However, some false positive interactions can arise, as the β-galactosidase activity in the yeast two-hybrid system results from a number of factors such as plasmid copy number, the level of protein expression, the stability of the chimerical fusion proteins, conformational effects, and the possible interaction of the fusion proteins with endogenous yeast proteins (Ye and Worman, 1995).

Additional in vitro experiments with a different approach are needed in order to confirm the results of Y2HS. No studies reported in the literature so far have addressed alternative biochemical approaches to define more precisely the minimal sequence(s) required for the interaction of lamins with emerin, since only one

additional study has mapped the interaction of emerin with the tail domain of Lamin A using the same approach as described here (Sakaki et al., 2001). Interestingly, one study using lamin B1 tail domain-vimentin chimeras in human breast adenocarcinoma (MCF7) and human adrenal cortex carcinoma cell lines demonstrated that the vimentin chimera was able to recruit LBR and emerin to nuclear vimentin-bodies (Dreger et al., 2002).

3.3.2. Over-expressing nuclear envelope proteins in emerin deficient cell lines.

Cell lines derived from patients, "naturally" deficient in one or more proteins, are excellent models to study the function of a particular protein, as most of the cellular pathways remain "unaffected" by experimental manipulations. Here we have used human dermal fibroblasts derived from XL- EDMD patients to further investigate the interaction between emerin and lamins, which are affected in different forms of EDMD.

Additionally, fluorescent proteins have proved to be useful tools to study the distribution of polypeptides in the cell, or to monitor cell migration in animal models (Lu et al., 2003). Some studies have shown that the distribution of fluorescent tagged proteins can be affected by the tag (Soling et al., 2002; Zhang et al., 2003) and due to over-expression (Bechert et al., 2003). However, the general approach is still useful for unravelling or confirming some biological and biochemical properties of proteins in living cells. With this in mind, transfection experiments were carried out to investigate the behaviour of lamins and emerin in cell lines lacking emerin.

Ectopic expression of GPF-Lamin A and DSRed2-Lamin C induced the formation of either normal nuclear rim localisation or intranuclear aggregates of these tagged proteins. Although the results of transfection into normal fibroblasts suggest that the aggregates can arise either through the nature of the fluorescent protein, due

to over-expression, or both, some valuable data can be conclusive. In the case of the patient cell line, the data might reflect a combination of the effect of over-expression of tagged proteins and the biochemical effect induced by the lack of emerin. Nevertheless, the differences between the control and the patient in the case of GFP-Lamin A ($Z= -5.657$; $p=0.0001$) and DSRed2-lamin C ($Z= -6.782$; $p=0.0001$) were highly significant. These results suggest that with a very high probability (> 99%), the absence of emerin in the patient cell line leads to the accumulation of A-type lamins in intranuclear aggregates, confirming the molecular interaction between emerin and lamins (Clements et al., 2000; Sakaki et al., 2001). When pooled all together, GFP-Lamin A and DSRed2-lamin C as A-type lamins, the difference between the control and the patient cell line ($Z= -6.455$; $p=0.0001$) was still highly significant. This is evidence for the interaction of emerin with lamins as has been demonstrated in other studies using other approaches (Clements et al., 2000; Sakaki et al., 2001; Vaughan et al., 2001).

Transfected cells stained with different antibody combinations showed that the aggregation of A-type lamins did not affect the distribution of endogenous Emerin. Neither GFP-Lamin A nor DSRed2-Lamin C over-expression produced any re-distribution of the endogenous Emerin from the nuclear rim, suggesting that emerin remains attached to the nuclear envelope through its carboxy-terminus transmembrane domain, the interaction with its binging partners (Lamin B1?) or both. As expected, Lamin B1 remained more stable at the nuclear rim since its localisation was never affected by any of the over-expressed fusion proteins.

It has been shown that A-type lamins are disassembled when the cell enters mitosis by reversible phosphorylation (Heald and McKeon, 1990; Ottaviano and Gerace, 1985; Peter et al., 1990), but B-type lamins remain attached to the nuclear vesicles and associated to the LBR (Chaudhary and Courvalin, 1993; Meier and

Georgatos, 1994). Live imaging experiments have shown emerin and LBR are recruited early to reforming nuclear envelopes during mitosis as patches, and become more homogeneous at later stages (Haraguchi et al., 2000). Other live imaging studies have shown different pathways of assembly of A and B-type lamins into the "novo" nuclear envelope following mitosis. Immediately after mitosis and until early G1, Lamin A is distributed homogenously throughout the nucleoplasm, but Lamin B1 is targeted directly to the periphery of the chromosomes before any de-condensation begins, and remains attached to the nuclear boundaries (Moir et al., 2000). As A-type lamins are soluble during mitosis, they are automatically excluded as interacting partners for emerin, at least at this stage of the cell cycle.

Our results show that lamin B1 is stably localized with emerin at the NE when A-type lamins are mislocalized to aggregates, which suggest that the retention of emerin at the NE in fibroblasts may be due to its stable interaction with B-type lamins. This observation is distinctively different from what happens in HeLa cells, where mis-localisation of A-type lamins to aggregates causes retraction of emerin to the ER (Vaughan et al., 2001). Perhaps there are other factors in fibroblast responsible for retaining emerin in the NE, e.g. low level of retention of A-type lamins at the lamina. However, during mitosis, emerin and Lamin B1 co-localize with LBR, so it is possible that emerin remains attached to the surface of the chromosomes through its direct association with Lamin B1, or indirectly through the formation of a transient complex that involves the Lamin B1 and other interacting partners yet to be discovered. Most probably, the ubiquitous interaction of emerin with all lamin subtypes may warranty that emerin remains stable attached to the NE during the cell cycle.

Figures Chapter 3

Figure 3.1

Emerin was cloned in pAS1 vector. A) Plasmid DNA digestion with restriction enzymes produced a band of approximately 700 bp as expected for the emerin gene. B) pAS1-Emerin was sequenced using the Big Dye terminator technology and the data acquired in an ABI377DNA Sequencer (Applied Biosystems). The ATG initiation codon is highlighted (Met) and the sequence upstream was analyzed showing the ATG codon is in the correct reading frame to produce the putative Emerin protein. C) Emerin sequence obtained after sub-cloning the gene into pAS1, was analyzed by the BLASTN (Basic Local Alignment Search Tool Nucleotide) for nucleotide homology. Distribution of 13 BLAST hits shows 100% similarity of the query to the reported emerin gene (highest scores).

Figure 3.1

A)

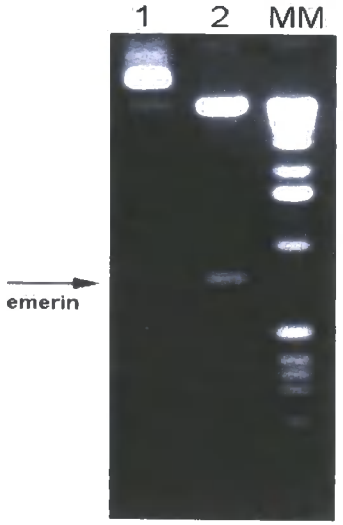

B)

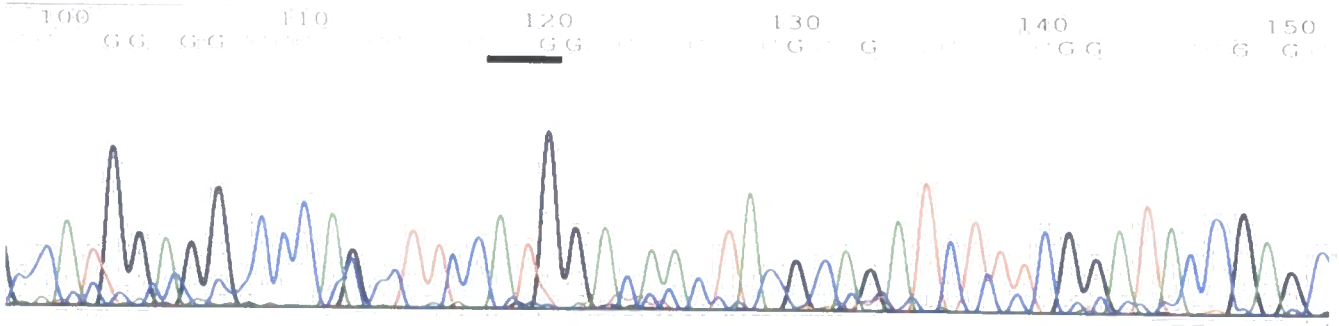

C)

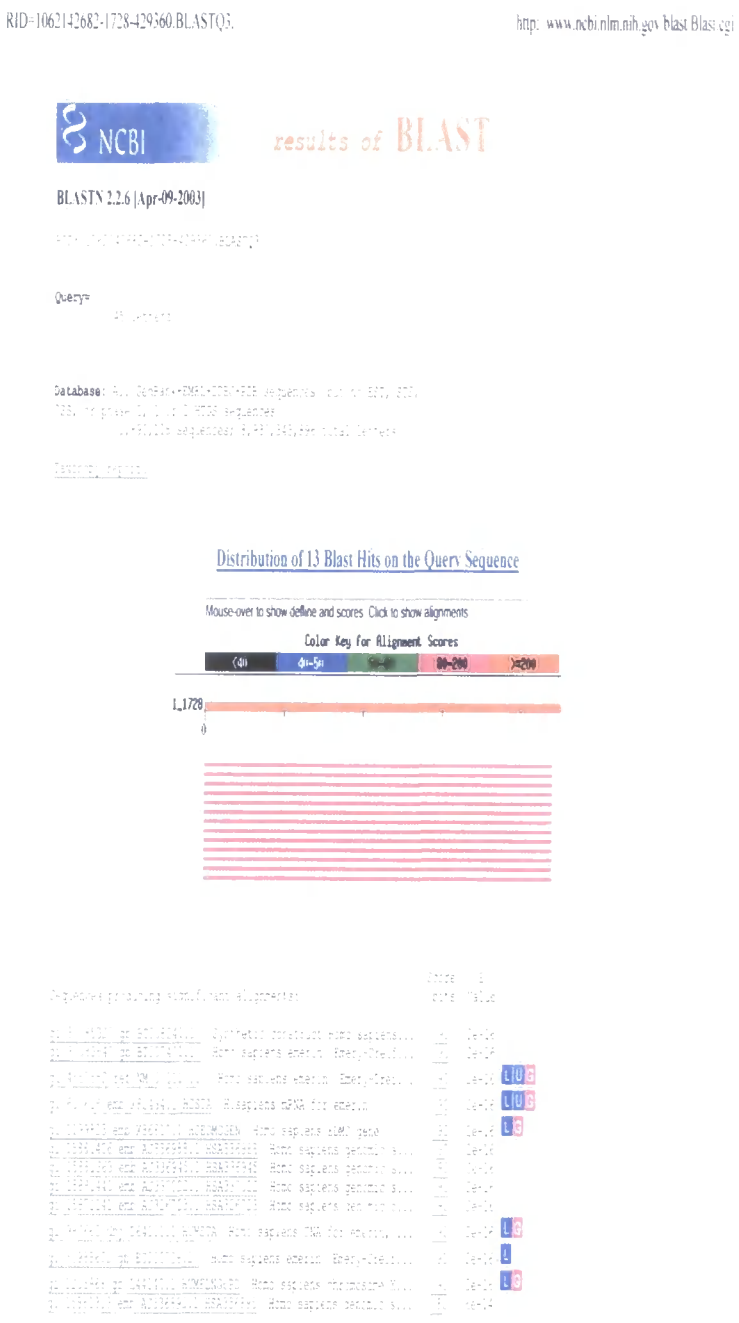
RID=1062142682-1728-429360.BLASTQ3.
http://www.ncbi.nlm.nih.gov/blast/Blast.cgi
NCBI
results of BLAST
BLASTN 2.2.6 [Apr-09-2003]
Query=
Database:
Distribution of 13 Blast Hits on the Query Sequence
Mouse-over to show defline and scores. Click to show alignments
Color Key for Alignment Scores
<40
40-50
50-80
80-200
>=200
1_1728
0

Figure 3.1

Figure 3.2

A transcriptional activation assay was set up in Y190. Yeast were co-transformed with 0.5 μg of the "empty" pAS1 vector and the pAS1/BD-emerin construct using the lithium acetate transformation method, and plated on agar plates containing different selective media to test for auto-activation of the RNA transcriptase activity in the yeast two-hybrid assay from the bait construct.

Figure 3.2

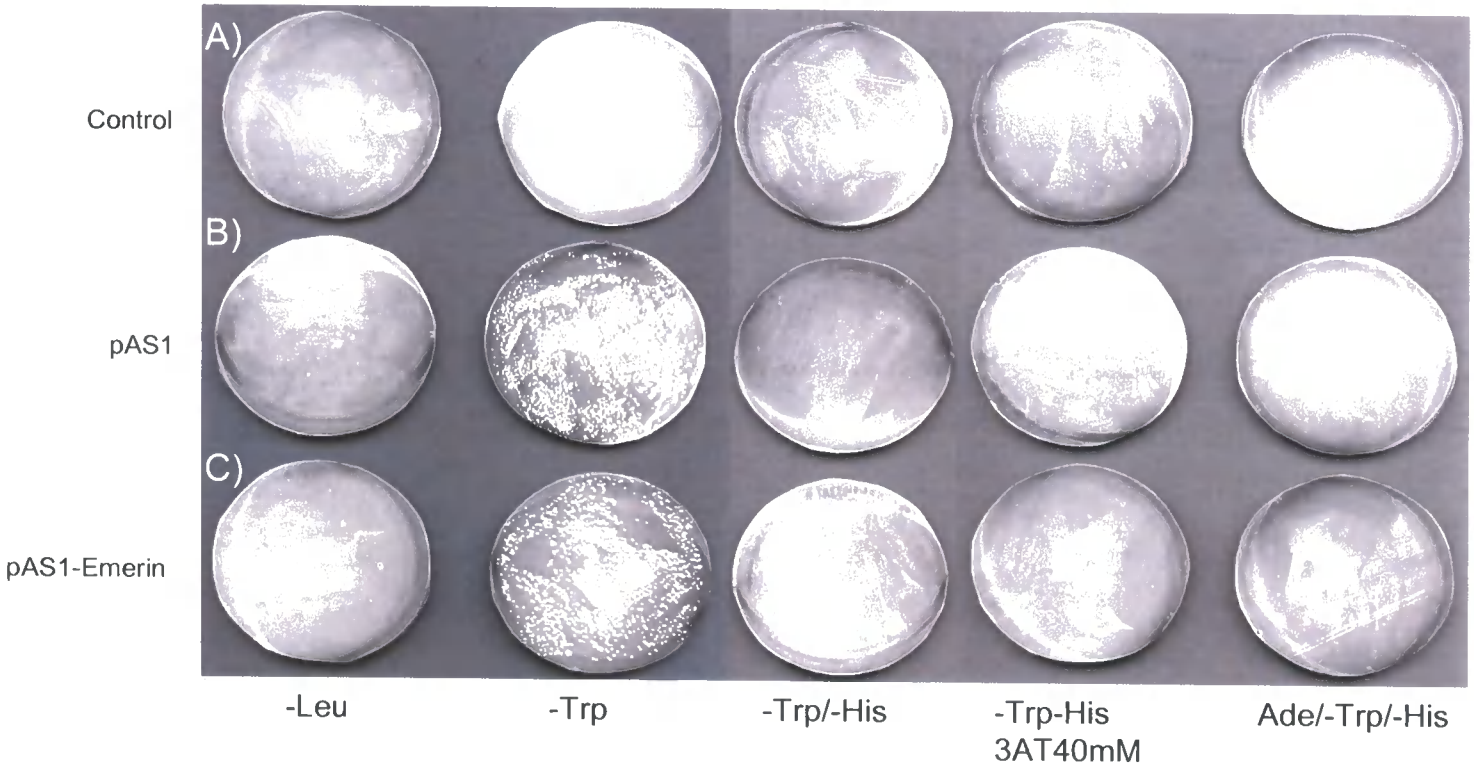
A)
B)
C)
Control
pAS1
pAS1-Emerin
-Leu
-Trp
-Trp/-His
-Trp-His
3AT40mM
Ade/-Trp/-His

Figure 3.3

β-galactosidase lift assay A. pAS1-Emerin was co-transformed with full length emerin, lamin A, lamin B1 and lamin C tagged to the activation domain of GAL4. Y190 was transformed using the lithium chloride method and grown on agar plates containing selective media. Yeast was grown for 4 days after transformation, when colonies were about 3 mm in diameter and streaked on plates containing selective media. After colonies appeared, the β-galactosidase lift assay was set up and color development stabilized at 2 hours.

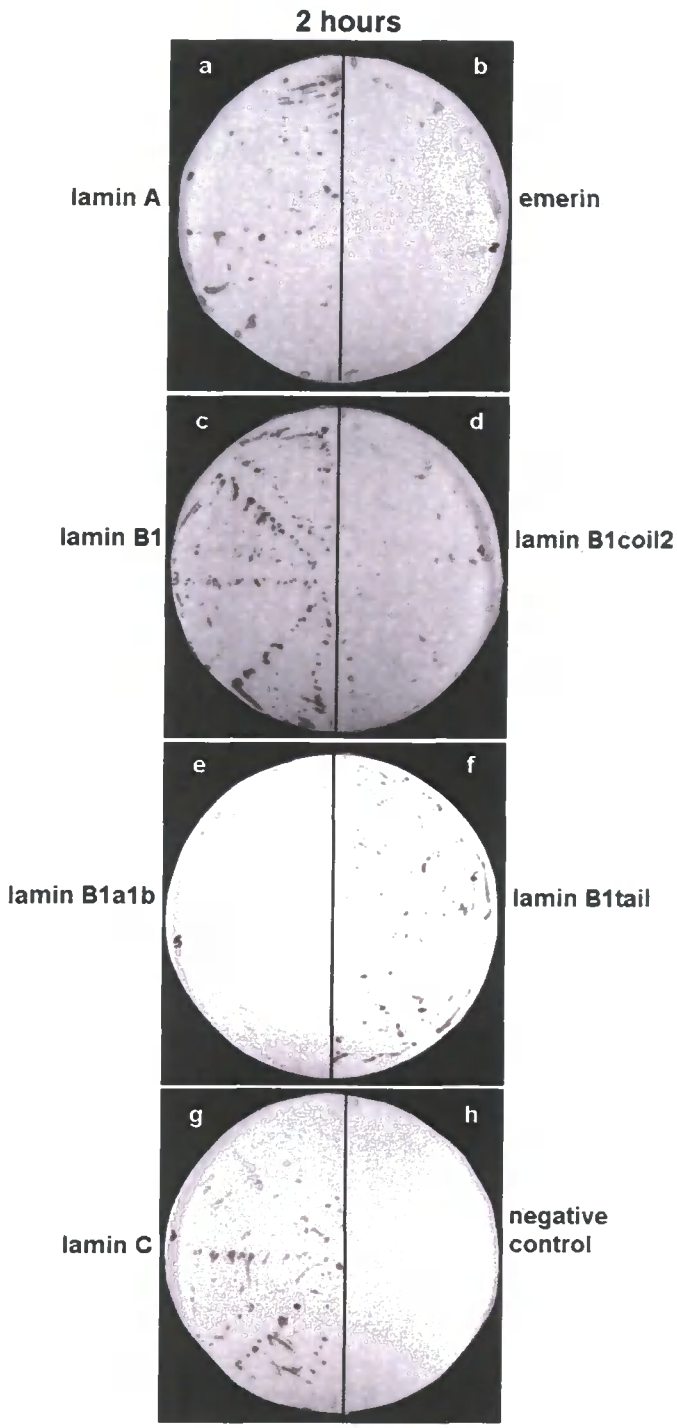
2 hours
a
b
lamin A
emerin
c
d
lamin B1
lamin B1coil2
e
f
lamin B1a1b
lamin B1tail
g
h
lamin C
negative
control

Figure 3.3

Table 3.1

A summary of the time course of β-galactosidase lift assay in the yeast two-hybrid experiment to assess the level of interaction between emerin and lamins. 0.5 μg of each construct was co-transformed in the yeast strain Y190 using the lithium acetate transformation method. Time was recorded as soon as the filters were in touch with the reaction buffer containing X-gal. The strength of the color of the colonies is represented by √.

Time (h)	Emerin Lamin A	Emerin Lamin B1	Emerin Lamin B1Coil2	Emerin Lamin B1tail
T_0	0	0	0	0
$T_{0.5}$	√	√√	0	√√
T_2	√√	√√√√	√	√√√√
T_3	√√	√√√√	√	√√√√

Table 3.1

Figure 3.4

β-galactosidase lift assay B. pAS1 BD-Emerin was co-transformed with full length lamin A and lamin B, and different deletions mutants of lamin B1 tagged to the activation domain of GAL4. Y190 was transformed using the lithium acetate method and growth on agar plates containing selective media. Yeast was grown for 2 - 4 days after transformation, when colonies were about 3 mm in diameter and streaked on plates containing selective media. After colonies appeared, the β-galactosidase lift assay was set up, and color development recorded at 2 hours.

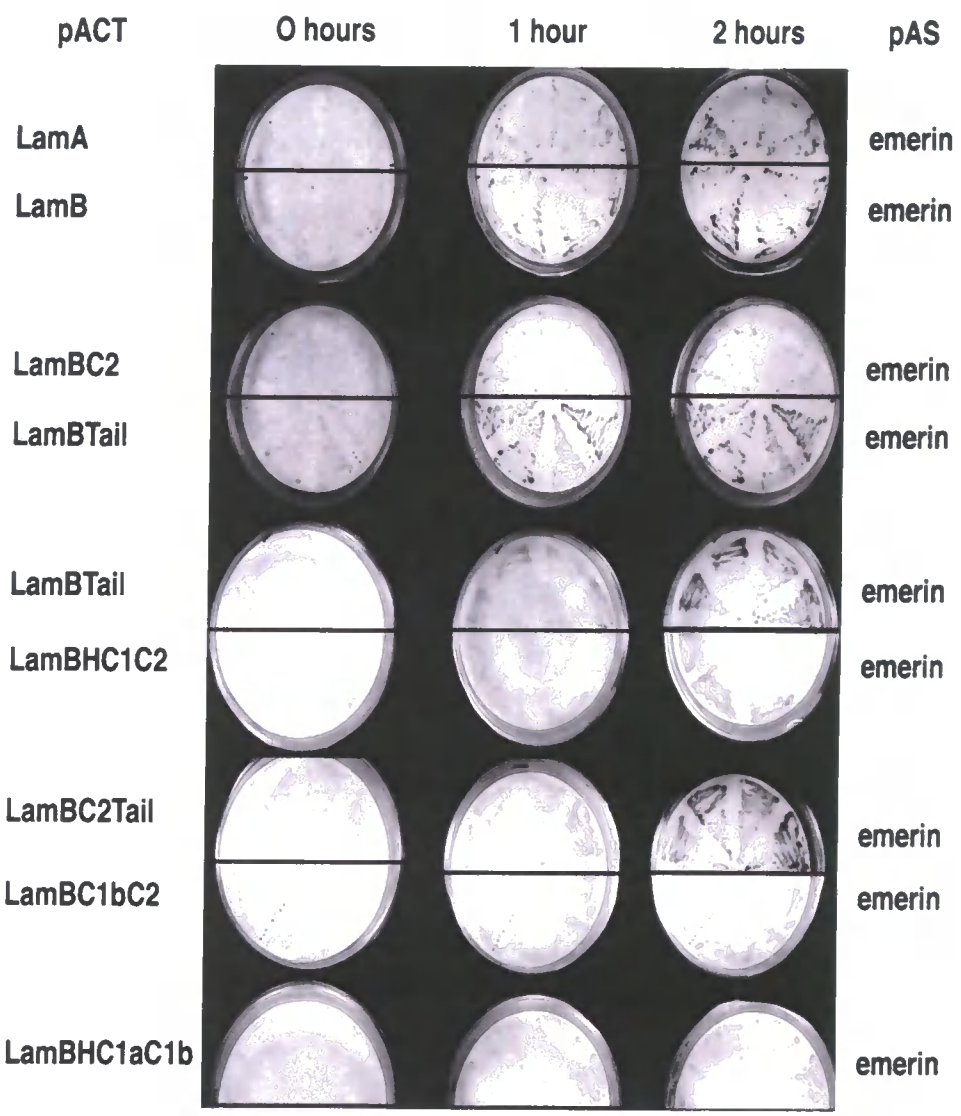
pACT
O hours
1 hour
2 hours
pAS
LamA
emerin
LamB
emerin
LamBC2
emerin
LamBTail
emerin
LamBTail
emerin
LamBHC1C2
emerin
LamBC2Tail
emerin
LamBC1bC2
emerin
LamBHC1aC1b
emerin

Figure 3.4

Table 3.2

Summary of the constructs used in the yeast two-hybrid experiments. Ye, Q. and Worman, H. J. (1995).

	ACTIVATION DOMAIN pGAD424	BINDING DOMAIN pAS1
1	Lamin A (1-646 a. a)	Emerin
2	Lamin B1 (1–586 a. a)	Emerin
3	Lamin B1 Coil2 (241-394a. a)	Emerin
4	Lamin B1 Tail (395-586 a. a)	Emerin
5	Lamin B1 HC1a1b2	Emerin
6	Lamin B1 HC1a1b	Emerin
7	Lamin B1 C1a1b	Emerin
8	Lamin B1 C1b2	Emerin

Table 3.2

Figure 3.5

Liquid β-galactosidase assay. Y190 was co-transformed with pASIBD-Emerin and full length emerin, lamin A, lamin Bland lamin C, and the fragments lamin B1C2, lamin B1a1b and lamin B1 tail fused to the AD of GAL4. Transformants were grown ON at 30°C with constant shaking at 250 rpm in selective media, and yeast processed for the liquid assay. Samples were set up by triplicate. For the full length constructs, Lamin B1 showed the strongest value of β-galactosidase activity, as in the lift assays A and B. The tail domain of lamin B1 showed the strongest value between the fragments.

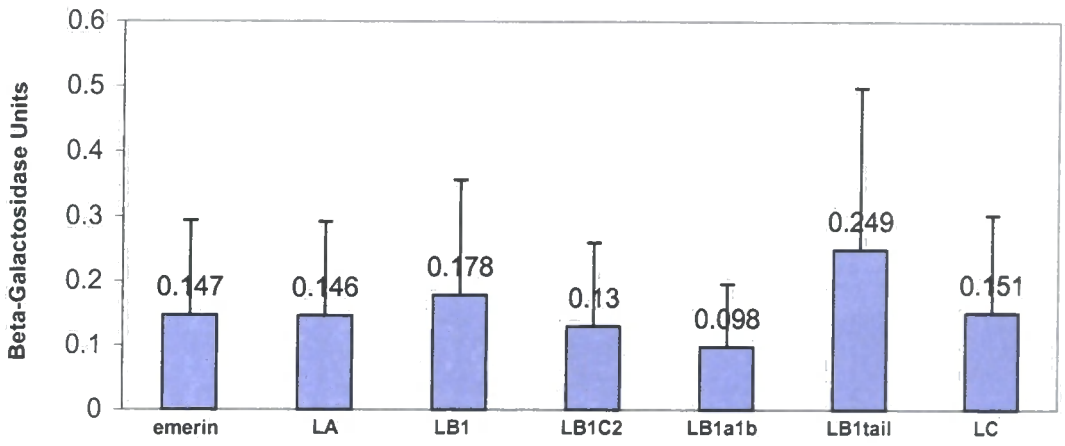
Beta-Galactosidase Units
0.6
0.5
0.4
0.3
0.2
0.1
0
0.147
0.146
0.178
0.13
0.098
0.249
0.151
emerin
LA
LB1
LB1C2
LB1a1b
LB1tail
LC

Figure 3.5

Figure 3.6

Transfection of GFP-Lamin A (wild type) and DSRed2-lamin C (wild type) in Human Dermal Fibroblasts from a healthy donor and from an EDMD X-linked patient. Cells were transfected with 0.5 μg of the plasmid DNAs using the electroporation system from Eppendorf. 300 cells were counted and the number of aggregates recorded. The statistical significance was calculated using the Wilcoxon test. Both increments of aggregates were highly significant with $p = 0.0001$.

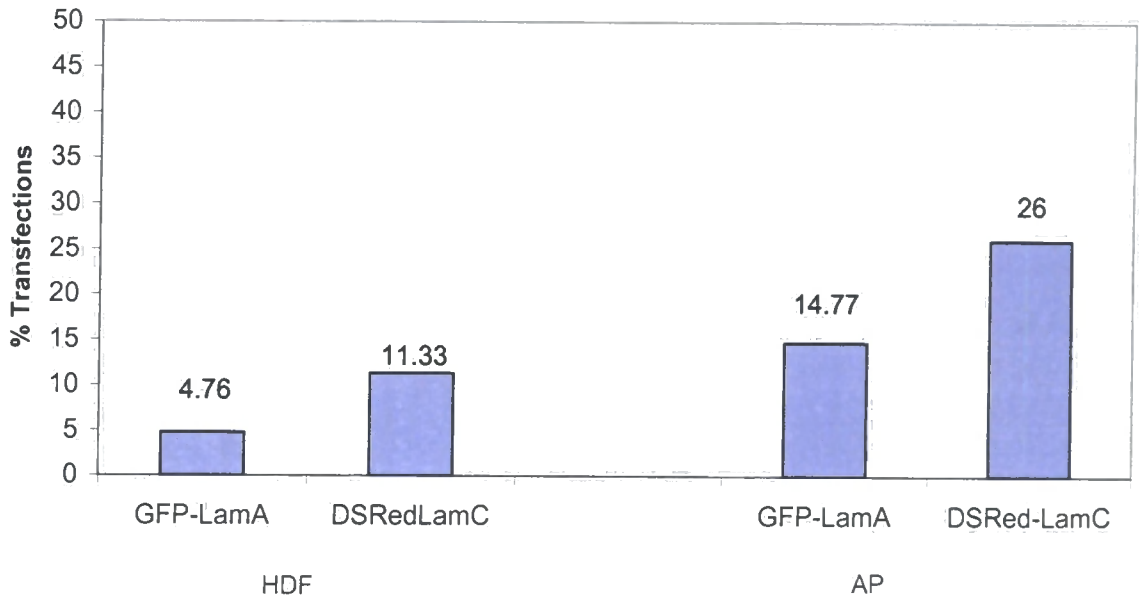
50
45
40
35
30
25
20
15
10
5
0
% Transfections
4.76
11.33
14.77
26
GFP-LamA
DSRedLamC
GFP-LamA
DSRed-LamC
HDF
AP

Figure 3.6

Figure 3.7

Fibroblasts from a healthy donor and X-linked EDMD cell lines were transfected with GFP-laminA (wild type) and stained with anti-emerin antibody. Different distribution patterns of the exogenous protein were observed. In control fibroblasts, when GFP-LaminA was localized to the nuclear rim (GFP-laminA i, iii and v), endogenous emerin showed a normal distribution (emerin i). Aggregation of the reporter protein in control fibroblasts (GFP-laminA ii) did not cause mis-localization of endogenous emerin into aggregates (emerin ii). GFP-laminA formed "honeycomb" like structures in the patient fibroblasts (GFP-LaminA v). Panels iii - vi) in the red channel showed no emerin expression in the patient cell lines.

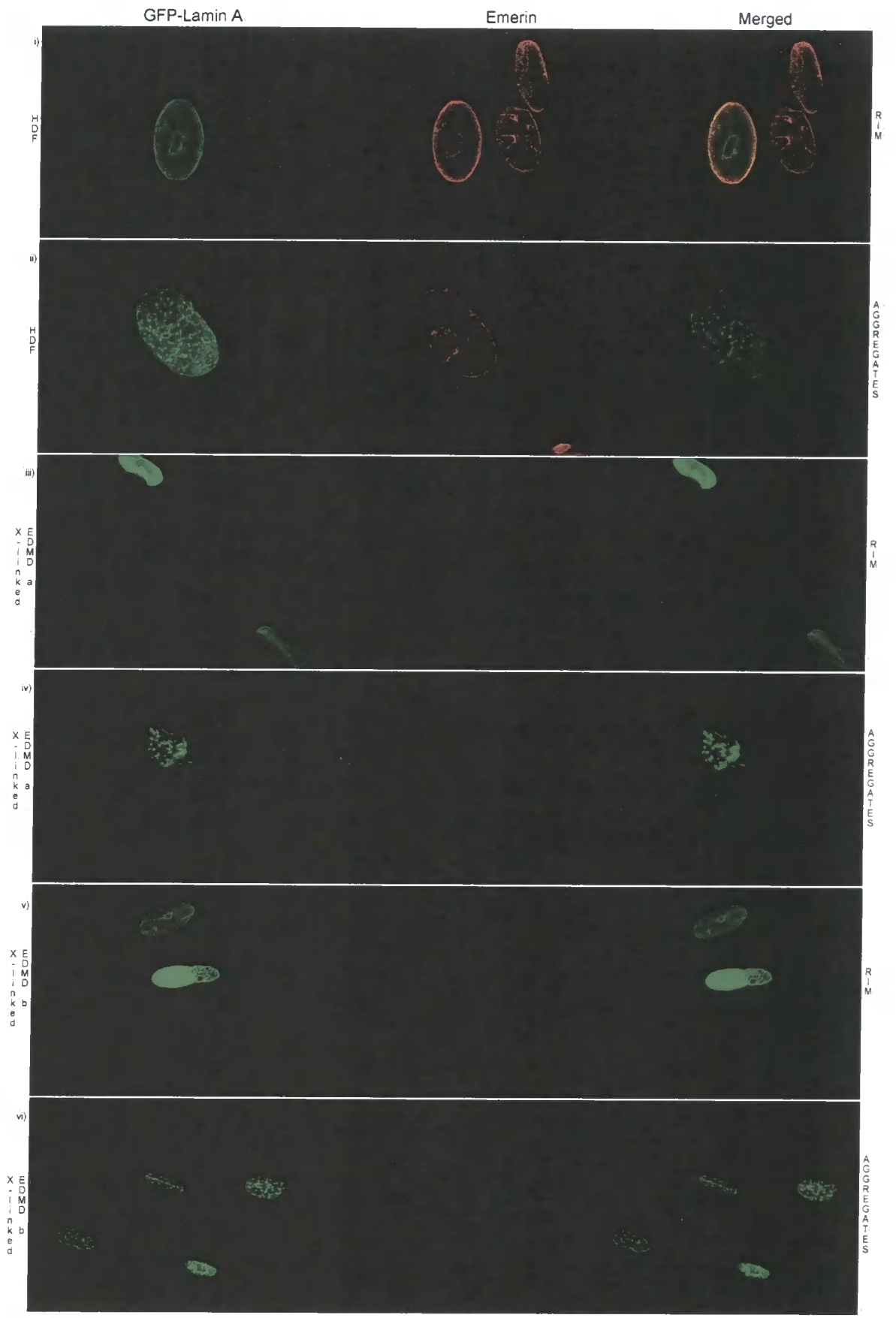
GFP-Lamin A
Emerin
Merged
i)
HDF
RIM
ii)
HDF
AGGREGATES
iii)
X-linked EDMD a
RIM
iv)
X-linked EDMD a
AGGREGATES
v)
X-linked EDMD b
RIM
vi)
X-linked EDMD b
AGGREGATES

Figure 3.7

Figure 3.8

Fibroblasts from a healthy donor and X-linked EDMD cell lines were transfected with GFP-laminA (wild type) and stained with anti-lamin C antibody. Different patterns of distribution of the exogenous protein were observed. In control and X-linked EDMD fibroblasts, when GFP-LaminA was localized to the nuclear rim (GFP-laminA i, iii and v), endogenous lamin C showed a normal distribution (lamin C i, iii and v). Aggregation of the reporter protein (GFP-laminA ii, iv and vi) caused mis-localization of endogenous lamin C into aggregates in control fibroblasts (lamin C ii), but only partial mis-localization in the patient cell lines (Lamin C iv and vi).

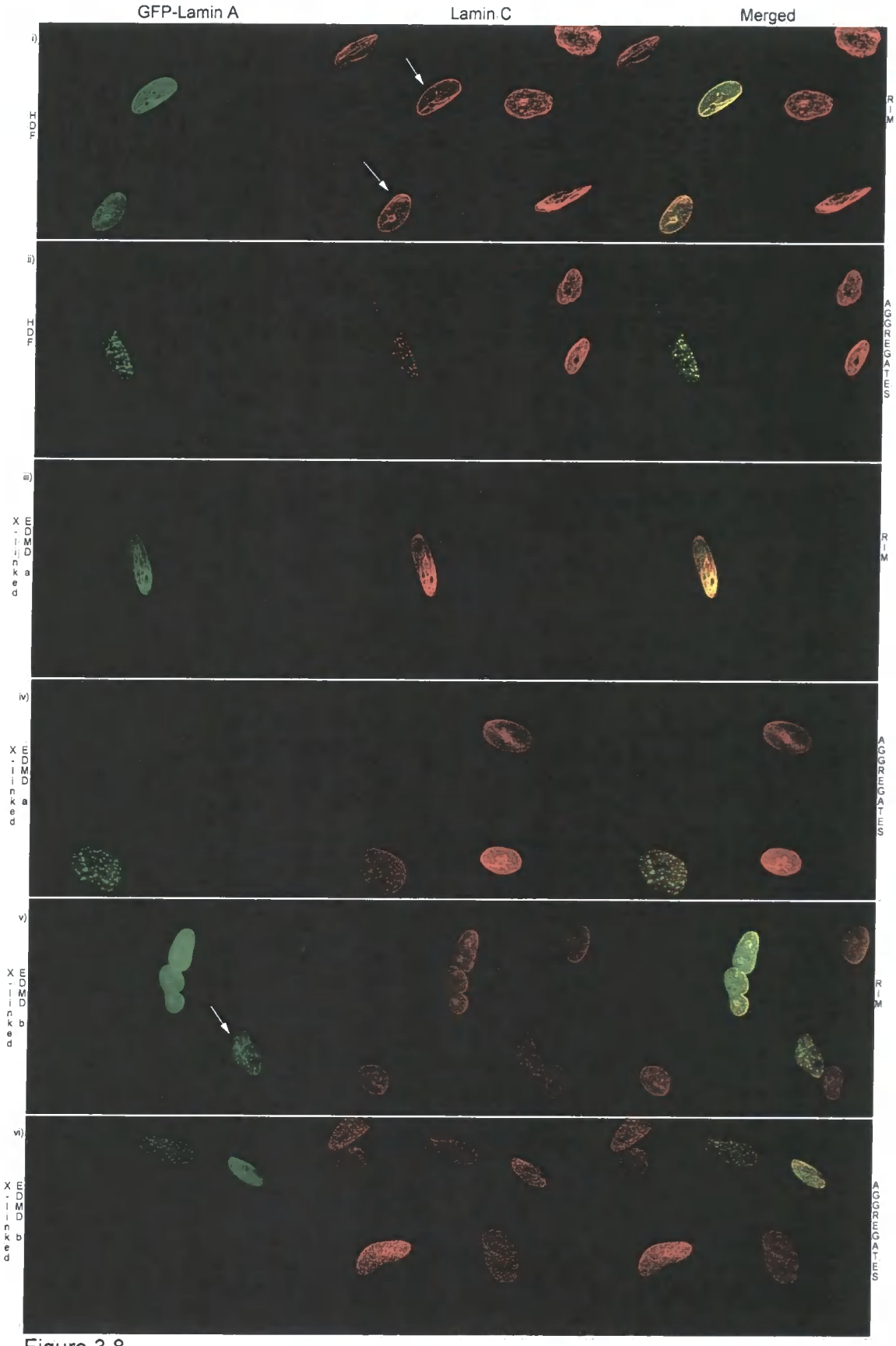
GFP-Lamin A
Lamin C
Merged
i)
HDF
RIM
ii)
HDF
AGGREGATES
iii)
X-linked EDMD a
RIM
iv)
X-linked EDMD a
AGGREGATES
v)
X-linked EDMD b
RIM
vi)
X-linked EDMD b
AGGREGATES

Figure 3.8

Figure 3.9

Fibroblasts from a healthy donor and X-linked EDMD cell lines were transfected with GFP-laminA (wild type) and stained with anti-lamin B1 antibody. Different patterns of distribution of the exogenous protein were observed. In control and X-linked EDMD fibroblasts, GFP-LaminA was localized to the nuclear rim (GFP-laminA i, iii and v), and into aggregates (GFP-LaminA ii, iv and vi). Endogenous lamin B1 localization at the nuclear rim was never affected by the distribution adopted by the reporter protein (LaminBI i - vi). Absence of lamin B1 from one pole of the nucleus co-localized with the absence of GFP-LaminA aggregates at the same area (Lamin B1 iv).

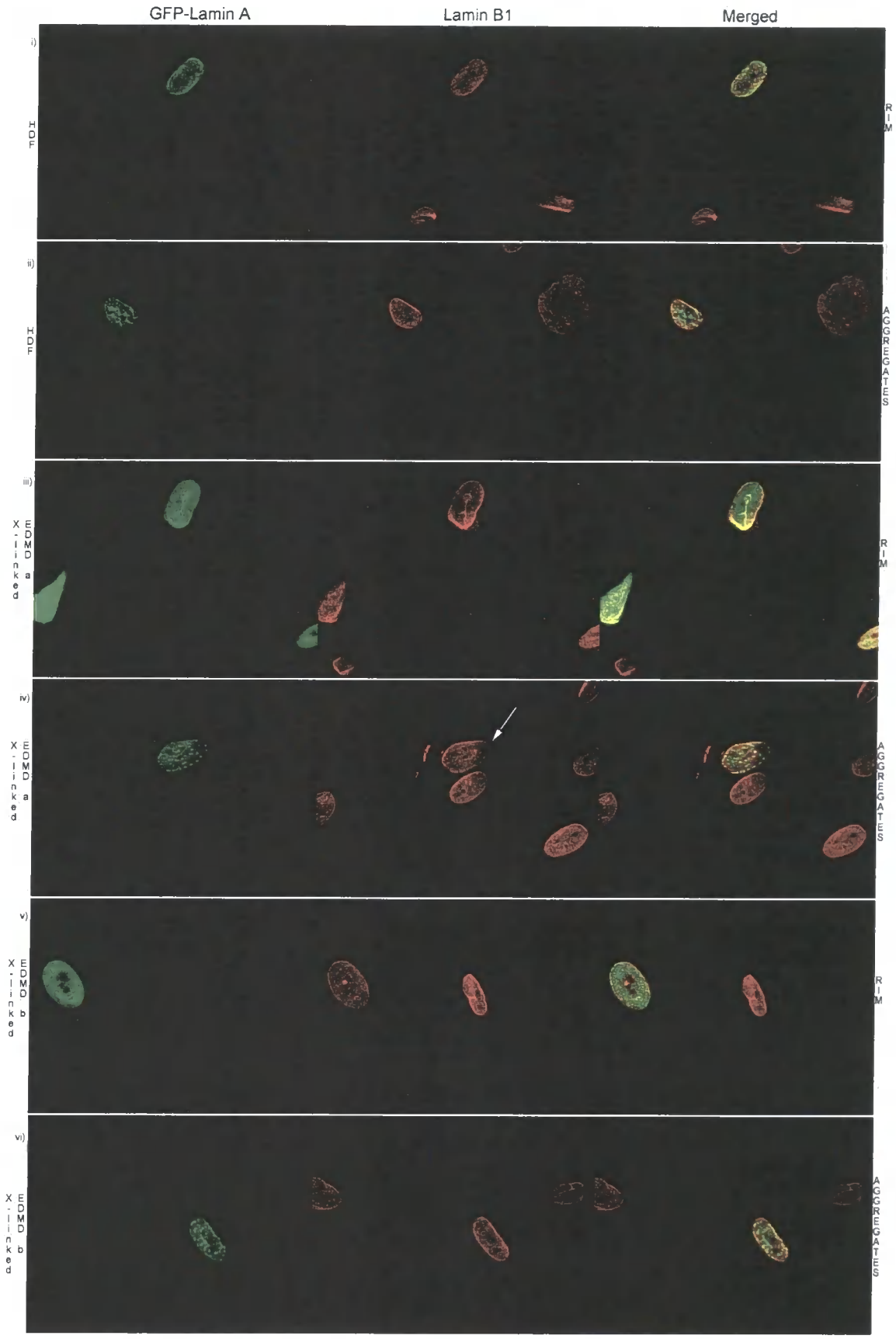
GFP-Lamin A
Lamin B1
Merged
i)
HDF
RIM
ii)
HDF
AGGREGATES
iii)
X-linked EDMD a
RIM
iv)
X-linked EDMD a
AGGREGATES
v)
X-linked EDMD b
RIM
vi)
X-linked EDMD b
AGGREGATES

Figure 3.9

Figure 3.10

Fibroblasts from a healthy donor and X-linked EDMD cell lines were transfected with DSRed2-LaminC (wild type) and stained with anti-emerin antibody. Different patterns of distribution of the exogenous protein were observed. In control fibroblasts, DSRed2-LaminC was localized to the nuclear rim (DSRed2-LaminC i, iii and v) and into aggregates (DSRed2-LaminC ii, iv and vi). Endogenous emerin localization at the nuclear rim was not affected by the distribution adopted by the reporter protein in the control fibroblasts (Emerin i -ii). Panels iii - vi) in the green channel showed no emerin expression in the patient cell lines.

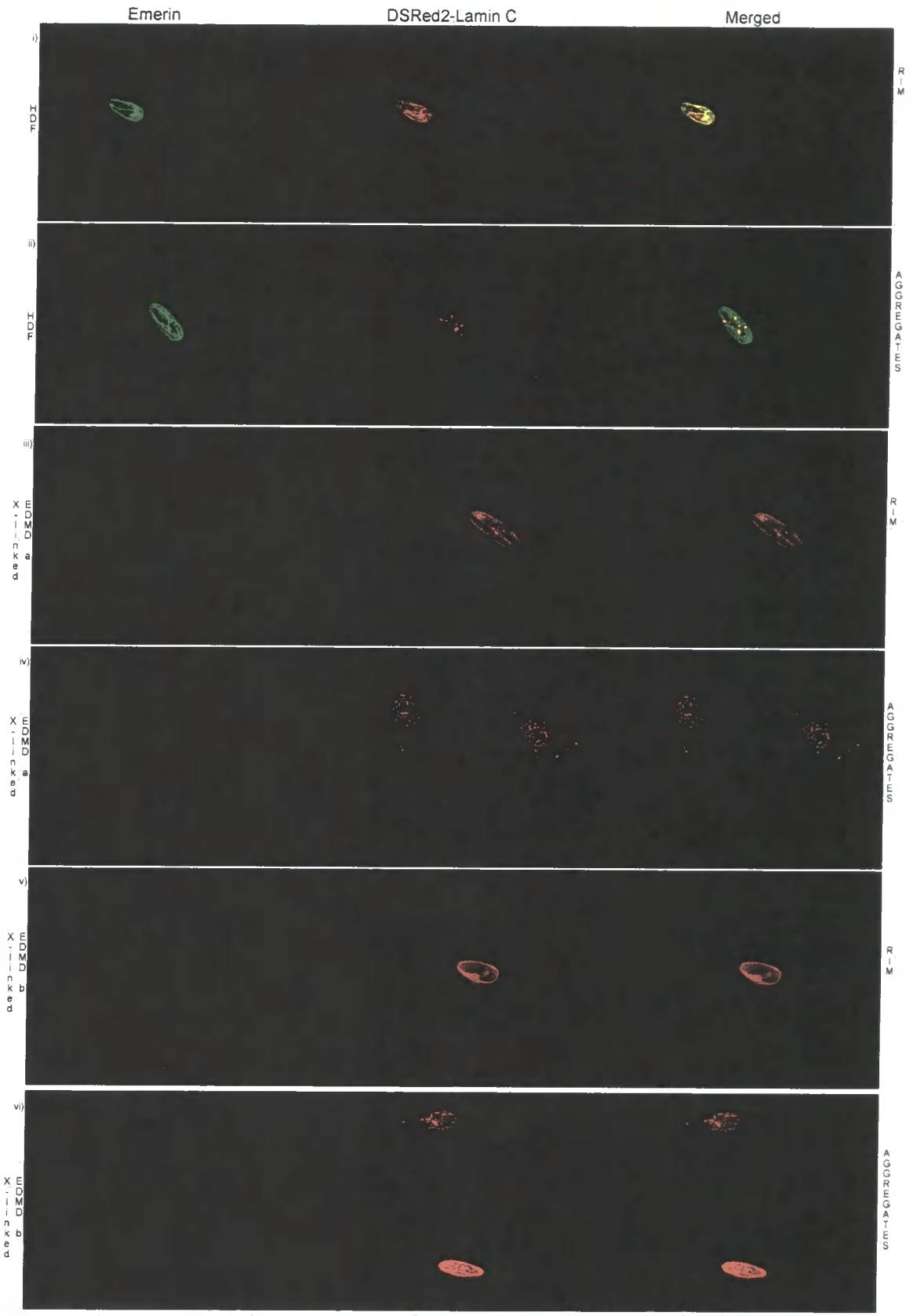
Emerin
DSRed2-Lamin C
Merged
i)
HDF
RIM
ii)
HDF
AGGREGATES
iii)
X-linked EDMD a
RIM
iv)
X-linked EDMD a
AGGREGATES
v)
X-linked EDMD b
RIM
vi)
X-linked EDMD b
AGGREGATES

Figure 3.10

Figure 3.11

Fibroblasts from a healthy donor and X-linked EDMD cell lines were transfected with DSRed2-LaminC (wild type) and stained with anti-lamin A antibody. Different patterns of distribution of the exogenous protein were observed. In control and X-linked EDMD fibroblasts, DSRed2-LaminC was localized to the nuclear rim (DSRed2-LaminC i, iii and v), and into aggregates (DSRed2-LaminC ii, iv and vi). Endogenous Lamin A localization at the nuclear rim was not affected by the distribution adopted by the reporter protein in the control fibroblasts (Lamin A i - ii), nor in the patient cell lines (Lamin A iv - vi).

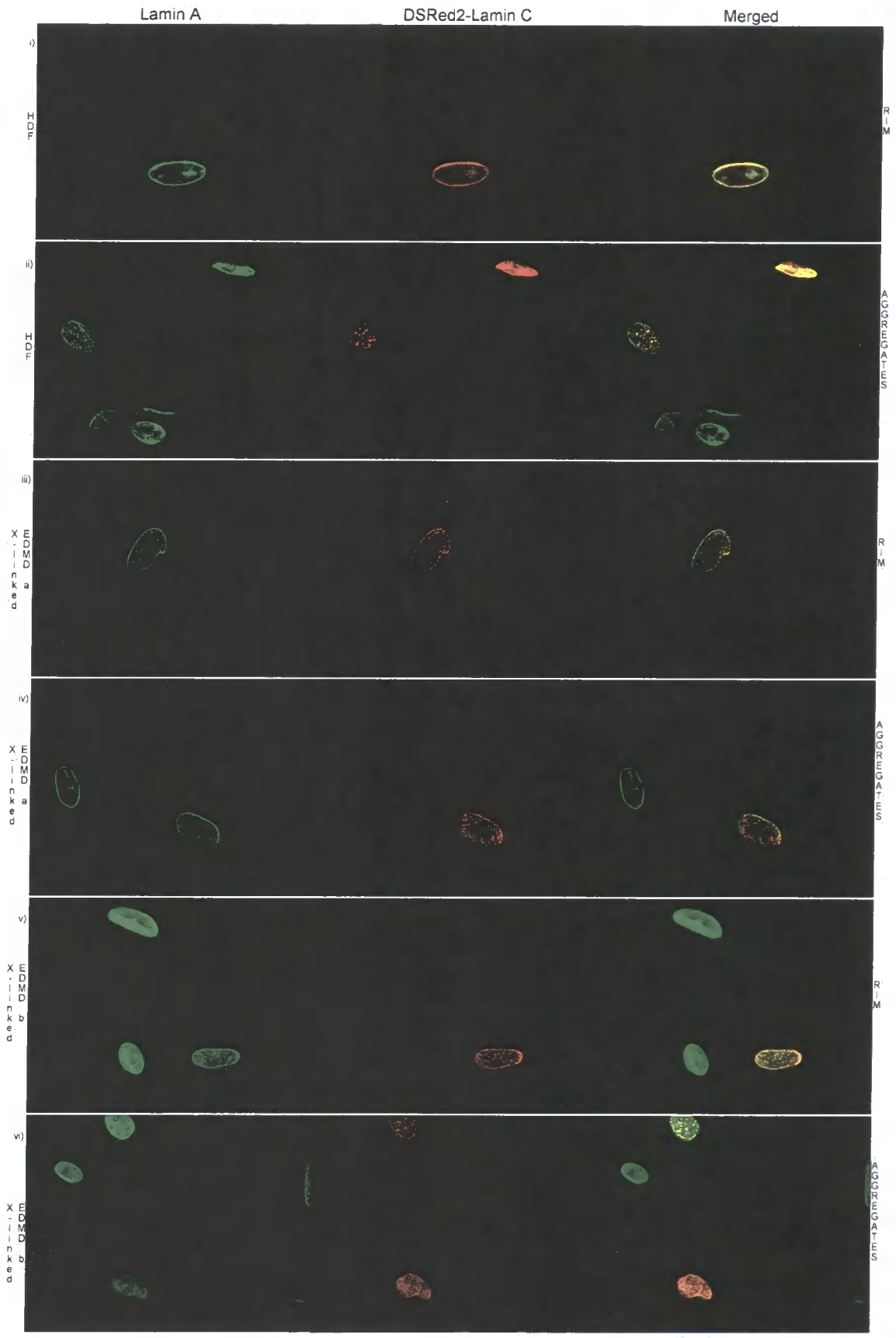
Lamin A
DSRed2-Lamin C
Merged
i)
HDF
RIM
ii)
HDF
AGGREGATES
iii)
X-linked EDMD a
RIM
iv)
X-linked EDMD a
AGGREGATES
v)
X-linked EDMD b
RIM
vi)
X-linked EDMD b
AGGREGATES

Figure 3.11

Figure 3.12

Fibroblasts from a healthy donor and X-linked EDMD cell lines were transfected with DSRed2-laminC (wild type) and stained with anti-laminB1 antibody. Different patterns of distribution of the exogenous protein were observed. In control and X-linked EDMD fibroblasts, DSRed2-LaminC was localized to the nuclear rim (DSRed2-LaminC i, iii and v), and into aggregates (DSRed2-LaminC ii, iv and vi). Endogenous lamin B1 localization at the nuclear rim was not affected by the distribution adopted by the reporter protein neither in the control or patients fibroblasts (laminB1 i - vi).

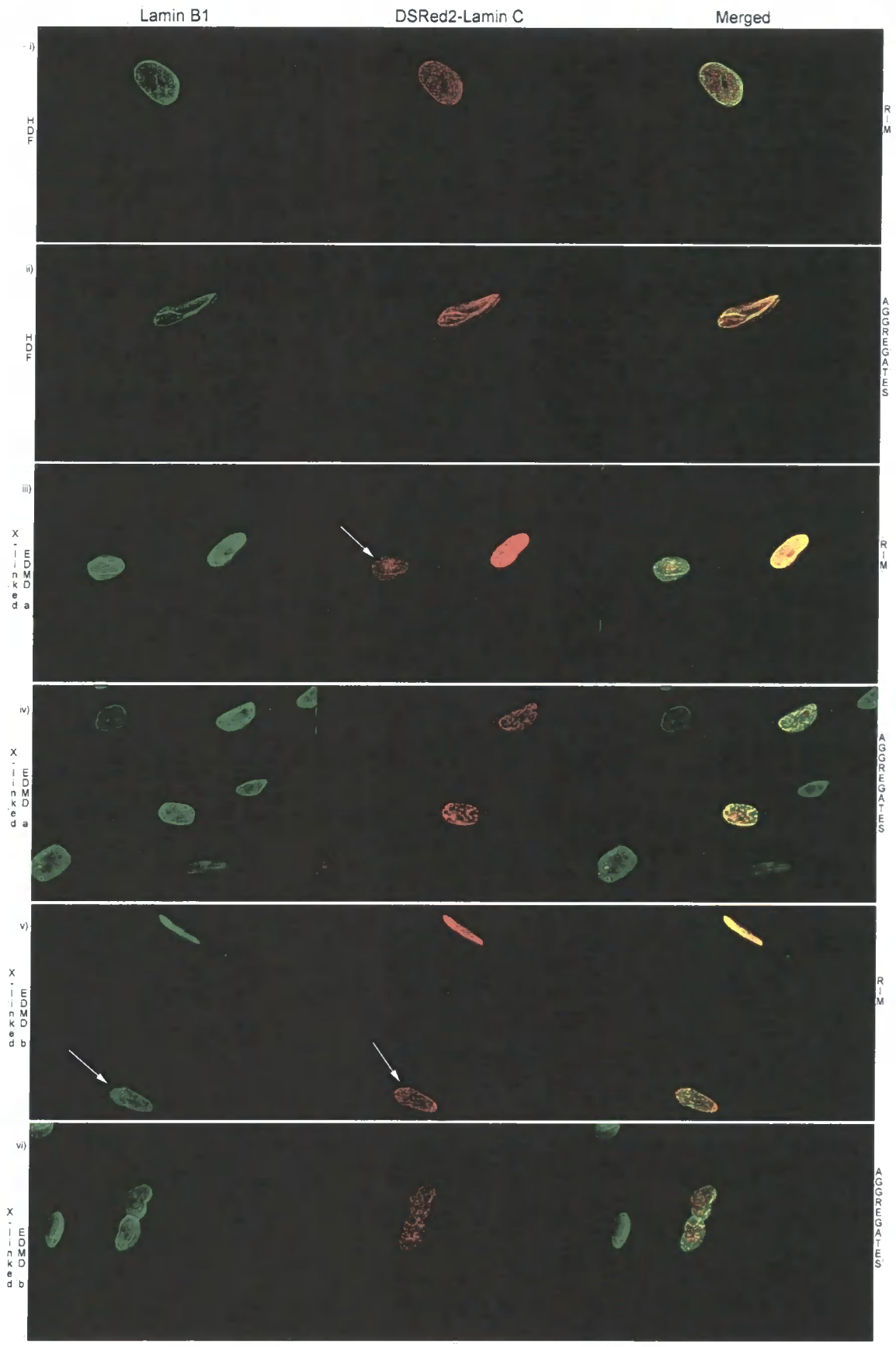
Lamin B1
DSRed2-Lamin C
Merged
i)
HDF
RIM
ii)
HDF
AGGREGATES
iii)
X-linked EDMD a
RIM
iv)
X-linked EDMD a
AGGREGATES
v)
X-linked EDMD b
RIM
vi)
X-linked EDMD b
AGGREGATES

Figure 3.12

Figure 3.13

Fibroblasts from a healthy donor and X-linked EDMD cell lines were transfected with GFP-Emerin (wild type) and stained with anti-laminA antibody. Different distribution patterns of the exogenous protein were observed. In control and X-linked EDMD fibroblasts, when GFP-Emerin was localized to the nuclear rim (GFP-Emerin i, iii and v), endogenous laminA showed a normal distribution (laminA i, iii and v). Aggregation of the reporter protein in control and patient fibroblasts did not cause miss-localization of endogenous laminA (lamin A ii, iv and vi) into aggregates. GFP-Emerin was often localized in the cytoplasm, either in a smooth distribution (GFP-Emerin ii, iii and vi) or into aggregates (GFP-Emerin iii and iv).

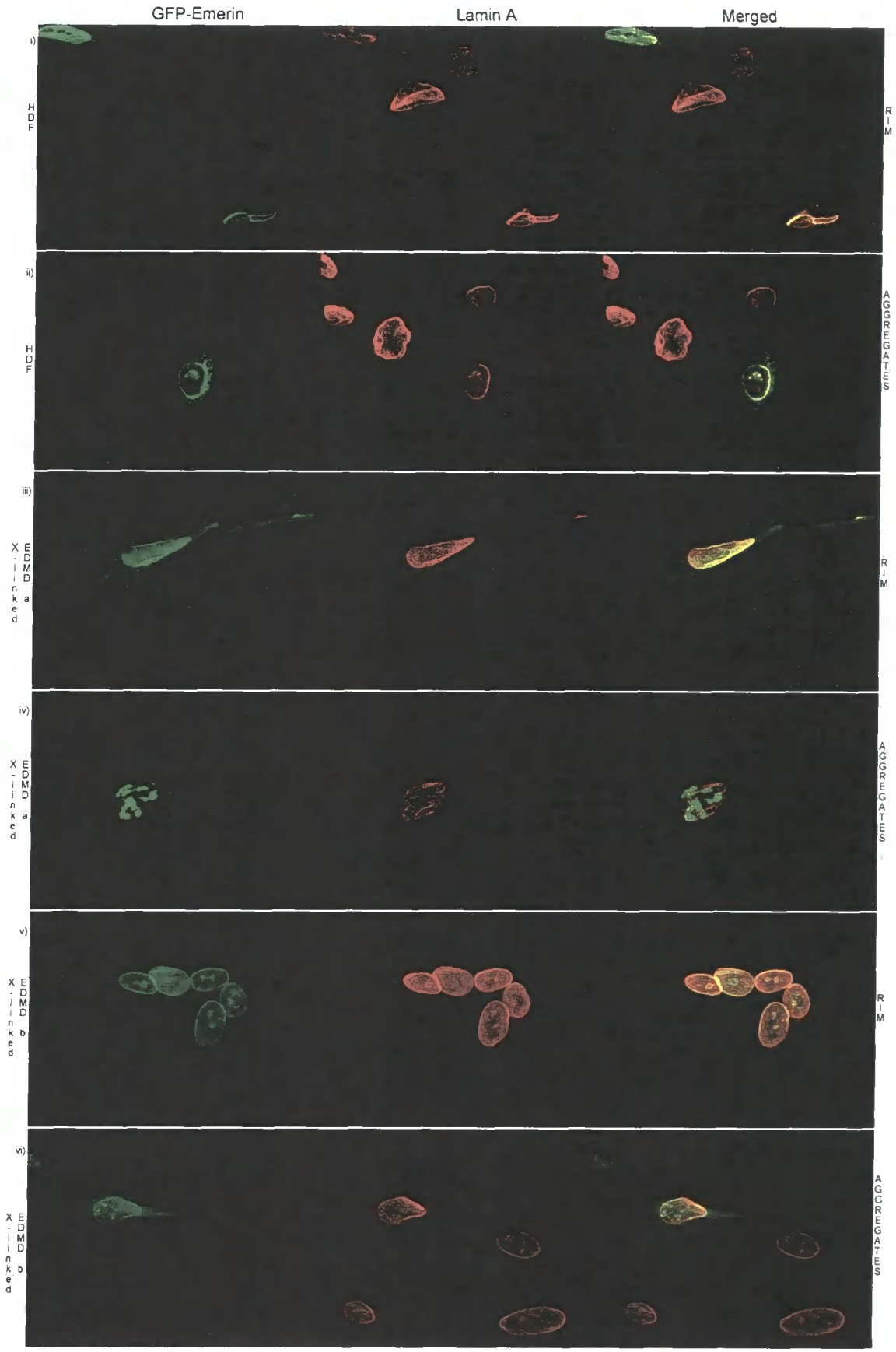
GFP-Emerin
Lamin A
Merged
i)
HDF
RIM
ii)
HDF
AGGREGATES
iii)
X-linked EDMD a
RIM
iv)
X-linked EDMD a
AGGREGATES
v)
X-linked EDMD b
RIM
vi)
X-linked EDMD b
AGGREGATES

Figure 3.13

Figure 3.14

Fibroblasts from a healthy donor and X-linked EDMD cell lines were transfected with GFP-Emerin (wild type) and stained with anti-lamin C antibody. Different distribution patterns of the exogenous protein were observed. In control fibroblasts, when GFP-Emerin was localized to the nuclear rim (GFP-Emerin i, iii and v), endogenous lamin C showed a normal distribution (lamin C i, iii and v). Aggregation of the reporter protein in control cells did cause miss-localization of endogenous lamin C (lamin C ii) into the nucleoplasm. In the patient cell lines, aggregation of the GFP-Emerin did not caused miss'-localization of the endogenous lamin C, but in this case, GFP-Emerin aggregates were localized mainly to the perinuclear space (GFP-Emerin iv and vi, lamin C iv and vi). GFP-Emerin was often localized in the cytoplasm, either in a smooth distribution (GFP-Emerin ii and vi) or into aggregates (GFP-Emerin iv and vi).

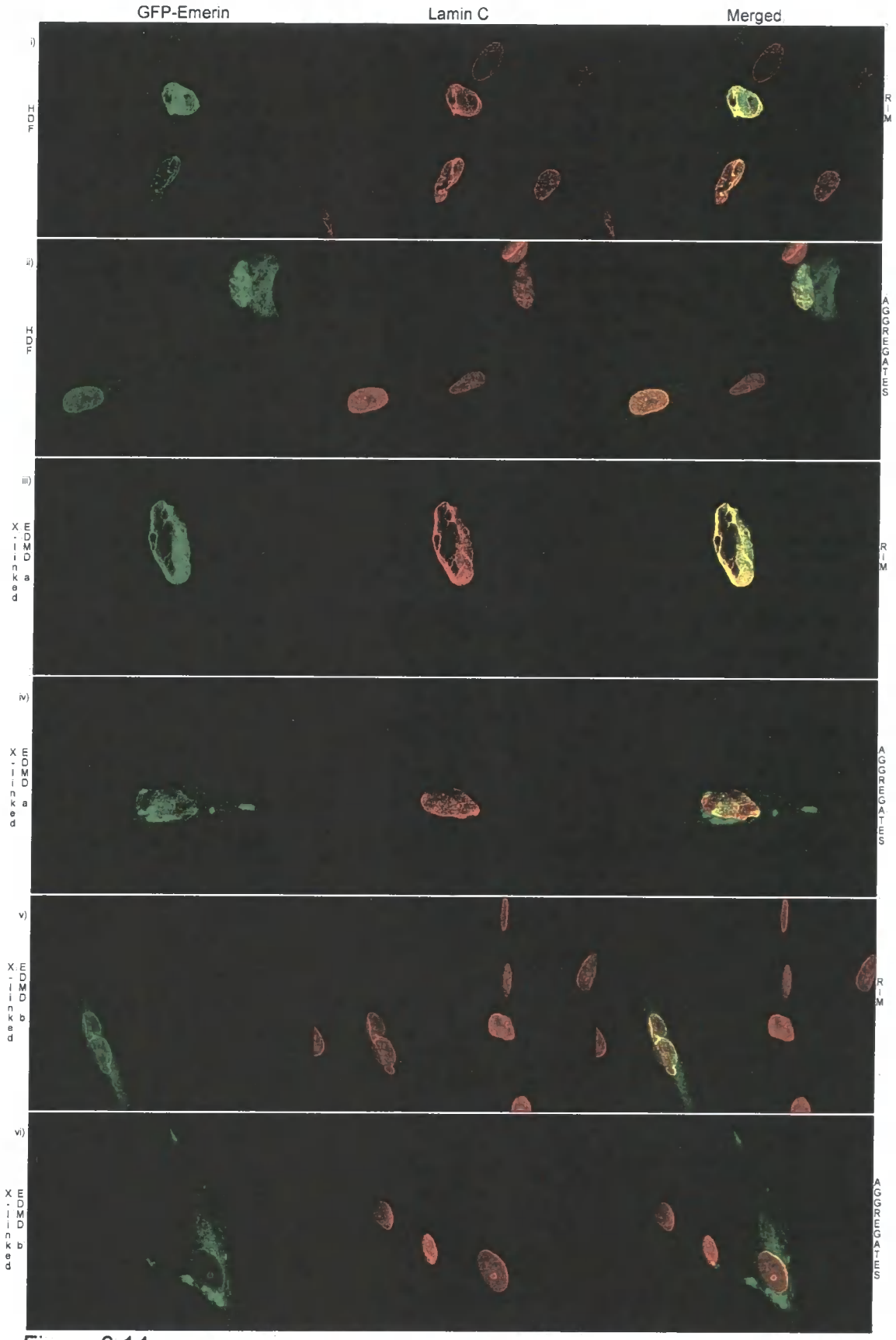
GFP-Emerin
Lamin C
Merged
i)
HDF
RIM
ii)
HDF
AGGREGATES
iii)
X-linked EDMD a
RIM
iv)
X-linked EDMD a
AGGREGATES
v)
X-linked EDMD b
RIM
vi)
X-linked EDMD b
AGGREGATES

Figure 3.14

Figure 3.15

Fibroblasts from a healthy donor and X-linked EDMD cell lines were transfected with GFP-Emerin (wild type) and stained with anti-lamin B1 antibody. Different patterns of distribution of the exogenous protein were observed. In control and X-linked EDMD fibroblasts, GFP-Emerin was localized to the nuclear rim (GFP-Emerin i, iii and v), and into aggregates (GFP-Emerin ii, iv and vi). Endogenous lamin B1 localization at the nuclear rim was never affected by the distribution adopted by the reporter protein (LaminB1 i - vi). GFP-Emerin was often localized in the cytoplasm, either in a smooth distribution (GFP-Emerin i and vi) or into aggregates (GFP-Emerin ii and vi).

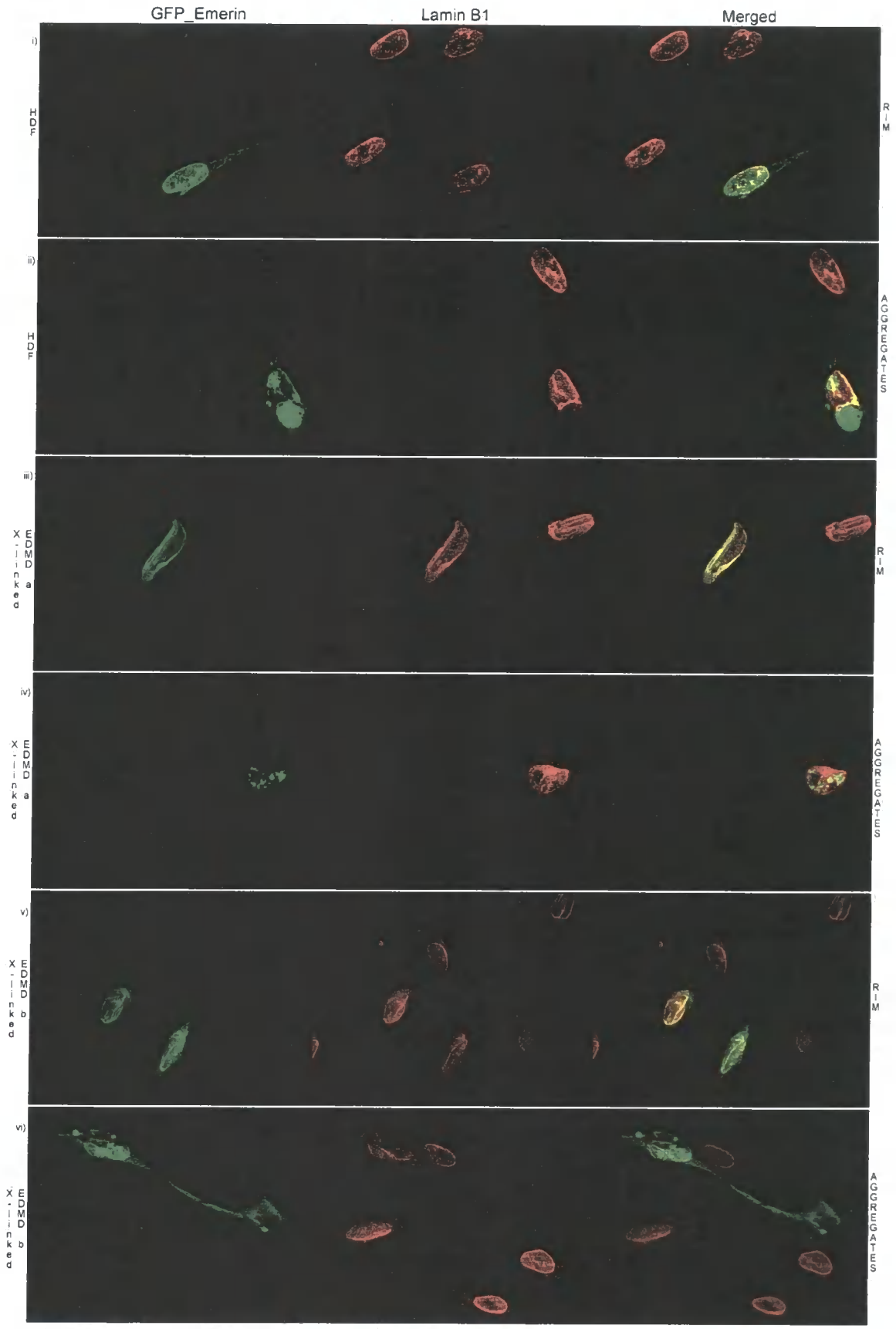
GFP_Emerin
Lamin B1
Merged
i)
HDF
RIM
ii)
HDF
AGGREGATES
iii)
X-linked EDMD a
RIM
iv)
X-linked EDMD a
AGGREGATES
v)
X-linked EDMD b
RIM
vi)
X-linked EDMD b
AGGREGATES

Figure 3.15

Table 3.3

Summary of the transfection/immunofluorecence results. Most relevant observations are highlighted.

		Endogenous Protein Localization							
		Lamin A		Lamin B1		Lamin C		Emerin	
Tagged Protein	Tagged Protein Localization	Control	Patient	Control	Patient	Control	Patient	Control	Patient
GFP-Lamin A	Normal	N/A	N/A	Normal	Normal	Normal	Normal	Normal	N/A
	Aggregates	N/A	N/A	Normal	Normal	**High**	**Low**	**Low**	N/A
DS-Red-Lamin C	Normal	Normal	Normal	Normal	Normal	N/A	N/A	Normal	N/A
	Aggregates	Normal	Normal	Normal	Normal	N/A	N/A	Normal	N/A
GFP-Emerin	Normal	Normal	Normal	Normal	Normal	Normal	Normal	N/A	N/A
	Aggregates	Normal	Normal	Normal	Normal	**High**	Normal	N/A	N/A

Table 3.3

4. Chapter Four - Changes in the distribution of nuclear and cytoplasmic proteins in Autosomal Dominant Emery- Dreifuss muscular dystrophy.

4.1. Introduction

Laminopathies are a group of diseases caused by underlying mutations in the genes encoding Lamins A and C or in their associated proteins (**Cohen et al., 2001; Hutchison et al., 2001; Morris and Manilal, 1999**). Positional cloning revealed that mutations in the gene encoding Lamin A/C (LMNA) or in the gene encoding Emerin (STA, also called EMD) give rise to Emery Dreifuss muscular dystrophy (EDMD). There are three forms of this disease: autosomal dominant or recessive (AD-EDMD and AR-EDMD) are both caused by mutations in LMNA. XL- EDMD caused by mutations in STA display similar phenotypes that are atypical of other muscular dystrophies (**Emery, 2000; Morris, 2000**). The disease starts with stiffness of joints in the neck, elbows and Achilles tendons. Muscle weakness progresses very slowly and the life threatening condition associated with this disease is a conduction block and progressive cardiomyopathy. Five other diseases are related to mutations in LMNA. These include Dilated Cardiomyopathy with Conduction System Disease (DCM-CD) (**Brodsky et al., 2000; Fatkin et al., 1999**), Dunnigan-type Familial Partial Lipodystrophy (FPLD) (**Cao and Hegele, 2000; Shackleton et al., 2000**), a sub-set of Limb Girdle Muscular Dystrophy (type 1B) (LGMD1B) (**Muchir et al., 2000**), Charcot-Marie-Tooth disorder type 2 (AR-CMT2) (**De Sandre-Giovannoli et al., 2002**) and Mandibuloacral Dysplasia (MAD) (**Novelli et al., 2002**). Other recently described disorders involving mutations in the LMNA gene are Hutchinson-Gilford (**Eriksson et al., 2003**) and Werner syndrome (**Chen et al., 2003**).

Lamins A/C and Emerin are components of the nuclear Lamina and the inner nuclear membrane (INM) respectively. Emerin is a type II integral

membrane protein (**Ellis et al., 1997; Manilal et al., 1996; Nagano et al., 1996**) that binds Lamins A/C and B1 (**Clements et al., 2000; Vaughan et al., 2001**), Barrier-to-Autointegration Factor (BAF) (**Haraguchi et al., 2001**), Splicing-Associated Factor YT521-B (**Wilkinson et al., 2003**), Nesprin 1α (**Mislow et al., 2002**), Transcriptional Repressor Germ-Cell-Less (GCL) (**Holaska et al., 2003**) and Actin (**Lattanzi et al., 2003; SEB-Symposia, 2003**) and is anchored to the INM by its C-terminal domain (**Yorifuji et al., 1997**). Lamins A and C are members of the type V intermediate filament proteins (**Fisher et al., 1986; McKeon et al., 1986**). They form part of the nuclear Lamina, a flattened filamentous structure lining the entire face of the INM (**Aebi et al., 1986; Hutchison, 2002**) where they bind to chromatin (**Glass et al., 1993**), Emerin (**Fairley et al., 1999; Vaughan et al., 2001**), transcription and splicing factors (**Dreger et al., 2002; Jagatheesan et al., 1999; Markiewicz et al., 2002a**), histones (**Goldberg et al., 1999**), Nesprin 1α (**Mislow et al., 2002**), Actin (**Sasseville and Langelier, 1998**) and other Lamina Associated Proteins (**Hutchison et al., 2001**).

There is some debate concerning the mechanisms by which mutations in nuclear membrane proteins that are ubiquitously expressed give rise to tissue specific diseases (**Hutchison et al., 2001; Muchir et al., 2000**). Two models have been proposed to explain how disease phenotypes arise. The first, called the structural model, is based upon the fact that Lamins and their associated proteins form a filamentous nucleoskeleton that supports the NE (**Hozak et al., 1995; Zhang et al., 1996**). It has been suggested that mutations in Emerin and Lamins A/C cause structural abnormalities within the Lamina and in turn this causes fragility in the NE particularly in contractile tissues such as skeletal and cardiac muscle (**Fidzianska et al., 1999; Hutchison et al., 2001; Sullivan et al., 1999**). In the second model, it has been suggested that mutations in Emerin and Lamins A/C cause

changes in gene expression, which ultimately promote the pathophysiology of the various diseases (**Cohen et al., 2001; Hutchison, 2002**).

Recent support for the structural hypothesis has emerged in three separate studies using skin fibroblasts from Laminopathy patients. Fibroblasts from FPLD patients displayed characteristic alterations in the distribution of nuclear membrane proteins and Lamins together with "herniations" in the nuclear envelope. In addition, all Lamins displayed increased solubility properties in biochemical assays (**Vigouroux et al., 2001**). In a complementary investigation of fibroblasts from LGMD1B patients, which were null for Lamin A/C, nuclei were misshapen and contained multiple lobules. Lamin B1, the nuclear membrane protein LAP2P and the nucleoporin Nup153 were all excluded from the lobules, whereas Emerin, while mainly located in the ER, was also concentrated in the lobules. The nuclear abnormalities were more apparent in early passage cultures and disappeared at late passages (**Muchir A, 2002**). A third report describes the solubility properties and localization of Lamins and Lamin Associated Proteins in fibroblasts from XL-EDMD patients. All Lamin sub-types displayed increased solubility properties in the absence of Emerin. In addition, Lamin C was redistributed from the nuclear envelope to the nucleoplasm, while the Lamin A/C binding protein LAP2α accumulated in "nuclear caps". However, herniations and lobules were not reported (**Markiewicz et al., 2002b**). Despite the differences in details between these three investigations, all indicate that mutations in Lamins or in Emerin can lead to structural weakness of the nuclear envelope. Given the very different clinical nature of these three diseases, the relevance of structural weakness to the disease etiologies must be questioned.

The lack of experimental evidence to support the gene expression theory in EDMD as a main cause of the disease created a high level of scepticism between

researchers when first proposed, as it is still not understood how nuclear Lamins and/or inner nuclear membrane proteins could be involved in control of gene expression (**Hutchison et al., 2001; Wilson, 2000**). Although yet to be proved, it is clear that A-type Lamins must be in some way involved in the control of gene expression, considering the early reports of the appearance of A-type Lamins in differentiated cell types (**Benavente et al., 1985; Lehner et al., 1987**). Other sources of indirect evidence for the role of A-type Lamins in transcriptional regulation derived from other studies, where the C-terminal of the SIR4 protein in yeast, protein required for transcriptional silencing of the HM mating-type loci, showed a high similarity with a unique 43-aminoacid region of the coil 1b domain of A-type Lamins (**Diffley and Stillman, 1989**). Other studies have shown that expression or changes of Lamin A occurs at differentiation, where certain genes are required to be expressed (**Collard et al., 1992; Lourim and Lin, 1992; Muralikrishna et al., 2001**). Current approaches involving powerful technologies like micro-arrays or proteomics may give rise to new insights in the specific set of genes under the control of A-type Lamins.

Other aspect of great importance to be considered in the pathogenesis of muscular dystrophies is the heterogeneous genetic nature of this group of diseases. Focusing only on EDMD, mutations in the Emerin gene give rise to one phenotype, the XL form of EDMD, and up to six phenotypes are associated with mutations in the LMNA gene (AR and AD-EDMD, LGMD1B, DCM-CD, FPLD, AR-CMT2 and MAD). Routine mutational analysis in patients with a classical EDMD phenotype revealed that only 40% were linked to mutations in the STA or LMNA gene. The other 60 % of the cases clearly indicates that further genes must be involved in EDMD (**Gisele Bonne and al, 2003**). The lack of large families or sufficient numbers of sib pairs have forced the functional candidate gene approach to be taken as a strategy for new linkage or association studies in order to identify other

genes involved in the development of the disease. Genes encoding proteins exclusively expressed in skeletal muscle and heart or those located in the nuclear membrane or Lamina that interact with Emerin or Lamin A/C or have structural similarities to these proteins have been considered as functional candidates, in particular: SMPX (small muscular protein), FLNC (filamin C), LMNB1 (Lamin B1), LMNB2 (Lamin B2), LBR (Lamin B receptor), LAP1 (Lamina-Associated Peptide 1), LAP2 (Lamina-Associated Peptide 2), MAN1 (man1), NRM (nurim), BAF (Barrier-to-Autointegration Factor), PSME3 (Proteasome Activator Subunit 3), DDX16 (DEAD/H-box polypeptide). Monomorphic genes were excluded (SMPX, LMNB2, LAP1 and BAF); intronic variation and frequent single nucleotide polymorphisms (SNPs) were considered not likely to cause the disease phenotype (MAN1, LMNB1, PSME3, LBR were excluded). Partially unique exonic DNA-variations causing amino acid exchanges were found in the remaining genes: FLPC (filamin C), LAP2, NRM (nurim) and DDX16 (DEAD/H-box polypeptide) (Manfred Wehnert in (**Gisele Bonne and al, 2003**)). Other genes will need to be included in these studies like the newly described Actin-binding proteins Nesprins and/or Nuance, members of a giant gene family that will require an extensive experimental effort to analyze their entire sequences in order to find evidences for DNA variations in samples from EDMD patients.

In this study, I investigated structural abnormalities in the nuclear envelopes of fibroblasts from AD-EDMD patients. I found that changes of the type described for FPLD, MAD and LGMD1B were observed in AD-EDMD fibroblasts but the frequency with which they were observed was dependent upon the conditions of fixation. In addition, these structural changes in the nuclear Lamina can be induced by serum starvation/re-stimulation and by over-confluence, which clearly indicates that re-arrangements of the nuclear Lamina may be affected during the intriguing events following exit or re-entrance to the cell cycle, especially in the patients carrying

mutations in the LMNA gene. This raises further doubt as to whether the structural changes described are a primary cause of any Laminopathy. Rather they may reflect fundamental changes in Lamin-Lamin associations, which affect different cells in different ways, but may be increased in the nuclear Lamina of cell lines derived from patients where A-type Lamins are mutated.

In search for new proteins involved in EDMD, I studied Nesprins and HSP70 distribution in EDMD cell lines. I confirmed the experimental evidences described in other studies that Nesprin 1 splicing isoforms, containing the original N-terminal region, might be involved in the interaction with Actin fibres (**Zhang et al., 2002**), an event that may be of special significance for natural and/or disease-induced process involving quiescence. The N-terminal of Nesprin 1α has been shown to be able to bind full length Emerin (**Mislow et al., 2002**), which together with the putative interaction of Nesprin 1 N-terminal with α-S-Actin confirm the theoretical speculations that a macromolecular protein complex may exist in the nucleus that combine Emerin and Actin with other nuclear proteins (Katherine Wilson and Juliet Ellis in (**SEB-Symposia, 2003**)). I also describe here the re-distribution of HSP70 protein in cells derived from EDMD patients under metabolic stress.

4.2. Results

4.2.1. Distribution of Emerin and A and B-type Lamins revealed by methanol: acetone fixation.

In previous investigations, LMNA mutations causing FPLD, LGMD1B and EDMD have been reported to promote abnormalities in the organization and distribution of Lamins and nuclear envelope proteins in fibroblasts (**Muchir A, 2002; Vigouroux et al., 2001**). Moreover, when mutant Lamin A or Lamin C are overexpressed as epitope-tagged proteins in model cell lines they may give rise to abnormal distributions of each protein, including the formation of intra-nuclear aggregates (**Ostlund et al., 2001; Raharjo et al., 2001**). I therefore investigated the distribution of all Lamin sub-types as well as the nuclear envelope protein Emerin and nucleoporins in control and AD-EDMD fibroblasts. Initially, cells were fixed in methanol: acetone and co-stained with anti-Emerin and anti-Lamin C antibodies (Figure 4.1 A). In control cells the vast majority of nuclei were oval shaped. Emerin and all Lamin types displayed a uniform perinuclear staining pattern, in which each protein co-localized with the others (Figure 4.1Ai - Ci). In AD-EDMD cultures, Lamin C displayed a honeycomb like appearance typically orientated towards one pole in 15 - 20% of cells (Figure 4.1A ii and iii Lamin C). The distribution of Lamin C in the remaining cells was identical to controls (Figure 4.1Ai Lamin C). Emerin was also present in the honeycomb structures (Figure 4.1Aii and iii Emerin) where it co-localized precisely with Lamin C (Figure 4.1Aii and iii Merged).

Next I compared the distributions of Lamin C (green) and Lamin B1 (red). Once again Lamin C was organised into honeycomb structures, in as many as 20% of cells in AD-EDMD cultures (Figure 4.1Bii and iii Lamin C). Lamin B1 was relatively depleted from the honeycomb structures (Figure 4.1B ii and iii Lamin B1), and therefore in these areas of the nucleus, Lamin C and Lamin B1 did not co-localise.

In contrast, in control fibroblasts (Figure 4.1Bi) and in AD-EDMD fibroblasts, which appeared normal (not shown), Lamin C and Lamin B1 co-localised throughout the nuclear envelope. Finally, I compared the distribution of Lamin B2 (green) and Lamin B1 (red) (Figure 4.1C). In all experiments, honeycomb structures were observed in ~20% of cells in AD-EDMD cultures. In all instances, there was complete co-localisation between the two B-type Lamins. Since Lamin C and Lamin B1 do not co-localise within the honeycomb I infer that within this structure A and B-type Lamins segregate away from each other. While the honeycomb structures observed in this study were superficially similar to those described in other studies (**Vigouroux et al., 2001**), under the conditions of fixation used here I rarely observed the associated "herniations" described in FPLD fibroblasts. In this study 98% of cells in controls displayed a uniform perinuclear rim for all antibodies used. In 2% of cells, internal staining was observed corresponding to intra nuclear tubes. These are normal structures that have been described previously (**Fricker et al., 1997**).

4.2.2. Distribution of Emerin and A and B-type Lamins revealed by Para-formaldehyde fixation.

To further investigate structural abnormalities in AD-EDMD fibroblasts I performed double immunofluorescence on fibroblast cultures fixed in Para- formaldehyde (PFA) and permeabilized with Triton X-100. In control cultures, Emerin and all Lamin types were uniformly distributed at the nuclear periphery (Figure 4.2 Ai and ii Lamin C (double arrow) and Figures 4.2B - D). Under these conditions of fixation, the nuclear envelope was always defined more discretely than with methanol: acetone fixation, indicating better preservation of the structure. Honeycomb structures were detected in control (Figure 4.2 Ai and ii Lamin C single arrow) and AD-EDMD fibroblasts (Figure 4.2 Bii-iii Emerin and Lamin C, 4.2 Cii-iii Nucleoporin and Lamin C, and 4.2 Dii-iii Nucleoporin and Lamin B1)

fixed with PFA. However, the frequency at which they were observed was <5%. As with methanol: acetone fixation, Emerin (Figure 4.2 Bii-iii Emerin) and Lamin C (Figure 4.2 Bii-iii Lamin C) co-localised precisely within the honeycomb (Figure 4.2 Bii-iii Merged). B-type Lamins were reported to be absent from "honeycomb" structures in LGMD1B fibroblasts that were null for Lamins A/C and FPLD patients with missense mutations in the LMNA gene (**Lattanzi et al., 2003; Muchir A, 2002**). In the study on LGMD1B fibroblasts, the nucleoporin Nup153 co-localised with Lamin B1 and was consequently depleted from the honeycomb structure. To determine whether nucleoporin proteins were depleted from honeycomb structures in the AD-EDMD fibroblasts, cells were co-stained with anti-Lamin C and the XFXG nucleoporin antibody 414 or with anti-Lamin B1 and 414. When the distribution of nucleoporins was compared to Lamin C there was less nucleopore protein within the honeycomb (Figure 4.2 Cii-iii Nucleoporin and Lamin C). When the distribution of nucleoporins was compared to Lamin B1, both types of protein were absent (Lamin B1) or depleted (XFXG nucleoporins) from the honeycomb (Figure 4.2 Dii-iii Nucleoporin and Lamin B1). Thus the distribution and behaviour of proteins in AD-EDMD fibroblasts harbouring Lamin A/C mutations was similar if not identical to LGMD1B fibroblasts where Lamins A/C are null.

To confirm these findings my study was extended to include six AD-EDMD fibroblast cell lines. Comparison of methanol: acetone fixation revealed a higher incidence of honeycombs in five patient cell lines compared to the control. Using PFA fixation, a higher incidence was observed in three out of six patient cell lines (Figure 4.3). To assess the statistical significance of the difference between the fixation methods, I used Wilcoxon-Mann-Whitney Z test for paired-samples using SPSS® 11.1 (for Windows®). All Z values were significant at $p<0.001$, except cell line AD-EDMD 4 ($Z= -2.000$), which was

significant at $p < 0.05$ (Table 4.1). Taken together, these results confirm that by using the strongest fixation method (methanol: acetone), a higher number of structural abnormalities can be displayed at the nuclear Lamina.

4.2.3. Lamins expression and conformation in AD-EDMD.

In this study, fibroblasts from four AD-EDMD patients with LMNA mutations were investigated. Two cell lines had mutations, one in the rod (R249Q) and the other one in the tail domain (R401C). I did not have the DNA sequencing data for the other two AD-EDMD cell lines at the time of writing this thesis. The two of them had been sent to our lab from Poland.

In a previous investigation a LMNA mutation Y259X giving rise to LGMD1B was shown to promote haplo-insufficiency for Lamins A/C in the heterozygote and a null phenotype in the homozygote (**Muchir et al., 2003**). In order to investigate whether LMNA causing AD-EDMD had similar effects and honeycomb structures could arise from re-arrangements of the nuclear Lamina, I compared the level of expression of Lamins A/C in each patient cell line to an age-matched control under reduced and non-reduced conditions. Since one mutation introduced a cysteine residue into the tail domain (R401C), I investigated the possibility that this would permit aberrant disulphide bond formation between Lamin polypeptides or with other proteins.

Therefore cell extracts were prepared from control and patient cell lines for immunoblotting, treated with the alkylating agent NEM to trap disulphide linked proteins and resolved on SDS-PAGE under reducing and non-reducing conditions. Levels of expression of Lamin C were similar in each cell line (Figure 4.4 A and B), while Lamin A was particularly expressed at a higher level in the cell line that presented the mutation in the rod domain (R249Q) of Lamin A (Figure 4.4 A, lanes 2 and 8). When cell extracts were resolved under non-reducing conditions, there

was no evidence of cross-linking between Lamin polypeptides (Figure 4.4 A and B). As a positive control for cross-linking through cysteine residues, the same samples were probed with antibodies against the E.R. protein, PDI (**Benham et al., 2000**). Intermediate disulphide bonded complexes were clearly obtained under non-reducing conditions, as expected (Figure 4.4 C).

While this evidence does not rule out the possibility that mutations introduce conformational changes in the Lamins, this data suggests that mutations introducing new cysteine do not lead to synthesis of unstable proteins and the residue does not permit unusual disulphide bond formation between Lamin polypeptides or with other proteins in the nuclei.

4.2.4. Lamina assembly may be affected in G1 → GO → G1.

Normal cells usually cease to proliferate in a cell-cycle-specific way. They arrest in G1 or enter a state of quiescence (GO) from G1 after depletion of serum or growth factors (**Pardee, 1974; Temin, 1971**) or nutrients (**Prescott, 1976**) or after cell crowding (**Nilausen and Green, 1965; Zetterberg and Auer, 1970**). Previous studies carried out in our lab have shown the dynamics of the nuclear Lamina in quiescence and re-stimulated normal human dermal fibroblasts (**Dyer et al., 1997**). These studies have suggested that in cells induced to exit the cell cycle, the steady-state of the nuclear Lamina changes probably due to biochemical modifications or re-arrangements of A-type Lamins, evidenced by the change in availability of epitopes for monoclonal antibodies against Lamin A and/or C.

Based on this evidence, I set up experiments to further investigate whether the honeycomb structures observed in the AD and XL-EDMD cell lines with different fixation methods were an artefact of the staining procedures or represented a real change in the nuclear Lamina, related to a particular stage of the cell cycle. Exponentially growing fibroblasts from a healthy donor (control HDF), AD and XL-

EDMD patients were serum starved for 5 days and then re-stimulated with fresh media containing 10% NCS. After 30 hour, cells were fixed with 3.5% Para-formaldehyde and stained with anti-Lamin A/C and anti-Emerin antibody at mid passages and late passages. AD-EDMD fibroblasts showed the higher amount of honeycombs compared to the control and XL-EDMD (Figure 4.5)

At mid passages, in control and X-linked fibroblasts, the great majority of the nuclei presented normal staining for Lamin C (Figures 4.6 and 4.7 A - C i and iii), Emerin (Figures 4.14 and 4.16 A - C i and iii) or Lamin A/C (Figures 4.15 and 4.17 A - C i and iii) at the nuclear rim, with honeycomb structures present at very low percentages (2-3%) in proliferative, quiescence and re-stimulated cultures. In contrast, the number of honeycomb structures in the AD-EDMD cell line was increasingly altered as cells progressed from proliferating to quiescent and back to a proliferating state with Lamin C (Figures 4.6 and 4.7 C ii), Emerin (Figures 4.14 and 4.16 C ii) and Lamin A/C (Figures 4.15 and 4.17 C ii). Other studies have shown that inducing quiescence by over-confluence also increases the amount of honeycomb structures in the nucleus of AD-EDMD cell lines in 3 fold (Chris J. Hutchison, Personal Communication). In all cases, wherever a honeycomb structure was present, lack of chromatin was observed in the area, highlighted by the DAPI staining, as reported previously.

Late passage cultures showed honeycomb structures as well when cells were stained with anti-Emerin or anti-Lamin A/C antibodies. But in this case, the amount of honeycombs in the AD-EDMD cultures was less than in the growth inhibition experiments (Figures 4.18 and 4.19 Band C).

4.2.5. Indirect evidence for cytoskeleton re-organization: Heat Shock Proteins distribution.

Diverse physiological stresses like heat, hemodynamics, mutant proteins and

oxidative injury, produce multiple changes in a cell that ultimately affect protein structure and function. Under these circumstances, molecular chaperons (for example heat shock proteins, HSPs) actively participate in a cascade of cellular events, including cytoprotection. In the case of disease states caused by expression of mutant proteins, elevated levels of misfolded or denatured proteins are potent inducers of HSPs gene expression (**Ananthan J et al., 1986; Benjamin and DR, 1998**). Conceivably, mutations in Lamins or other proteins might be considered as a source of stress in Laminopathies, so potentially heat shock proteins can be expressed or re-distributed. As metabolic stress is not known as a stimulus to induce heat shock proteins expression, I decided to test the distribution of some members of this family of proteins in AD-EDMD fibroblast harbouring missense mutations in the rod and tail domain of the filaments, throughout exit and re-entrance to the cell cycle induced by serum starvation.

Human dermal fibroblasts from a healthy donor, AD-EDMD (R401C) and XL-EDMD were used at mid passage. Proliferating cultures at 60% confluence were serum starved for 5 days using media containing 0.5% NCS. On day five, fresh media containing 10% NCS was added and cells were allowed to grow for 30 hours before fixation with 3.5 % PFA and staining with anti-HSP27 (green) and anti-Lamin C (red) antibodies.

In proliferating cells (Figure 4.6 A), HSP27 was localized into a homogeneous pattern within the cytoplasm in all cell lines. No significant staining was observed in any nucleus. During quiescence, morphological changes in cell shape were accompanied by re-location of HSP27 into fibres throughout most of the cytoplasm, but a homogeneous pattern remained in the perinuclear space with no significant difference between cell lines. The nucleus remained partially negatively stained for HSP27 (Figure 4.6 B). Re-stimulation produced a re-distribution of

HSP27 to the homogeneous pattern observed in the proliferative stage, with an increased intensity in the signal for the heat shock protein (Figure 4.6 C).

Other members of the family of the Heat Shock Proteins have been described to be altered in many diseases, including cardiovascular disorders. One of these members that have been studied in more details is HSP70 (**Benjamin and DR, 1998**). To further analyze whether this protein is affected in EDMD patients and/or is involved in the re-arrangements of the nuclear Lamina observed in the EDMD cell lines, samples were double stained with anti-HSP70 (green) and anti-Lamin C (red) antibodies (Figure 4.7). Proliferating cultures showed a homogenous diffuse pattern of staining within the cytoplasm in all cell lines (Figure 4.7 A). The nucleoplasm of AD-EDMD cells contained more HSP70 than the control or the XL-EDMD samples (Figure 4.7 A ii). When cells were serum starved for 5 days (Figure 4.7 B), morphological changes were accompanied with HSP70 redistributed strongly to the outer perinuclear space in 74% of the AD-EDMD cells (Figure 4.71 B ii), while the control and the XL-EDMD cell lines showed a weak re-distribution in only 3 and 6 % respectively. The presence of nuclear HSP70 staining was reduced compared to proliferating cultures. Re-stimulated cells showed a re-location of HSP70 into the homogeneous pattern observed during proliferation (Figure 4.7 C), but 24 % of the XL-EDMD cells displayed perinuclear localization. HSP70 staining re-appeared in the nucleoplasm of AD-EDMD cells (Figure 4.7 C ii).

Are HSP70 expression levels altered in AD-EDMD patients? To answer this question, I determined the levels of expression of HSP70 in proliferating cultures of AD-EDMD cell lines. Cell extracts were prepared from control and patient cell lines resolved on SDS-PAGE, transferred and immunoblotted (Figure 4.8). Levels of expression of HSP70 were almost identical in each cell line, suggesting that the increased levels of HSP70 in the quiescence AD-EDMD cultures might be due to re-

location of its cytoplasmic pool into the nuclei or induction of HSP70 expression, rather than due to differences in protein content.

It is well known that chaperones interact with several members of the cytoskeleton and influence their organization. During quiescence-induced metabolic stress, an abnormal re-arrangement of HSP70 to the Endoplasmic Reticulum (ER) occurred at the exit (AD-EDMD cells) or re-entrance (XL-EDMD cells) to the cell cycle, which resembled the rearrangement of Nesprin 2 (N-terminal) in cultures under metabolic stress. Taking together, this data implies that probably there is a stress response due to the mutations in the Lamins, Nesprins and/or others (it did not happen in the controls), where HSP70, but not HSP27 accumulates in the ER to execute a cytoprotective pathway at a critical cell cycle checkpoint in fibroblasts from EDMD patients.

4.2.6. Nesprin 1 N-terminal co-localizes with the distribution of α-S-Actin fibres in skin dermal fibroblasts.

The observed changes in the frequencies of occurrence of honeycomb structures in response to serum starvation or confluence indicated that honeycombs may arise as a result of stress. In addition, my early observation in skin dermal fibroblasts under a phase contrast microscope revealed a high frequency of very large and flattened cells derived from AD-EDMD and X-linked patients when compared to controls (Figure 4.9, arrows). In my very first Nesprin single staining in human fibroblasts, the anti-Nesprin 1 N5 antibody (specific for the N-terminal of Nesprin 1) produced a characteristic phenotype in a sub-population of cells resembling the distribution of α-S-Actin in other cell types.

Together, these data indicate that EDMD fibroblasts may be subject to stress-related responses which involve not only the nucleoskeleton but also the cytoskeleton. To investigate this possibility, I studied the distribution of Nesprins

1 and 2 in human fibroblasts. Nesprins were selected because they are giant spectrin-repeat proteins which link the nuclear Lamina to the Actin cytoskeleton (**Zhang et al., 2001; Zhen et al., 2002**); therefore they are potentially candidate markers for stress-related reorganization of nucleo-cytoskeleton in response to growth inhibition. With this in mind, I used double immunofluorescence with anti-α-S-Actin and Nesprin 1 N5 antibody (specific for the N terminal of Nesprin 1) or Nesprin 2 CH3 antibody (specific for the N terminal of Nesprin 2) to investigate whether or not Nesprins and α-S-Actin where present in the same fibres.

Skin dermal fibroblasts derived from a healthy donor, EDMD patient and rat were stained with anti-α-S-Actin (green) and anti-Nesprin 1 N5 antibodies (red) (Figure 4.10 A). Very large and flattened cells were observed in all cases, in which α-S-Actin perfectly co-localized with antibodies against the N terminal of Nesprin 1. Nesprin 1 labelled with this antibody showed a homogeneous-diffuse pattern in the nucleoplasm in normal spindle/shaped cells. Parallel samples were double stained with α-S-Actin (green) and anti-Nesprin 2 CH3 antibodies (red) (Figure 4.10 B). Nesprin 2 CH3 produced nuclear signal excluding nucleoli in human cells (Figure 4.10 B i - ii, Nesprin2 CH3). Rat nuclei presented a diffuse pattern through the nucleoplasm (Figure 4.10 B iii Nesprin2 CH3). In all cases, Nesprin 2 C-terminal never co-localized with α-S-Actin fibres when present in the cytoplasm. α-S-Actin positive cells always had a large flattened shape, resembling the phenotype of non-migrating senescent cells.

Nesprin gene family was originally identified in search for Vascular Smooth Muscle Cell (VSMC) differentiation markers (**Zhang et al., 2001**). In association with a number of diseases, VSMC becomes functionally impaired, when made quiescent. To further investigate whether the distribution of Nesprin 1 fibres was related or not to the cell cycle, in particular to quiescence, human dermal fibroblasts from a

healthy donor, AD-EDMD (R401C) and XL-EDMD were analyzed (Figure 4.11). Proliferating cultures at 60% confluence were serum starved for 5 days using media containing 0.5% NCS. On day five, fresh media was added and cells were allowed to grow for 30 hours before fixation with 3.5 % PFA and staining with α-S-Actin (green) and Nesprin 1 N5 (red) antibodies.

In proliferating cultures (Figure 4.11 A) heterogeneous patterns of Nesprin 1 and α-S Actin positive cells were observed. In some cells, Nesprin 1 co-localized with α-S-Actin stress fibres (Figure 4.11 A i and iii, single arrows). In other cells, stress fibres were absent and Nesprin 1 was distributed at the nuclear envelope and diffusely through the cytoplasm (Figure 4.11 i double arrows). In a third class of cells, Nesprin 1 partially co-localized with α-S-Actin stress fibres but was also concentrated in the nucleus. This third class of cells was found predominantly in the AD-EDMD cell line (Figure 4.11 A ii, triple arrows).

Induction of quiescence by serum starvation caused almost all cells in control and AD-EDMD cultures to adopt shapes that were reminiscent of cells having α-S-Actin stress fibres in proliferating cultures. In contrast, a significantly high number of cells in XL-EDMD cultures maintained a bipolar shape. All cultures showed a dramatic re-distribution of Nesprin 1 towards the plasma membrane that co-localized with re-distribution of α-S-Actin. In control and XL-EDMD cells, Nesprin 1 re-location to the plasma membrane was independent of the expression of α-S-Actin (Figure 4.11 B i and iii, arrows). In AD-EDMD cells, the vast majority of the cells were positive for Nesprin 1 and α-S-Actin, with both co-localising strongly towards the edge of the cells (Figure 4.11 B ii, arrows). After serum re-stimulation, staining patterns for both α-S-Actin and Nesprin 1 antibodies reverted to the distributions reported previously for proliferating cultures (Figure 4.11 C and see Figure 4.10 A and B).

Parallel samples from the same cultures were double stained with anti-α-S-Actin (green) and anti-Nesprin2 (N terminal) (red) antibodies (Figures 4.12 A - C). In all cases, Nesprin 2 N-terminal was always absent from α-S-Actin fibres. Its localization, as in previous experiments (Figure 4.10 B), was strong in the nucleus, but clearly absent in the nucleoli.

In proliferating cultures (Figure 4.12 A), Nesprin 2 produced a diffuse cytoplasmic stain in all cell types. As cells became quiescent, there was a shift of cytoplasmic Nesprin 2 towards the perinuclear space in a high percentage of the AD-EDMD (Figure 4.12 B ii). In XL-EDMD cells (Figure 4.12 B iii), but not in the controls (Figure 4.12 B i), the shift appeared to occurs from the nucleoplasm, as the nucleoplasm staining was weaker. As in previous experiments, most of the AD-EDMD cells showed α-S-Actin re-distributed to the edges of the plasma membrane and the shape of the cells was large and flattened. Some XL-EDMD fibroblasts remained resistant to change their shape (Figure 4.12 B iii). In all cell types, following re-stimulation of the cultures, Nesprin 2 relocated to the nucleus and to the cytoplasm as in proliferating cultures (weak background) (Figure 4.12 C). Cells recovered their original shape, but still the control and AD-EDMD cultures showed a higher fraction of α-S-Actin positive cells (Figure 4.12 C ii), which was absent in XL-EDMD fibroblasts (Figure 4.12 C iii).

Since Nesprin 1 N-terminal clearly re-distributes in response to entry and exit from a quiescent state, I investigated whether this also happens during "natural" cell aging or senescence. Fibroblasts from a healthy donor and AD-EDMD patient (R401C) were grown through serial passage to generate senescent cells. Control fibroblasts became senescent at passage 40, while AD-EDMD fibroblasts became senescent at passage 45. Cultures were double labelled with anti-α-S-Actin (green) and anti-Nesprin 1 N5 (red) antibodies. In both cases, large and flattened

cells predominated in senescent cultures, with a higher percentage in the patient cell line. Senescent cells resembled both in shape and in the distribution of α-S-Actin and Nesprin 1 those quiescent cells induced by serum starvation. The vast majority of the patient cells displayed double positive fibres for α-S-Actin and Nesprin 1 N-terminal (Figure 4.13 A i-ii). When senescent cells were co-stained with anti-α-S-Actin and Nesprin 2 (N terminal), there was no co-localization between the two antibodies. However, as in quiescent cells, cytoplasmic Nesprin 2 became concentrated at the perinuclear space in AD-EDMD cells, and absent in the nucleoli (Figure 4.13 B i-ii).

4.2.7. C-terminal of Nesprins during proliferation, quiescence and re-entrance to the cell cycle.

To further investigate the significance of growth-related changes in Nesprin distribution, I performed immunofluorescence on human fibroblasts with antibodies specific for the C-terminal of Nesprins 1 and 2. As previously, proliferating cultures at 60% confluence were serum starved for 5 days using media containing 0.5% NCS. On day five, fresh media was added and cells were allowed to grow for 30 hours before fixation with 3.5 % PFA and staining with anti-Emerin (green) and Nesprin 1 C1 (C-terminal)(red) antibodies (Figure 4.14 A - C) or anti-Lamin A/C (green) and anti-Nesprin 1 C1 (C-terminal)(red) antibodies (Figure 4.15 A-C).

Nesprin 1 produced a heterogeneous weak-diffuse pattern in both the nucleus and the cytoplasm in the control (Figure 4.14 A - C i) and in the patient cell lines (Figure 4.14 A - C ii - iii). Nesprin 1 antibody never rendered fibre-like structures. A slightly stronger signal in the nucleus of the AD-EDMD cell line was observed (Figure 4.14 and 4.15 A ii). No cell-cycle dependent re-distribution occurred.

Parallel cultures were double stained with anti-Emerin (green) and Nesprin 2

N2(C-terminal)(red) antibodies (Figure 4.16 A - C) or anti-Lamin A/C (green) and anti-Nesprin 2 N2 (C-terminal)(red) antibodies (Figure 4.17 A - C). The nuclear distribution pattern of Nesprin 2 C-terminal was not as evident as for Nesprin2 N-terminal at different stages of the cell cycle. However, as with the N-terminal antibody, there was a relatively higher amount of Nesprin 2 C-terminal in the nucleus of the cell lines derived from EDMD patients (Figures 4.16 A ii-iii, 4.16 B ii-iii and 4.17 A ii-iii), compared to controls.

Control and AD-EDMD fibroblasts were grown to late passages and double stained with anti-Emerin (green)/Nesprin 1 C1(C-terminal)(red) antibodies (Figure 4.18 B) or anti-Lamin A/C (green)/anti-Nesprin 1 C1 (C-terminal)(red) antibodies (Figure 4.18 C). As in the previous experiments, the Nesprin 1 C-terminal antibody produced a diffuse staining pattern throughout the cell with some concentration of the signal in the patient cell line. Staining of stress fibres was not observed (Figures 4.18 B ii and 4.18 C ii). Almost identical results were obtained with antibody specific for Nesprin 2 C terminal (Figures 4.19 B - C).

4.2.8. Expression of Nesprins in human fibroblasts.

Next I investigated the expression pattern of Nesprin 1 in AD-EDMD cell lines on Western Blots. Similar experiments for Nesprin 2 were not set up due to the higher amount of isoforms recognised by anti-Nesprin 2 antibodies on Western Blots.

Cell extracts from control and three AD-EDMD cell lines were used at mid and late passage. Extracts were resolved on 10% SDS-PAGE and blotted with either Nesprin 1 C-terminal or Nesprin 1 N-terminal antibodies (Figure 4.20 A - B respectively). A complex pattern of staining was observed in each instance. With Nesprin C terminal antibody, bands with molecular weights of 250 KDa, 140 kDa, 95 kDa, 52 kDa, 40kDa and 21 kDa were predominantly detected. The 140 kDa species (Figure 4.20 A *) was only detected in mid passage AD-EDMD cultures. The 52

kDa species (Figure 4.20 +) was detected strongly in AD-EDMD cultures at mid and late passage. The 21 kDa species was detected in control and in AD-EDMD cultures at mid passage but was absent from all cultures at late passage.

The predominant species detected by Nesprin 1 N terminal antibody migrated at ~ 250 kDa, 240 kDa, 78 kDa, 60 kDa, 51 kDa 45 kDa and 35 kDa. Again differences in expression level between AD-EDMD and control were observed as well as differences between passage numbers. The ~78 kDa species (Figure 4.20 B *) was expressed more strongly in mutation R249Q than in any other cell line and was absent from late passage control cell line. In addition, the ~45 kDa (+) and ~35 kDa (•) (Figure 4.20 B) were expressed more strongly in mid passage cultures of all cell lines compared to late passage cultures.

4.2.9. Aging in AD-EDMD cultures.

Data shown previously in this chapter has indicated that the expression and distribution patterns of Nesprin 1, normally associated with a senescent phenotype, occurs in mid passage culture of AD-EDMD fibroblasts. This may be explained if AD-EDMD fibroblast age prematurely in culture. To test this hypothesis, I established a simple experiment to compare the proliferation index of three AD-EDMD cultures with an age matched control through serial passage.

Cells were grown from passage 14 onwards, and stained with the proliferation marker ki67. Two hundred cells were counted randomly in duplicate samples and in replicate experiments. Results were expressed in percentage of ki67 positive cells at each passage (Table 4.2). At passage 15, all cultures displayed indices of proliferation between 62 -82 %. The proliferation index of control cultures had declined to 10 % by passage 38. In contrast, two AD-EDMD cultures (R249Q and R453W) had proliferation indices of 0% at passage 25. A third AD-EDMD culture (R401C) had a proliferation index of 40% at passage 45. Taken together, these

results might indicate that some AD-EDMD fibroblasts can enter a senescent state at twice the rate of age matched controls.

4.3. Discussion

In this chapter, I reported changes in the distribution of lamins, nuclear membrane proteins, nucleoporins and cytoplasmic proteins in fibroblasts from AD and XL-EDMD patients. In the case of AD-EDMD cell lines, the presence of mutations in different regions of Lamin A/C apparently lead to haploinsufficiency or high expression of A-type Lamins since their levels were differentially expressed when compared to control fibroblasts. Apparently, mutations gave rise to similar changes in the distribution of Lamins, nuclear membrane proteins (Emerin) and nucleoporins in immunofluorescence. These changes resulted in the detection of A-type Lamins and Lamin binding proteins (Emerin) within a honeycomb structure orientated to one pole of the nucleus. B-type Lamins and nucleoporins were either absent or depleted from these structures. The appearance of the structures detected by immunofluorescence varied with fixation procedure but not with passage number, and they were induced by metabolic stress.

Similar structures have been reported in two other diseases, which involve mutations in the LMNA gene, namely FPLD and DCM-CD (**Muchir A, 2002; Vigouroux et al., 2001**). The variation in frequency of the structures with fixation procedure reported here reflects the extreme conditions of the methanol: acetone method compared to PFA. This must reflect underlying weakness in the nuclear Lamina and therefore a decreased resistance to chemical stress. Thus, in this study the use of harsh fixation procedures (methanol: acetone) generates the structures at a higher frequency than does by using mild fixation procedures (PFA). To my knowledge, this is the first study interconnecting critical changes in the distribution of Lamins, Nesprins and HSPs at the exit and re-entrance of the cell cycle, which might reflect the cell dynamics at early stages of the embryonic development in

AD-EDMD patients.

4.3.1. The representation of different Lamins in honeycomb structures implies a disruption of Lamin-Lamin associations in the presence of LMNA mutations.

One of the most striking features of this and previous studies (**Vigouroux et al., 2001**) is the segregation of A-type from B-type Lamins into different parts of the nuclear envelope in the presence of LMNA mutations. Depletion of B-type Lamins from one pole of the nuclear envelope also occurs in the complete absence of A-type Lamins (**Muchir A, 2002**). These changes in behaviour of Lamins have two important implications for Lamin associations in the nucleus. First the absence of B-type Lamins from the honeycomb implies that in the absence of A-type Lamins or in the presence of mutant Lamins A or C, B-type Lamins may form closer associations with other structures in the nucleus or nuclear envelope (for example chromatin or NPCs). Presumably, these associations now determine the distribution of B-type Lamins in the nucleus. For example, it has been reported previously that chromatin is depleted from honeycomb structures in the nucleus (**Muchir A, 2002**). If the association of B-type Lamins and peripheral chromatin in Laminopathy fibroblasts is tighter than in normal fibroblasts, it is self evident that B-type Lamins will be observed in regions of the nucleus where chromatin is concentrated and absent from regions where chromatin is depleted. The co-segregation of NPCs with B-type Lamins is expected because NPCs are anchored to Lamin filaments through interactions between the nucleoporin Nup153 and B-type Lamins (**Hutchison, 2002; Smythe et al., 2000; Walther et al., 2001**).

A second implication of this and previous studies, is that LMNA mutations lead to an aberrant clustering of A-type Lamins in the absence of B-type Lamins. In previous studies it has been reported that A-type Lamins are normally incorporated into existing B-type Lamin filaments (**Dyer et al., 1999;**

Hutchison et al., 2001). Within honeycombs, A-type Lamins are present in the absence of B-type Lamins. While it is an assumption these A-type Lamins are organized into filaments, the presence of the Lamin A/C binding protein Emerin in the honeycomb supports this assumption. These observations imply that mutations in the rod and tail domain abrogate the dependency for Lamins A/C to form filaments through association with B-type Lamins but do not disrupt Lamin-Emerin associations. At present I can only speculate as to the mechanism by which this occurs. The most obvious mechanism is that both types of mutation lead to weakened interactions between A-type and B-type Lamins, which causes them to polymerize independently. Alternatively, the mutations alter A-type Lamins-chromatin interactions, which may in turn promote the assembly of homotypic A-type Lamin filaments in areas of the nucleus depleted of chromatin.

A third possibility might derive from the incorporation pathway of individual A-type Lamins into the existing B-type Lamina after mitosis. The smallest soluble oligomers of intermediate filaments detected in vivo and in vitro were tetramers (**Quinlan et al., 1984**). If A-type Lamins incorporate as tetramers (or dimers) into the pre-assembled B-type Lamina, and if the mutation is heterozygous, one might expect a random mixture of normal A-type Lamins and their mutant counterparts in the oligomers. The heterozygosity of the A-type Lamins homo-oligomers might then cause a change in the tertiary structure of the complexes that compromise its interaction with B-type Lamins polymers, segregating these subunits from a normal Lamina, and facilitating the formation of A-type Lamins homo-filaments and its accumulation in one pole of the nuclei. The co-localization of ectopic-mutant Lamin A with endogenous-wild type Lamin C supports this hypothesis (**Favreau et al., 2003**).

4.3.2. Interconnecting cytoplasmic and nuclear abnormalities at the exit and re-entrance to the cell cycle in EDMD fibroblasts.

The effect of serum deprivation on the cell cycle and the down-stream events regulating gene expression and protein concentration in G1→ GO → G1 has been well documented (**Pardee, 1974; Temin, 1971**). Serum starved and re-stimulated human fibroblasts have shown changes in the distribution of A-type Lamins, revealed by epitope masking at several points along the filament in quiescent and re-stimulated cells, as a result of protein phosphorylation, Lamin-Lamin or Lamin-chromatin interactions, or specific binding to unidentified nuclear partners (**Dyer et al., 1997**). In this chapter I report structural changes at the exit/re-entrance to the cell cycle in AD-EDMD fibroblasts harbouring mutations in the LMNA gene that might be related to a nuclear checkpoint at these cell cycle events.

The role of Nesprins during G_0 stage of the cell cycle it is one of the interesting findings of my study in normal and EDMD human skin dermal fibroblasts. Nesprins were originally isolated from a cDNA library of vascular smooth muscle cells (VSMCs) in search for a marker of differentiation (**Zhang et al., 2001**). The critical redistribution of Nesprin 1 (N-terminal) and its co-localization with α-S-Actin, and redistribution of Nesprin 2 (N-terminal) during exit and entrance to the cell cycle in human dermal fibroblasts revealed the value of Nesprins as markers for differentiation not only in humans but as a conserved pathway in other species (rat). In addition, proliferating cultures of human fibroblasts harbouring mutations in the LMNA gene appeared to present a senescent phenotype in a higher percentage of cells compared to the controls, and an altered pattern of Nesprins expression, suggesting a possible implication of Nesprins in EDMD an revealing a possible involvement of an aging process in vitro. A recent investigation have demonstrated that Nesprin 1α N-terminal binds Emerin and its C-terminal binds Lamin A (**Mislow et al., 2002**).

Compiling our experimental evidences in the cell cycle experiments, increased percentage of Nesprin 1 (N-terminal) fibres, co-localization of Nesprin 1 (N-terminal) with α-S-Actin during quiescence, and re-distribution of the original pool of HSP70 and Nesprin 2 (N-terminal) towards the perinuclear space in cells derived from AD-EDMD patients might well be interconnected events, rather than isolated experimental records. These data might reflect underlying conveying processes that affect in some way the overall homeostasis of the early events involved in the development of the heart and skeletal muscle in patients carrying mutations in the LMNA gene, yet to be considered the main cause of the disease, or part of the plethora of cumulative genetic defects.

I conclude that nuclear Lamina abnormalities described here in AD-EDMD fibroblasts but previously reported in FPLD, XL-EDMD, LGMD and MAD fibroblasts (**Muchir A, 2002; Novelli et al., 2002; Vigouroux et al., 2001**) might well reflect the steady-state of nuclear Lamins in EDMD patient cells in a proliferative state or G1→GO→G1, rather than artefacts due to the fixation methods. Defective Lamina (honeycomb structures) can be induced by serum starvation or over-confluence, both in vitro manipulations that end up in exit from the cell cycle to a G_0 stage, where critical interactions between nuclear proteins (Lamin-Lamins, Lamins-other partners, or Lamin-independent interactions) may affect key elements in the cellular program to re-enter the cell cycle at G1.

4.3.3. Implications for disease.

The structural defects reported here (honeycomb structures) are similar to structural defects reported in other diseases caused by mutations in LMNA, namely FPLD and LGMD1B (**Muchir A, 2002; Vigouroux et al., 2001**). While LGMD1B shares certain pathophysiological features in common with EDMD, FPLD is distinctly different. Its major phenotype is an absence of white fat from the trunk,

deposition of white fat around the neck and secondary type II diabetes. Given that FPLD mutations affect adipocytes, whereas EDMD and AD-EDMD mutations affect skeletal and cardiac muscle it seems unlikely that the structural changes in nuclear envelope morphology and organisation reported here are the primary causes of these diseases. The mechanical stress to which adipose tissue is exposed it is minimal compared to heart or skeletal muscle. As indicated above, the structural changes occur as a result of changes in the organisation and association of A-type and B-type Lamins in the cell. These changes give rise to structural weakness (as revealed in this study) and altered associations between Lamins and chromatin and Lamins and NPCs. Moreover, in a recent investigation of the organisation of nuclear envelope proteins in XL-EDMD fibroblasts, the formation of honeycomb structures was not an obvious feature; instead the major defect observed was a redistribution of Lamin C from the nuclear envelope to the nucleoplasm (**Markiewicz et al., 2002b**).

The results of this study were very similar to the results reported in other studies. Munchir and co-workers also found that in XL-EDMD fibroblasts, the major change was a redistribution of A-type Lamins from the nuclear envelope to the nucleoplasm. They also reported that mutations in the tail domain promoted the formation of honeycomb structures and that B-type Lamins were absent from these structures. They did not report the presence of honeycomb structures in fibroblasts harbouring LMNA mutations in the rod domain. However, the mild fixation conditions (Para-Formaldehyde) used in their study might not reveal a honeycomb in these cells (**Muchir et al., 2003**). Since the phenotypes of the X-linked form of EDMD are almost identical to those of AD-EDMD, the current and previous findings (**Markiewicz et al., 2002b**) together with those of (**Muchir A, 2002**) suggests that the presence of honeycomb structures are indicative of underlying causes of disease rather being the primary cause. I propose that change in

Lamin-Lamin and Lamin-chromatin associations are promoted by all Laminopathy mutations. In skeletal muscle, evidence that weakness of the nuclear envelope leads to damage has been presented in XL-EDMD patients (**Fidzianska et al., 1998; Markiewicz et al., 2002b**) but is as yet missing in other tissues. The obvious explanation for physical weakness of the nuclear envelope promoting pathology in skeletal muscle is that in these cells, nuclei are close to the plasma membrane and are therefore more acutely subjected to the stress of muscle contractions. In adipocytes, nuclei are located centrally in the cell and the cells neither contract nor are they motile. Therefore weakness in the nuclear envelope may be inconsequential in adipocytes.

Changes in Lamin-chromatin interactions are likely to affect gene expression (**Hutchison, 2002**). Again I propose that changes in Lamin-chromatin interactions are promoted by all Laminopathy mutations. I further propose that altered gene expression contribute to pathology in all Laminopathies. However, it seems likely that in some Laminopathies altered gene expression is the sole basis of the pathology (e.g. FPLD), whereas in other Laminopathies (e.g. EDMD) a combination of physical damage caused by a weak nuclear envelope together with altered patterns of gene expression both contribute to the pathology. Use of DNA expression profiling in model systems should help to address this hypothesis.

Changes in Lamin-Lamin or Lamin-binding partners associations are likely to result in physical weakness of the NE in all EDMD cases but this weakness may only contribute to pathology in some cells. With this in mind, and considering the data obtained from the cell cycle experiments, I suggest that the physical weakness of the NE and the Lamina is particularly important during early differentiation events in skeletal and heart muscle during embryogenesis. At this stage, precise positioning of the Lamin filaments may orchestrate key control of gene expression

directly or indirectly, which may produce a general failure to maintain a homogeneous population of "healthy post-mitotic cells". This might be the beginning of a chain of events that ends in abnormal development of affected tissues in EDMD by the childhood.

Figures Chapter 4

Figure 4.1

Exponentially growing cultures of fibroblasts were fixed in methanol: acetone 1:1 (v/v). Dual labeled cells were imaged sequentially in the FITC and TRITC channels using a MicroRadiance 2000 confocal microscope (BioRad). Central sections were projected as individual colors or as merged overlays (a, b and c merged). Control is shown in panel a, AD-EDMD fibroblasts are shown in panel b (R249Q) and c (R401C). The percentage of cells displaying normal or honeycomb morphology was calculated by counting two hundred cells each on duplicate slides. Scale bar =10 μm.

A. Double staining with anti-emerin and anti-Lamin C antibodies

B. Double staining with anti-Lamin C and anti-lamin B1 antibodies

C. Double staining with anti-lamin B2 and anti-lamin B1 antibodies


Emerin
Lamin C
Merged
i) HDF
ii) AD-EDMD R249Q
10 uM
iii) AD-EDMD R401C

Figure 4.1 A

Figure 4.1 B

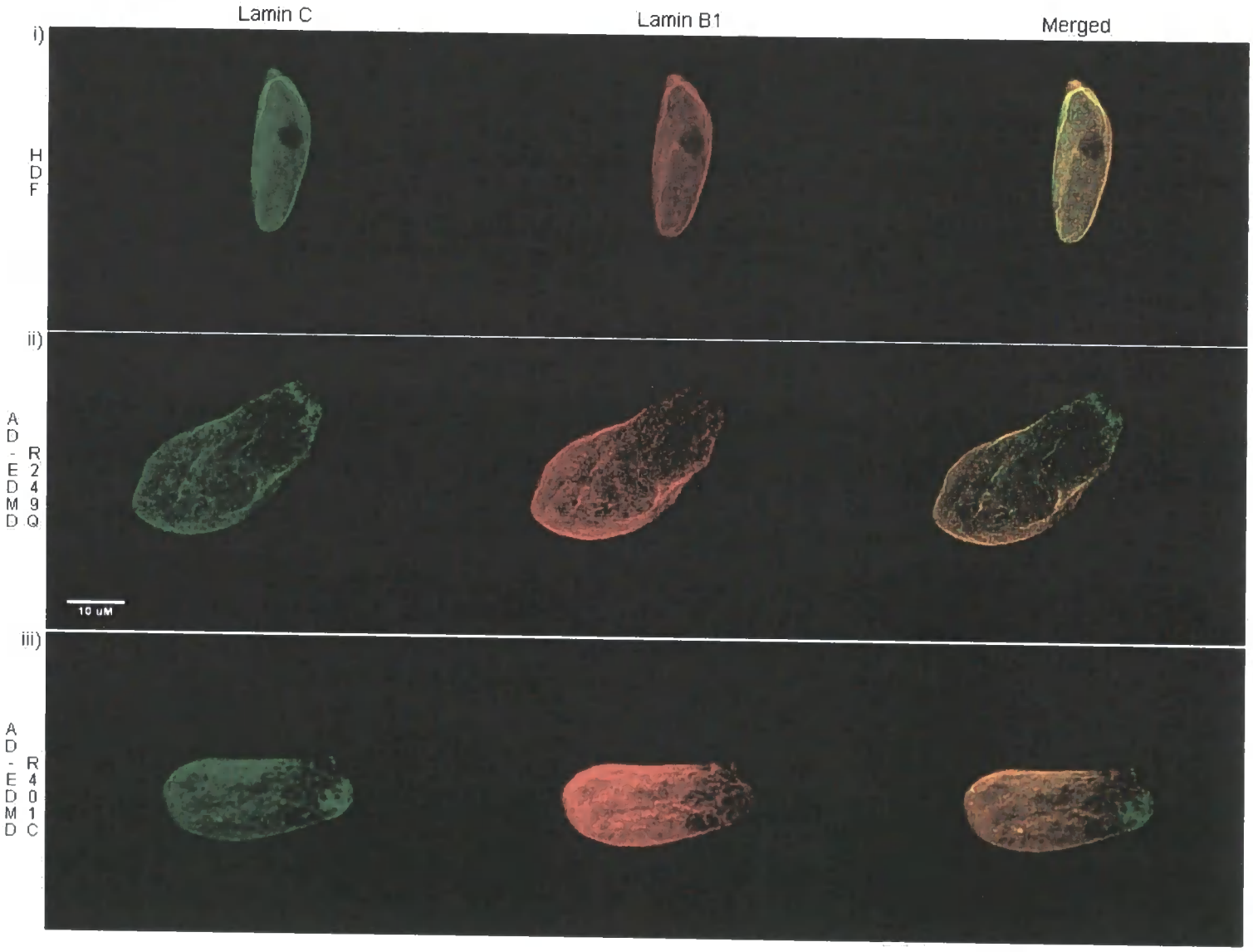
Lamin C
Lamin B1
Merged
i)
HDF
ii)
AD-EDMD R249Q
10 uM
iii)
AD-EDMD R401C

Figure 4.1 C

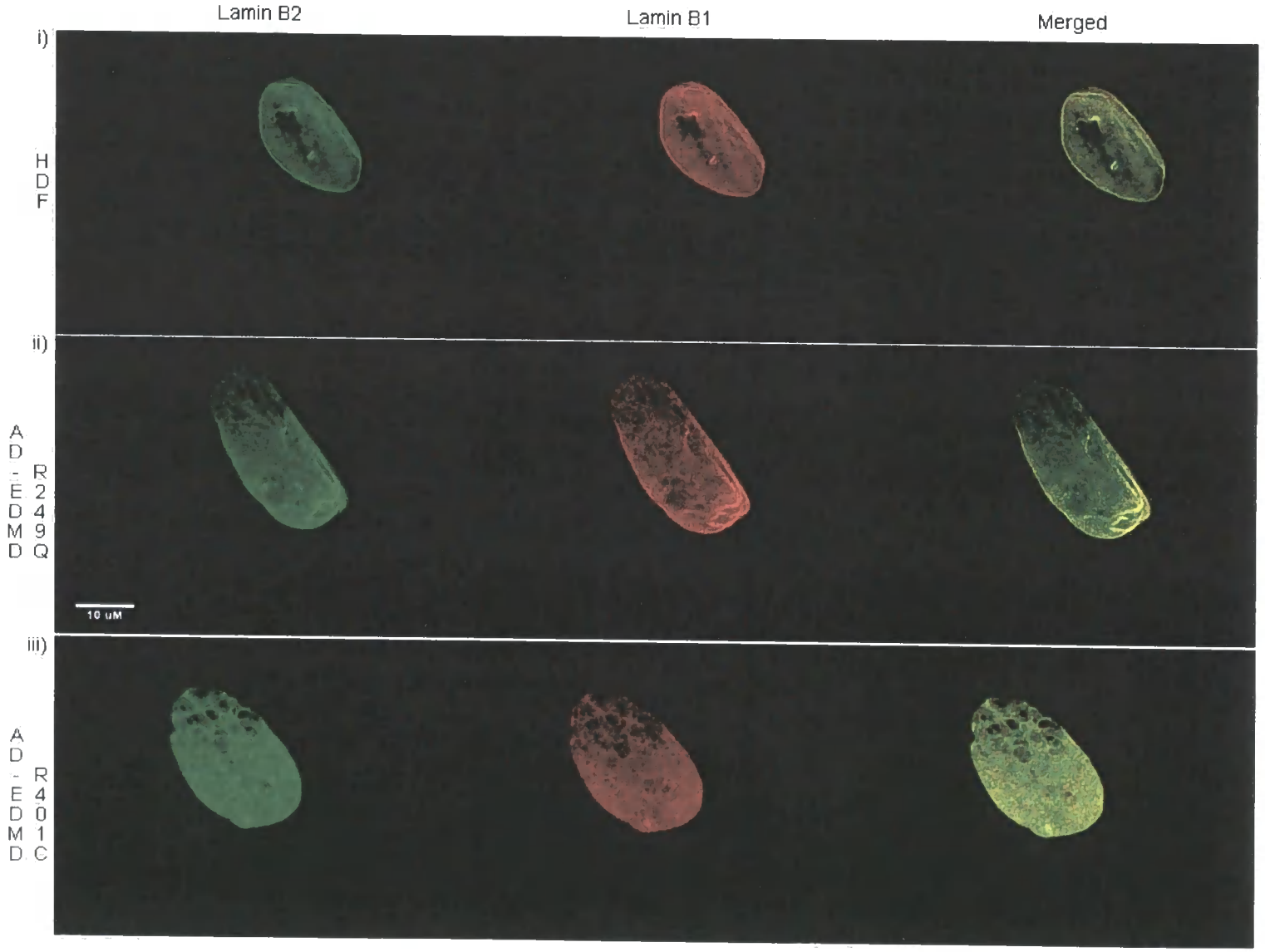
Lamin B2
Lamin B1
Merged
i)
HDF
ii)
AD-EDMD R249Q
10 uM
iii)
AD-EDMD R401C

Figure 4.2

Exponentially growing cultures of fibroblasts were fixed in 4 % Para-formaldehyde. Dual labeled cells were imaged sequentially in the FITC and TRITC channels using a MicroRadiance 2000 confocal microscope (BioRad). Central sections were projected as individual colors or as merged overlays (a, b and c merged). Control is shown in panel a, AD-EDMD fibroblasts are shown in panel b (R249Q) and c (R401C). The percentage of cells displaying normal or honeycomb morphology was calculated by counting two hundred cells each on duplicate slides. Scale bar = 10 μm

A. Exponentially growing cultures of normal human skin dermal fibroblasts were fixed in Para-formaldehyde and double stained with anti-ki67 and anti-Lamin C antibodies (a - b). Cells displaying honeycomb morphology (one arrow) are present at a very low percentage in normal cultures. Normal lamina is shown by a double arrow.

B. Double staining with anti-emerin and anti-Lamin C antibodies

C. Double staining with anti-nucleoporin and anti-Lamin C antibodies

D. Double staining with anti-nucleoporin and anti-lamin B1 antibodies

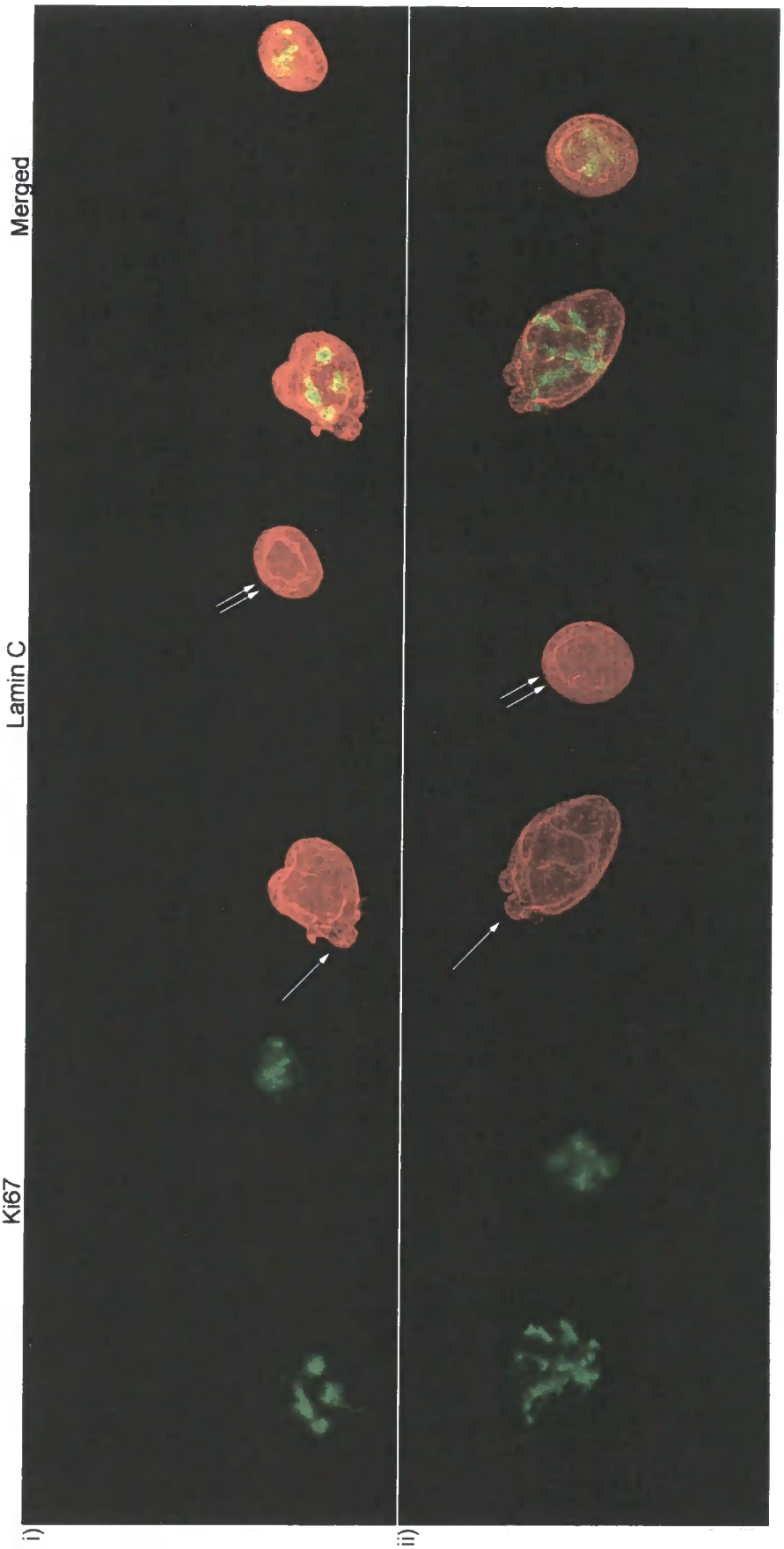

Figure 4.2 A

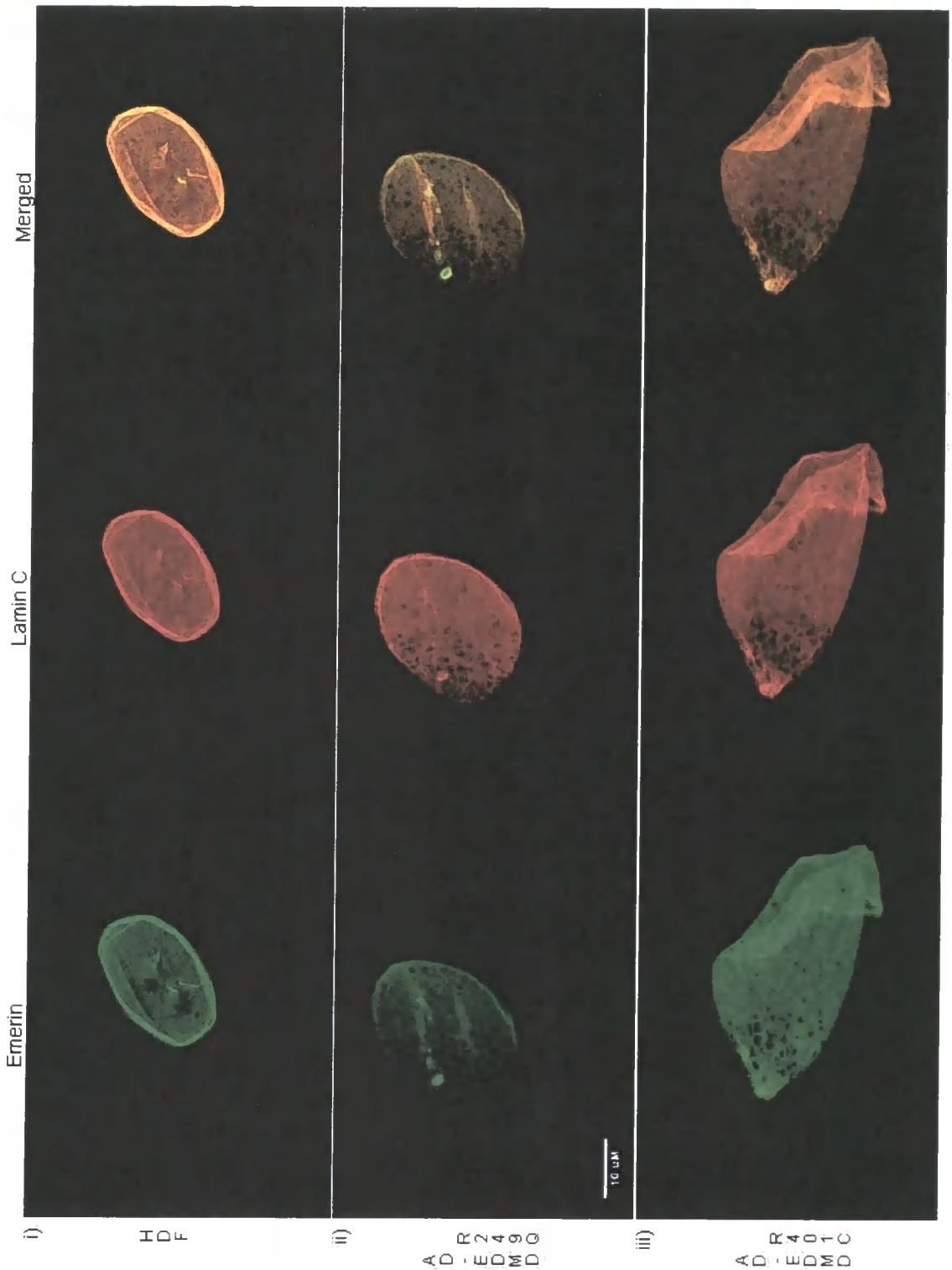

Figure 4.2 B

Figure 4.2 C

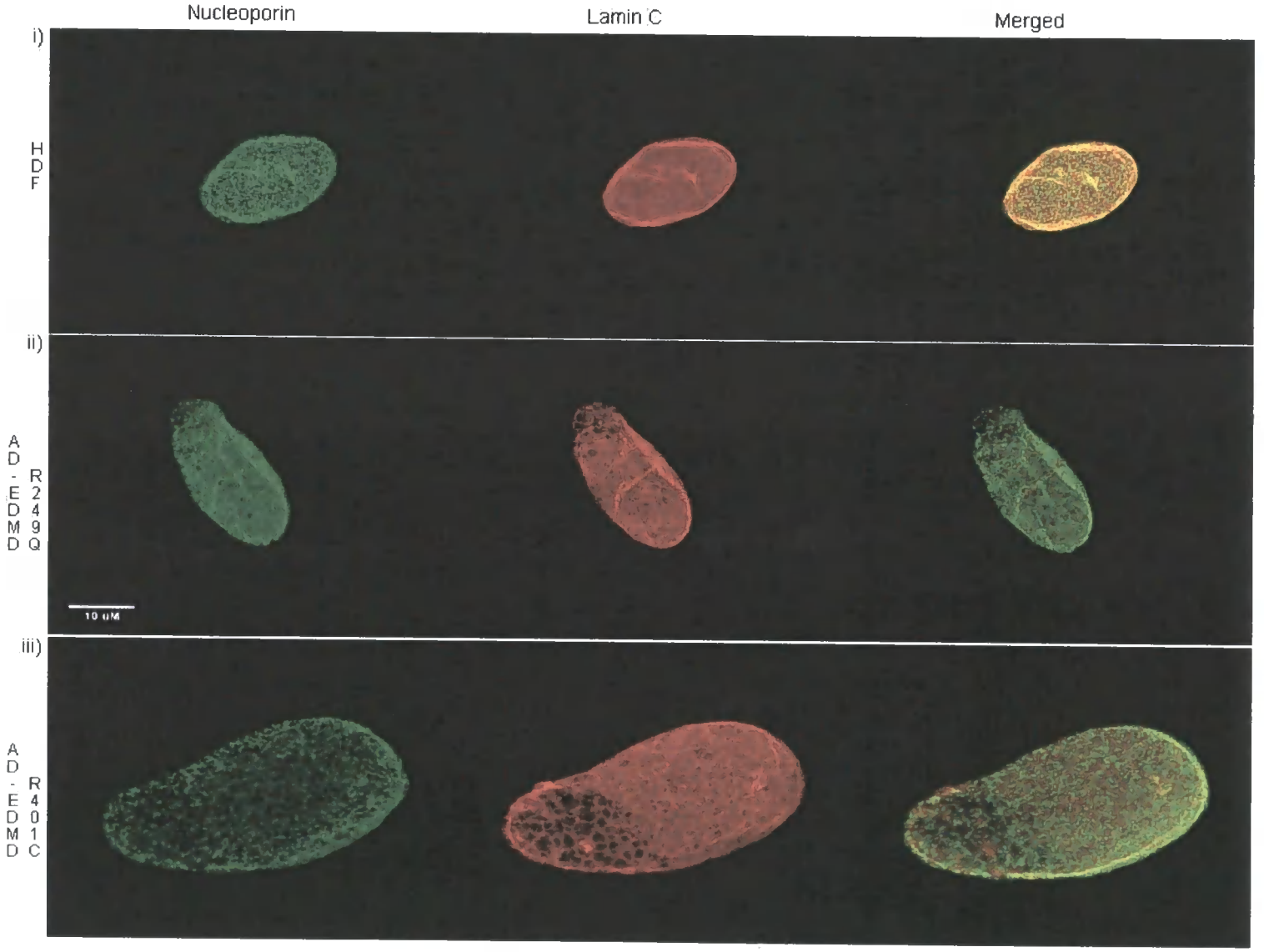
Nucleoporin
Lamin C
Merged
i)
HDF
ii)
AD-EDMD R249Q
10 uM
iii)
AD-EDMD R401C

Figure 4.2 D

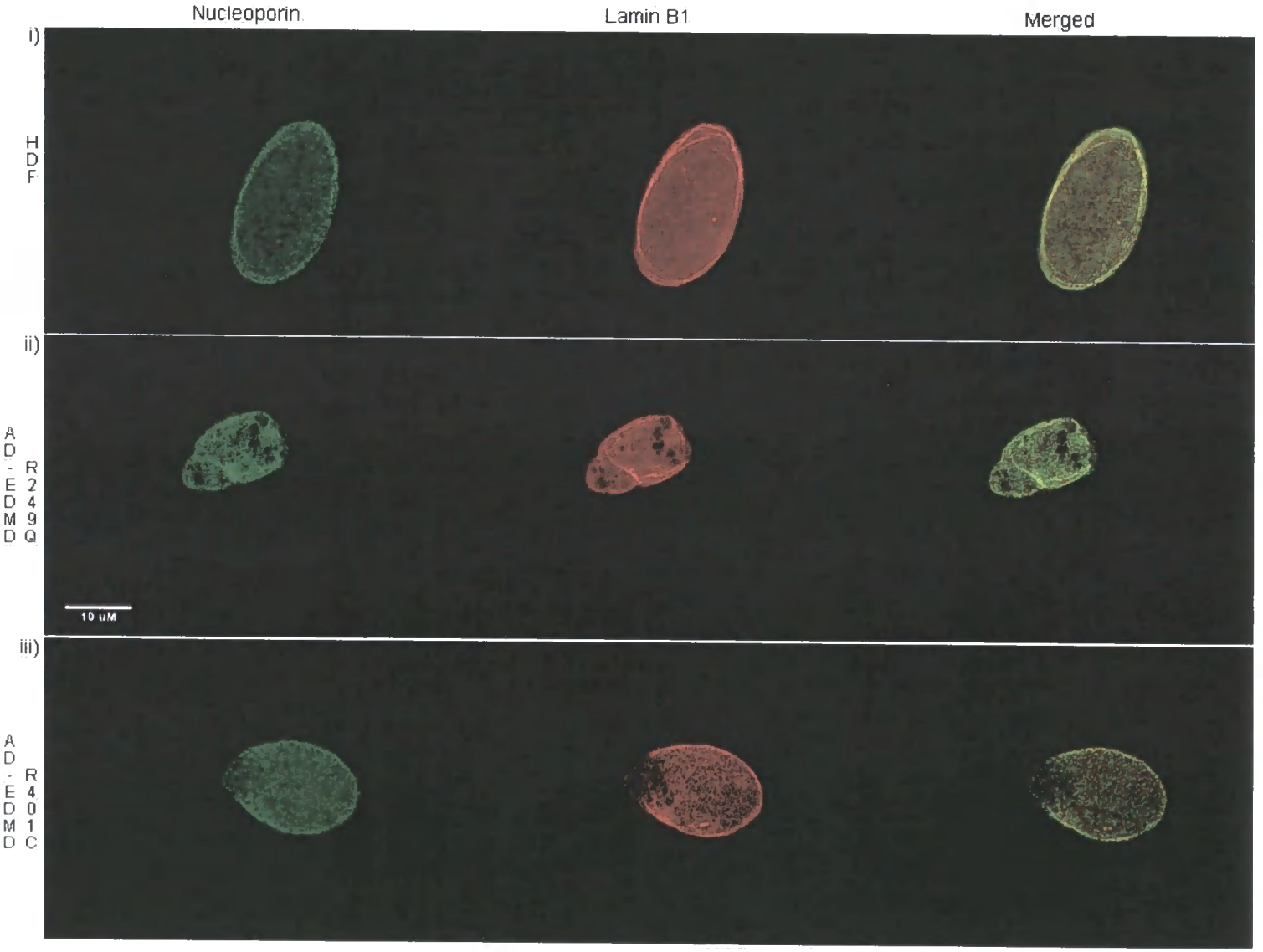
Nucleoporin
Lamin B1
Merged
i)
HDF
ii)
AD-EDMD R249Q
10 uM
iii)
AD-EDMD R401C

Figure 4.3

Honeycomb structures distribution in AD-EDMD cell lines. Cells were grown up to 80% confluence, fixed in methanol: acetone or Para-formaldehyde and stained with anti-lamin A/C and lamin C antibodies. Two hundred cells were counted and lamins distribution in honeycomb like-structure was recorded as normal or honeycomb.

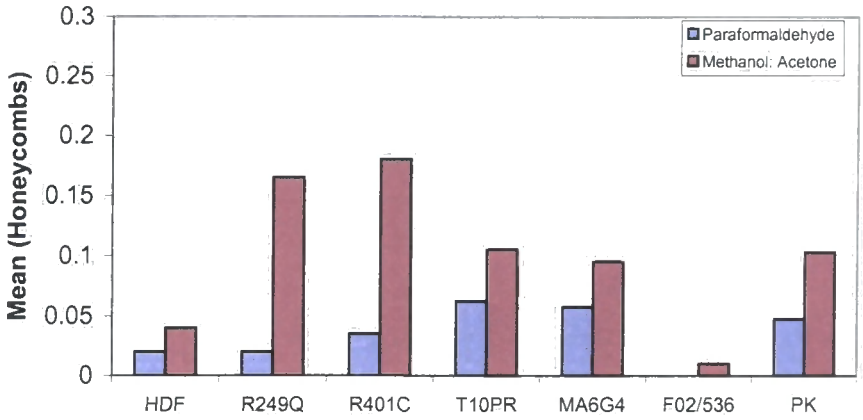
0.3
0.25
0.2
0.15
0.1
0.05
0
Mean (Honeycombs)
Paraformaldehyde
Methanol: Acetone
HDF
R249Q
R401C
T10PR
MA6G4
F02/536
PK

Figure 4.3

Table 4.1

Proliferation index in EDMD cell lines. Cells were grown to mid passages in DMEM supplemented with 10 % NCS and seeded on glass coverslips for Para-formaldehyde fixation followed by staining with anti-Ki67 antibody. Old passages were grown until passage 30 in DMEM supplemented with 10 % NCS. Afterwards, serial passages were maintained in DMEM supplemented with 5% NCS/5% FBS until a morphological change was observed under a phase contrast microscope. Data was recorded by counting 200 cells randomly from duplicate samples in duplicate experiments.

	Mid passage		Old passage (Senescent)	
	Passage number	% Ki67 +	Passage number	% Ki67 +
HDF	14	79.5	38	10
R249Q	16	62	25	0
R401C	15	82	45	40
R453W	16	70.5	25	0

Table 4.1

Figure 4.4

Expression patterns for lamins A/C (A) and lamin C (B) in control and AD-EDMD fibroblasts. Comparison of lamins expression in control (lanes land 7) and AD-EDMD fibroblasts (lanes 2 and 6: R249Q, lanes 3 and 9: R401C, lanes 4 and 10 MA6G4 and lanes 5 and 11: T10PR). Cell extracts were prepared from exponentially growing fibroblasts in the presence of NEM. Fifteen μg of total protein per lane were resolved on 12% SDS-PAGE, transferred to a membrane and immunoblotted with monoclonal antibody Jol2 (A). Samples were run under reducing and non-reducing conditions, to resolve intact S-S bonded complexes. As a control, parallel blots were probed with antibodies against the ER protein PDI, which is known to form disulphide bonded intermediates (C). Molecular weight markers are in kDa.

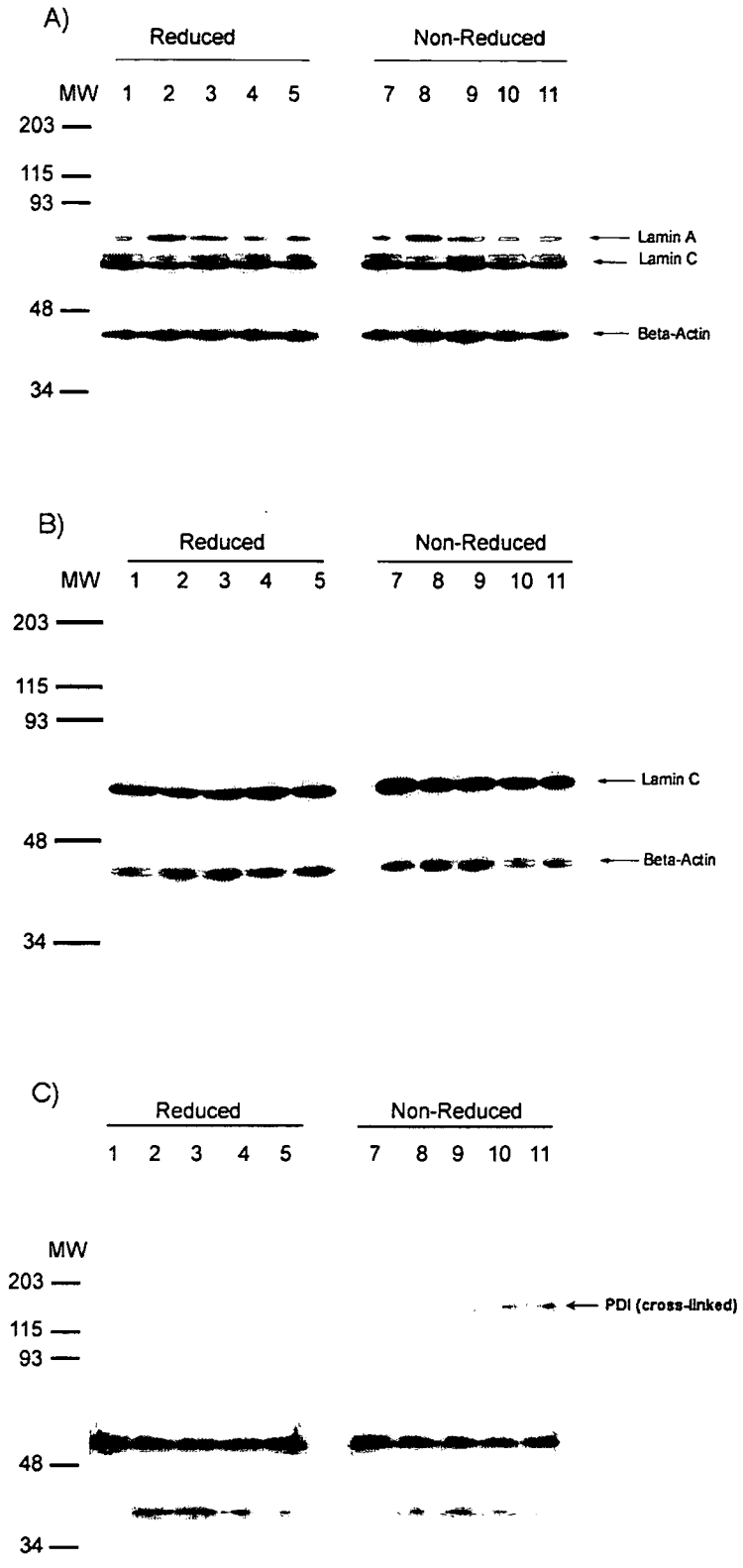
A)
Reduced
Non-Reduced
MW 1 2 3 4 5 7 8 9 10 11
203
115
93
48
34
Lamin A
Lamin C
Beta-Actin
B)
Reduced
Non-Reduced
MW 1 2 3 4 5 7 8 9 10 11
203
115
93
48
34
Lamin C
Beta-Actin
C)
Reduced
Non-Reduced
1 2 3 4 5 7 8 9 10 11
MW
203
115
93
48
34
PDI (cross-linked)

Figure 4.4

Figure 4.5

Control (HDF), AD-EDMD (R401C) and X-linked cell lines were serum-starved, re-stimulated by adding serum to the culture after 5 days of starvation and stained after 30 hours of re-stimulation. Control and X-linked cell lines did not show any significant change in the amount of honeycomb structures, but AD-EDMD R401C showed an increasing amount as it went through proliferation, quiescence and re-stimulation states.

A. Control fibroblasts

B. AD-EDMD R401C

C. X-Linked-EDMD

A)

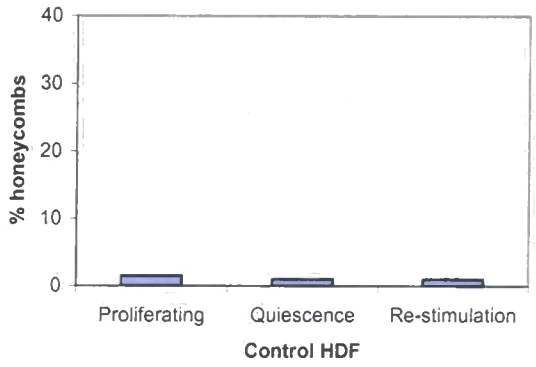

B)

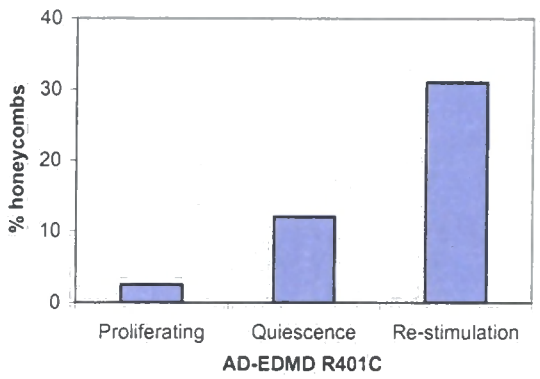

C)

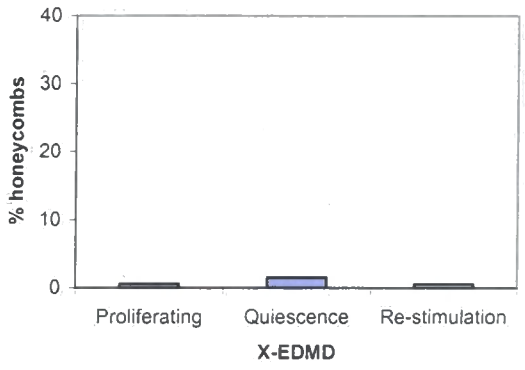

Figure 4.5

Figure 4.6

Human Dermal Fibroblasts from a healthy donor (i), AD-EDMD patient (ii) and X-linked EDMD patient (iii) were grown until 80% confluence, fixed with 3.5 % para-formaldehyde and double stained with anti-Lamin C (red) and anti-Heat Shock Protein 27 (HSP27) (green). DAPI-containing mounting media was used to label the DMA (blue).

A. Cultures in proliferating state

B. Cultures in quiescence state

C. Cultures after 30 hours of serum re-stimulation

Figure 4.6 A

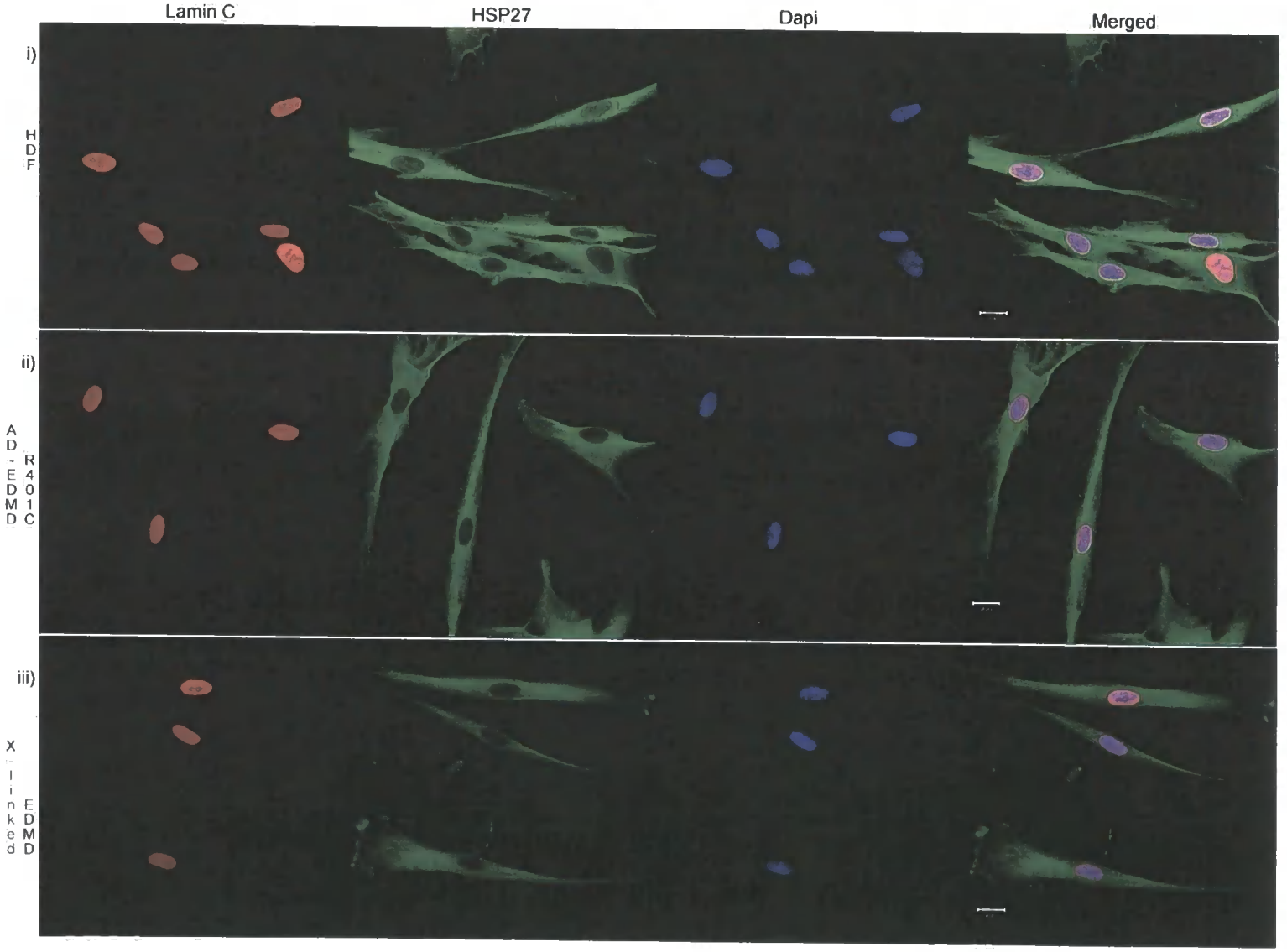
Lamin C
HSP27
Dapi
Merged
i)
HDF
ii)
AD-EDMD R401C
iii)
X-linked EDMD

Figure 4.6 B

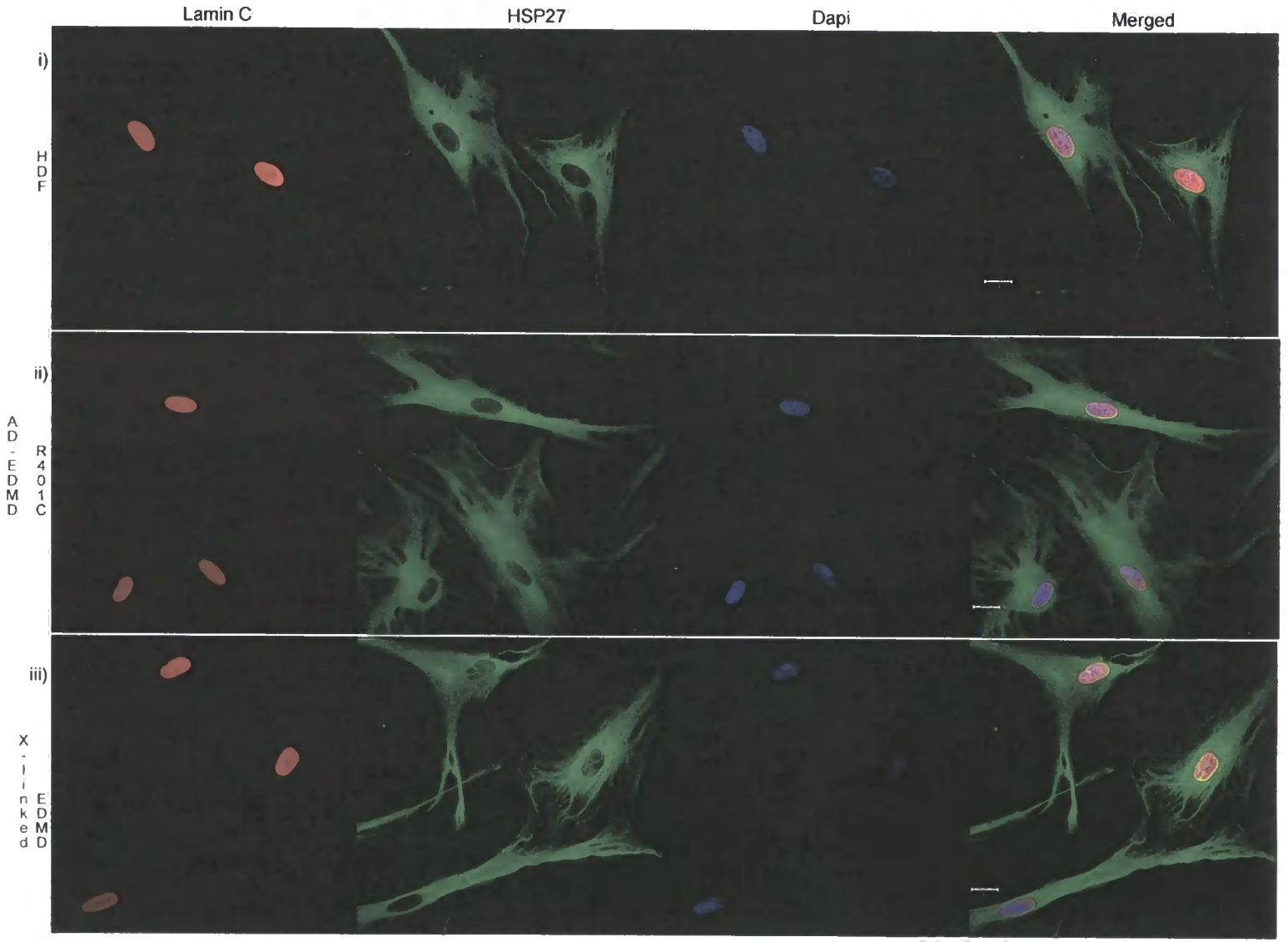
Lamin C
HSP27
Dapi
Merged
i)
HDF
ii)
AD-EDMD R401C
iii)
X-linked EDMD

Figure 4.6 C

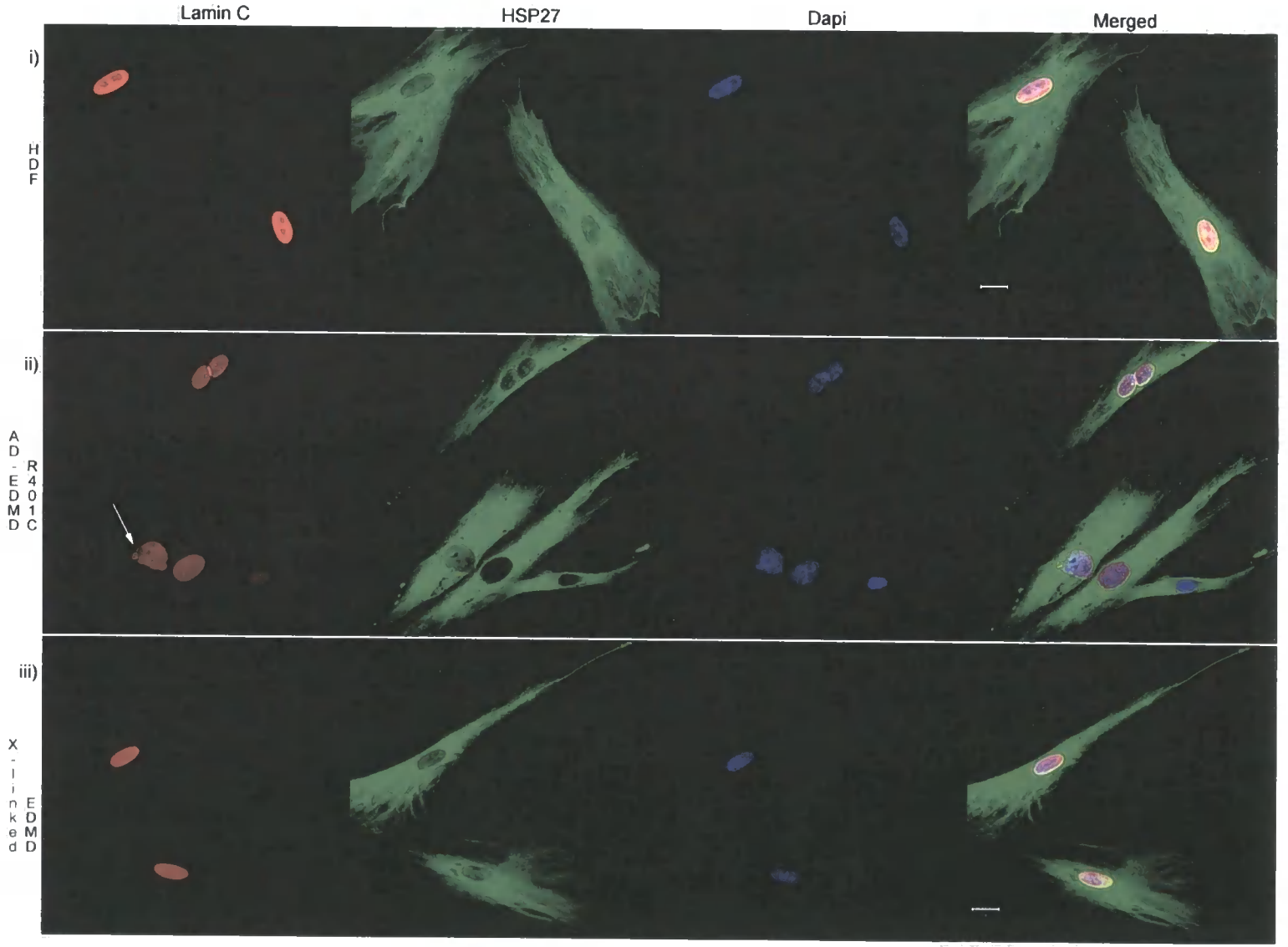
Lamin C
HSP27
Dapi
Merged
i)
HDF
ii)
AD-EDMD R401C
iii)
X-linked EDMD

Figure 4.7

Human Dermal Fibroblasts from a healthy donor (i), AD-EDMD patient (ii) and X-linked EDMD patient (iii) were grown until 80% confluence, fixed with 3.5 % para-formaldehyde and double stained with anti-Lamin C (red) and anti-Heat Shock Protein 70 (HSP70) (green). DAPI-containing mounting media was used to label the DNA (blue).

A. Cultures in proliferating state

B. Cultures in quiescence state

C. Cultures after 30 hours of serum re-stimulation

Figure 4.7 A

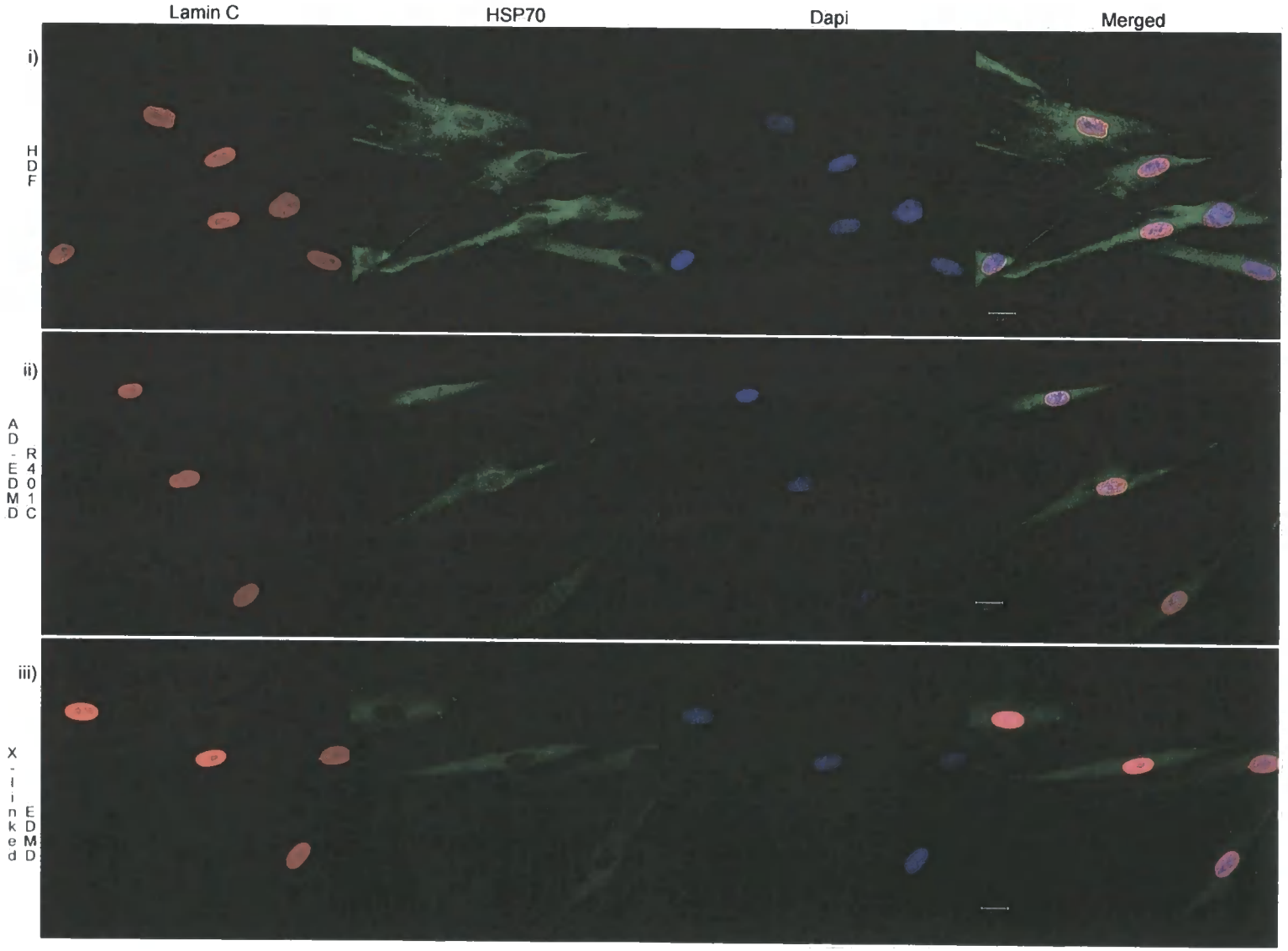
Lamin C
HSP70
Dapi
Merged
i)
HDF
ii)
AD-EDMD R401C
iii)
X-linked EDMD

Figure 4.7 B

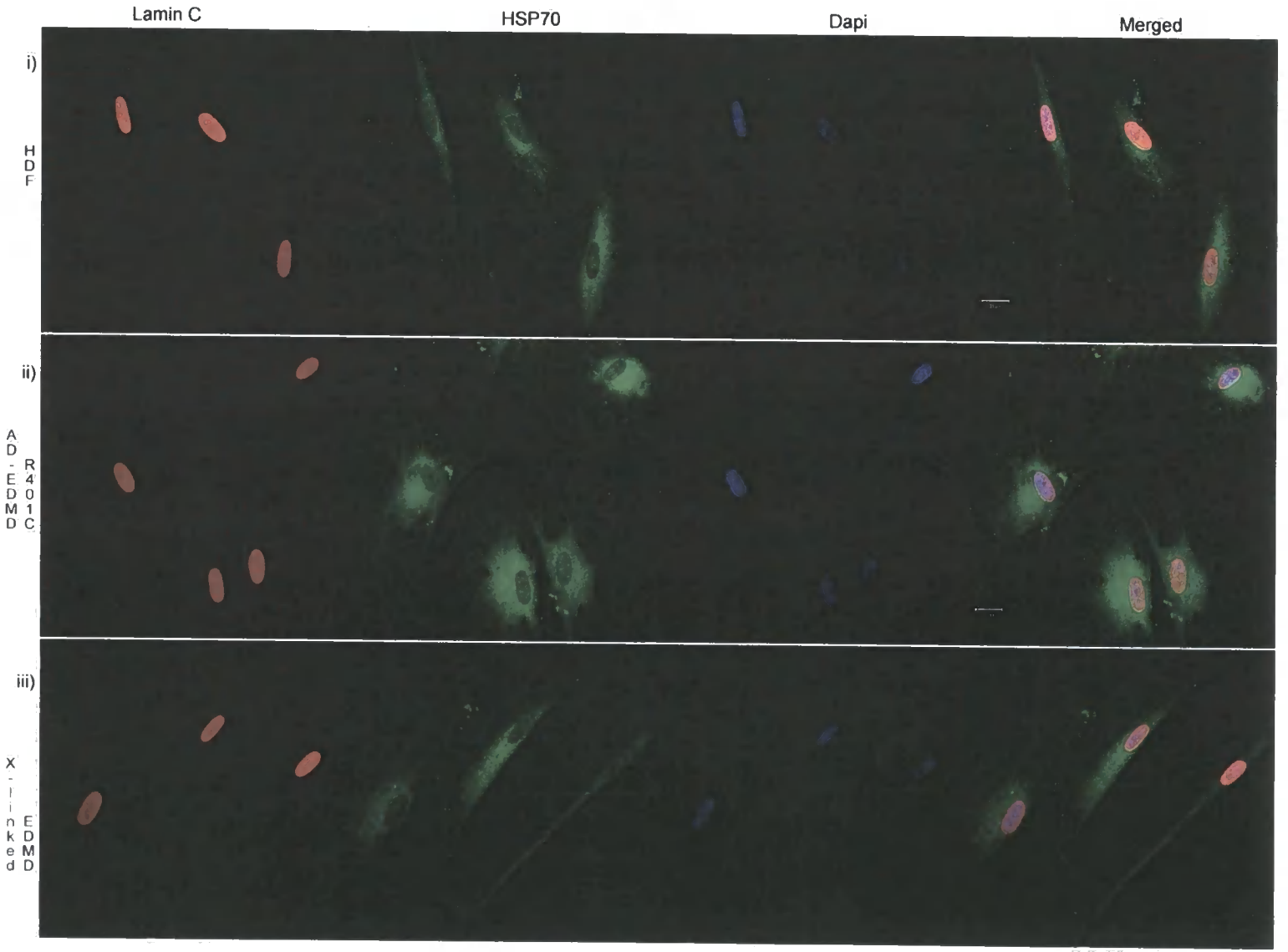
Lamin C
HSP70
Dapi
Merged
i)
HDF
ii)
AD-EDMD R401C
iii)
X-linked EDMD

Figure 4.7 C

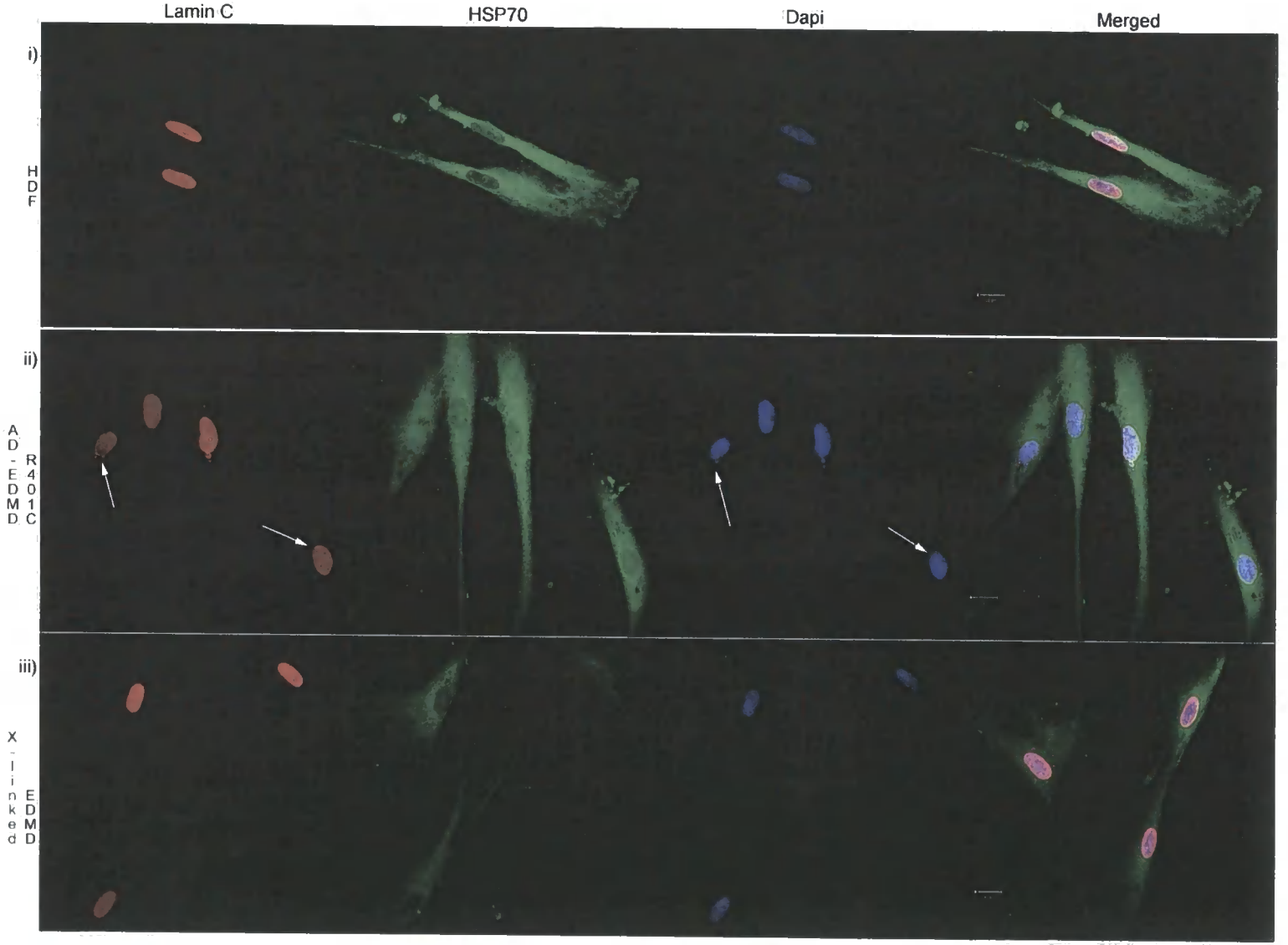
Lamin C
HSP70
Dapi
Merged
i)
HDF
ii)
AD-EDMD R401C
iii)
X-linked EDMD

Figure 4.8

Expression patterns of HSP70 in proliferating human dermal fibroblasts from AD-EDMD patients. Cell extracts were prepared from sub-confluent cultures in the presence of protein inhibitors cocktail (Sigma) and 5 g of total protein were loaded per well. Samples were separated in a 10% SDS-PAGE, transferred and immuno-blotted with HSP70 antibody. Lane 1: control human dermal fibroblast, Lane 2: AD-EDMD mutation R249Q, Lane 3: AD-EDMD patient mutation R401C and Lane 4: AD-EDMD patient (unknown mutation). Molecular markers are in kDa.

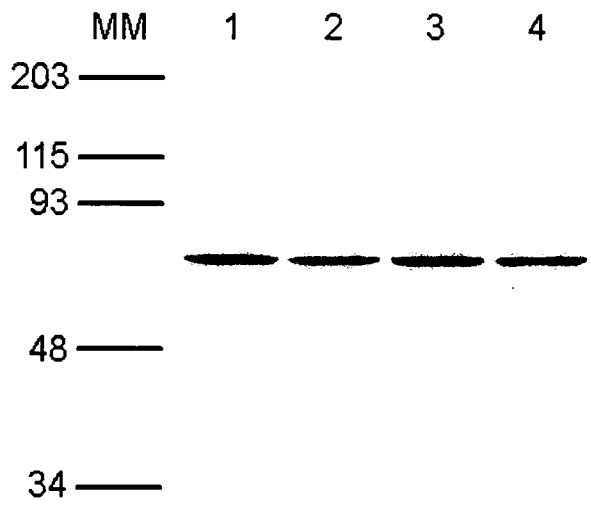

Figure 4.8

Figure 4.9

Phase contrast images of human dermal fibroblasts from a healthy donor (HDF, control), AD-EDMD and X-linked patients. Images were taken 48 hours after cells were seeded at $3x10^4$cells/ml in 60mm culture dishes. Flattened cells are shown by arrows.

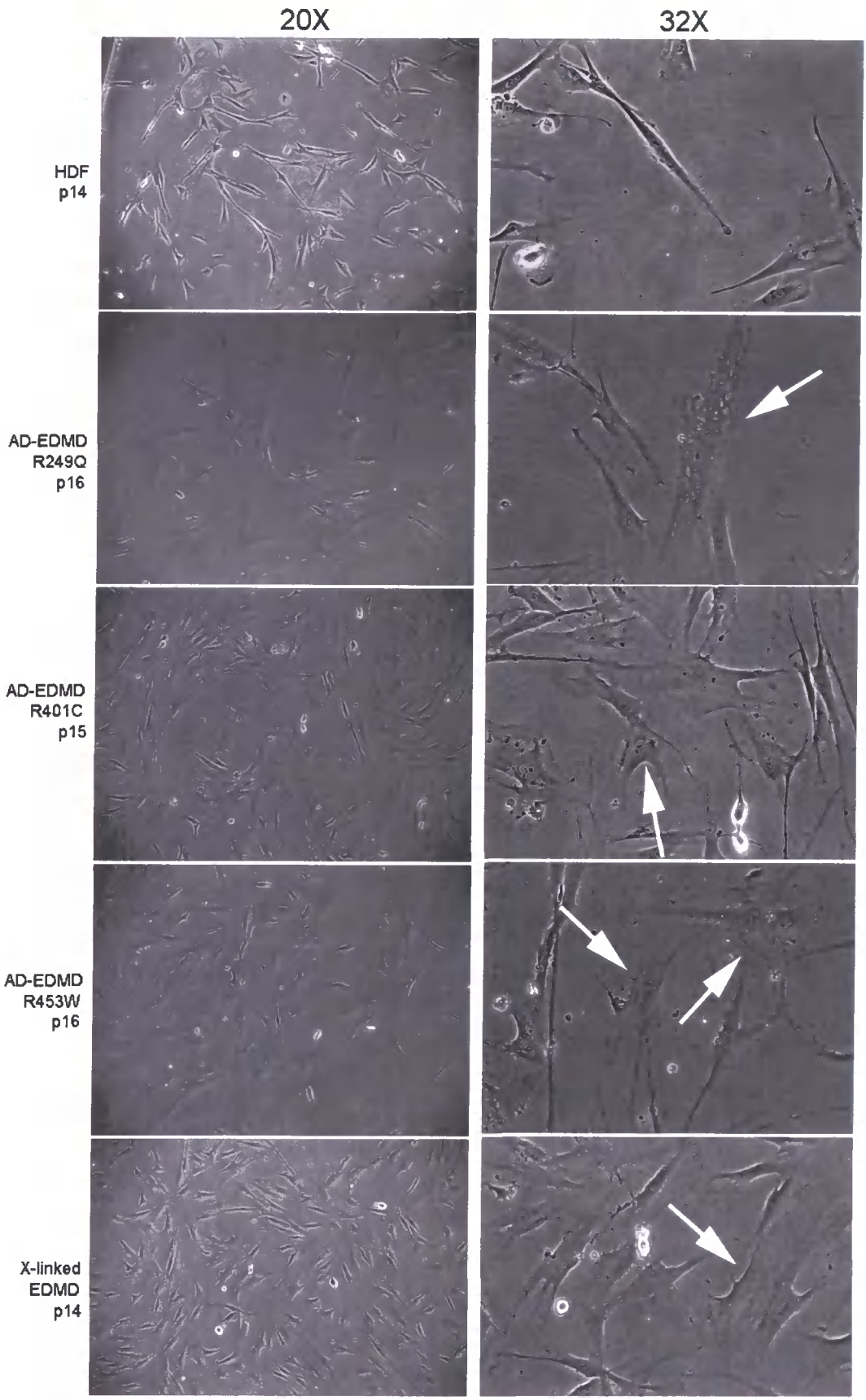
20X
32X
HDF
p14
AD-EDMD
R249Q
p16
AD-EDMD
R401C
p15
AD-EDMD
R453W
p16
X-linked
EDMD
p14

Figure 4.9

Figure 4.10

Nesprin 1 is in fibers, co-localizing with α-S-Actin in skin dermal fibroblasts from a healthy donor, EDMD patient and healthy rat. Cells were grown until 80% confluence, fixed with 3.5% Para-formaldehyde and double stained with anti-alpha-S-actin (green) and anti-Nesprin 1 N5 antibodies (red) (A), or anti-α -S-actin (green) and anti-Nesprin 2 CH3 antibodies (red) (B). Co-localization of Nesprin 1 (N-terminal) with α-S-Actin fibers, but not Nesprin 2 (N-terminal), is a common feature between these species.

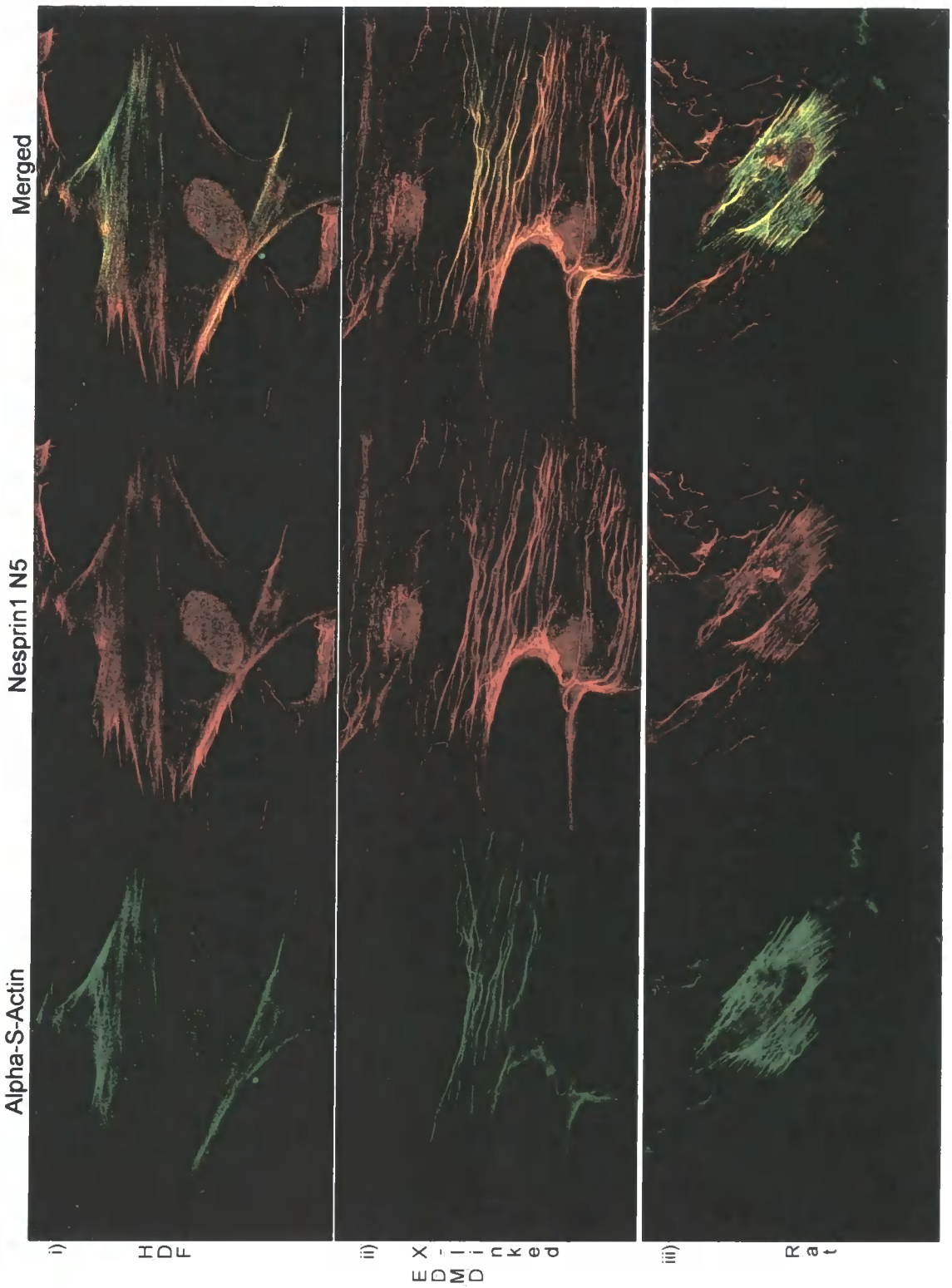

Figure 4.10 A

Figure 4.10 B

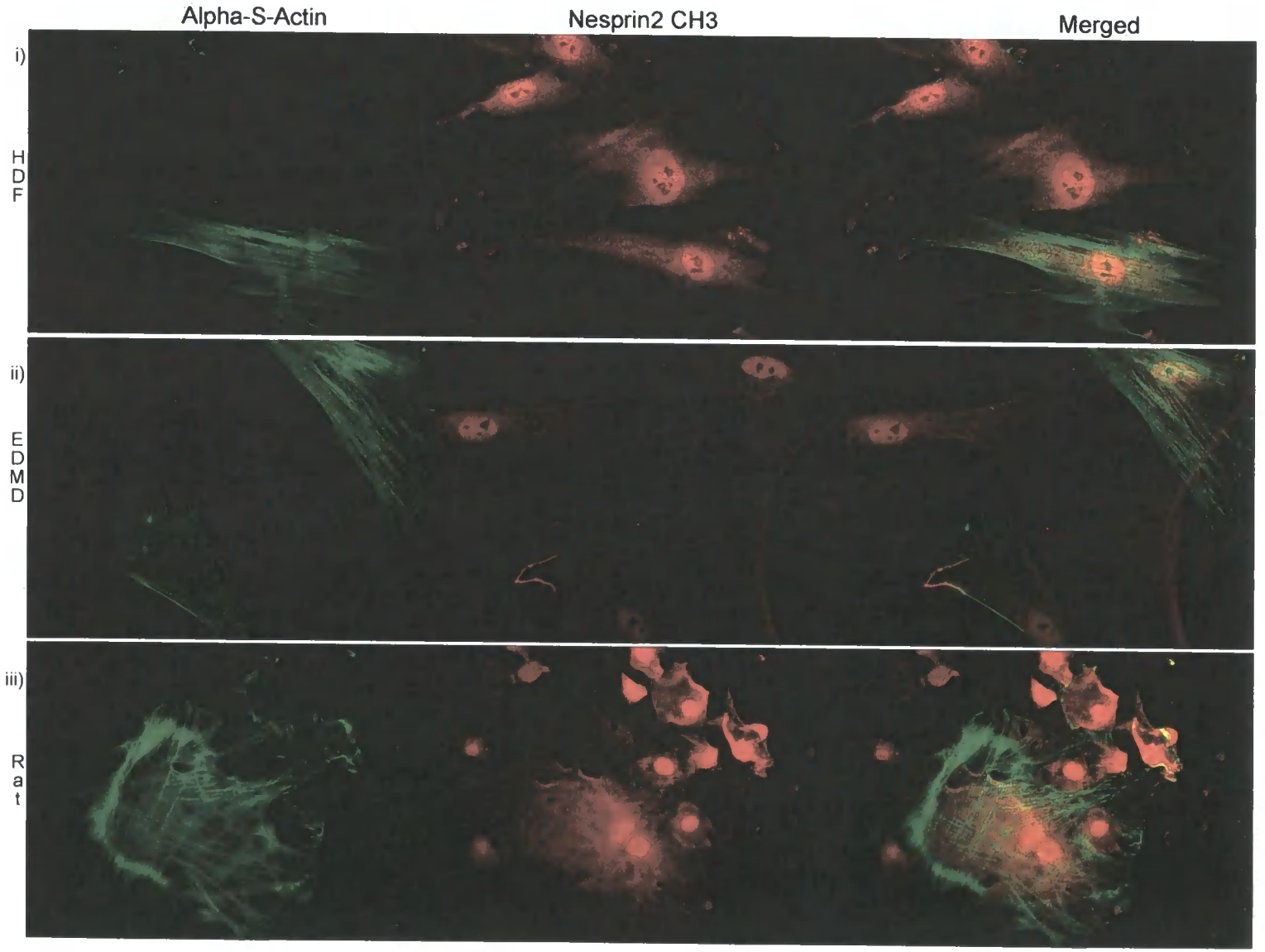

Figure 4.11

Human Dermal Fibroblasts from a healthy donor (i), AD-EDMD patient (ii) and X-linked EDMD patient (iii) were grown until 80% confluence, fixed with 3.5 % Para-formaldehyde and double stained with α-S-Actin (green) and anti-nesprin 1 N5 (N-terminal) (red) antibodies. DAPI-containing mounting media was used to label the DNA (blue).

Cultures in proliferating stage. Control (25.5%) and X-linked EDMD (17.5%) fibroblasts presented Nesprin 1 fibers. Only 2.5% (control) and 4% (x-linked EDMD) of the cells remain co-expressing Nesprin 1 and α-S-actin. In contrast, 33.5% of the AD-EDMD cells express Nesprin 1 in fibers and 21% of the total cultures co-express both proteins in fibers.

A. Cultures in quiescent stage. Control (25%) and X-linked EDMD (21.5%) fibroblasts presented fibers either for Nesprin 1 or alpha-s-actin. AD-EDMD dramatically presented all the cells with fibers, 95% of the culture co-expressing both proteins. Nesprin 1 relocated to the plasma membrane (thicker fibers), and the nucleoplasm in control fibroblasts, but no dramatic change was observed in the patient cell lines. X-linked EDMD cell line co-expressed both fibers in only 3% of the cells under these culture conditions.

B. Cultures after 30 hours of serum re-stimulation. Control (2%) and X-linked EDMD (2.5%) fibroblasts presented fibers either for Nesprin 1 or α-s-actin, resembling the distribution of fibers at the proliferating stage. AD-EDMD presented 12% of the cells co-expressing the fibers. Most of the cells in all three cell lines did not express any fiber.

Figure 4.11 A

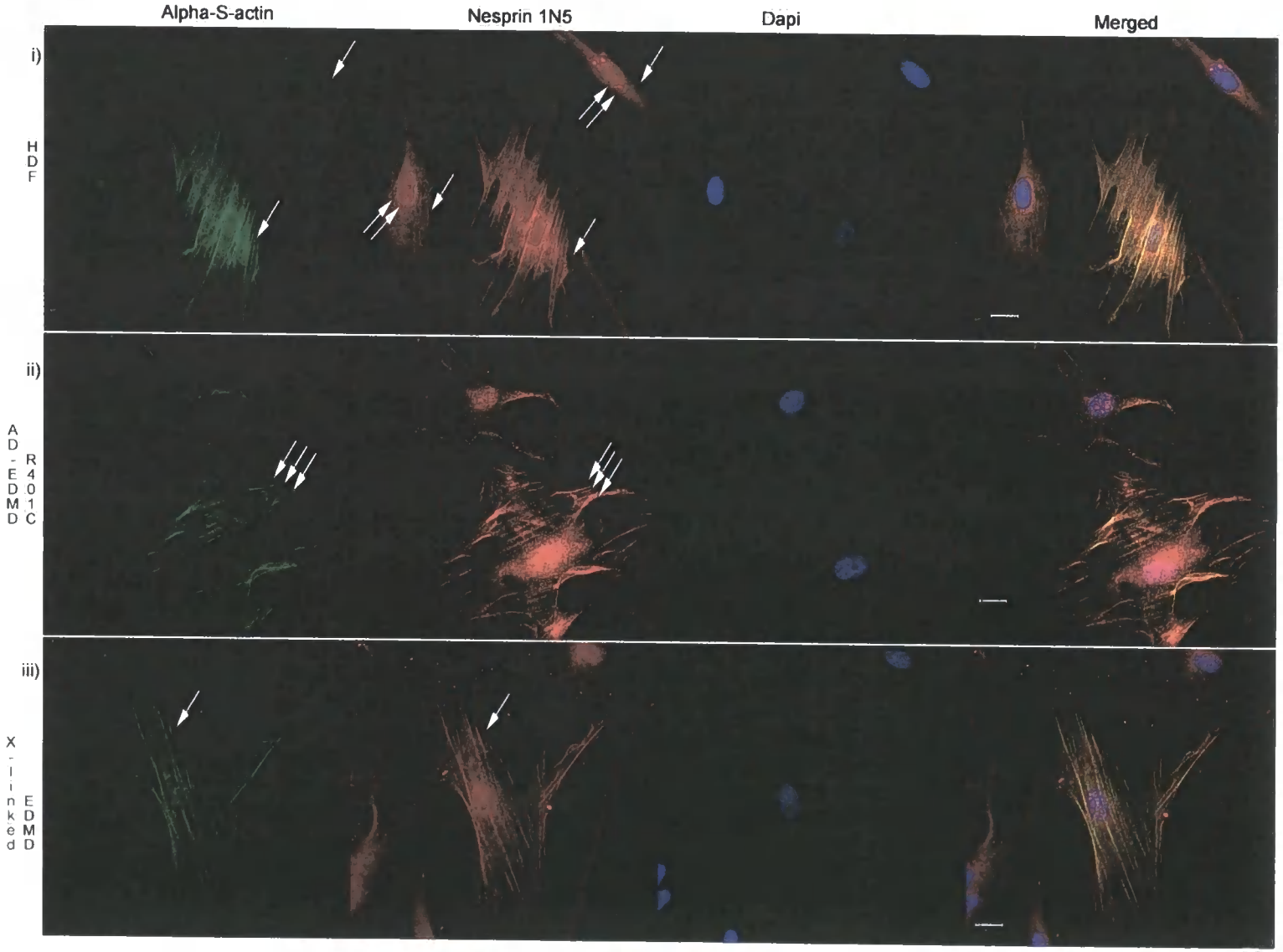
Alpha-S-actin
Nesprin 1N5
Dapi
Merged
i)
HDF
ii)
AD-EDMD R401C
iii)
X-linked EDMD

Figure 4.11 B

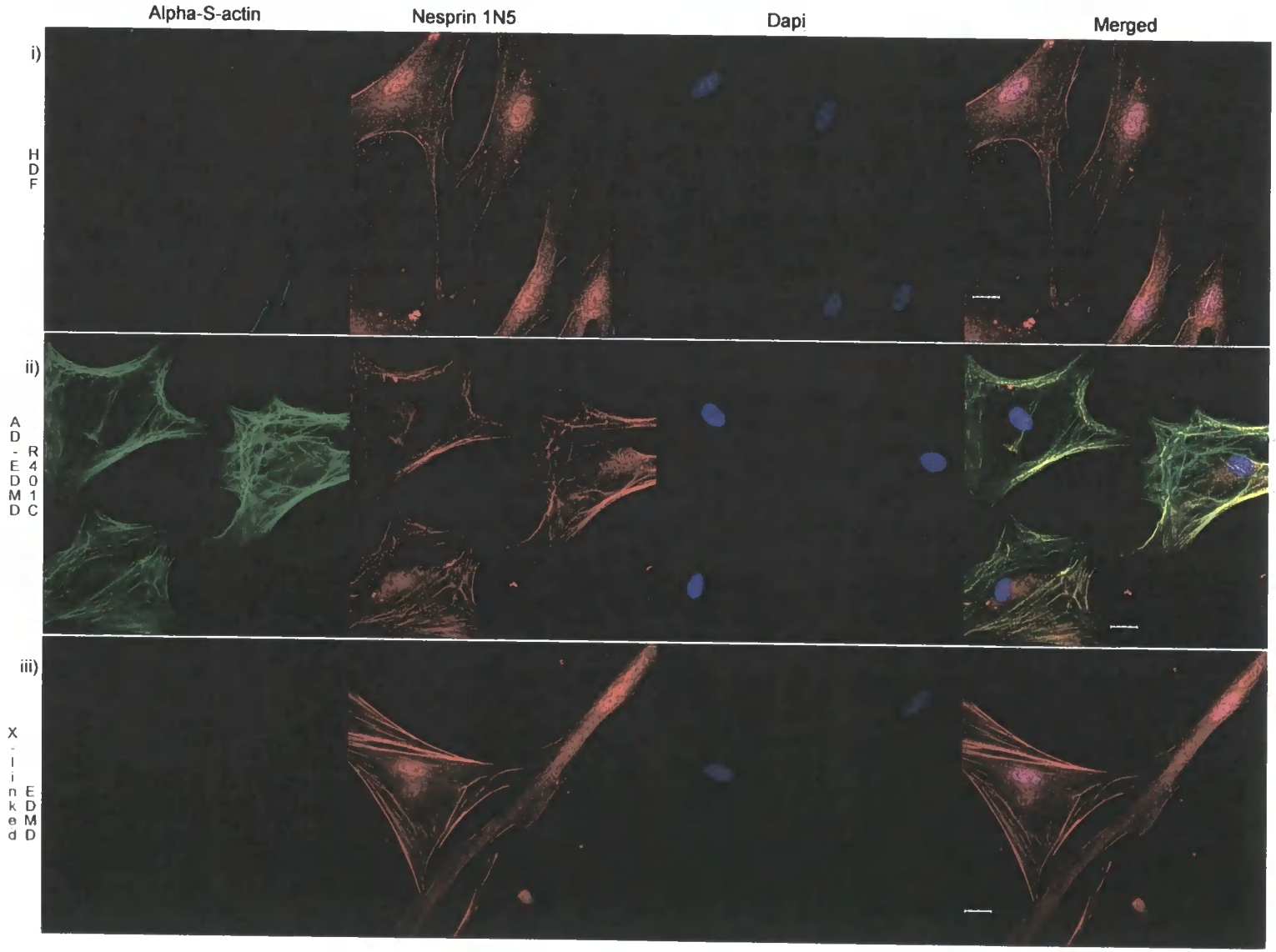
Alpha-S-actin
Nesprin 1N5
Dapi
Merged
i)
HDF
ii)
AD-EDMD R401C
iii)
X-linked EDMD

Figure 4.11 C

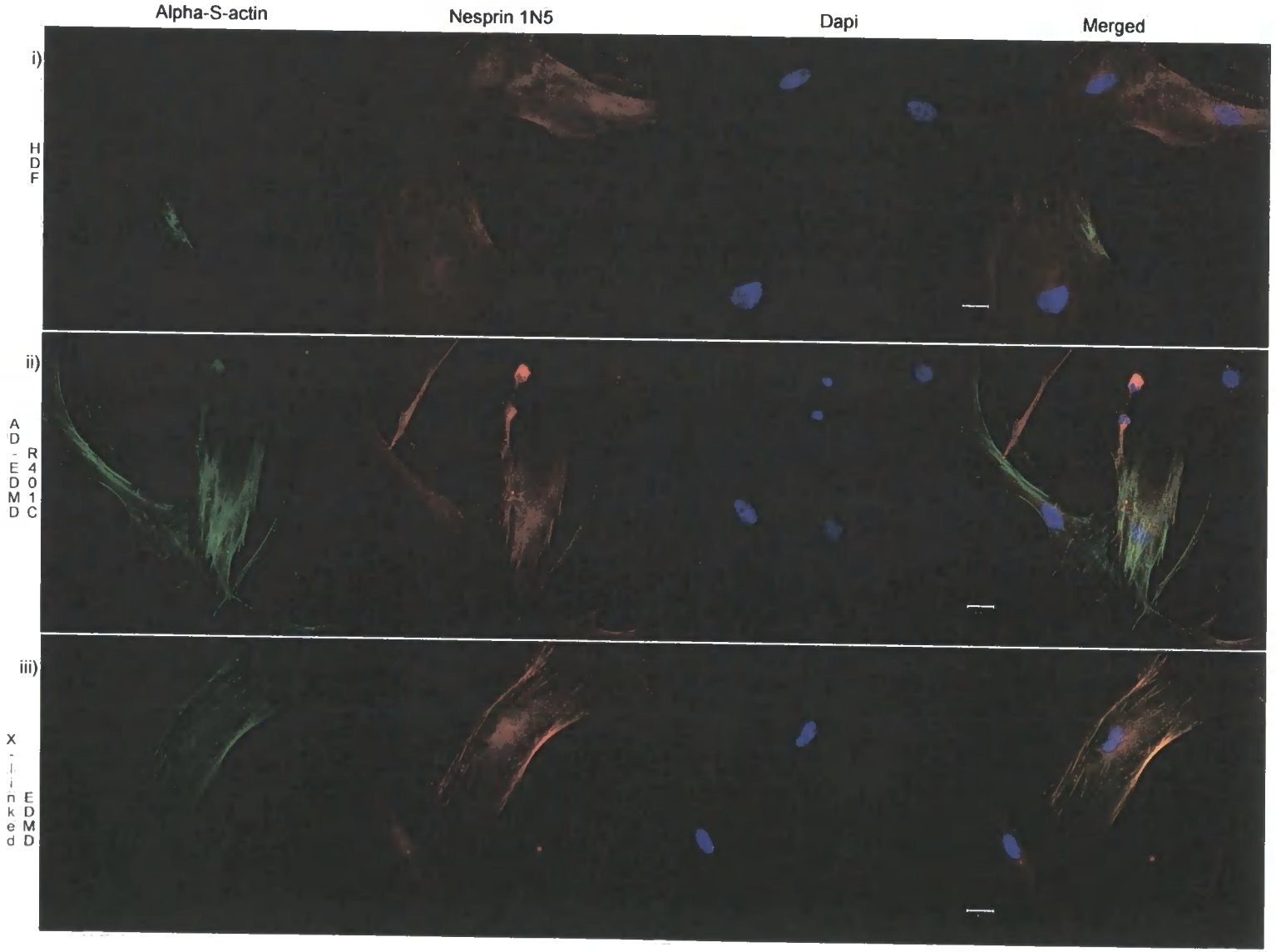
Alpha-S-actin
Nesprin 1N5
Dapi
Merged
i)
HDF
ii)
AD-EDMD R401C
iii)
X-linked EDMD

Figure 4.12

Human Dermal Fibroblasts from a healthy donor (i), AD-EDMD patient (ii) and X-linked EDMD patient (iii) were grown until 80% confluence, fixed with 3.5 % Para-formaldehyde and double stained with α-S-Actin (green) and anti-Nesprin 2 CH3 (N-terminal) (red) antibodies. DAPI-containing mounting media was used to label the DNA (blue).

A. Cultures in proliferating stage. Nesprin 2 labeled at the N-terminal had a nuclear localization, with diffuse cytoplasmic staining in all cell lines. Nuclear staining was particularly stronger in X-linked EDMD cells. Nesprin 2 N-terminal was always absent in the nucleoli.

B. Cultures in quiescent stage. Nesprin 2 re-organized in the perinuclear space in all cell lines (resembling HSP70 distribution?). In control and AD-EDMD fibroblast, the nuclear localization remained as in proliferating cells, but X-linked EDMD cells appeared, as less Nesprin 2 was present in the nucleus. Nucleoli lack Nesprin 2.

C. Cultures after 30 hours of serum re-stimulation. Nesprin 2 re-localized back to the cytoplasm and the strong signal was not yet present in the X-linked EDMD fibroblasts.

Figure 4.12 A

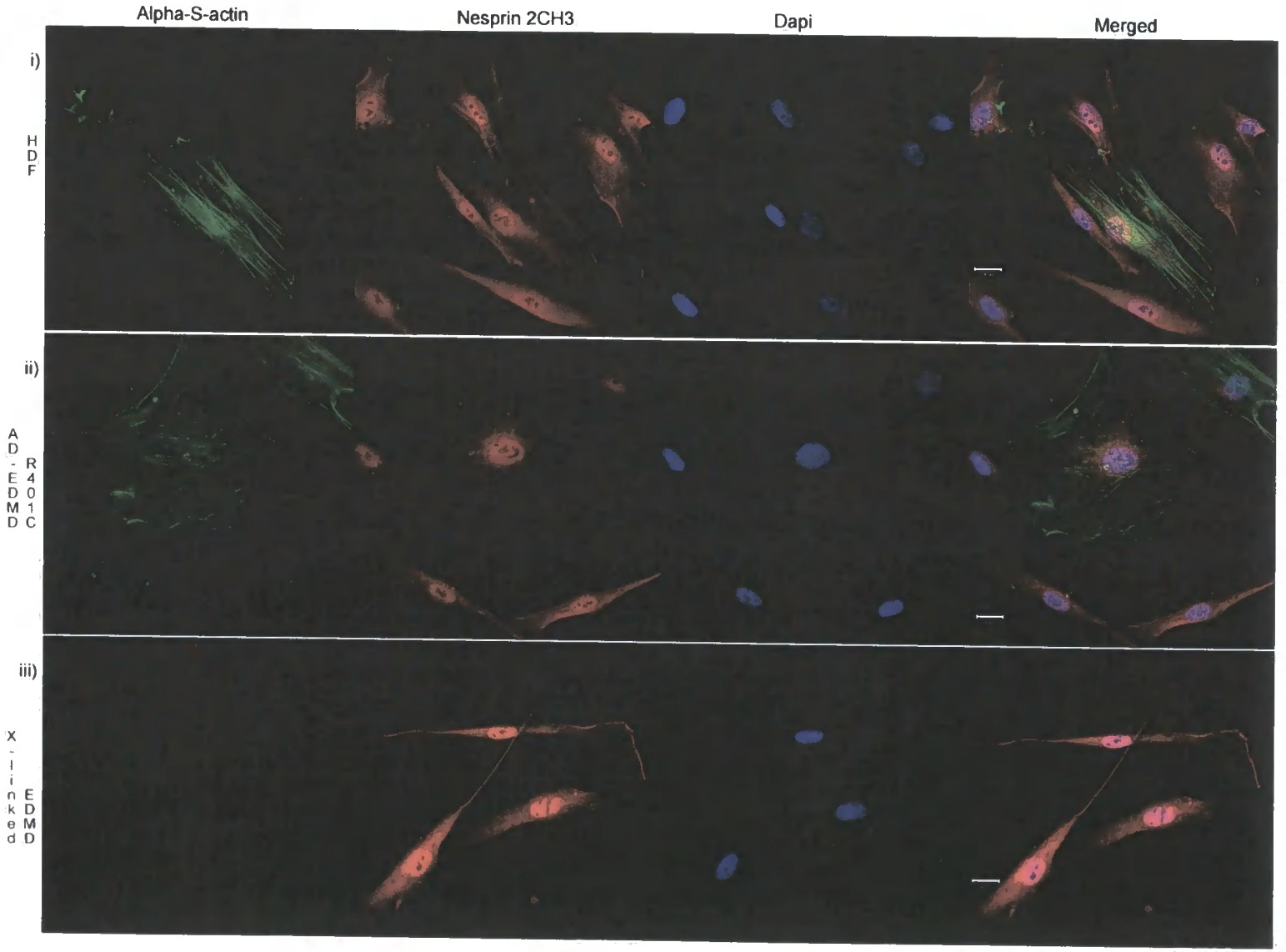
Alpha-S-actin
Nesprin 2CH3
Dapi
Merged
i)
HDF
ii)
AD-EDMD R401C
iii)
X-linked EDMD

Figure 4.12 B

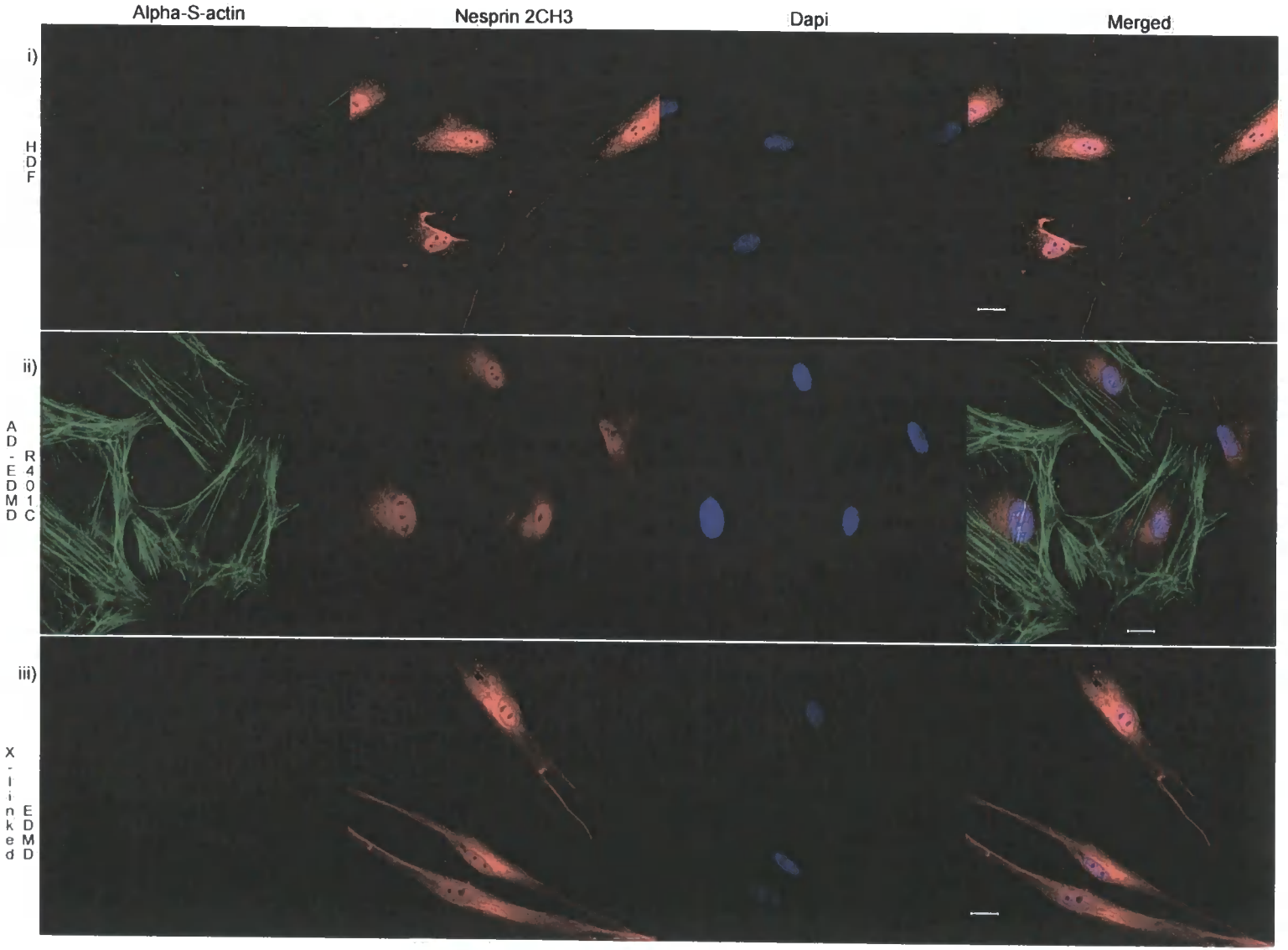
Alpha-S-actin
Nesprin 2CH3
Dapi
Merged
i)
HDF
ii)
AD-EDMD R401C
iii)
X-linked EDMD

Figure 4.12 C

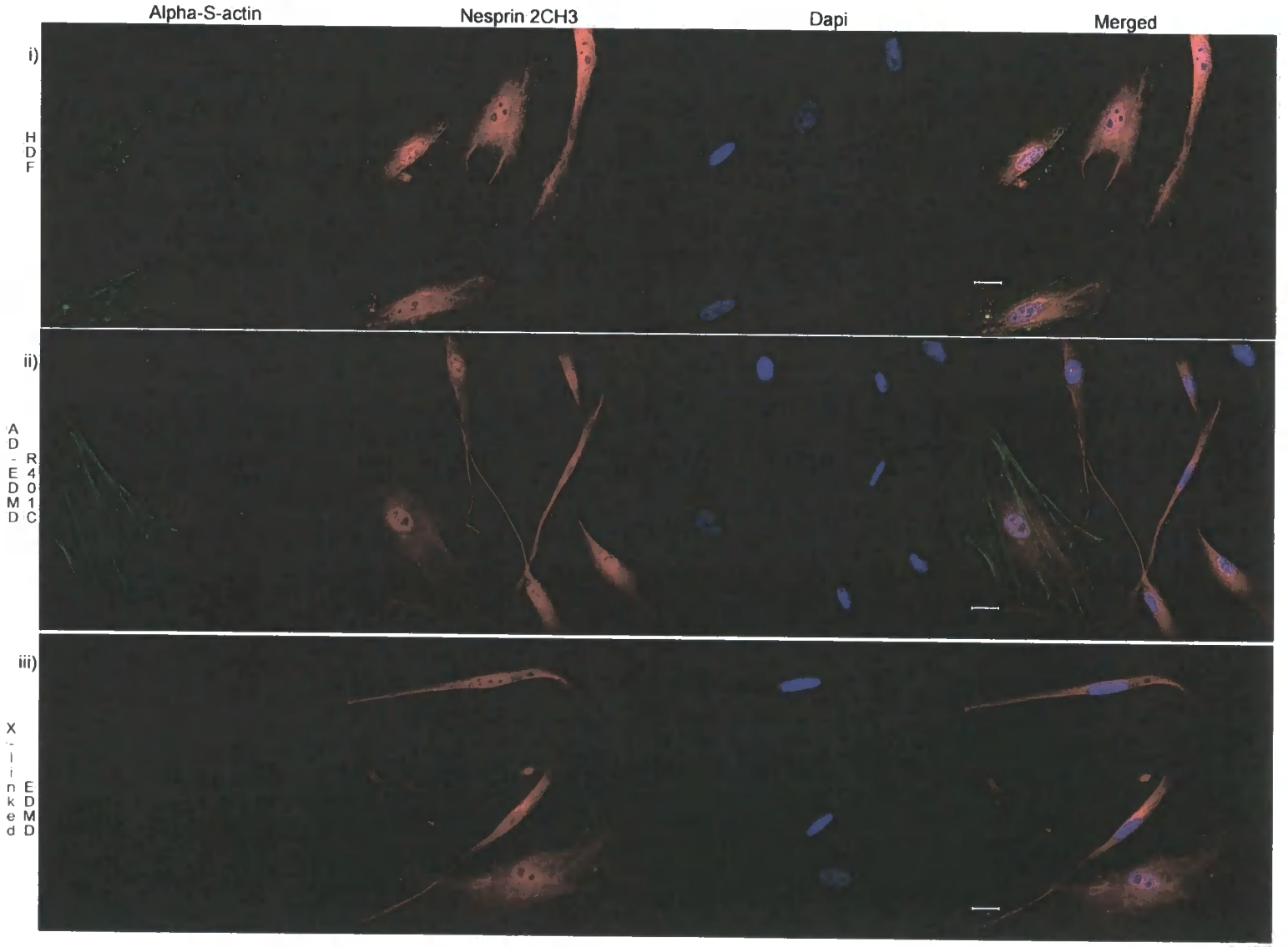
Alpha-S-actin
Nesprin 2CH3
Dapi
Merged
i)
HDF
ii)
AD-EDMD R401C
iii)
X-linked EDMD

Figure 4.13

Human dermal fibroblasts from a healthy donor and AD-EDMD patient were grown at late passages. Cells were grown in 10% NCS until passage 30, then were grown in 5%NCS / 5%FBS as far as they were proliferating and the cells looked healthy. Cultures were split 1:3 every time they reached 80% confluence. Cells were cultured on 13mm glass coverslips, fixed with 3.5 % Para-formaldehyde and double stained with α-S-Actin (green) and Nesprin 1 N5 (red) (A) or Nesprin 2 CH3 (B) antibodies. (N-terminal of Nesprins 1 and 2 respectively).

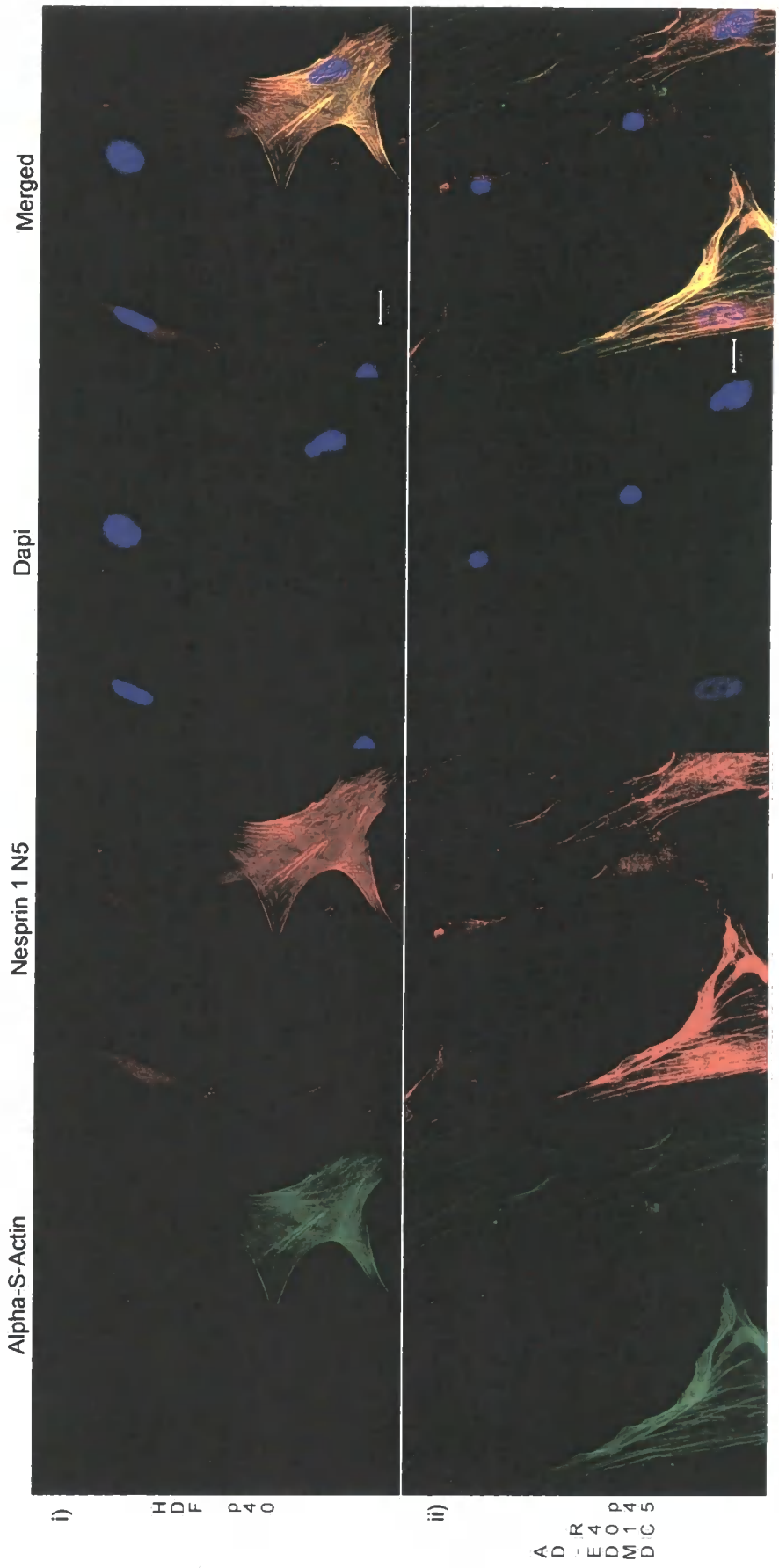
Merged
Dapi
Nesprin 1 N5
Alpha-S-Actin
i)
HDF p40
ii)
ADR-E40p
DM14
DC5

Figure 4.13 A

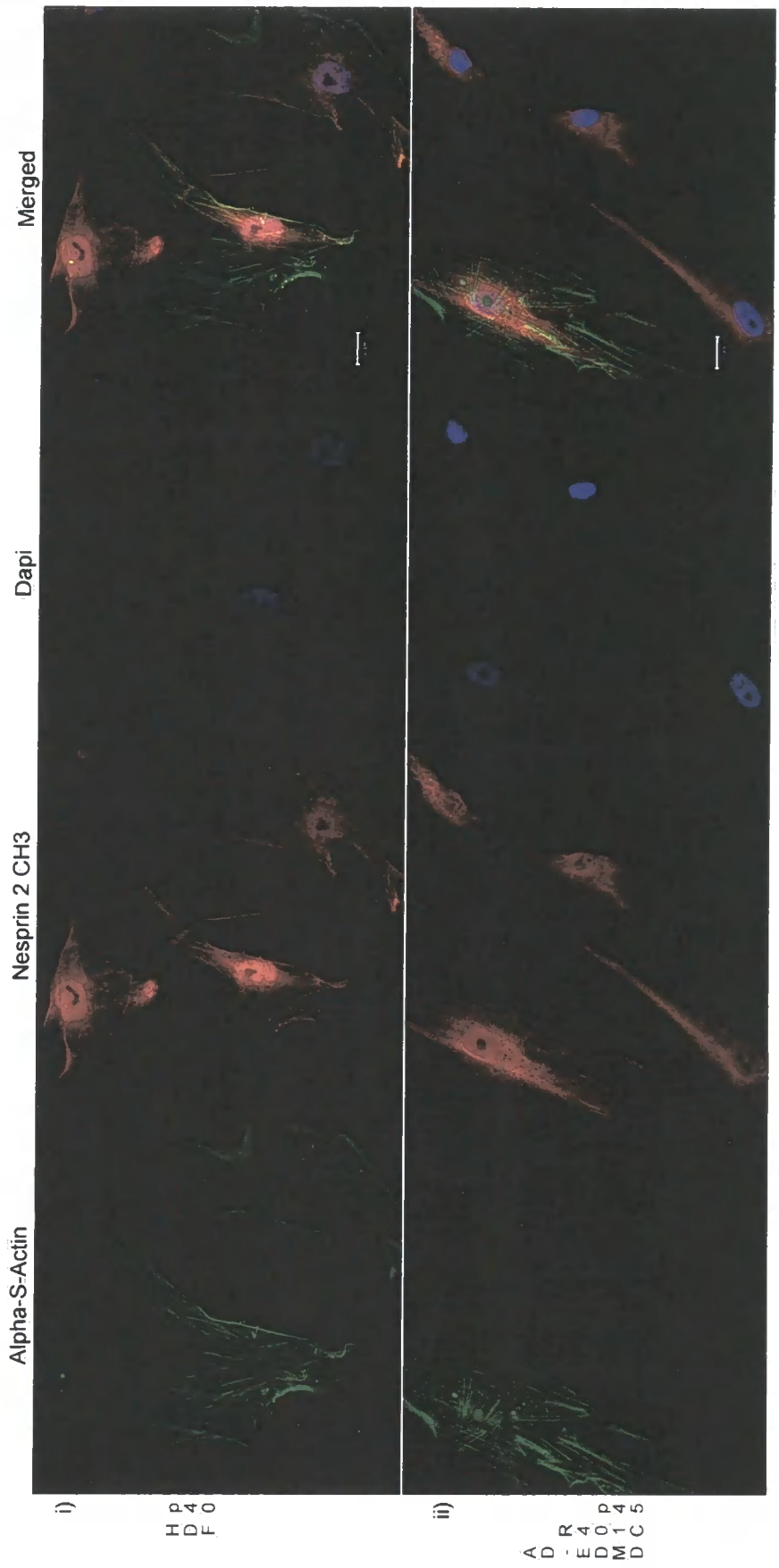
Alpha-S-Actin
Nesprin 2 CH3
Dapi
Merged
i)
HpD4F0
ii)
ADR-E4D0PM14DC5

Figure 4.13 B

Figure 4.14

Human Dermal Fibroblasts from a healthy donor (i), AD-EDMD patient (ii) and X-linked EDMD patient (iii) were grown until 80% confluence, fixed with 3.5 % Para-formaldehyde and double stained with anti-emerin (green) and anti-Nesprin 1 C1 (C-terminal) (red) antibodies. DAPI-containing mounting media was used to label the DNA (blue).

A. Cultures in proliferating state. Nesprin 1 did not form any fibers when stained with the antibody specific for the C-terminal region. Control fibroblasts presented a very diffuse staining across the cell. AD-EDMD and X-linked cells presented more nucleoplasmic staining than the control.

B. Cultures in quiescence state. Nesprin 1 re-locates to the nuclear ring and perinuclear space, in the control and the AD-EDMD cells but it stayed diffuse in the X-linked EDMD cell line.

C. Cultures after 30 hours of serum re-stimulation. Nesprin 1 distributed in across the cell in control and X-linked EDMD fibroblasts but AD-EDMD cells still conserved the nuclear distribution.

Figure 4.14 A

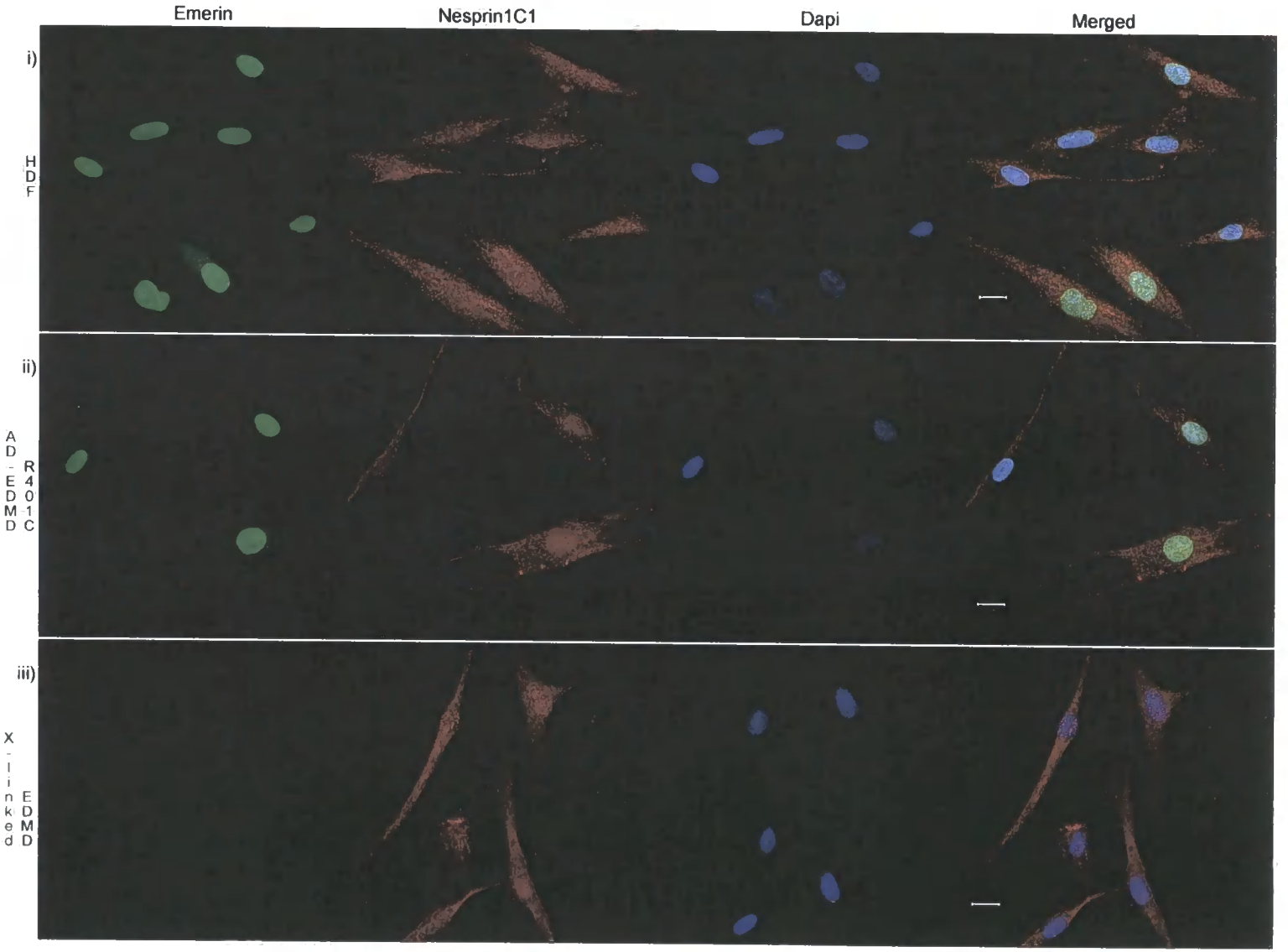
Emerin
Nesprin1C1
Dapi
Merged
i)
HDF
ii)
AD-EDMD R401C
iii)
X-linked EDMD

Figure 4.14 B

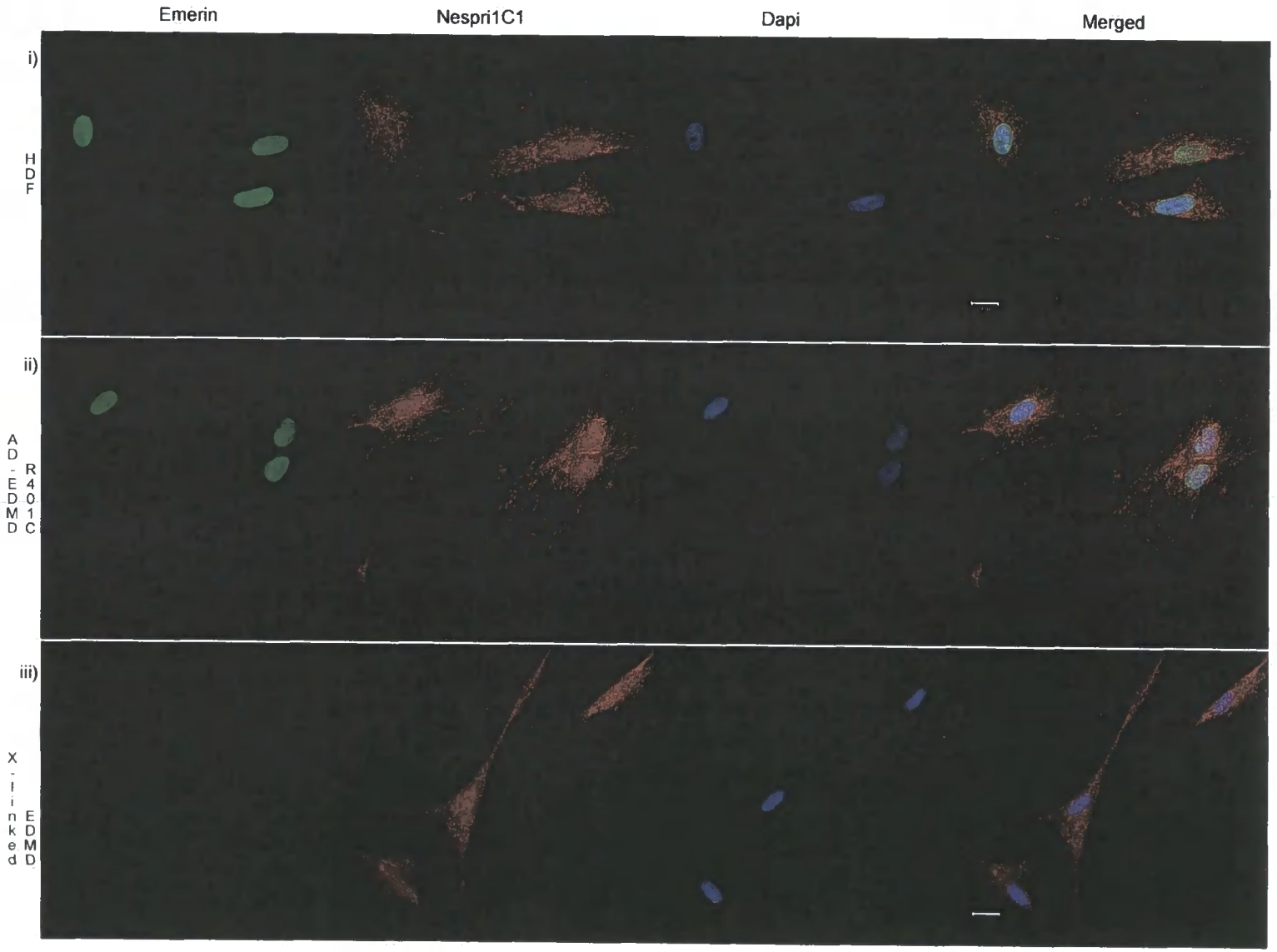
Emerin
Nespri1C1
Dapi
Merged
i)
HDF
ii)
AD-EDMD R401C
iii)
X-linked EDMD

Figure 4.14 C

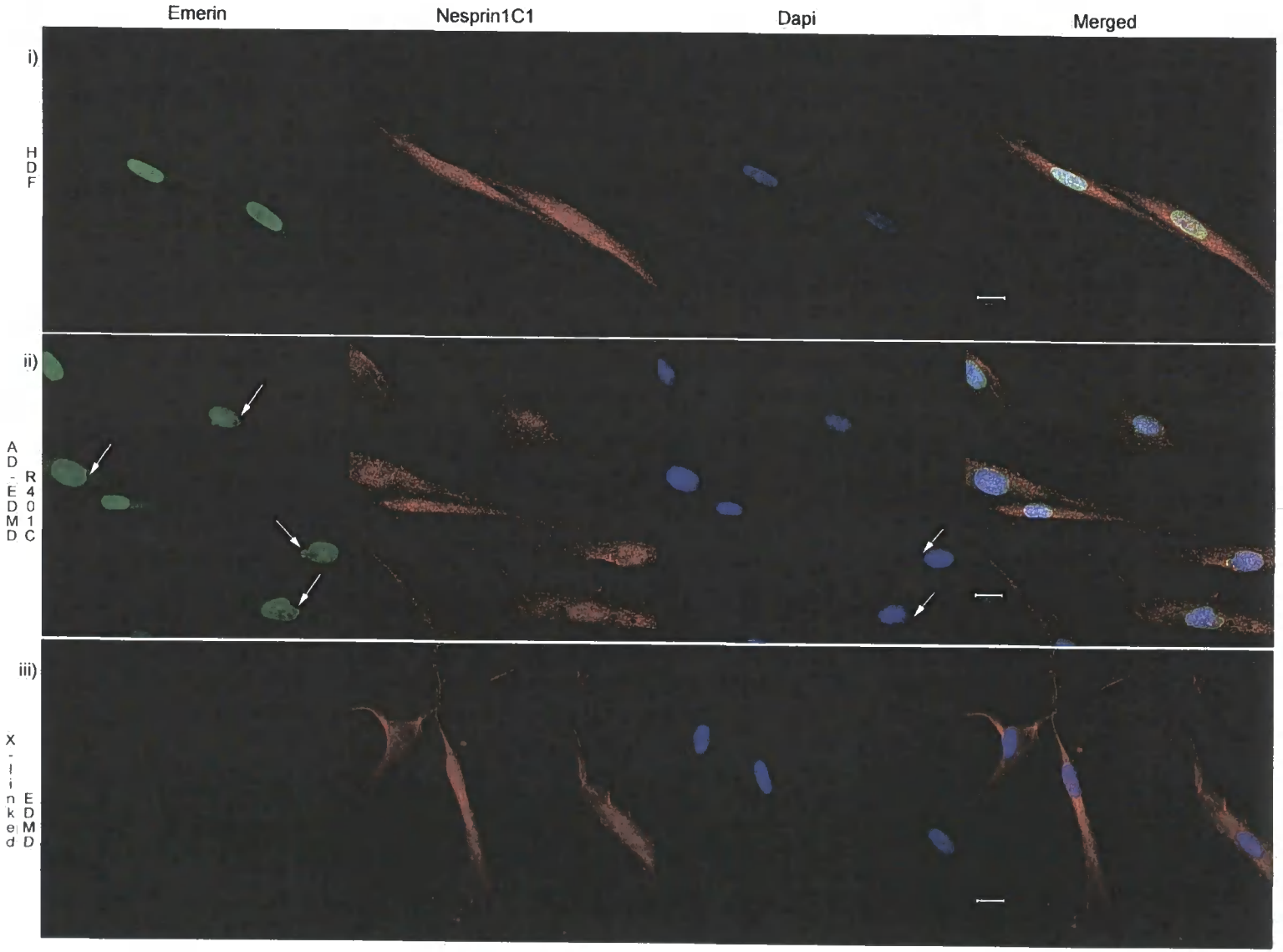
Emerin
Nesprin1C1
Dapi
Merged
i)
HDF
ii)
AD-EDMD R401C
iii)
X-linked EDMD

Figure 4.15

Human Dermal Fibroblasts from a healthy donor (i), AD-EDMD patient (ii) and X-linked EDMD patient (iii) were grown until 80% confluence, fixed with 3.5 % Para-formaldehyde and double stained with anti-lamin A/C (green) and anti-Nesprin 1 C1 (C-terminal) (red) antibodies. DAPI-containing mounting media was used to label the DNA (blue).

A. Cultures in proliferating state. Nesprin 1 did not form any fibers when stained with the antibody specific for the C-terminal region. Control fibroblasts presented a very diffuse staining across the cell. AD-EDMD and X-linked cells presented more nucleoplasmic staining than the control.

B. Cultures in quiescent state. Nesprin 1 re-locates to the nuclear ring and perinuclear space, in the control and the AD-EDMD cells but it stayed diffuse in the X-linked EDMD cell line.

C. Cultures after 30 hours of serum re-stimulation. Nesprin 1 distributed across the cell in control and X-linked EDMD fibroblasts but AD-EDMD cells still conserved the nuclear distribution.

Figure 4.15 A

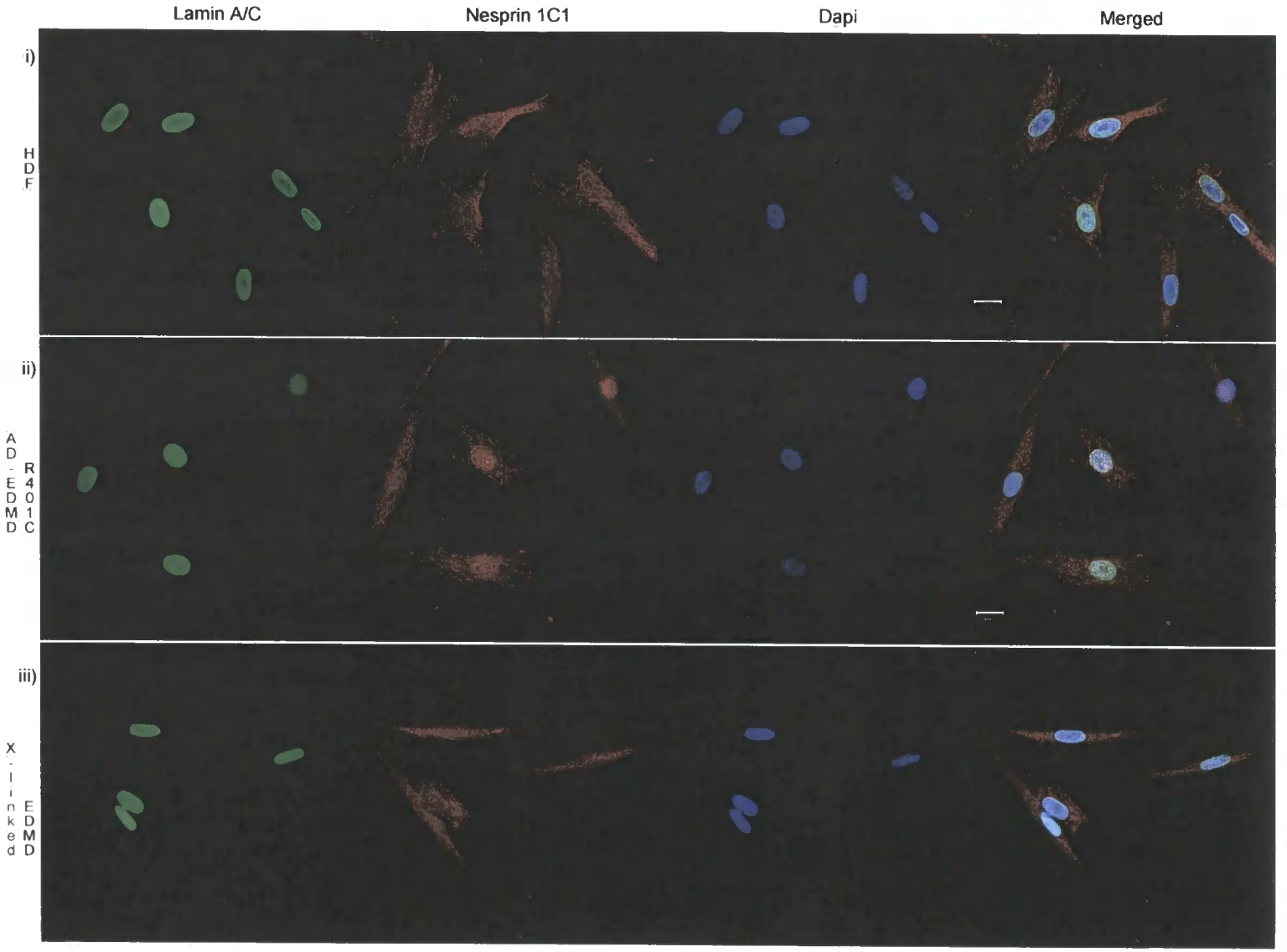
Lamin A/C
Nesprin 1C1
Dapi
Merged
i)
HDF
ii)
AD-EDMD R401C
iii)
X-linked EDMD

Figure 4.15 B

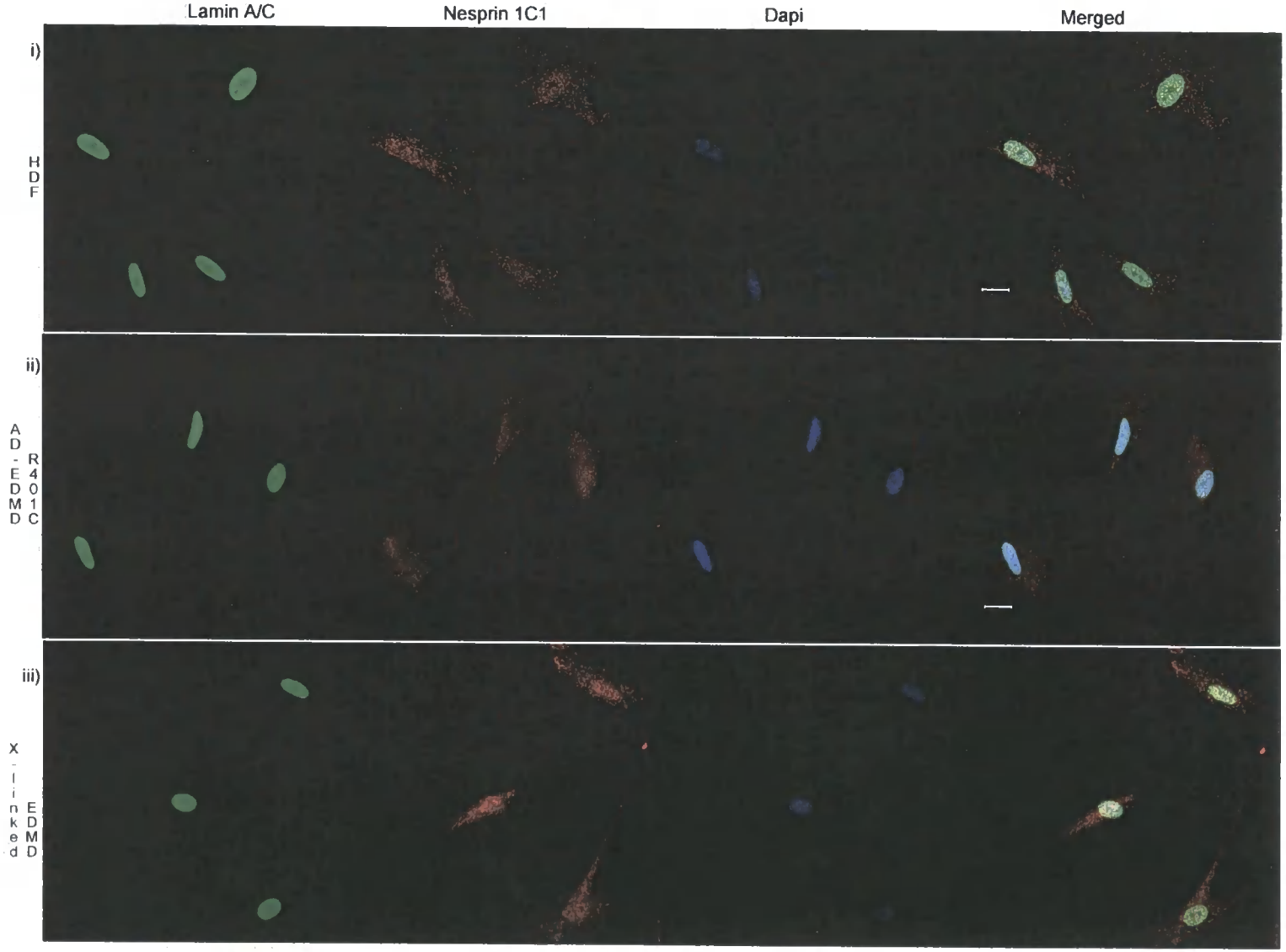
Lamin A/C
Nesprin 1C1
Dapi
Merged
i)
HDF
ii)
AD-EDMD R401C
iii)
X-linked EDMD

Figure 4.15 C

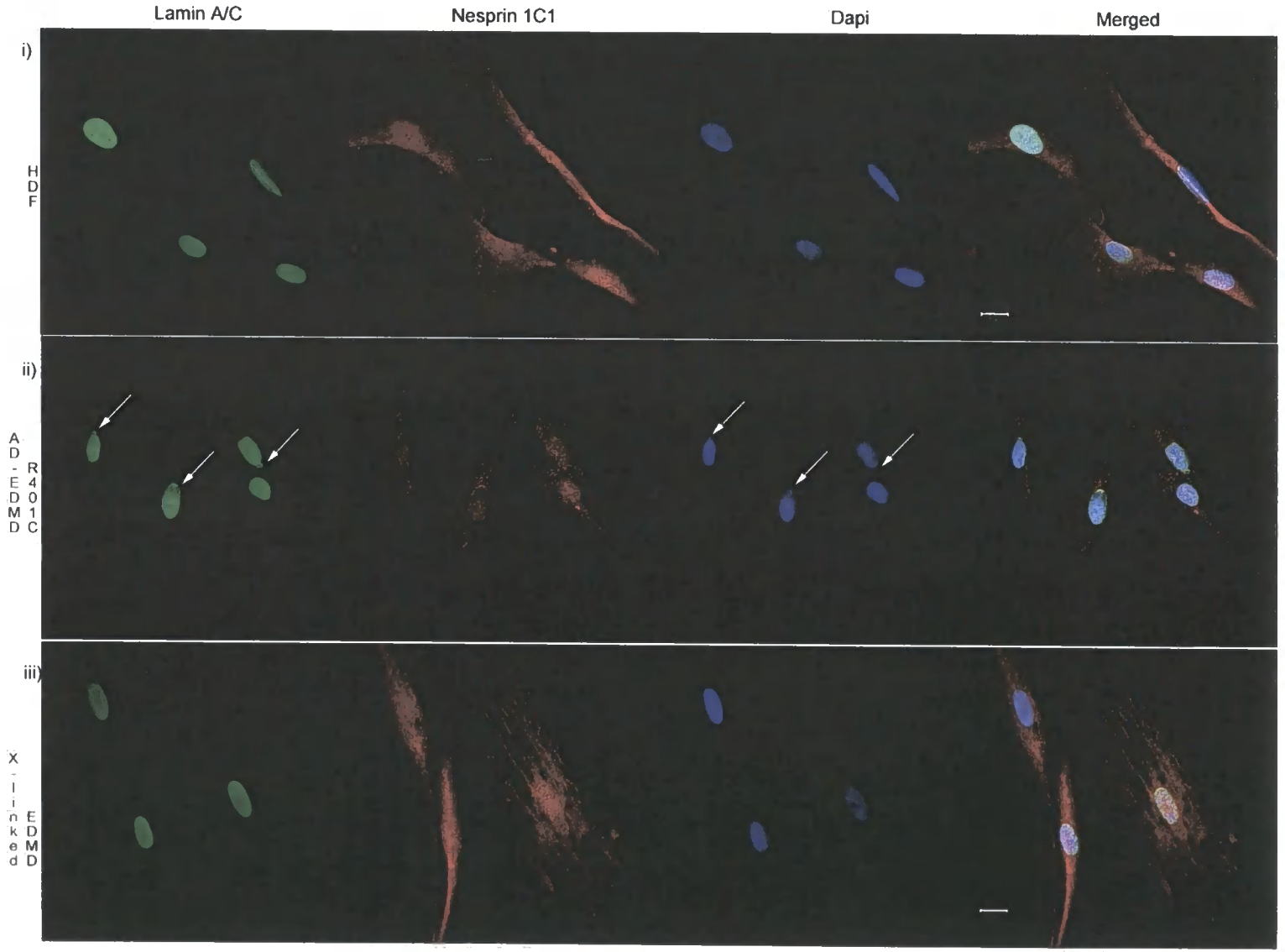
Lamin A/C
Nesprin 1C1
Dapi
Merged
i)
HDF
ii)
AD-EDMD R401C
iii)
X-linked EDMD

Figure 4.16

Human Dermal Fibroblasts from a healthy donor (i), AD-EDMD patient (ii) and X-linked EDMD patient (iii) were grown until 80% confluence, fixed with 3.5 % Para-formaldehyde and double stained with anti-emerin- (green) and anti-Nesprin 2 N2 (C-terminal) (red) antibodies. DAPI-containing mounting media was used to label the DNA (blue).

A. Cultures in proliferating state. Nesprin 2 labeled at the C-terminal presented a diffuse pattern of staining across the control cells, but in the patient cell lines the staining was stronger in the nucleus, with the X-linked cell line presenting the clearer nuclear localization. The absence of the C-terminal from the nucleoli was not as dramatic as the absence of the N-terminal.

B. Cultures in quiescent state. Nesprin 2 C-terminal re-organized to the nucleus in all cells, but still was stronger in the X-linked EDMD cell line.

C. Cultures after 30 hours of serum re-stimulation. Nesprin 2 still remained in the nucleus, particularly in the X-linked EDMD fibroblasts.

Figure 4.16 A

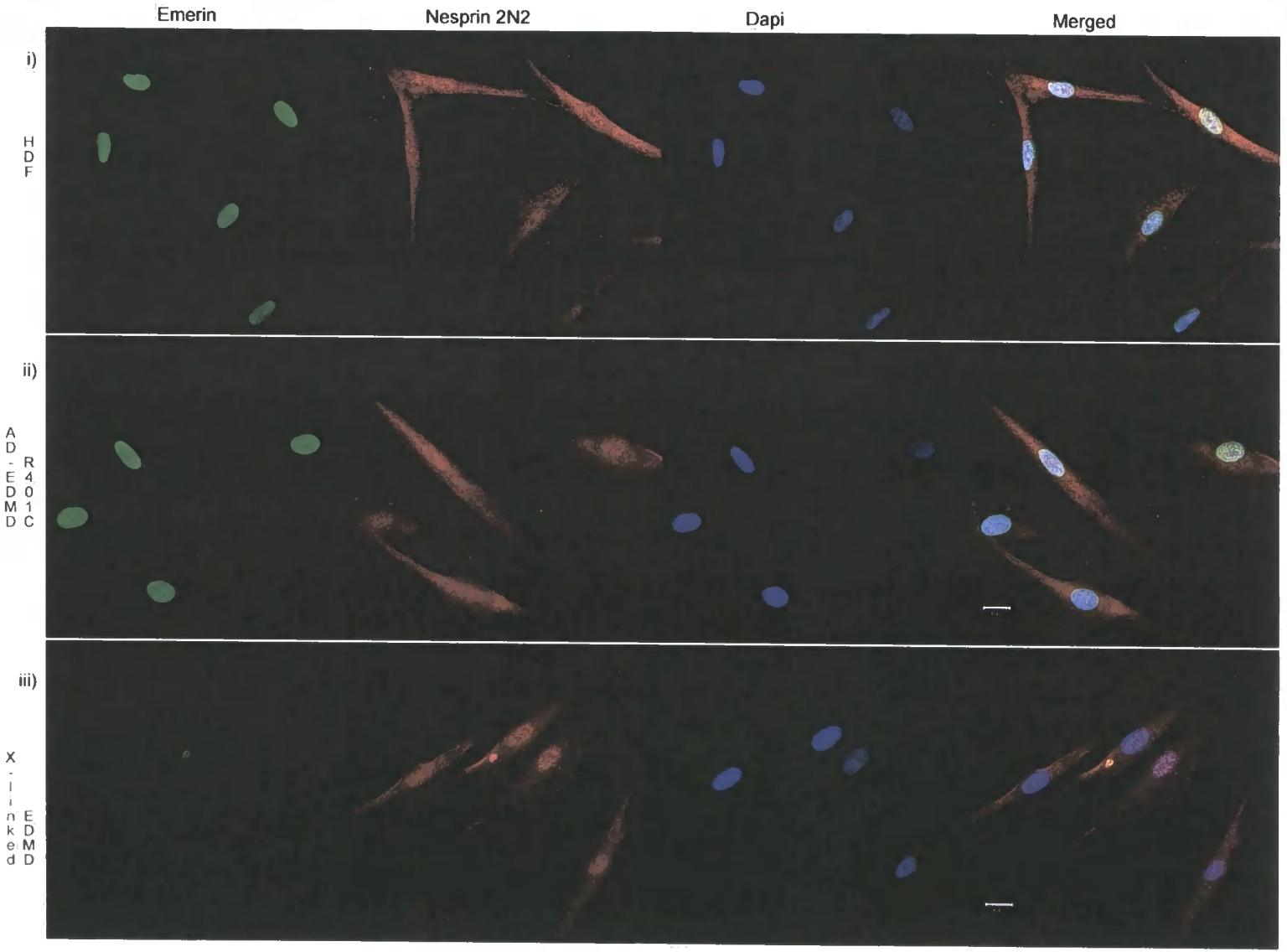
Emerin
Nesprin 2N2
Dapi
Merged
i)
HDF
ii)
AD-EDMD R401C
iii)
X-linked EDMD

Figure 4.16 B

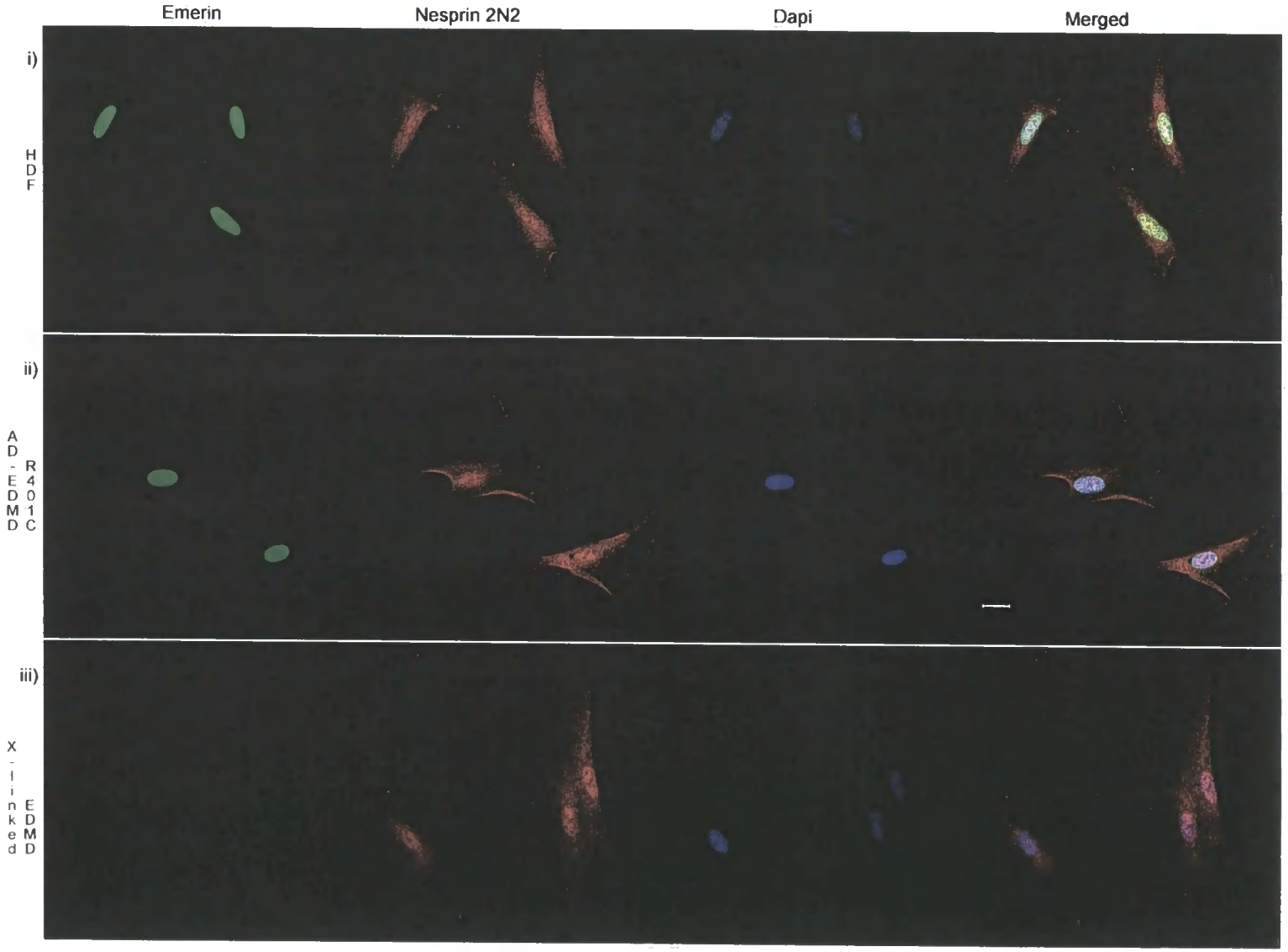
Emerin
Nesprin 2N2
Dapi
Merged
i)
HDF
ii)
AD-EDMD R401C
iii)
X-linked EDMD

Figure 4.16 C

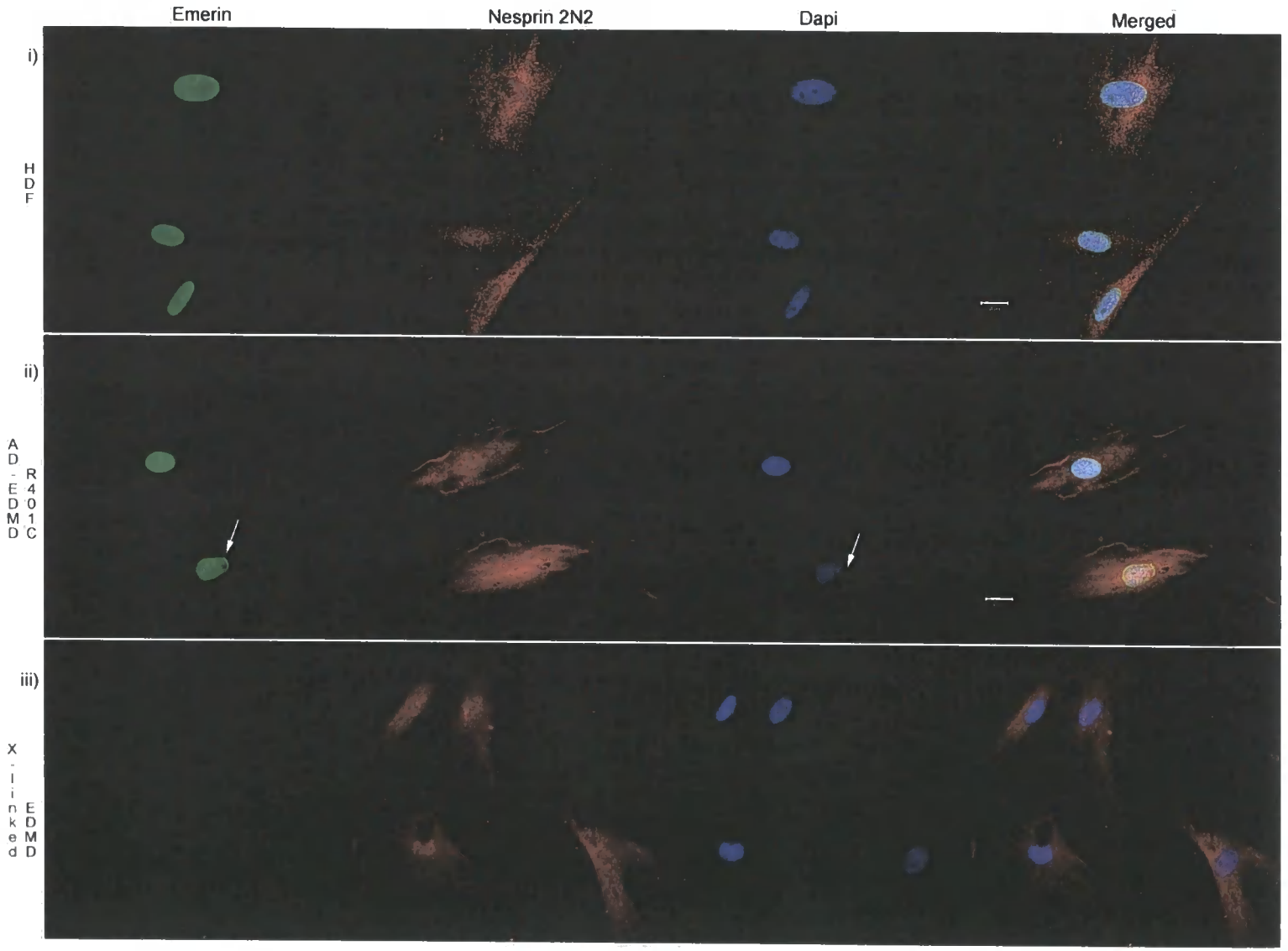
Emerin
Nesprin 2N2
Dapi
Merged
i)
HDF
ii)
AD-EDMD R401C
iii)
X-linked EDMD

Figure 4.17

Human Dermal Fibroblasts from a healthy donor (i), AD-EDMD patient (ii) and X-linked EDMD patient (iii) were grown until 80% confluence, fixed with 3.5 % Para-formaldehyde and double stained with anti-lamin A/C (green) and anti-Nesprin 2 N2 (C-terminal) (red) antibodies. DAPI-containing mounting media was used to label the DNA (blue).

A. Cultures in proliferating state. Nesprin 2 labeled at the C-terminal presented a diffuse pattern of staining across the control cells, but in the patient cell lines, the staining was stronger in the nucleus, with the X-linked cell line presenting the clearer nuclear localization. The absence of the C-terminal from the nucleoli was not as dramatic as the absence of the N-terminal.

B. Cultures in quiescent state. Nesprin 2 C-terminal re-organized to the nucleus in all cells, but still was stronger in the X-linked EDMD cell line.

C. Cultures after 30 hours of serum re-stimulation. Nesprin 2 still remained in the nucleus, particularly in the X-linked EDMD fibroblasts.

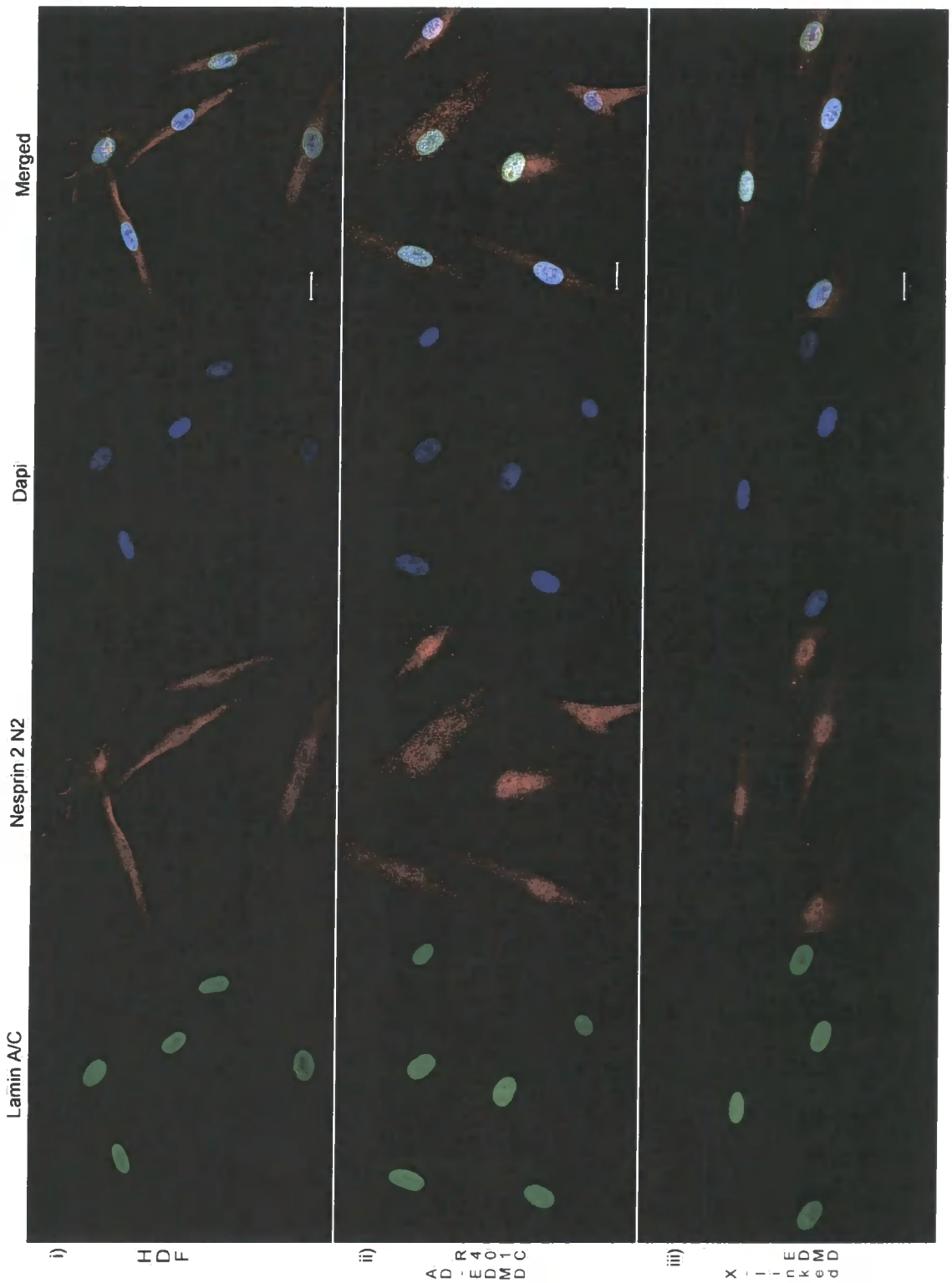

Figure 4.17 A

Figure 4.17 B

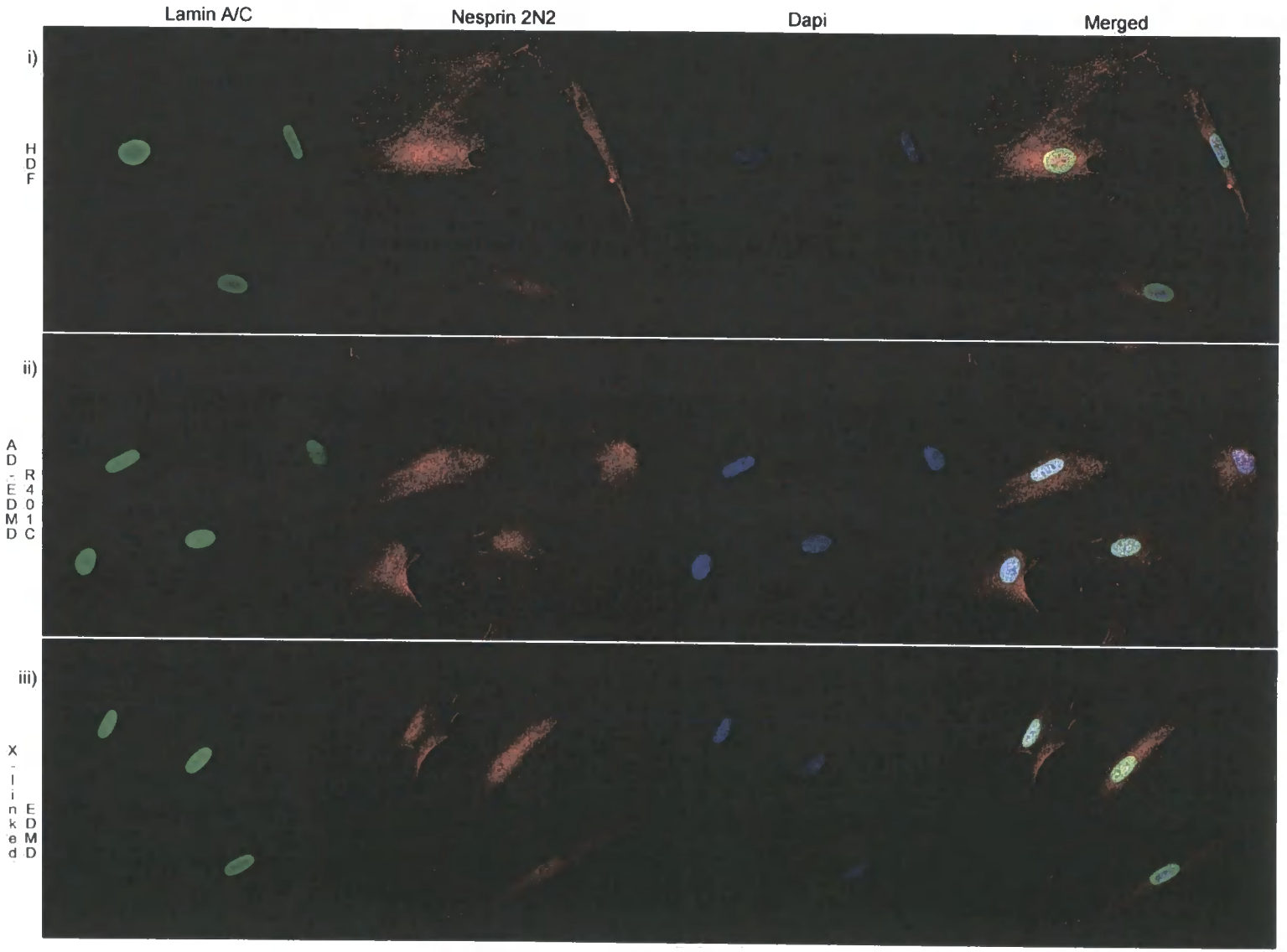
Lamin A/C
Nesprin 2N2
Dapi
Merged
i)
HDF
ii)
AD-EDMD R401C
iii)
X-linked EDMD

Figure 4.17 C

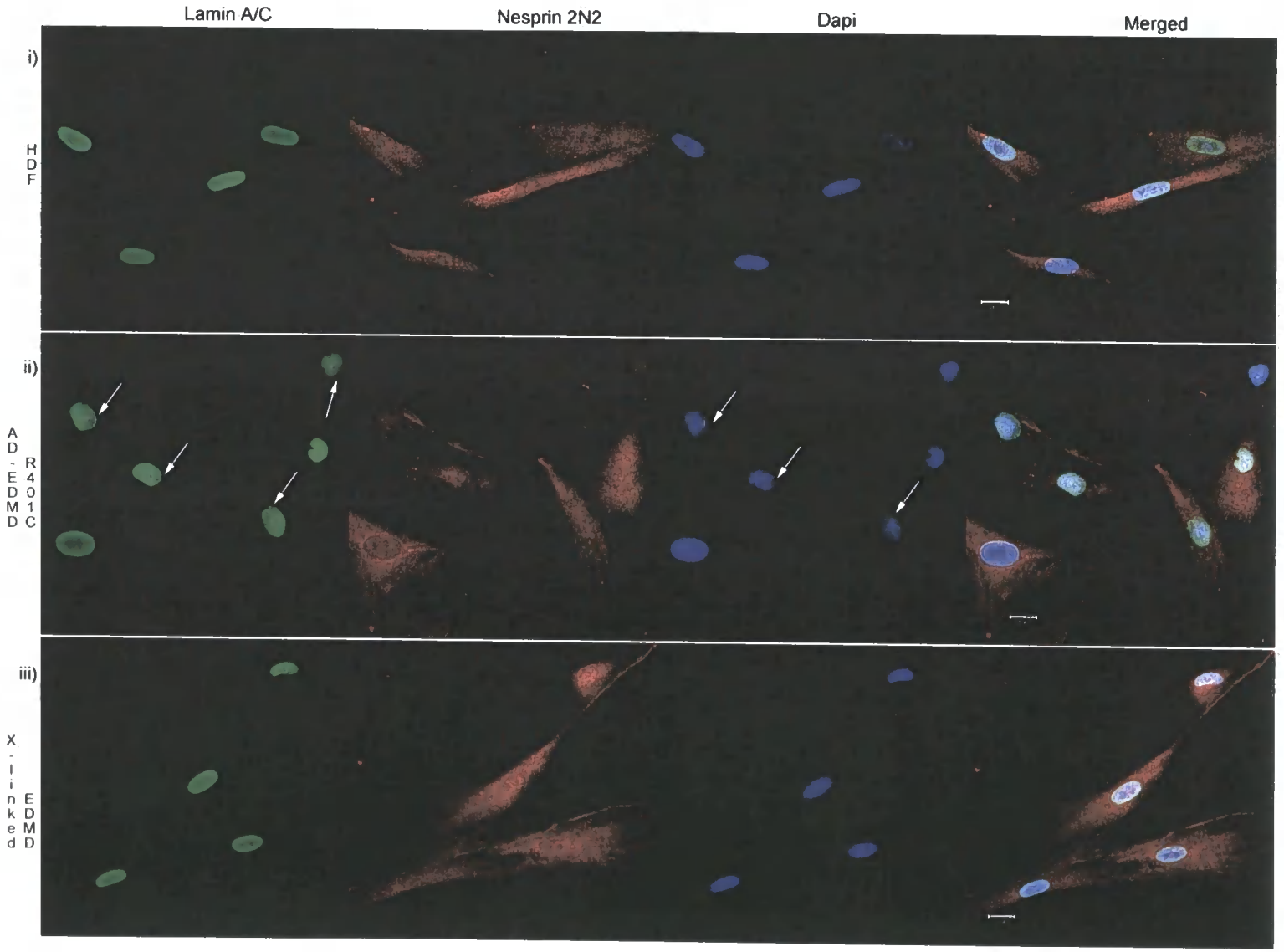
Lamin A/C
Nesprin 2N2
Dapi
Merged
i)
HDF
ii)
AD-EDMD R401C
iii)
X-linked EDMD

Figure 4.18

Human dermal fibroblasts from a healthy donor and AD-EDMD patient were grown at late passages. Cells were grown in 10% NCS until passage 30, then they were grown in 5% NCS/ 5% FBS as far as they were proliferating and the cells looked healthy. Cultures were split 1:3 every time they reached 80% confluence. Cells were cultured on 13mm glass coverslips, fixed with 3.5 % Para-formaldehyde and double stained with:

A. Anti-Ki67 (green) and nesprin 1 N5 (red) antibodies.

B. Anti-emerin (green) and nesprin 1 C1 antibodies.

C. Anti-laminA-C (green) and nesprin 1 C1 antibodies

Figure 4.18 A

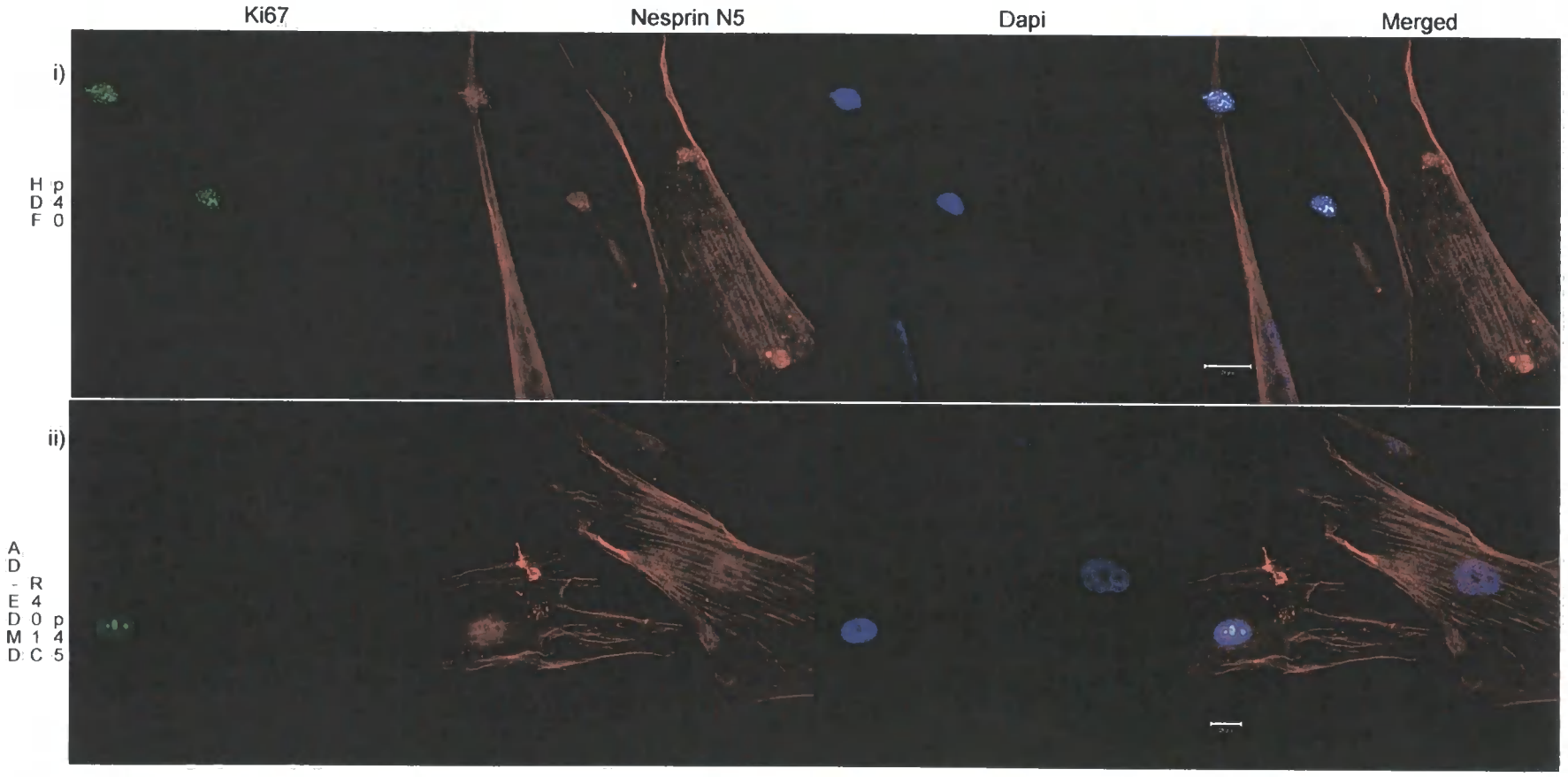

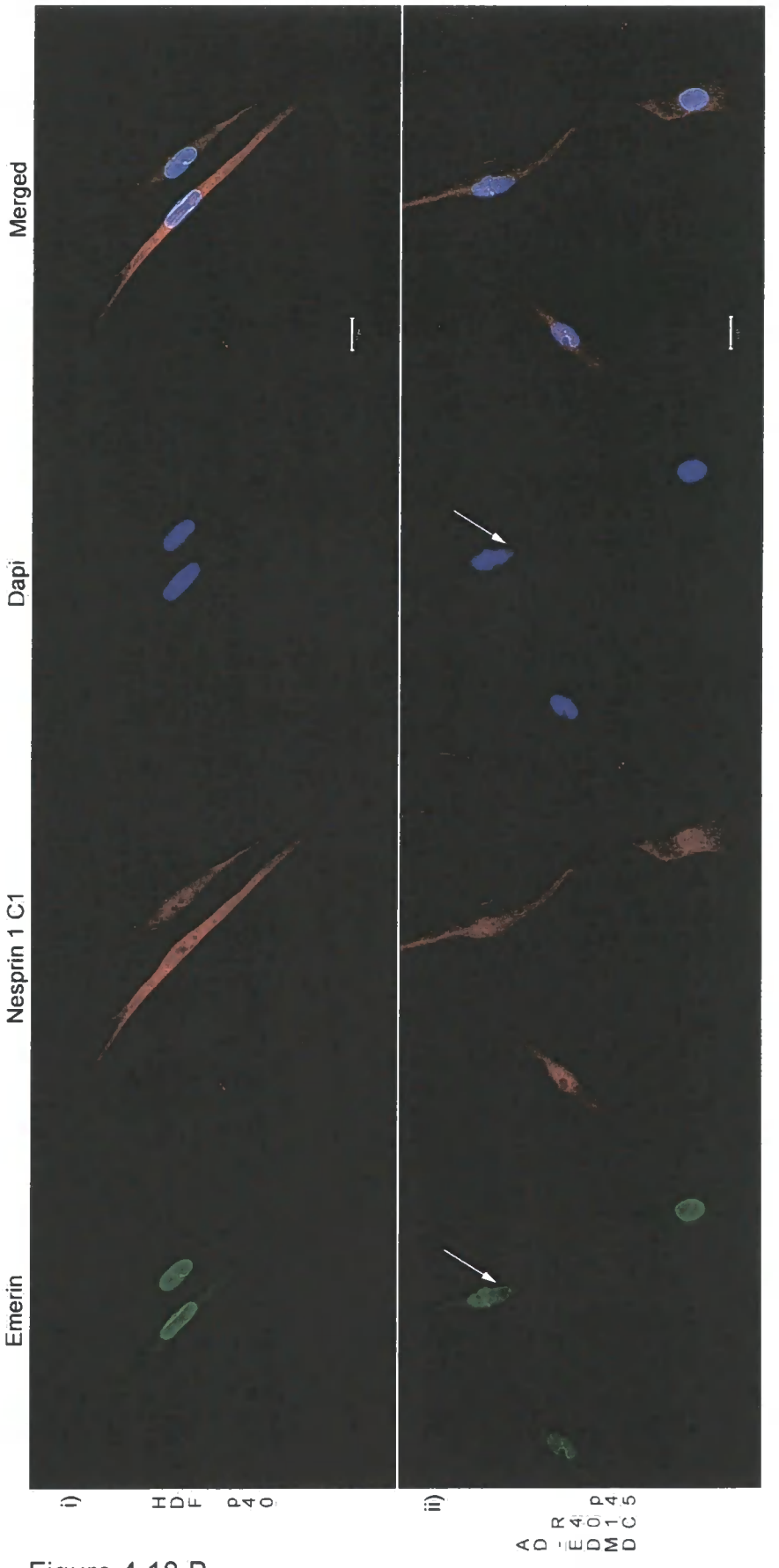

Figure 4.18 B

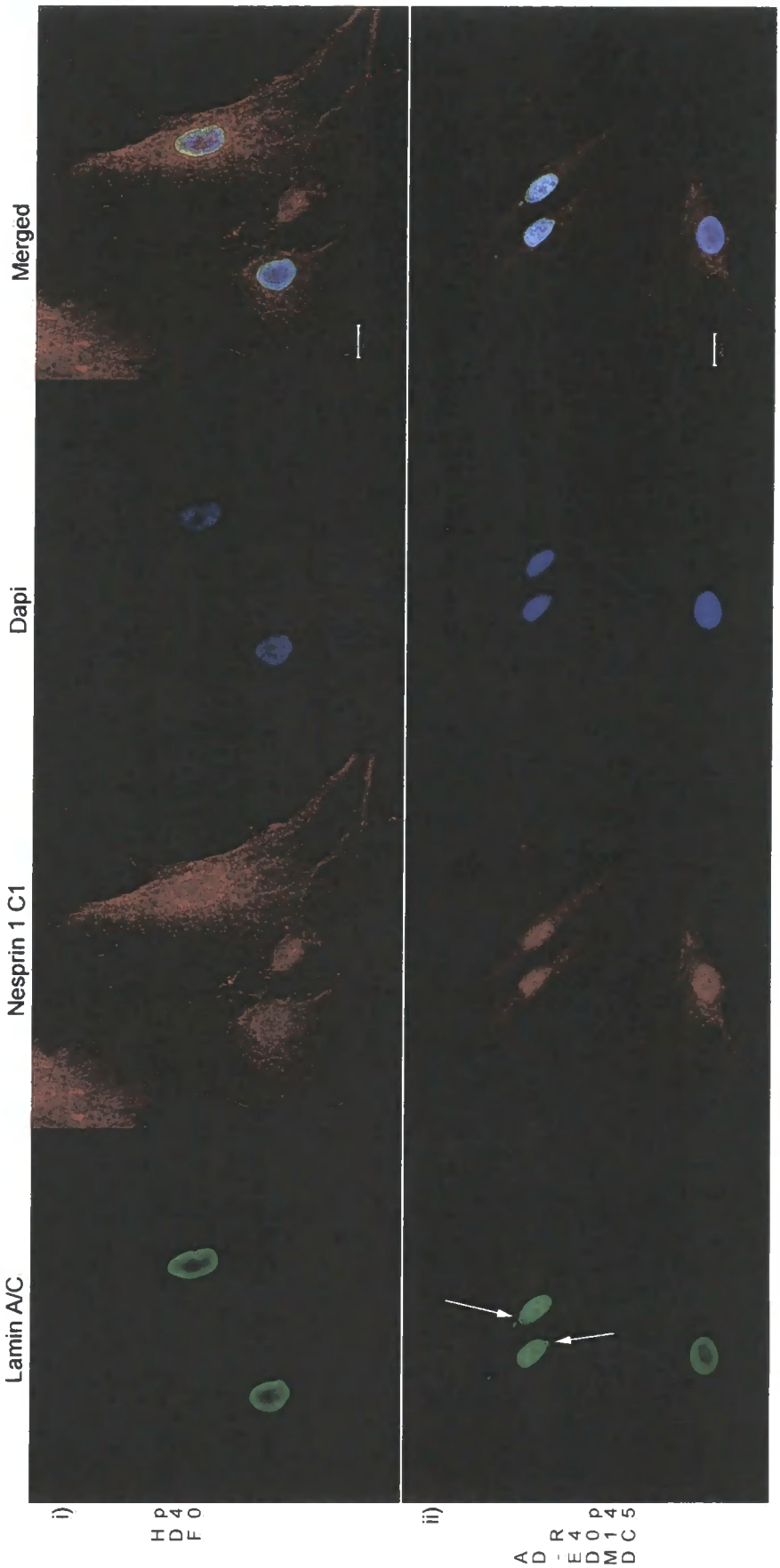
Merged
Dapi
Nesprin 1 C1
Lamin A/C
i)
HpD4F0
ii)
ADR-E4D0pM14DC5

Figure 4.18 C

Figure 4.19

Human dermal fibroblasts from a healthy donor and AD-EDMD patient were grown at late passages. Cells were grown in 10% NCS until passage 30, then they were grown in 5% NCS / 5% FBS as far as they were proliferating and the cells looked healthy. Cultures were split 1:3 every time they reached 80% confluence. Cells were cultured on 13mm glass coverslips, fixed with 3.5 % Para-formaldehyde and double stained with:

A. Anti-Ki67 (green) and Nesprin 2 CHS (red) antibodies.

B. Anti-emerin (green) and Nesprin 2 N2 antibodies.

C. Anti-laminA-C (green) and Nesprin 2 N2 antibodies

Figure 4.19.A

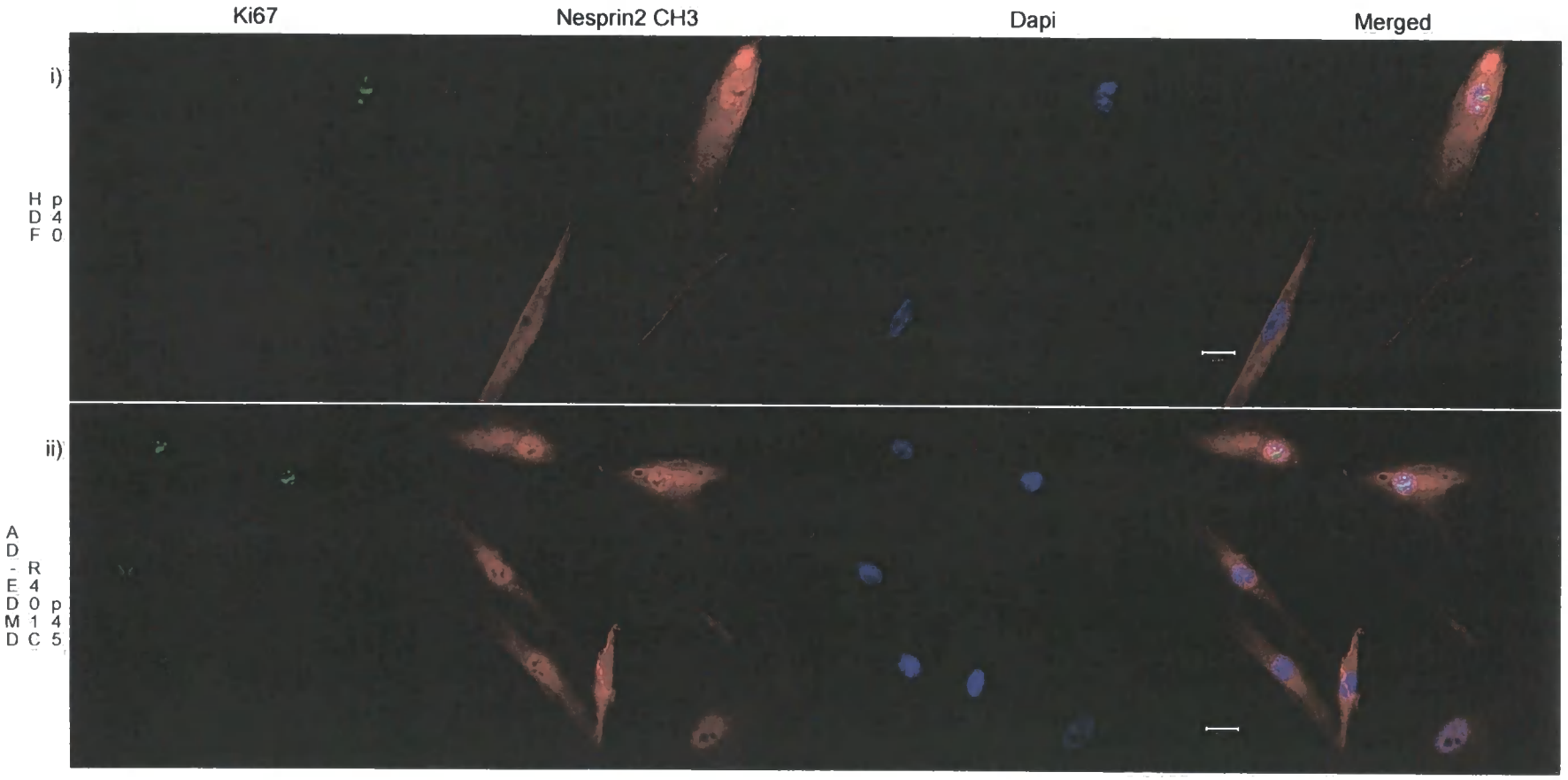

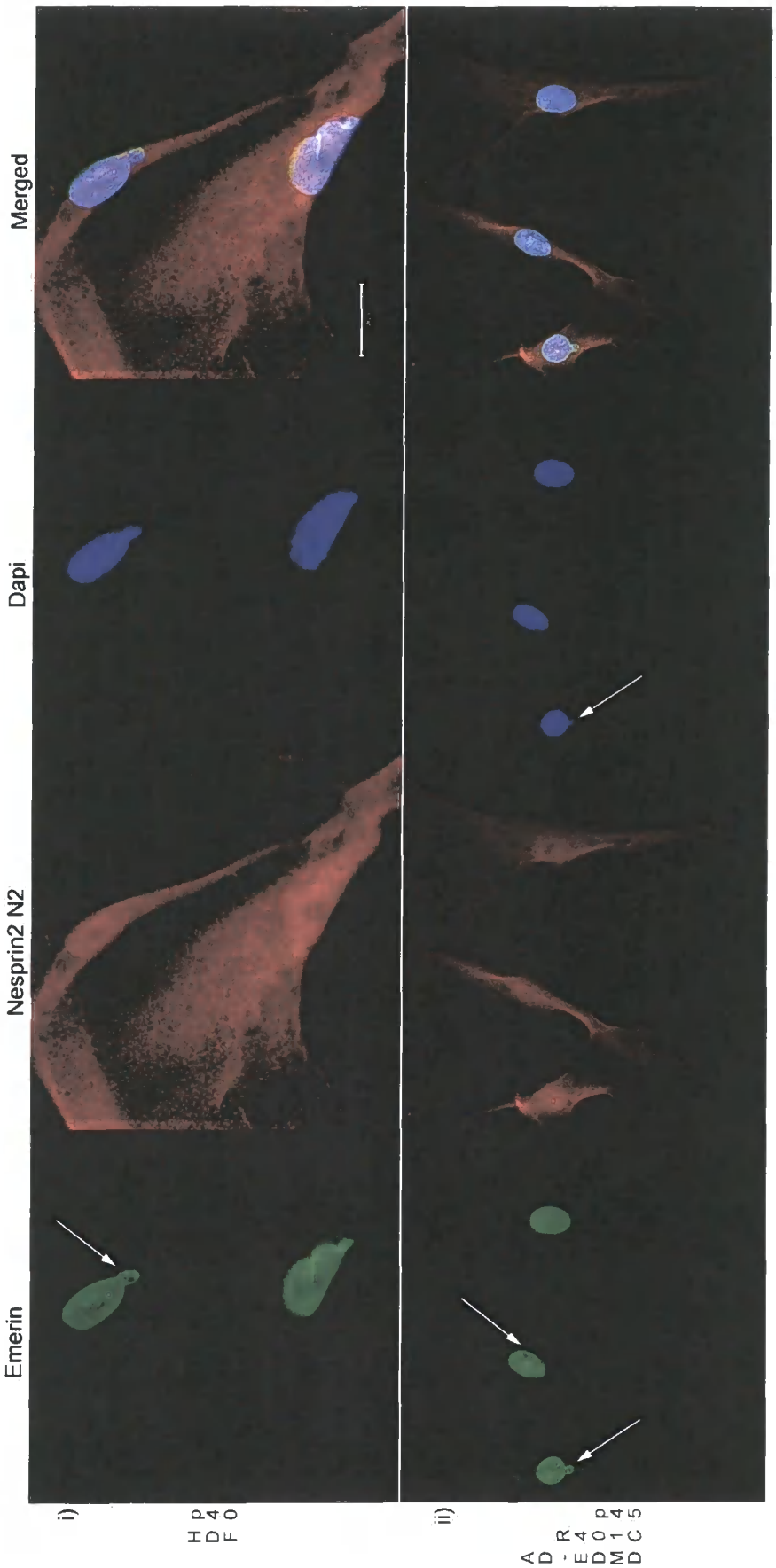

Figure 4.19 B

Figure 4.19 C

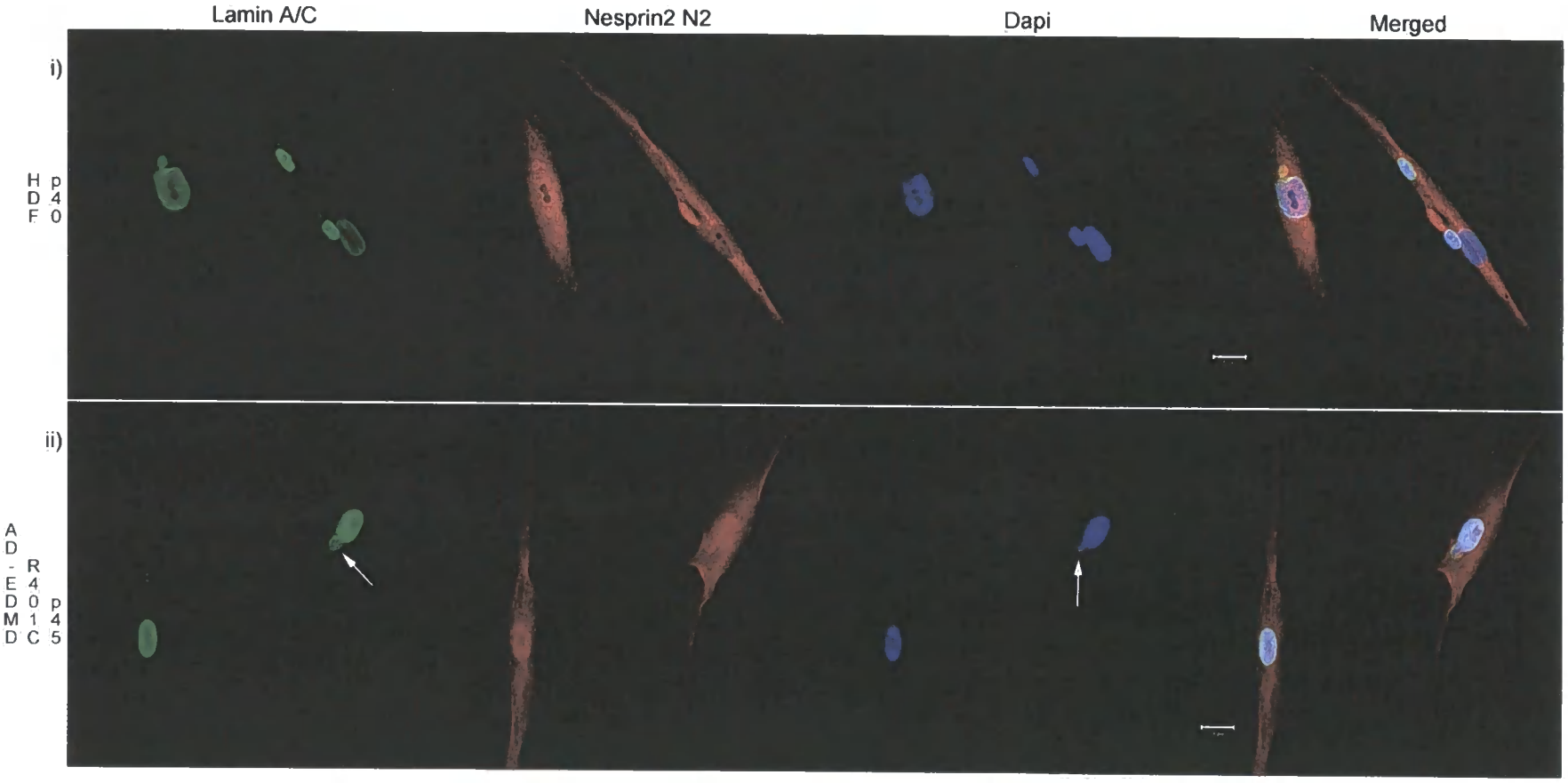
Lamin A/C
Nesprin2 N2
Dapi
Merged
i)
HDF p40
ii)
AD-EDMD R401C p45

Figure 4.20

Expression patterns for Nesprin 1 in control and AD-EDMD fibroblasts revealed.

A. Cell extracts were prepared from sub-confluent cultures in the presence of protein inhibitors cocktail (Sigma) and 5 jig of total protein were loaded per well. Samples were separated in a 10% SDS-PAGE, transferred and immuno-blotted with anti-Nesprin 1 C1 antibody (C-terminal). Mid passage (20): Control (lanel), AD-EDMD patients (lanes 2: R249Q, lane 3: R401C and lane 4: MA6G4). Late passage: Control (passage 38, lane 5) and AD-EDMD (passage 42, lane 6). Molecular markers are in KD.

B. Cell extracts were prepared from non-confluence cultures in the presence of protein inhibitors cocktail (Sigma) and 5 |j.g of total protein were loaded per well. Samples were separated in a 10% SDS-PAGE, transferred and immuno-blotted with anti-Nesprin 1 N5 antibody (N-terminal). Mid passage (20): Control (lanel), AD-EDMD patients (lanes 2: R249Q, lane 3: R401C and lane 4: MA6G4). Late passage: Control (passage 38, lane 5) and AD-EDMD (passage 42, lane 6). Molecular markers are in KD.

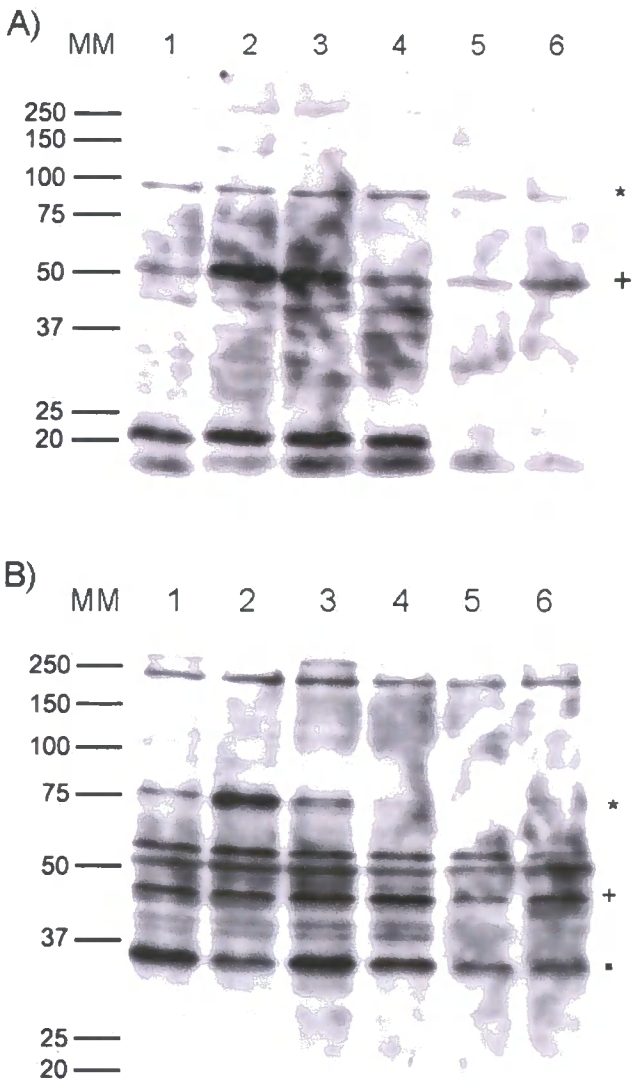
A)
MM
1
2
3
4
5
6
250
150
100
75
50
37
25
20
*
+
B)
MM
1
2
3
4
5
6
250
150
100
75
50
37
25
20
*
+
-

Figure 4.20

Table 4.2

Statistical analysis of honeycomb distribution with different fixation methods using Wilcoxon-Mann-Whitney Z test for paired-sample using SPSS® 11.1 (for Windows®). * represents significance at $p<0.05$.

AD-EDMD Cell Line	Variance		Mean		Standard Deviation		Difference between PFA - M:A Wilcoxon Test (Z)	Significance
	PFA	M:A	PFA	M:A	PFA	M:A		
HDF	0.0196	0.0385	0.02	0.04	0.14	0.196	(-2.828)	0.005
R249Q	0.0196	0.138	0.02	0.165	0.14	0.371	(-7.616)	0.0001
R401C	0.0338	0.147	0.035	0.18	0.184	0.384	(-7.616)	0.0001
T10PR	0.0587	0.0942	0.0625	0.105	0.242	0.306	(-4.123)	0.0001
MA6G4	0.0543	0.0861	0.0575	0.095	0.233	0.293	(-3.873)	0.0001
F02/536	0	0.0099	0	0.01	0	0.099	(-2.000)*	0.046
PK	0.04536	0.0092	0.0475	0.103	0.219	0.303	(-4.690)	0.0001

Table 4.2

5. Chapter five - ARMS- RT-PCR assay for AD-EDMD

5.1. Introduction

The importance for medical science of identifying the genetic basis underlying individual differences becomes obvious from the observation that individuals differ in their susceptibility to disease. The identification of gene variants predisposing to certain diseases allows assessment of risk and facilitates prevention. Similarly, genetic factors determine the reaction of individuals to therapeutic agents, by affecting drug metabolism or the predisposition to develop adverse reactions, or their interaction with the environment. Genetically determined individual differences are the result of polymorphisms in the genome, and complex processes, like susceptibility to most diseases, are often associated with variations in quantitative traits that are influenced by multiple gene loci. Quantitative trait loci must be polymorphic and their alleles must differ in their contribution to the quantitative trait (Rothenburg, Koch-Nolte et al. 2001).

Considerable progress has been made in mapping quantitative trait loci, but it is very difficult to identify the mutations underlying a disease phenotype. Mutations with phenotypic consequences may be of two types: 1) mutation affecting coding regions, which may result in structural change in the gene product and lead to an altered function of the encoded protein. This is the easiest scenario to establish a causal link between the mutation and the disease phenotype; 2) mutations within non-coding regions, which are frequently more subtle in their effects as they lead to quantitative rather than qualitative variation of gene expression. Quantitative differences in gene expression are generally assumed to be due to mutations in regulatory sequences, such as promoter or enhancer elements, which directly affect the ability of transcription factors to bind target sequences. Polymorphisms occurring in promoter regions upstream to the transcriptional

start site may potentially affect the process of transcription whereby RNA polymerases are recruited to the gene and the nascent mRNA synthesized. This complex process requires the coordinated action of multiple regulatory proteins through complex protein-DNA and protein-protein interactions (Orphanides and Reinberg 2002). Variation in the DNA sequence may potentially alter the affinities of existing protein-DNA interactions or, indeed, recruit new proteins to bind to the DNA, altering the specificity and kinetics of the transcriptional process (Tournamille, Colin et al. 1995; Buckley, Dean et al. 1999; Knight, Udalova et al. 1999; Udalova, Richardson et al. 2000).

The most abundant source of polymorphisms in the mammalian genome is the presence of repetitive DNA sequences, due to defects in the DNA repairing machinery during nucleic acid replication, and Single Nucleotide Polymorphisms (SNPs). DNA repeats can modulate the role of regulatory sequences by different mechanisms like differential DNA methylation (Bird 1986; Rothenburg, Koch-Nolte et al. 2001) or left-handed Z-DNA formation (Schwartz, Rould et al. 1999).

In diploid organisms, the vast majority of genes are expressed by both alleles, but mono-allelic expression has been reported in a growing number (Mostoslavsky and Bergman 1997; Ohlsson, Tycko et al. 1998). In most of the instances investigated so far, the choice of which allele is expressed is determined either by the parental origin, as in genomic imprinting, or is stochastic, as in the allelic exclusion of the immuno-receptor genes (Chess, Simon et al. 1994; Held, Roland et al. 1995; Nutt, Vambrie et al. 1999). Many biological processes are regulated by random selection of expressed alleles. In all instances, the choice for the activation or repression of a given allele is made at some point in the development of an ancestral cell and then passed on

to its descendants by clonal expansion (Ohlsson, Tycko et al. 1998). Depending on the time-point of the activating or repressing event, this would result in fixation of the choice within a whole organism or in a given cell lineage. In the case of a disease phenotype, it is not difficult to imagine what the consequences for the patient can be if the allele chosen is altered by a polymorphism that affects the regulatory sequences.

Many techniques are currently used for DNA polymorphism genotyping: Micro-arrays, Real-Time PCR, Nucleotide extension, Cleavage, Ligation-Reaction product detection and display, each of them with its own advantages and disadvantages (Kirk, Feinsod et al. 2002). One of the simplest and most widely used SNP genotyping strategies is allele-specific PCR (AS-PCR). This DNA amplification method is based on positioning the 3' base of a PCR primer to match one of SNP allele and accurately extend only the correct matched primer under stringent conditions (Bottema, Sarkar et al. 1993). AS-PCR has the advantage of combining the amplification and detection events, with no additional probes or enzymes required. By using standard DNA primers, this approach generally produces false priming of certain nucleotides leading to inaccurate genotyping when G:T, C:A, A:C or T:G combinations are present if special care is not taken during the design process (Huang, Arnheim et al. 1992; Ayyadevara, Thaden et al. 2000).

The specificity and reliability of DNA primers for AS-PCR have been improved by different approaches. Some strategies are based on the template or the primer like switching strand for analysis or incorporation of additional mismatches in the allele specific primer near the 3' end (Allelic Refractory Mutation Specific-Polymerase Chain Reaction: ARMS-PCR) (Newton, Graham et al. 1989). Others use biochemical approaches like titration of critical PCR reaction components to near-limiting levels (Bottema, Sarkar et al. 1993) or enrichment of target template by PCR prior to

adding allele-specific primer (Kaltenbock and Schneider 1998). Some use modifications like truncated Taq DNA polymerase (Stoffel fragment) lacking 5' and 3' exonuclease activity (Lawyer, Stoffel et al. 1993) or nucleotide analogs to facilitate conversion at 3' mismatched sites (Day, Bergstrom et al. 1999). The latest approaches use apyrase to degrade dNTPs when reaction kinetics is slow at mismatched 3' ends (AMASE) (Ahmadian, Gharizadeh et al. 2001) or bidirectional Real-Time allele specific PCR with SYBR® Green fluorescent melt curve analysis of amplified products (Waterfall and Cobb 2002). Each of these AS-PCR optimization strategies has limitations. For example, inclusion of additional ARMS mismatches requires careful design, strand selection, and development that can create additional primer stability. Titration of reagents and target enrichment are time-consuming and complicate primer multiplex design. The use of Stoffel fragment requires high concentration of enzyme and is not compatible with 5' exonuclease probe cleavage in Real-Time AS-PCR. The other variations require either more expenses via reagents (probe or enzymes) or specific instrumentation for detection analysis.

Specificity and sensitivity of AS-PCR has recently increased by the introduction of a new modified nucleotide termed locked nucleic acid (LNA) at the 3' terminal position of the primers. LNA is a nucleic acid analog with a 2'-O, 4'-C methylene bridge (Kumar, Singh et al. 1998). This bi-cyclic structure locks the ribose moiety into a C3'-endo conformation, which generally increases hybrid Tm when an oligonucleotide containing LNA is hybridized with its complement (Nielsen, Singh et al. 1999). The use of this innovative family of nucleic acid analog does not restrict to AS-PCR, but to a series of applications including immobilized capture probes, micro-array analysis, and anti-sense and decoy oligonucleotide technologies (Nielsen, Singh et al. 1999; Orum, Jakobsen et al. 1999; Wahlestedt, Salmi et al. 2000; Braasch and Corey 2001; Crinelli, Bianchi et al. 2002; Jacobsen, Bentzen et

al. 2002).

Individual lamins and integral nuclear envelope proteins have been demonstrated to play a crucial role in maintaining the integrity and functionality of the cell nucleus, assessed by their involvement in several genetic disorders. Mutations in the STA gene (emerin) produce the X-linked form of EDMD, while point mutations in the gene encoding for A-type lamins have been linked up to six different clinical phenotypes so far (Gisele Bonne and al 2003). Interestingly, other patients with no mutation in the LMNA gene have been included within some of the same clinical classifications caused by point mutations in A-type lamins (e.g. cardiac, muscle involvement (Gisele Bonne and al 2003) and FPLD (Hegele, Yuen et al. 2001)). Despite the intensive research in the laminopathies field, focused on biochemical, cellular biology and human genetics approaches, no studies so far have been published to address the question whether non-coding mutations affecting regulatory elements in the LMNA gene or other candidates are involved in this group of muscular dystrophies. The biggest attempt to find novel genes and mutations involved in the disease by a functional candidate gene approach has been focused in the coding region of candidate genes and has clearly discarded any intronic variations, short tandem repeats and frequent SNPs in non-coding regions (Gisele Bonne and al 2003). Other studies using genomic DNA sequencing approach found mutations in the coding and non- coding regions of LMNB1 and LBR genes in FPLD patients whose LMNA gene sequence was normal (Hegele, Yuen et al. 2001). In contrast to studies by Wehnert et al (see (Gisele Bonne and al 2003)), the Hegele's study has considered LMNB1 and LBR as potential candidates for FPLD in patients with no mutations in LMNA, and has suggested focused analyses on its promoter region.

The genomic structure of the A-type lamins gene and its promoter region in humans, mice and rats has been determined (Lin and Worman 1993; Nakajima

and Abe 1995; Tiwari, Muralikrishna et al. 1998). The 5' promoter region have been analyzed and several regulatory elements have been found: a GC box that can bind to Sp1 and Sp3 transcription factors (Lin and Worman 1993; Tiwari, Muralikrishna et al. 1998; Muralikrishna and Parnaik 2001); a TATA box, and an AP-1 motif that can bind to c-Jun and c-Fos, which play a key role in the activation of the lamin A promoter in Drosophila and Mouse embryonal carcinoma cells (Hass, Brach et al. 1991; Muralikrishna and Parnaik 2001); Lamin-Retinoic Acid Regulatory Element (L-RARE) (Okumura, Nakamachi et al. 2000) and DNaseI hypersensitive sites (Nakamachi and Nakajima 2000). In addition, the LMNA locus is under the control of at least two promoters: a somatic cell-acting promoter (for lamins A and C) and a testis-specific promoter (for lamin C2). Expression of lamins A and C is controlled by differential selection of poly-A sites and lamin A-specific splicing (Nakajima and Abe 1995). It is well known that LMNA is a developmental regulated gene, which appears late in embryogenesis and it is up regulated when cells exit the cell cycle (Dyer, Kill et al. 1997). As described above, several regulatory elements are involved in this complex process, so it becomes obvious that mutations in regulatory elements would have an effect, subtle or dramatic, in the expression of A-type lamins, and might determine the disease phenotype. The effect of polymorphisms in susceptibility to diseases has been demonstrated (Knight, Udalova et al. 1999; Udalova, Richardson et al. 2000).

Since the cell lines used in this study are heterozygous, two related question arose during the course of the experimental work: 1); are both alleles of the LMNA gene equally transcribed?; 2) is there any haplo-insufficiency at the protein levels of the mutant and the wild type A-type lamins as a result of any differential allelic transcription? The latter has been addressed in Chapter Four.

Here I describe the design, optimization and successful use of ARMS primers for RT-PCR to detect single nucleotide polymorphisms in cell lines derived from AD-EDMD patients with mutations in the rod (R249Q) and tail domain (R401C) of lamins A and C (Figure 5.1). Alternative primers design is given (LNA primers) in combination with powerful instrumental analysis (CEQ-8000). I found evidence for differential allelic expression, apparently not related to the mutations, for both lamin A and lamin C mRNA levels in the two cases analyzed. The different pattern of expression for the mutations studied may open more questions related to whether the disease-associated genetic variants linked to the LMNA gene in AD-EDMD are functionally important or serve only as a genetic marker with the functional locus co-inherited on the polymorphic allele.

5.2. Results

5.2.1. DNA primer design for ARMS-RT-PCR

Originally, the analysis of the ARMS-PCR products was planned to be carried out using a CEQ-8000 genotyper (Beckman-Coulter), so the primers specific for the mutations (sense) were all labelled at the 5' end with different fluorescent probes in order to differentiate the wild type and mutant alleles on the same sample using a multiplex reaction. But technical difficulties with the CEQ-8000 made it impossible to separate the fragments by capillary electrophoresis, so the analysis had to be performed on agarose gels. The presence of the fluorescent probe at the 5' end of the primers produced a predictable shift in the mobility of the fragments separated in 2% agarose gels.

Amplification of specific point mutations restricts the strategies to design ARMS-PCR primers because the mutant base must be at the very 3' end of each primer and a mismatch at the second or third last base (Table 5.1). For example, in the case of the mutation R249Q (G746A) if the mutant sequence is:

Mutant Sequence: 5' g a t g c g c t g c a g g a a c t g c A

And the wild type sequence is:

Wild type Sequence: 5' g a t g c g c t g c a g g a a c t g c C

Then the mutant primer for the mutant allele will be:

Mutant Primer: 5' g a t g c g c t g c a g g a a c t A c A

And the wild type primer for the wild type allele will be:

Wild type Primer: 5' g a t g c g c t g c a g g a a c t A c C

The same approach was used to design the ARMS-PCR primers for the mutation R401C (C1201T). With this in mind, using NetPrimer PCR online software I designed combinations of ARMS-PCR primers with the optimal theoretical parameters to ensure a successful assay. The coding region containing the

mutation R249Q (746 G→A) allowed designing of the best possible combination of primers for both lamin A and lamin C anti-sense specific probes. Melting points (Tm: theoretical temperature, based on the nucleotide composition, at which 50% of the primer molecules remain annealed to the template) were very similar between the sense and anti-sense primers, GC content was > 55% in all cases but not higher than 60%, and secondary structures were kept to the minimum (Hairpin, Dimer primers, Cross-linking, Palindromes) (Table 5.1).

In the case of mutation R401C (1201C→T), the region where the mutation is only allowed designing sense primers with 5 - 10°C difference in the Tm regarding their anti-sense combinations for both lamin A and C, when keeping the secondary structures to the minimum. The high Tm reflects the elevated GC content of this region, forcing the design of primers with 70 - 75% of GC in their nucleotide composition. In the case of the combination of primers R401C (1201C→T) / Lamin C, a relative high number of cross-linking (4) (see Table 5.1) could account for the very high stability of this couple of primers at annealing temperatures above the Tm in the RT-PCR reaction (Figure 5.6 A - D).

5.2.2. Annealing temperature optimization for mutations R249Q (746 G →A) and R401C (1201 C→T) using ARMS primers

Every PCR reaction requires optimization in some, if not all of its parameters before any interpretation and conclusion is made out of the data obtained. The purpose of the ARMS-RT-PCR assay described in this chapter was to provide a fast, reliable and relatively cost effective assay that allows a large number of samples to be processed, in search for evidences of differential expression of the LMNA alleles in cell lines or clinical samples (blood, biopsies, etc) from heterozygous AD-EDMD patient.

Genotyping of mutation R249Q was optimized for both lamin A (Figure 5.2) and

Lamin C (Figure 5.3) specific mRNAs by using ARMS DNA primers. In both cases, the mutant allele was expressed at lower levels compared to the wild type during the entire gradient tested, even at the most stringent temperatures near the Tm. The design for the mutant primer proved to be optimum, considering it did not produce any amplification in the control mRNA. The combination of primers for the lamin C splicing variant produced a neater amplification when compared to the Lamin A one, where weak background fragments were observed between 500 and 800 bp, but this should not affect the interpretation of the data. None of the primers produced any significant amount of secondary structures empirically (dimer primers, hairpins, cross-linking) as no bands were observed below 100 bp. PCR products were sequenced to confirm that the amplified fragments were specific for the region of interest. In both cases the sequence obtained corresponded to the wild type and mutant alleles as expected (data not shown). Although this was not a quantitative assay, it is important to note that at optimum annealing temperature for each combination of primers, the expression level of wild type lamins A and C transcripts was very similar to the control. In addition, the level of expression of lamin C transcripts was always higher when compared to lamin A. The primer specific for the mutation never produced any amplification in the control (Figures 5.2 and 5.3 A) and B) lanes 2 and 6).

A pilot experiment was set up to analyze whether a multiplex RT-PCR reaction could differentiate between wild type and mutant allele using the CEQ-8000. Mutation R249Q (746 G→A) and control RNA were amplified for lamin C at 60°C and 2 μl of the products were mixed with Di-methylformamide. The mixture was injected in the CEQ-8000 and the fragments analyzed for molecular weight and fluorescent signal (Figure 5.4). The multiplex reaction did differentiate the wild type from the mutant allele, and the reduction pattern is similar to the signal obtained by Ethidium Bromide in the agarose gels (Figure 5.3 B, lanes 5 -8). The

ratio of wild type/mutant allele is not similar, due to the difference in quantum efficiency of the WellRed® D3 dye compared to D4. This should affect only the quantitative approach of the assay rather than the qualitative outcome.

Amplification of the region containing mutation R401C was also successful. In contrast to the data obtained for mutation R249Q (lamin A), the combination of primers for lamin A and lamin C amplification in R401C produced a neat product in almost all the reactions. Lamin A specific primers showed a consistent differential amplification during the entire gradient, where the mutant allele in the patient cell line was always expressed at a higher level compared to the wild type, even at stringent conditions very near to the Tm (Figure 5.5 B) lanes 5 -8).

Optimization of ARMS-RT-PCR for the combination of primers specific for lamin C transcripts in the R401C mutant was intriguing, as the primers produced PCR products at very high temperatures, above the Tm for the primers. For this combination of oligonucleotides, a first temperature gradient was set up, which produced a very slight difference in the level of expression between wild type and mutant alleles in the patient (Figure 5.6). When a second, more stringent gradient was assayed, a clear differential pattern was obtained at critical temperatures, where the mutant allele was always present at higher level than the wild type (Figure 5.7 A - B), but still no inhibition of the annealing efficiency was observed. A third gradient was set up, to the maximum possible annealing temperature, and at a very stringent temperature (70°C), the same differential pattern of expression was observed. Only at 72°C, inhibition of the PCR reaction in both the control and the patient samples was observed (Figure 5.7 C - D). As in the case of the R249Q mutation, although the assay described here was not quantitative, all cases showed that the level of lamin A transcripts was lower than for lamin C, both in the control and in the patient. In addition, if the relative

amount of amplification products in the patient sample were put together both in lamin A and lamin C amplification, the levels were much lower in the patient than when compared to the control. A summary of all annealing temperature gradients tested are shown in Table 5.2.

Multiplex reactions were set up to assess the performance of this assay when primers specific for the wild type and mutant alleles were present in the same RT-PCR reaction, under the same conditions. At an optimum temperature (61 °C) (Figure 5.7 C lines 9 - 10), the multiplex RT-PCR produced results which were consistent with those obtained with separate primers at the same temperature (Figure 5.7 C lines 1 - 4), where an overall reduced amount of product was obtained. More stringent conditions (72°C) (Figure 5.6 D lines 9-10) affected the multiplex reaction in the same fashion as when separate primers were used at this temperature (Figure 5.7 D lines 5- 8). The primers specific for the mutation produced no amplification of lamin A or Lamin C in the control (Figures 5.5 and 5.6 A-B and 5.7 A - D, lanes 2 and 6).

In order to confirm the results using annealing temperature gradients, a final assay was set up including the optimum temperature at which no significant change in the intensity of the bands in the wild type and mutant alleles was obtained. Consistent results to those obtained in the optimization process were observed (Figure 5.8 A - B). Negative controls showed that the RNA samples used were free of any contaminants and β-Actin primers revealed the presence of an equal amount of mRNA in all samples (Figure 5.8 C).

Another important observation from these data, showed consistently throughout the gradients (Figures 5.2 to 5.7), the confirmation assay (Figure 5.8) and the multiplex RT-PCR analyzed in the CEQ-8000 (Figure 5.4), is the lower overall amount of transcripts in the patients compared to the control, both for lamin A

and C. The simplest conclusion from this study is that fewer transcripts mean less protein for both lamin A and C, and therefore haploinsufficiency in these patients.

5.2.3. Alternative primer modifications to detect Single Nucleotide Polymorphisms (SNPs) using the CEQ-8000 series of genotypers.

Technologies to detect known polymorphisms can be divided in two categories: hybridization-based or enzyme-based. Hybridization technologies include Micro-arrays, Real-Time PCR and AS-PCR. Enzymatic technologies include Nucleotide Extension, Cleavage, Ligation Reaction product detection and display. As methodologies, all of them have their own advantages and disadvantages. Apart from the technical inconveniences, possibly the most limiting aspect of genotyping techniques is the elevated cost when a large number of samples are processed or when a genome wide scale approach is needed (Kirk, Feinsod et al. 2002).

Optimization process is expensive, especially when genotyping technologies like ARMS-PCR (using labelled primers) demand a new primer design due to failure of the former primers to discriminate wild type from mutant alleles in heterozygous conditions. A new approach to increase the efficiency of primers to differentiate between wild type and mutant alleles in heterozygosis is the use of LNA primers (Latorra, Arar et al. 2003; Latorra, Campbell et al. 2003; Latorra, Hopkins et al. 2003). In addition, different fluorescent probes have been developed to be attached to the 5' end of primers. CEQ-8000 automatic DNA sequencers (Beckman- Coulter) use very accurate technology to separate labelled DNA fragments (using WellRed® dyes) based on size, but its advantage can be boosted if those DNA fragments are labelled with different fluorescent probes. Then it is possible to analyse different fragments at the same time, or what is more relevant in my case, it can differentiate the same fragment generated from different alleles in the same

heterozygous sample. With this in mind, and using the technologies available in the market, I designed a new generation of primers that allows high discrimination efficiency between mutant and wild type alleles in heterozygous samples, and time and cost saving during the primer design and optimization processes, by combining LNA and CEQ-8000 technologies.

Using NetPrimer PCR software online, I then designed primers that included a locked nucleic acid (LNA) at the 3' end for the mutant specific primer (at the position where the mutant base is in the mutant allele), and for the wild type specific primer (at the position where the wild type base is in the wild type allele) (Table 5.3). Then, a different WellRed® fluorescent probe was assigned to each primer, so each end contained a marker with different functions: a fluorescent probe at the 5' end, which allows discrimination of fragments with very similar size (including the same size), and a locked nucleic acid at the 3' end to increase allelic specificity. A recent study using cystic fibrosis as a model has shown that 3' LNA residues in AS-PCR primers increases allelic specificity and maintains high sensitivity compared with DNA primers. Its effect is independent of the specific mismatch involved and has proved to work efficiently with plasmid and human genomic DNA, with single and multiplex targets and using agarose gel detection or Real-Time PCR (SYBR®green) (Latorra, Campbell et al. 2003).

5.2.4. SNPs analysis in the regulatory elements of the LMNA genomic sequence: a bioinformatics approach

The Nuclear Lamina have been under intense study for nearly 20 years, as an effort to understand its biochemical properties, its behaviour during the cell cycle and its role in every kind of cell were their presence have been reported. However, very little has been done so far to understand how the transcription and translation of this important family of type V intermediate filaments is regulated. Since the finding that mutations in A-type lamins were linked to a disease

phenotype (AD-EDMD) (Bonne, Di Barletta et al. 1999), a very competitive field of research was set up in order to find the biochemical basis of these diseases. Although some advance have been made, it is still not clear how these mutations can cause the muscle wasting and heart failure observed in the patients and the broad range of phenotypes found due to mutations in the LMNA gene. Most of the mutations described to produce laminopathies are heterozygous, and some patients presenting the same clinical features do not have mutations in the LMNA gene. Taking this evidence together with the unexpected results of the ARMS-RT-PCR described in this chapter, a fertile ground was set up to formulate an obvious question: Are the point mutations in laminopathies the actual cause of the disease phenotype, or they are just a genetic marker that co-segregates with the actual disease-causing mutation/s on the polymorphic allele? The complete lack of sequencing data in the promoter region of the LMNA gene in patients with any of the laminopathies drives one to this hypothesis.

The first step to present this hypothesis was to analyze the regulatory elements contained in the human LMNA gene and map all known SNPs to this regions to check for overlap. A total of 99 SNPs were found, divided in 67% transitions and 32 % transversions; 1.5% of the transitions produced a silent variation (H566H [1698C→T]) while 3.1 % of the transversions produced a missense variation (R624P [1871G→C]). Interestingly, the SNP at position 1698 G→C, although produces a silent amino acid change, it occurs at the last position of the poly-histidine stretch on exon 10, changing the DNA sequence just at the splicing region for lamin C (Figure 5.1). Whether this affects the targeting of the splicing machinery and consequently alters the transcriptional ratio of lamin C has yet to be proved.

The LMNA sequence analyzed included 32kb upstream of ATG and 14.5 Kb

downstream of the TAA (57.5 Kb in total). This sequence was divided in four parts: Promoter region extending for 32360 bp upstream the ATG, genomic sequence for the LMNA gene from ATG to TAA (24188bp), downstream sequence from codon TAA (Stop), extending for 1013 bp and Full sequence analyzed, 57561 bp (Figure 5.9), where base's number starts at base number 1 relative to the sequence analyzed, not the actual position in chromosome 1. Four algorithms for promoter's analysis were used: GRAIL/Prom, TSSW/Prom, GENSCAN/Prom and FGenes/Prom. One algorithm analyzed for CgP islands (GRAIL/CpG) and one for Transcriptional Sites (Eponine) (Table 5.4). I mapped the predicted regulatory elements in the genomic sequence of the LMNA gene and its SNPs reported to date relative to the actual position in chromosome 1, in a graphic representation to scale, and classified the regulatory elements as good predictions (Figure 5.10) and marginal predictions (Figure 5.11).

In Figure 5.10 C, two DNA variations overlapped with two CpG islands upstream the ATG of LMNA gene. SNP 2502488 was inside the CpG Island 2502232 - 2502642 (at position -32054), and variation 2526065-2526066 was an AG deletion in the CpG Island 2526054 -2526282 (at position - 8477). None of the SNPs overlapped with any of the good promoters or transcriptional sites predicted by NIX analysis in the promoter region. CpG Island 2534300 - 2535000 extended from positions - 242 in the promoter region to + 458 into the first exon of LMNA gene (Figure 5.10 A and C) but no SNPs hit this region. LMNA genomic sequence contained a good predicted TATA (2547829) at intron 1, but no polymorphism was found in this area. Curiously, two SNPs were found in coding regions of the LMNA gene, specifically in exons 10 (2557366) and 11 (2558283). SNP in exon 10 produced a silent change of H - H while variation in exon 11 produced a change R→P. The region downstream the stop codon of LMNA gene showed one good prediction for a TATA box (2559385) but again no SNPs affected this region. Eight

polymorphisms were contained up to position + 421 after the TAA codon (Figure 5.10 D). Marginal predictions comprised only promoters and they were concentrated in the promoter region of the LMNA gene and its introns. None of them was hit by any SNP (Figure 5.11 A and C).

5.3. Discussion

In this chapter, two cell lines derived from AD-EDMD patients carrying mutations in the rod domain (R249Q/746G→A) and in the tail domain (R401C/1201C→T) of the A-type filaments were RNA extracted, together with a control cell line (HDF). RNAs were then used as templates to set up a one-step ARMS-RT-PCR assay using DNA primers including a mismatch at the third last base to increase specificity. The main results show that first, a differential allelic pattern of expression is present and the parental alleles are affected randomly, and secondly, the overall amount of A-type lamins transcripts is lower in both patients compared to the control. The point mutations in the coding region of the LMNA gene in the AD-EDMD fibroblasts studied here may not directly play a critical role in the disease phenotype, but rather they could be genomic markers that co-segregate with the polymorphic allele, with the true mutation/s not yet found, forming part of a haplotype not yet described.

Since the genomic structure of the LMNA gene was published, some studies have demonstrated the presence of regulatory elements in the promoter region of this gene, including TATA and GC boxes, AP1 motifs, L-RARE (Lamin-Retinoic Acid responsive Elements), CpG Islands, DNaseI hypersensitive sites and separate promoters for tissue specific lamins. Some of these studies have demonstrated that these regulatory elements are active, and are involved in the regulation of the LMNA gene during different biological processes. Despite these published data, genetic studies in laminopathies have mainly focused on searching for mutations in the coding region of the LMNA gene, even though some patients presenting the disease phenotype do not present any mutation in this gene or any other. So where is the lost link? Only one study has included the promoter region in their experimental design, while another one suggests that the promoter region should be analyzed. By coincidence, both studies were related to a lipodystrophy

phenotype

5.3.1. Differential allele expression

The results obtained in the ARMS-RT-PCR could be due to different mechanisms, but I will consider first they are due to the point mutations present in exon 10 (746 G→A) and exon 11(1201 C→T) of the LMNA gene. In both cases, there was an overall reduction of the amount of transcripts (adding up the wild type and the mutant one) compared to the control. If the lamina self-regulates its levels of transcription by interacting with specific elements in the nucleus, then it is possible that the mutations affect the nature of these interactions, resulting in a reduced amount of transcripts. However, one could expect that this is a general mechanism affecting both alleles at the same level, unless there is a stochastic transcription of A-type lamins alleles. In the case of a general allelic effect, it is difficult to explain that mutation 746 G→A reduces more the level of transcription in the mutant allele than mutation 1201 C→T does. If the effect is random, so alleles are affected independently, how can mutations in the coding regions affect the levels of mRNA for each allele? It is unlikely that this observation can be explained by RNA stability. Other regulatory mechanisms should be acting independently on separate alleles, so the transcriptional ratio differs.

5.3.2. Searching for the lost link

Compiling and analyzing information contained in current public databases can produce important conclusions on different subjects. Analysis of regulatory elements and DNA polymorphisms not reported in the literature to date for the genomic sequence of the human LMNA gene revealed interesting results. First, a number of DNA variations (SNPs and small deletions) are present in the promoter region of the LMNA gene, even inside regulatory elements not too far from the transcriptional site. Secondly, and probably more important at this point due to

clinical and experimental evidence, is the finding that 2 % (2 out of 99 SNPs) of the polymorphisms analyzed were present in coding regions of the LMNA gene. Fifty percent (1 out of 2 SNPs) were missense mutations (624R→P), and the other 50% were silent (566H→H), but a DNA variation occurred at the splicing region for lamin C. The finding that naturally occurring DNA variations (SNPs) are present in the promoter, introns and exons of the LMNA gene acquire more importance since several recent studies have demonstrated that a single SNP could not be associated to a particular disease risk or phenotype. Instead, the combination of several SNPs on a single chromosome, the haplotype, offered greater power to identify causative loci for a particular clinical feature (Drysdale, McGraw et al. 2000; Bader 2001; Judson and Stephens 2001).

One of the most intensely studied regulatory mechanisms that can influence the ultimate impact of a given protein on its biological role is transcriptional regulation. SNPs within regulatory elements in the promoter region of different genes have been shown to affect transcriptional activity (Zhang, Ye et al. 1999; Zhang, Stroud et al. 1999; Harendza, Lovett et al. 2003). Functional studies in MMPs have determined that a SNP (G→A) at position -1575 influenced transcriptional activity: the -1575 G allele functioned as an enhancer, whereas the -1575A allele (SNP) reduced transcriptional activity significantly by affecting the binding of the estrogen receptor to this region (Harendza, Lovett et al. 2003). A number of naturally occurring DNA variants in human genes have been identified and found to be associated with susceptibility/progression of several diseases. For example SNPs in the matrix metalloproteinase (MMP) gene promoters have been associated to ovarian cancer (MMP-1, SNP -1607) (Rutter, Mitchell et al. 1998), coronary atherosclerosis (MMP-9, SNP -1562) (Zhang, Ye et al. 1999) and MMP-12, SNP -82 (Jormsjo, Ye et al. 2000)). Other regulatory mechanisms that can affect a given biological process act at translational level.

As mentioned above, one of the most intriguing observations in the laminopathies field is that some patients with clinical symptoms of AD-EDMD, Cardiomyopathy with Conduction Defects and Familial Lipodystrophy have no mutations in the LMNA gene or in the coding region of any other functional candidate protein. Where is the disease-causing factor then? Some authors have suggested that there must be other genes involved in these genetically heterogeneous diseases, but the fact is that none has been found so far, despite the combined effort of different laboratories worldwide. Combining the results from the ARMS-RT-PCR with the SNPs analysis, or more explicitly, the differential allelic expression and reduced A-type lamins transcripts in AD-EDMD, together with the polymorphism's distribution in the human LMNA gene and its regulatory elements, I demonstrated that this gene deserves more attention regarding the study of the events that regulate its transcription, and perhaps, its translation. It would be interesting to test the possibility that the high-order array of the nuclear lamin and/or lamina subunits, tetramers or dimers control regulatory mechanisms of transcription or translation, like some members of the microtubule filaments system do, where tubulin monomers not bound to the filaments regulate their level of translation (Barlow, Gonzalez-Garay et al. 2002; Hari, Yang et al. 2003).

However, to understand regulatory mechanisms, we first need to know very well the structural details of the intermediate filaments structure. Current structural biology technologies have to be pushed to the limits and more innovative approaches have to be developed to unravel the biochemical dynamics of the assembly-disassembly processes of nuclear lamins in vitro and in vivo (Strelkov, Herrmann et al. 2003). Certainly, these findings may bring more insights to understand how subtle changes in the composition of the nuclear lamina can affect the assembly-disassembly processes in disease, and whether a subtle "defective" lamina unable to interact with its putative binding-partners in vivo can

be the answer to the already intriguing laminopathies.

The ARMS-RT-PCR design described in this chapter using DNA primers have proved to be a robust assay that can be used to easily screen a large number of patients to further statistically determine whether the differential allelic pattern of expression is a common feature in laminopathies, or whether it is a particular pattern in the AD-EDMD clinical phenotype. In addition, it showed the importance of testing mRNA as a template rather than genomic DNA when point mutations are present in the coding region of the affected genes, especially when the disease phenotype is not 100% linked to mutations. Extra analysis can be made to determine whether the mutation affects the levels of transcription, and which regulatory elements are affected, and ultimately translation, giving a deficiency or over-expression of a disease-related protein.

Here I have described a preliminary set of data that may bring light to the increasing concern in the laminopathies research community regarding the multi-factorial nature of this group of disorders. Nearly 60 different mutations in the LMNA gene have been reported so far, linked up to six different clinical phenotypes of muscle involvement, cardiomyopathy or lipodystrophy, plus an aging related disorder (Progeria). Only the latter one, where a large region in the tail domain specific for lamin A is affected, can explain the disease phenotype from a structural-biochemical point of view. Most of the other laminopathies involve point mutations along the filament, where biochemical studies have failed to demonstrate a dramatic disruption of putative protein-protein interaction of A-type lamins with their binding partners, and/or direct involvement of lamins in gene expression.

Finally, I consider it is important to highlight the potential use of LNA primers in Allelic-Specific RT-PCR including fluorescent probes at the 5' end. The analysis of

these amplification products, in a CEQ-8000 genotyper may give birth to a new high-throughput technology where mismatch combinations in genetic disorders can quickly be highly discriminated and semi-quantified, and bring back the reliability of the AS-PCR as a SNP genotyping technique (Latorra, Hopkins et al. 2003).

Figures Chapter 5.

Figure 5.1

mRNA and protein sequence for LMNA gene, showing the position of the mutations studied, relative to the exons and protein domains.

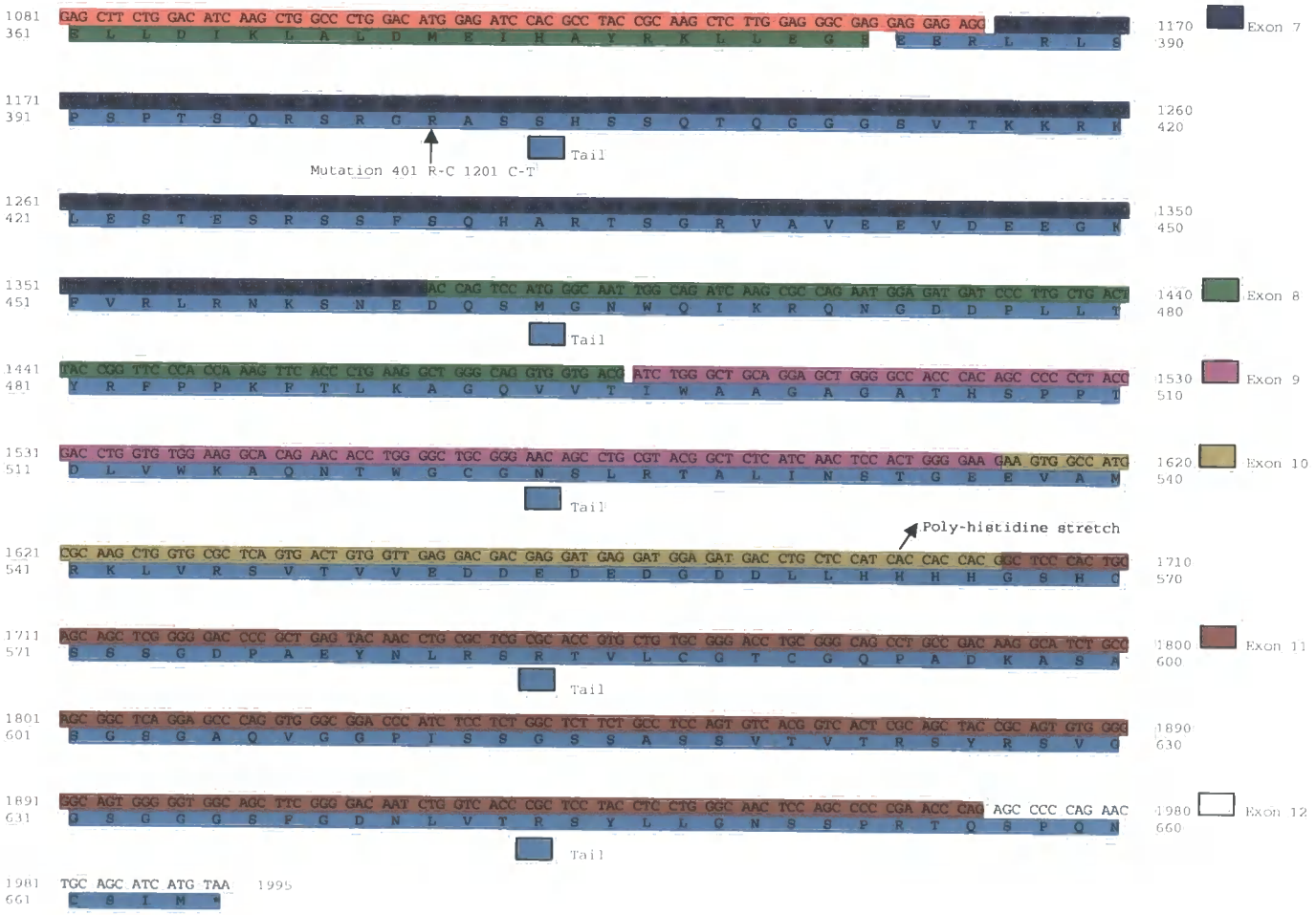
1081
361
GAG CTT CTG GAC ATC AAG CTG GCC CTG GAC ATG GAG ATC CAC GCC TAC CGC AAG CTC TTG GAG GGC GAG GAG GAG AGC
S L L D I K L A L D M E I H A Y R K L L E G E E E R L R L S
1170
390
Exon 7
1171
391
P S P T S Q R S R G P A S S H S S Q T Q G G G S V T K K R K
1260
420
Tail
Mutation 401 R-C 1201 C-T
1261
421
L E S T E S R S S F S Q H A R T S G R V A V E E V D E E G K
1350
450
1351
451
AAC CAG TCC ATG GGC AAT TGG CAG ATC AAG CGC CAG AAT GGA GAT GAT CCC TTG CTG ACT
F V R L R N K S N E D Q S M G N W Q I K R Q N G D D P L L T
1440
480
Exon 8
Tail
1441
481
TAC CGG TTC CCA CCA AAG TTC ACC CTG AAG GCT GGG CAG GTG GTG ACT ATC TGG GCT GCA GGA GCT GGG GCC ACC CAC AGC CCC CCT ACC
Y R F P P K F T L K A G Q V V T I W A A G A G A T H S P P T
1530
510
Exon 9
1531
511
GAC CTG GTG TGG AAG GCA CAG AAC ACC TGG GGC TGC GGG AAC AGC CTG CGT ACG GCT CTC ATC AAC TCC ACT GGG GAA GAA GTG GCC ATG
D L V W K A Q N T W G C G N S L R T A L I N S T G E E V A M
1620
540
Exon 10
Tail
Poly-histidine stretch
1621
541
CGC AAG CTG GTG CGC TCA GTG ACT GTG GTT GAG GAC GAC GAG GAT GAG GAT GGA GAT GAC CTG CTC CAT CAC CAC CAC GGC TCC CAC TGC
R K L V R S V T V V E D D E D E D G D D L L H H H H G S H C
1710
570
1711
571
AGC AGC TCG GGG CAC CCC GCT GAG TAC AAC CTG CGC TCG CGC ACC GTG CTG TGC GGG ACC TGC GGG CAG CCT GCC GAC AAG GCA TCT GCC
S S S G D P A E Y N L R S R T V L C G T C G Q P A D K A S A
1800
600
Exon 11
Tail
1801
601
AGC GGC TCA GGA GCC CAG GTG GGC GGA CCC ATC TCC TCT GGC TCT TCT GCC TCC AGT GTC ACG GTC ACT CGC AGC TAC CGC AGT GTG GGC
S G S G A Q V G G P I S S G S S A S S V T V T R S Y R S V G
1890
630
1891
631
GGC AGT GGG GGT GGC AGC TTC GGG GAC AAT CTG GTC ACC CGC TCC TAC CTC CTG GGC AAC TCC AGC CCC CGA ACC CAG AGC CCC CAG AAC
G S G G G S F G D N L V T R S Y L L G N S S P R T Q S P Q N
1980
660
Exon 12
Tail
1981
661
TGC AGC ATC ATG TAA 1995
C S I M *

Figure 5.1

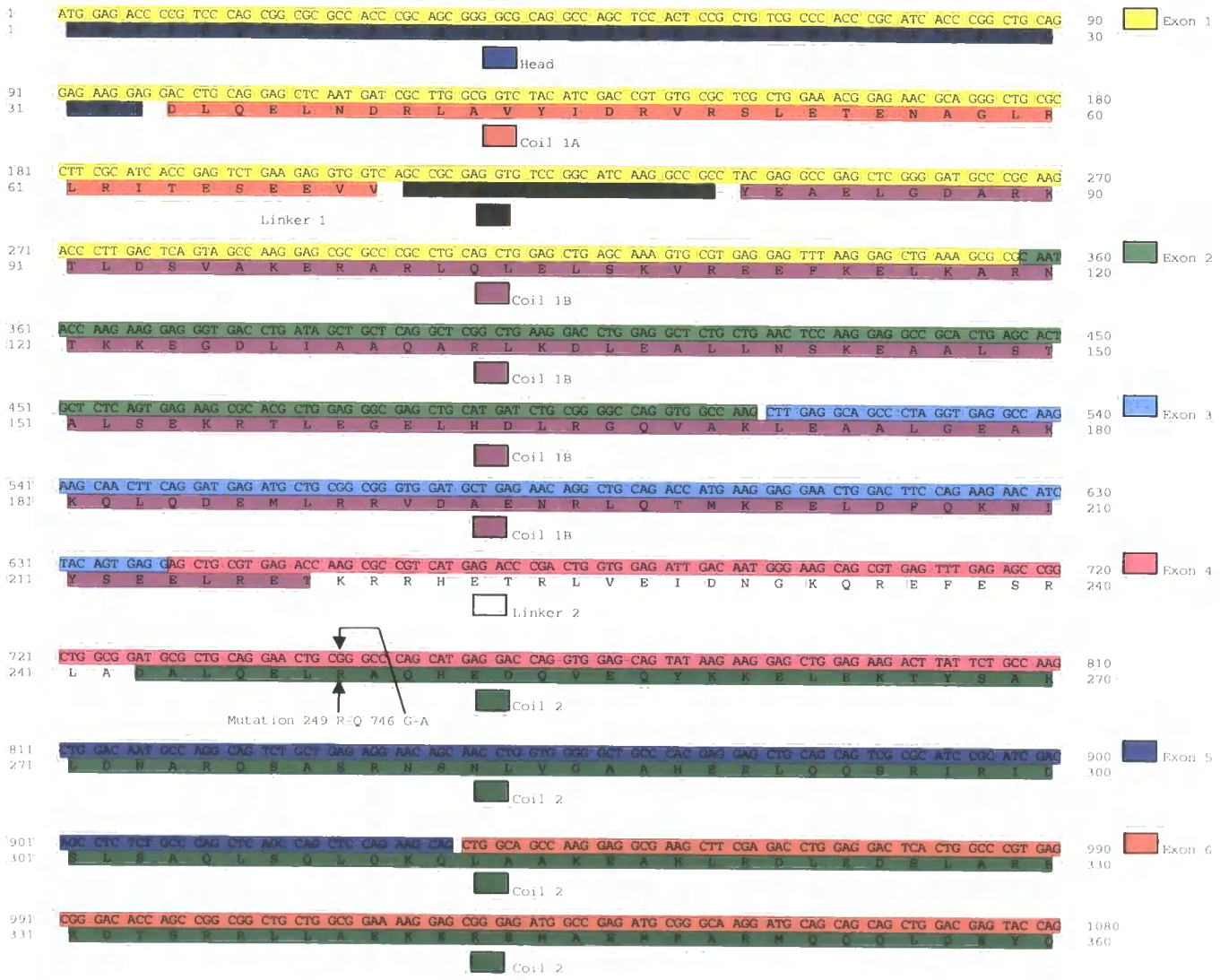
Exon 1
Head
Coil 1A
Linker 1
Exon 2
Coil 1B
Coil 1B
Exon 3
Coil 1B
Exon 4
Linker 2
Mutation 249 R-Q 746 G-A
Coil 2
Exon 5
Coil 2
Exon 6
Coil 2
Coil 2

Table 5.1

Summary of the DNA primers designed using NetPrimer software.

DNA Primers in WellRed Dyes

			Mutation R249Q LAMIN A AND C:	Prod size	Tm	GC%	BP	Hairpin	Dimers	Cross	Palind
Lamin A Specific antisen	5'	1842	c g t g a c a c t g g a g g c a g a a g a g		62	59	22	0	0	2	0
R249Q (G746A) WT sense	5'	727	g a t g c g c t g c a g g a a c t A c g	1115	62	60	20	0	2	2	1
Normal sequence	5'	727	g a t g c g c t g c a g g a a c t g c g								
Lamin A Specific antisen	5'	1842	c g t g a c a c t g g a g g c a g a a g a g		62	59	22	0	0	1	0
R249Q (G746A) Mutant sense	5'	727	g a t g c g c t g c a g g a a c t A c A	1115	60	55	20	0	2	1	1
Mutant sequence	5'	727	g a t g c g c t g c a g g a a c t g c A								
Lamin C Specific antisen	5'	1719	t c a g c g g c g g c t a c c a c t a c		63.5	65	20	1	0	1	0
R249Q (G746A) WT sense	5'	727	g a t g c g c t g c a g g a a c t A c g	992	62	60	20	0	2	1	1
Normal sequence	5'	727	g a t g c g c t g c a g g a a c t g c g								
Lamin C Specific antisen	5'	1719	t c a g c g g c g g c t a c c a c t a c		63.5	65	20	1	0	1	0
R249Q (G746A) Mutant sense	5'	727	g a t g c g c t g c a g g a a c t A c A	992	60	55	20	0	2	1	1
Mutant sequence	5'	727	g a t g c g c t g c a g g a a c t g c A								

			Mutation R401C LAMIN A AND C :	Prod size	Tm	GC%	BP	Hairpin	Dimers	Cross	Palind
Lamin A Specific antisen	5'	1842	c g t g a c a c t g g a g g c a g a a g a g		62	59	22	0	0	1	0
R401C (C1201T) WT sense	5'	1182	c t c g c a g c g c a g c c g t g A c c	660	72	75	20	0	1	1	0
Normal sequence	5'	1182	c t c g c a g c g c a g c c g t g g c c								
Lamin A Specific antisen	5'	1842	c g t g a c a c t g g a g g c a g a a g a g		62	59	22	0	0	1	0
R401C (C1201T) Mutant sense	5'	1182	c t c g c a g c g c a g c c g t g A c T	660	69	70	20	0	1	1	0
Mutant sequence	5'	1182	c t c g c a g c g c a g c c g t g g c T								
Lamin C Specific antisen	5'	1719	t c a g c g g c g g c t a c c a c t a c		63.5	65	20	1	0	4	0
R401C (C1201T) WT sense	5'	1182	c t c g c a g c g c a g c c g t g A c c	537	72	75	20	0	1	4	0
Normal sequence	5'	1182	c t c g c a g c g c a g c c g t g g c c								
Lamin C Specific antisen	5'	1719	t c a g c g g c g g c t a c c a c t a c		63.5	65	20	1	0	4	0
R401C (C1201T) Mutant sense	5'	1182	c t c g c a g c g c a g c c g t g A c T	537	69	70	20	0	1	4	0
Mutant sequence	5'	1182	c t c g c a g c g c a g c c g t g g c T								

Figure 5.2

ARMS-RT-PCR in one step for lamin A. R249Q (746G→A) AD-EDMD cell line was grown until 80% confluent on 90 mm culture dishes and RNA was extracted. After treatment with DNase-RNase free, 0.1 μg of total RNA was used to set up RT-PCR reactions. A temperature gradient was set up to standardize the optimal annealing temperature for the primers specific for the wild type and mutant Lamin A alleles.

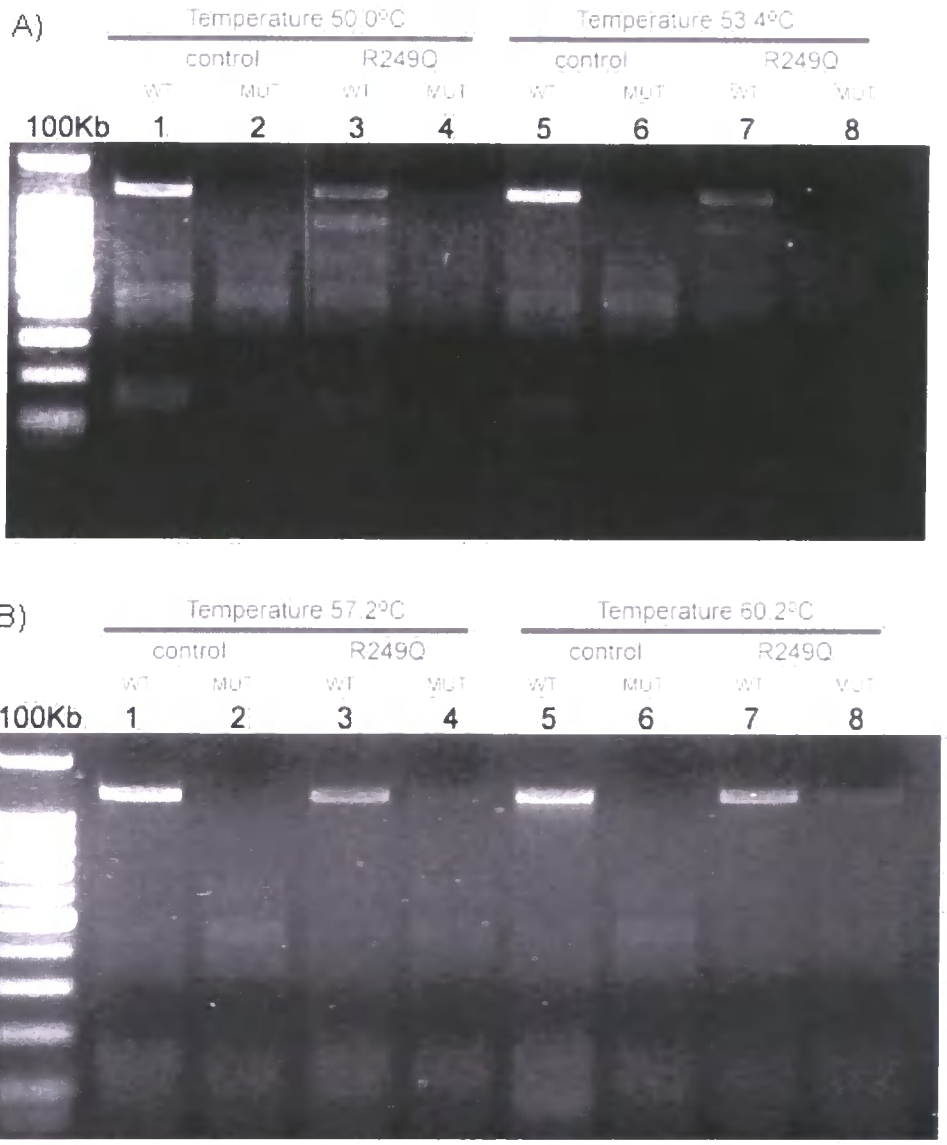
A)
Temperature 50.0°C
Temperature 53.4°C
control
R249Q
control
R249Q
WT
MUT
WT
MUT
WT
MUT
WT
MUT
100Kb
1
2
3
4
5
6
7
8
B)
Temperature 57.2°C
Temperature 60.2°C
control
R249Q
control
R249Q
WT
MUT
WT
MUT
WT
MUT
WT
MUT
100Kb
1
2
3
4
5
6
7
8

Figure 5.2

Figure 5.3

ARMS-RT-PCR in one step for lamin C. R249Q (746 G→A) AD-EDMD cell line was grown until 80% confluent on 90 mm culture dishes, and RNA was extracted. After treatment with DNase-RNase free, 0.1 μg of total RNA was used to set up RT-PCR reactions. A temperature gradient was set up to standardize the optimal annealing temperature for the primers specific for the wild type and mutant alleles.

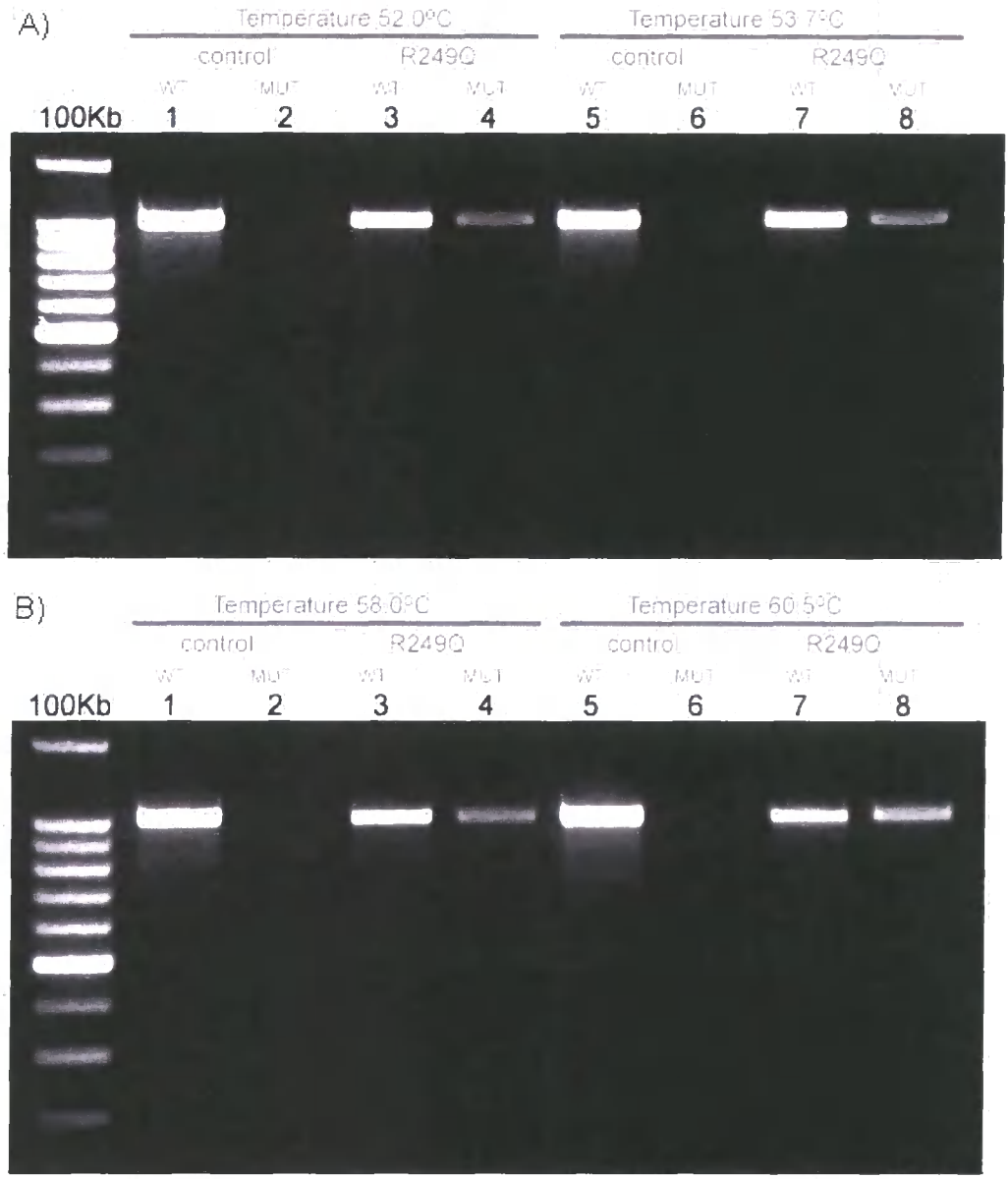
A)
Temperature 52.0°C
Temperature 53.7°C
control
R249Q
control
R249Q
WT
MUT
WT
MUT
WT
MUT
WT
MUT
100Kb
1
2
3
4
5
6
7
8
B)
Temperature 58.0°C
Temperature 60.5°C
control
R249Q
control
R249Q
WT
MUT
WT
MUT
WT
MUT
WT
MUT
100Kb
1
2
3
4
5
6
7
8

Figure 5.3

Figure 5.4

Multiplex ARMS-RT-PCR was analyzed in the automatic DNA Sequencer CEQ-8000 (Beckman-Coulter). PCR products were cleaned up using Qiagen's Clean Up System and 2 ml of each reaction were injected in the capillary system. A) Lamin C multiplex ARMS-RT-PCR for mutation R249Q (746 G→A). B) Control Human Dermal Fibroblasts. Legend: Blue line: wild type primer labelled with WellRed®D4; Green: mutant primer labelled with WellRed®D3.

A)

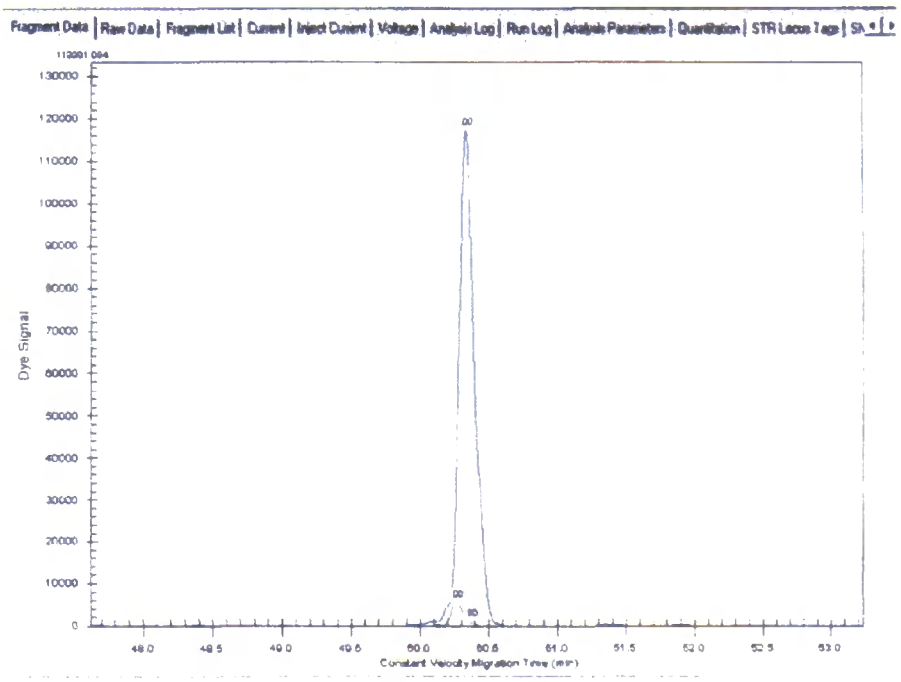
Fragment Data | Raw Data | Fragment List | Current | Inject Current | Voltage | Analysis Log | Run Log | Analysis Parameters | Quantitation | STR Locus Tags
Dye Signal
Constant Velocity Migration Time (min)

B)

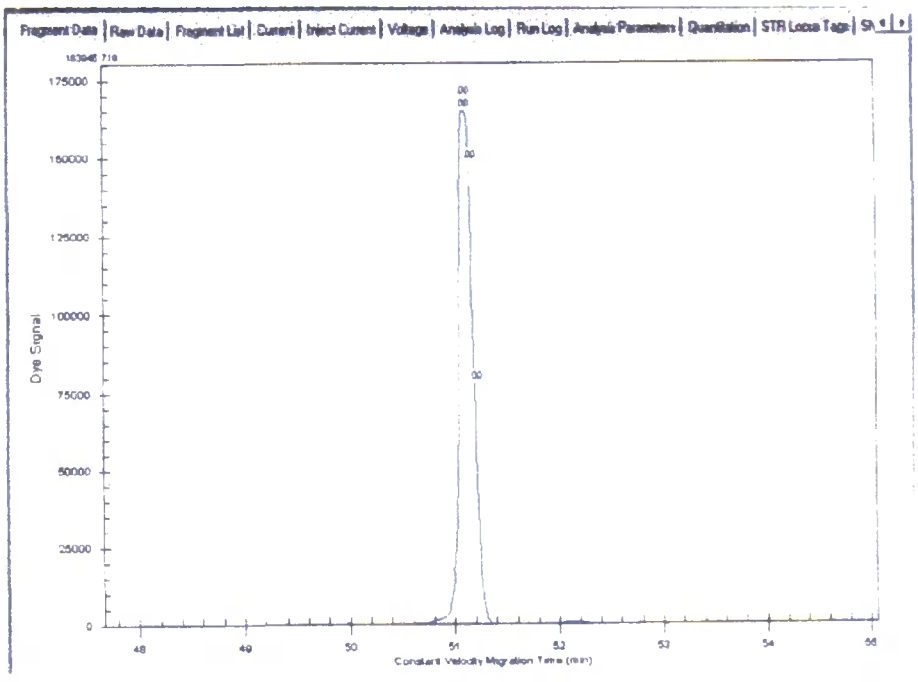
Fragment Data | Raw Data | Fragment List | Current | Inject Current | Voltage | Analysis Log | Run Log | Analysis Parameters | Quantitation | STR Locus Tags
Dye Signal
Constant Velocity Migration Time (min)

Figure 5.4

Figure 5.5

ARMS-RT-PCR in one step for lamin A. R401C (1201C→T) AD-EDMD cell line was grown until 80% confluent on 90 mm culture dishes, and RNA was extracted. After treatment with DNase-RNase free, 0.1 μg of total RNA was used to set up RT-PCR reactions. A temperature gradient was set up to standardize the optimal annealing temperature for the primers specific for the wild type and mutant alleles.

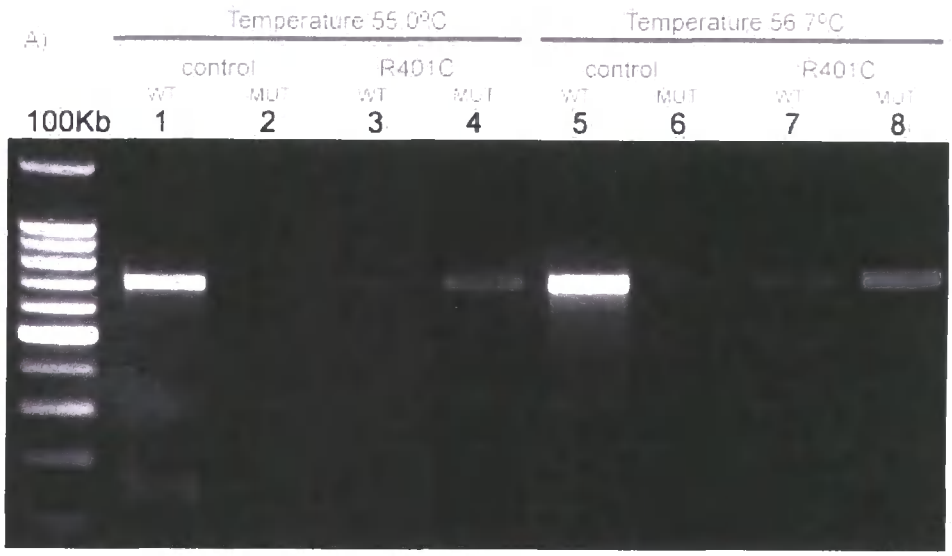
A)
Temperature 55.0°C
Temperature 56.7°C
control
R401C
control
R401C
WT
MUT
WT
MUT
WT
MUT
WT
MUT
100Kb
1
2
3
4
5
6
7
8

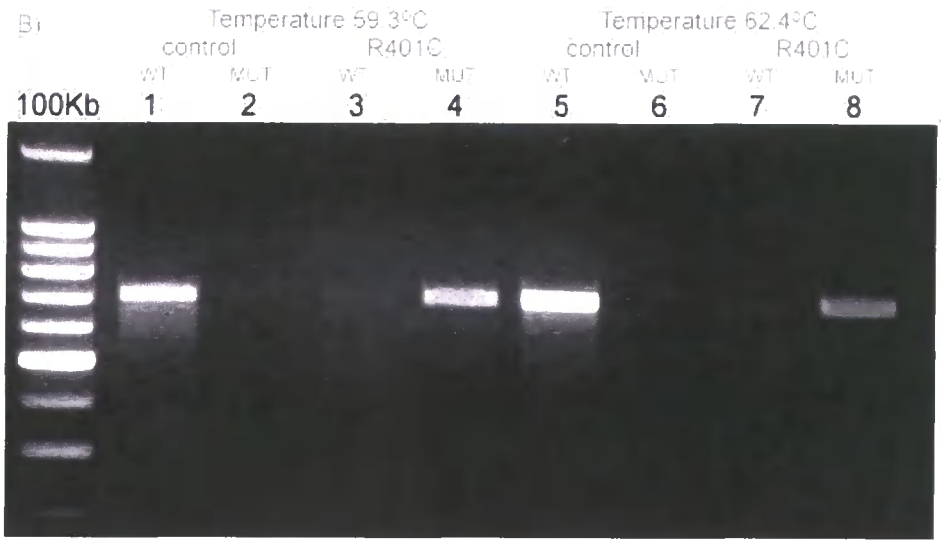
B)
Temperature 59.3°C
Temperature 62.4°C
control
R401C
control
R401C
WT
MUT
WT
MUT
WT
MUT
WT
MUT
100Kb
1
2
3
4
5
6
7
8

Figure 5.5

Figure 5.6

ARMS-RT-PCR in one step for lamin C (Gradient 1). R401C (1201C→T) AD-EDMD cell line was grown until 80% confluent on 90 mm culture dishes and RNA was extracted. After treatment with DNase-RNase free, 0.1 μg of total RNA was used to set up 25μl RT-PCR reactions. A temperature gradient was set up to standardize the optimal annealing temperature for the primers specific for the wild type and mutant alleles.

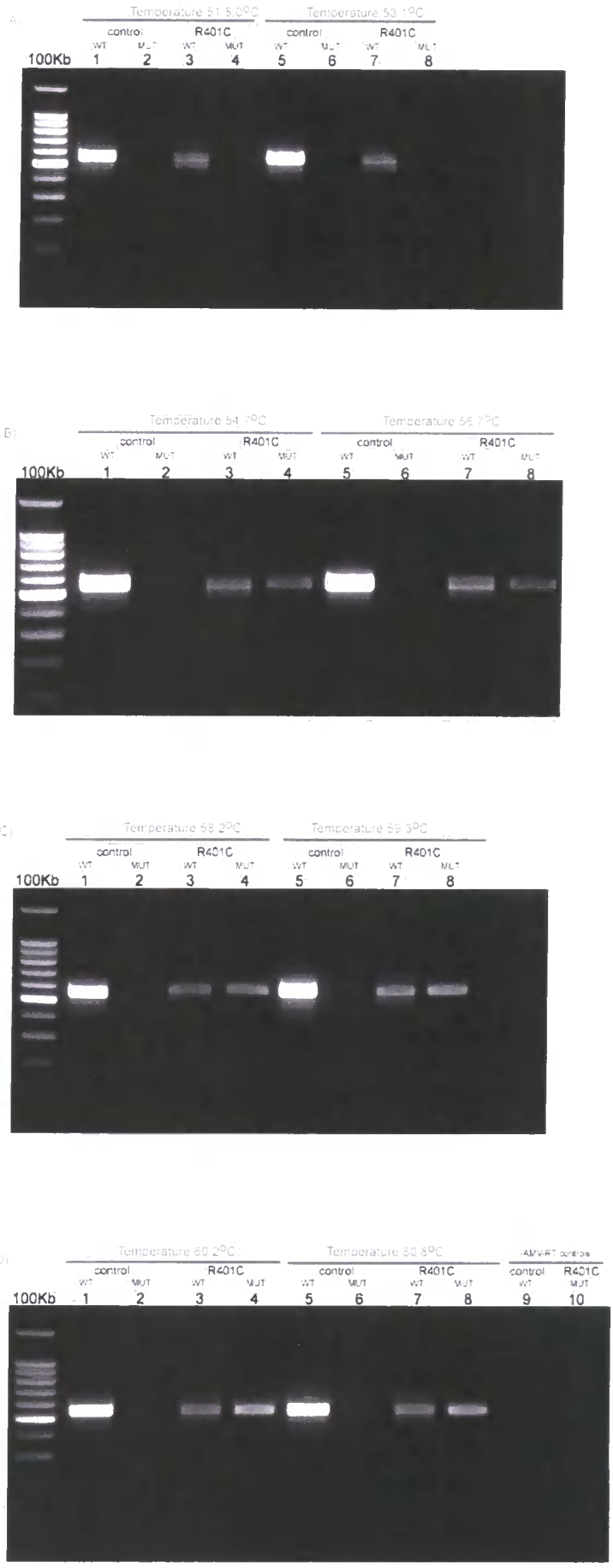
A)
Temperature 51.5°C
Temperature 53.1°C
control
R401C
control
R401C
WT
MUT
WT
MUT
WT
MUT
WT
MUT
100Kb
1
2
3
4
5
6
7
8
B)
Temperature 54.7°C
Temperature 56.7°C
control
R401C
control
R401C
WT
MUT
WT
MUT
WT
MUT
WT
MUT
100Kb
1
2
3
4
5
6
7
8
C)
Temperature 58.2°C
Temperature 59.3°C
control
R401C
control
R401C
WT
MUT
WT
MUT
WT
MUT
WT
MUT
100Kb
1
2
3
4
5
6
7
8
D)
Temperature 60.2°C
Temperature 60.8°C
AMV-RT control
control
R401C
control
R401C
control
R401C
WT
MUT
WT
MUT
WT
MUT
WT
MUT
WT
MUT
100Kb
1
2
3
4
5
6
7
8
9
10

Figure 5.6

Figure 5.7

ARMS-RT-PCR in one-step for lamin C. Gradient 2 (A and B) and Gradient 3 (C and D). R401C (1201C→T) AD-EDMD cell line was grown until 80% confluent on 90 mm culture dishes and RNA was extracted. After treatment with DNase-RNase free, 0.1 μg of total RNA was used to set up RT-PCR reactions. A temperature gradient was set up to standardize the optimal annealing temperature at higher values for the primers specific for the wild type and mutant alleles.

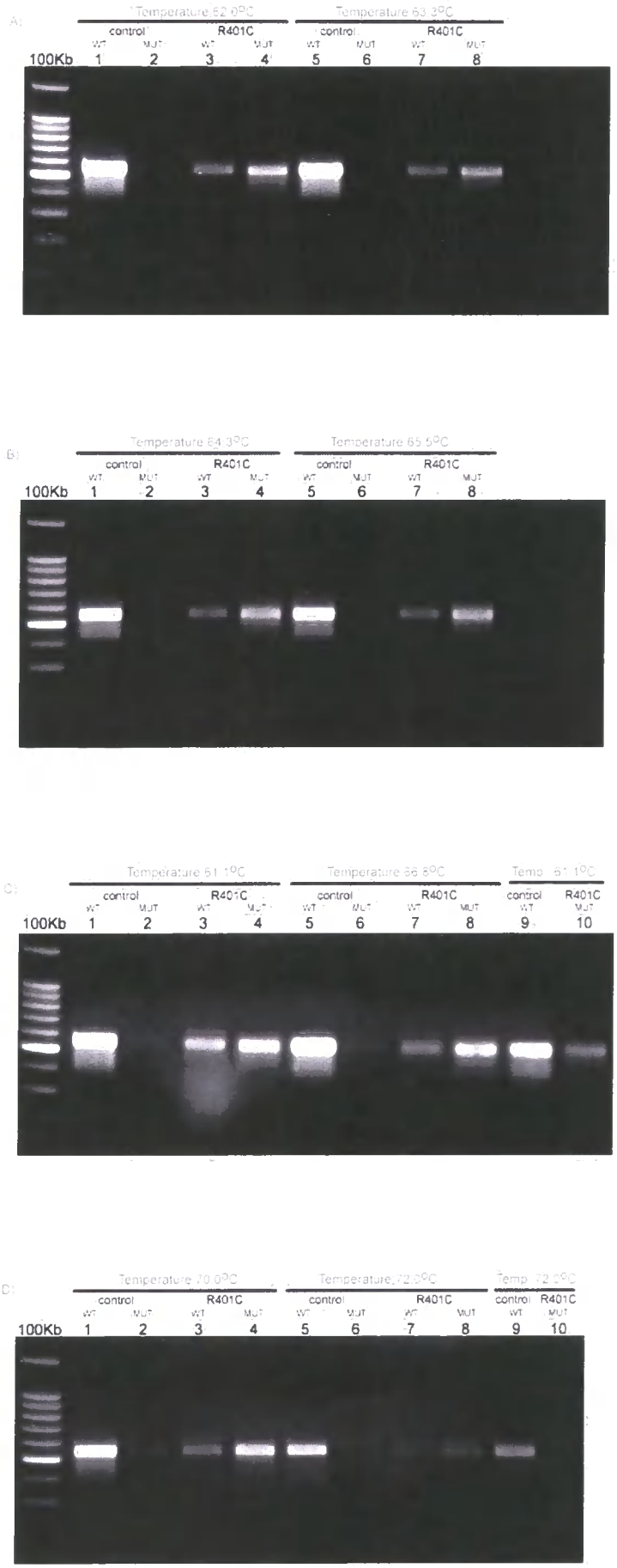
A)
Temperature 62.0°C
Temperature 63.3°C
control
R401C
control
R401C
WT
MUT
WT
MUT
WT
MUT
WT
MUT
100Kb
1
2
3
4
5
6
7
8
B)
Temperature 64.3°C
Temperature 65.5°C
control
R401C
control
R401C
WT
MUT
WT
MUT
WT
MUT
WT
MUT
100Kb
1
2
3
4
5
6
7
8
C)
Temperature 61.1°C
Temperature 66.8°C
Temp 61.1°C
control
R401C
control
R401C
control
R401C
WT
MUT
WT
MUT
WT
MUT
WT
MUT
WT
MUT
100Kb
1
2
3
4
5
6
7
8
9
10
D)
Temperature 70.0°C
Temperature 72.0°C
Temp 72.0°C
control
R401C
control
R401C
control
R401C
WT
MUT
WT
MUT
WT
MUT
WT
MUT
WT
MUT
100Kb
1
2
3
4
5
6
7
8
9
10

Figure 5.7

Table 5.2

Summary of the gradients used to optimize the annealing temperatures in the ARMS-RT-PCR.

Annealing Temperature Gradients

Mutation	Primer Specific	Gradient Number	Temperature Gradient											
R249Q	Lamin C	1	**52.00**	52.30	52.90	**53.70**	54.80	56.30	**58.00**	59.40	**60.50**	61.30	61.80	62.00
R249Q	Lamin A	1	**50.00**	50.30	51.10	52.00	**53.40**	55.20	**57.20**	58.90	**60.20**	61.10	61.80	62.00
R401C	Lamin C	1	50.00	50.30	51.00	**51.80**	**53.10**	**54.70**	**56.60**	**58.20**	**59.30**	**60.20**	**60.80**	61.00
		2	**62.00**	62.20	62.70	**63.30**	**64.30**	**65.50**	66.80	68.00	68.80	69.40	69.90	70.00
		3	59.00	59.30	60.10	**61.10**	62.70	64.60	**66.80**	68.60	**70.00**	71.00	71.80	**72.00**
R401C	Lamin A	1	**55.00**	55.30	55.90	**56.70**	57.80	**59.30**	61.00	**62.40**	63.50	64.30	64.80	65.00

Legend: Temperatures used

Table 5.2

Figure 5.8

Summary of ARMS- RT-PCR in one-step for lamins A and C in both patients studied using optimum annealing temperatures. R249Q (A) and R401C (B) AD-EDMD cell lines were grown until 80% confluent on 90 mm culture dishes, and RNA was extracted. After treatment with DNase-RNase free, 0.1 μg of total RNA was used to set up 25 μl RT-PCR reactions. Optimum annealing temperatures were used, considering the results obtained with each gradient. β-Actin primers (C, lines 1-4) were used as a positive control to assess the equal amount of the mRNA in each PCR reaction and to monitor the high efficiency of the assays. Negative controls were used to confirm no contaminants were influencing the quality of the data (C, lines 5 - 8).

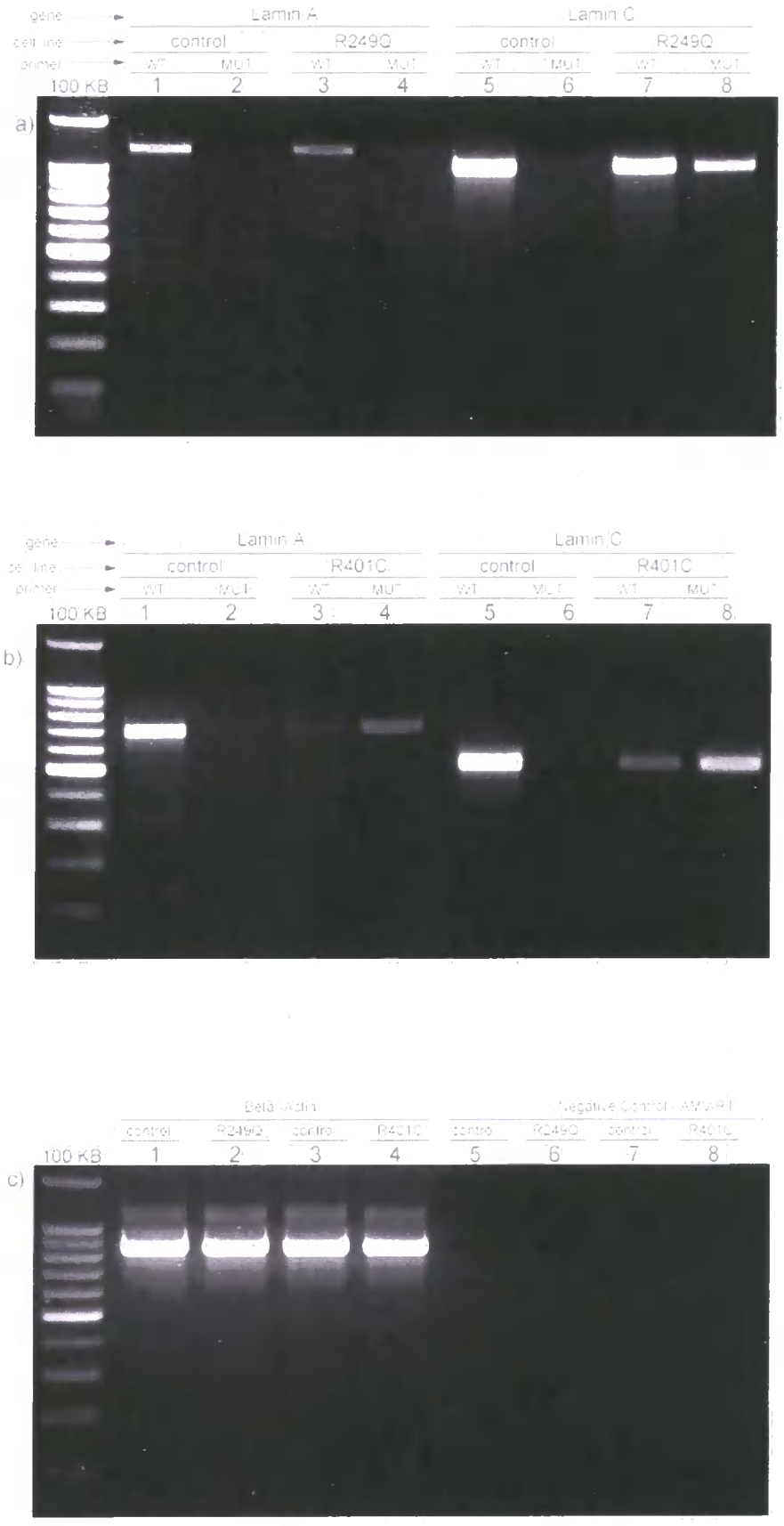
gene
cell line
primer
Lamin A
Lamin C
control
R249Q
control
R249Q
WT
MUT
WT
MUT
WT
MUT
WT
MUT
100 KB
1
2
3
4
5
6
7
8
a)
R401C
R401C
b)
Beta-Actin
Negative Control - AMV-RT
c)

Figure 5.8

Table 5.3

Summary of the RT-PCR results in control and AD-EDMD cell lines.

		Primers	
Cell Line	LMNA Mutation	Wild type	Mutant
Control HDF	None	OK	No Reaction
AD-EDMD 1	R249Q	⇑	⇓
AD-EDMD 2	R401C	⇓	⇑

Table 5.3

Table 5.4

Summary of the LNA primers designed using NetPrimer software.

LNA Primers in WellRed dyes

	Mutation R249Q LAMIN A AND C:	Prod size	Tm	GC%	BP	Hairpin	Dimers	Cross	Palind
Lamin A Specific antisen	5' 1842 c g t g a c a c t g g a g g c a g a a g a g		62	59	22	0	0	2	0
R249Q (G746A) WT sense	5' 730 g c g c t g c a g g a a c t g c G	1112	62	71	17	2	4	2	1
Normal sequence	5' 730 g c g c t g c a g g a a c t g c g								
Lamin A Specific antisen	5' 1842 c g t g a c a c t g g a g g c a g a a g a g		62	59	22	0	0	2	0
R249Q (G746A) Mutant sense	5' 731 c g c t g c a g g a a c t g c A	1111	54	62	16	1	3	2	1
Mutant sequence	5' 731 c g c t g c a g g a a c t g c A								
Lamin C Specific antisen	5' 1719 t c a g c g g c g g c t a c c a c t a c		63.5	65	20	1	0	2	0
R249Q (G746A) WT sense	5' 730 g c g c t g c a g g a a c t g c G	1112	62	71	17	2	4	2	1
Normal sequence	5' 730 g c g c t g c a g g a a c t g c g								
Lamin C Specific antisen	5' 1719 t c a g c g g c g g c t a c c a c t a c		63.5	65	20	1	0	2	0
R249Q (G746A) Mutant sense	5' 731 c g c t g c a g g a a c t g c A	1111	54	62	16	1	3	2	1
Mutant sequence	5' 731 c g c t g c a g g a a c t g c A								

	Mutation R401C LAMIN A AND C :	Prod size	Tm	GC%	BP	Hairpin	Dimers	Cross	Palind
Lamin A Specific antisen	5' 1842 c g t g a c a c t g g a g g c a g a a g a g		62	59	22	0	0	1	0
R401C (C1201T) WT sense	5' 1188 g c g c a g c c g t g g c G	654	60	86	14	0	3	1	0
Normal sequence	5' 1188 g c g c a g c c g t g g c c								
Lamin A Specific antisen	5' 1842 c g t g a c a c t g g a g g c a g a a g a g		62	59	22	0	0	0	0
R401C (C1201T) Mutant sense	5' 1188 g c g c a g c c g t g g c T	654	57	79	14	1	2	0	0
Mutant sequence	5' 1188 g c g c a g c c g t g g c T								
Lamin C Specific antisen	5' 1719 t c a g c g g c g g c t a c c a c t a c		63.5	65	20	1	0	5	0
R401C (C1201T) WT sense	5' 1188 g c g c a g c c g t g g c G	531	60	86	14	0	3	5	0
Normal sequence	5' 1188 g c g c a g c c g t g g c c								
Lamin C Specific antisen	5' 1719 t c a g c g g c g g c t a c c a c t a c		63.5	65	20	1	0	3	0
R401C (C1201T) Mutant sense	5' 1188 g c g c a g c c g t g g c T	531	57	79	14	1	2	3	0
Mutant sequence	5' 1188 g c g c a g c c g t g g c T								

Figure 5.9

NIX analysis of DNA regulatory elements in the LMNA gene using the algorithms available at the Human Genome Mapping Project (HGMP), Cambridge, UK. LMNA gene was searched in the OMIM database at the National Centre for Biotechnology Information (NCBI, USA, www.ncbi.nlm.nih.gov). LMNA sequence included 32kb upstream ATG and 14.5 Kb downstream the TAA, 57.5 Kb in total. Four algorithms for promoter's analysis were used: GRAIL/Prom, TSSW/Prom, GENSCAN/Prom and FGenes/Prom. One algorithm analyzed for CgP islands (GRAIL/CpG) and one for Transcriptional Sites (Eponine). Numbering of bases starts at base number 1 regarding the sequence analyzed, not the position in chromosome 1.

A. Promoter region extending for 32360 bp upstream the ATG

B. Genomic sequence for the LMNA gene from ATG to TAA (24188bp)

C. Downstream sequence to codon TAA (Stop), extending for 1013 bp

D. Full sequence analyzed, 57561 bp.

Figure 5.9

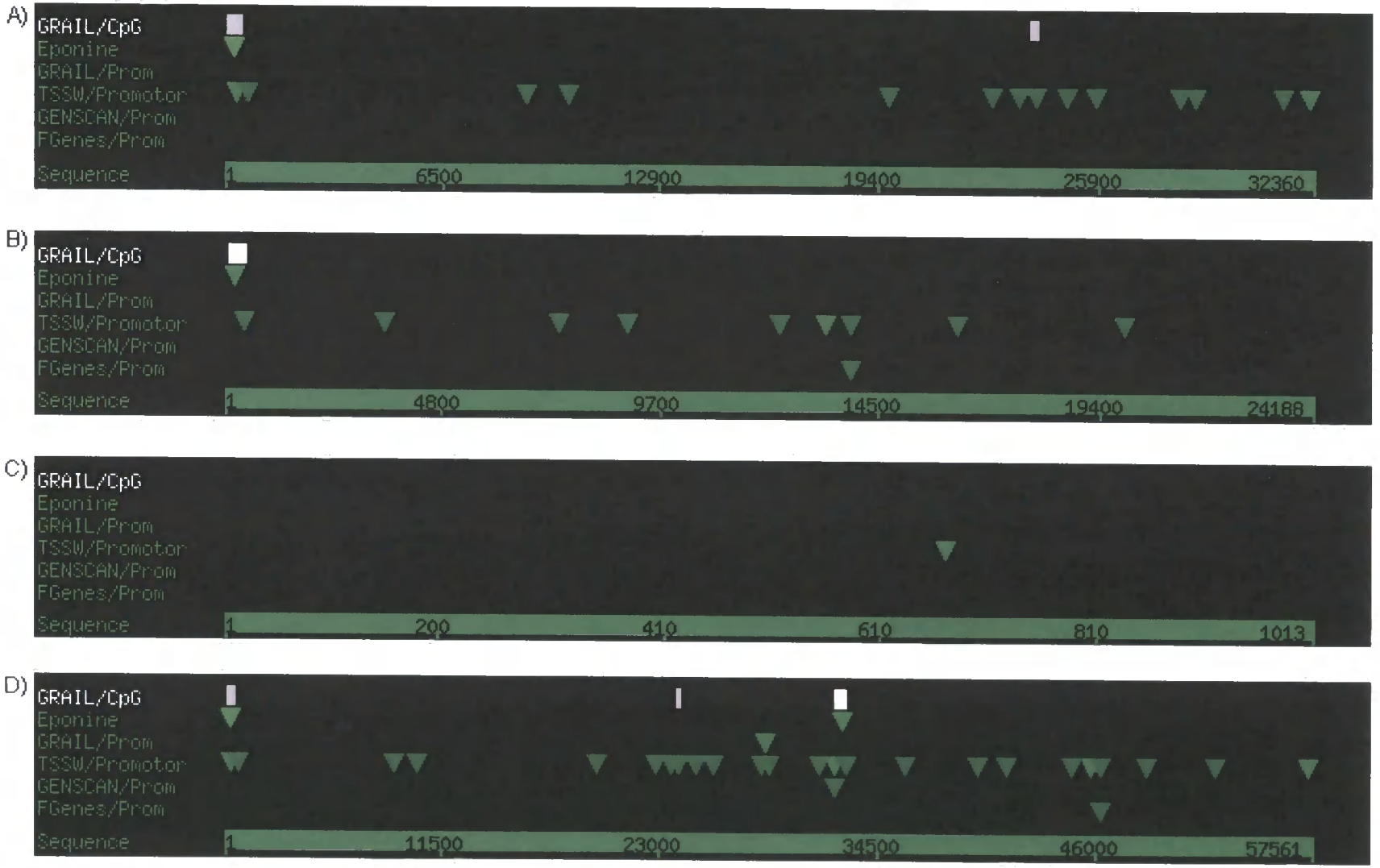
A)
GRAIL/CpG
Eponine
GRAIL/Prom
TSSW/Promotor
GENSCAN/Prom
FGenes/Prom
Sequence
1
6500
12900
19400
25900
32360
B)
GRAIL/CpG
Eponine
GRAIL/Prom
TSSW/Promotor
GENSCAN/Prom
FGenes/Prom
Sequence
1
4800
9700
14500
19400
24188
C)
GRAIL/CpG
Eponine
GRAIL/Prom
TSSW/Promotor
GENSCAN/Prom
FGenes/Prom
Sequence
1
200
410
610
810
1013
D)
GRAIL/CpG
Eponine
GRAIL/Prom
TSSW/Promotor
GENSCAN/Prom
FGenes/Prom
Sequence
1
11500
23000
34500
46000
57561

Table 5.5

NIX analysis summary.

Algorithm		Statistical Value	Prediction at:	Strand	Quality of prediction	Absolute positon in Chromosome 1
GrailEXP CpG islands	1	ratio 0.79	N/A	positive	good	2502232-2502642
	2	ratio 0.65	N/A	positive	good	2526054-2526282
	3	ratio 0.84	N/A	positive	excellent	2534300-2534998
Transcriptional Sites	1	score= 0.998	2502354	positve	good	2502354
	2	score= 0.998	2534725	positve	good	2534725
Grail Promoter	1	score 73	N/A	N/A	good	2530728
TSSW Promoter	1	LDF -16.46	2502428	positive	good	2502428
	2	LDF - 4.47	2511068	positive	marginal	2511068
	3	LDF - 4.62	2512338	positive	marginal	2512338
	4	LDF - 6.27	2521818	positive	marginal	2521818
	5	LDF - 8.74	2524884	positive	marginal	2524884
	6	LDF - 5.41	2527090	positive	marginal	2527090
	7	LDF - 5.41	2527942	positive	marginal	2527942
	8	LDF - 4.97	2530441	positive	marginal	2530441
	9	LDF - 5.42	2530914	positive	marginal	2530914
	10	LDF - 5.08	2533485	positive	marginal	2533485
	11	LDF - 13.65	2534301	positive	good	2534301
	12	LDF - 4.51	2538072	positive	marginal	2538072
	13	LDF - 4.15	2541909	positive	marginal	2541909
	14	LDF - 8.62	2543443	positive	marginal	2543443
	15	LDF - 11.10	2547829	positive	good	2547829
	16	LDF - 4.57	2548361	positive	marginal	2548361
	17	LDF - 4.41	2550729	positive	marginal	2550729
	18	LDF - 12.07	2559385	positive	good	2559385
Genescan Promoter	1	score - 4.91	2534295	positive	marginal	2534295
Fgenes Promoter	1	score 0.67	2548331	positive	marginal	2548331

Table 5.5

Figure 5.10

SNPs mapping in the genomic sequence for the human LMNA gene, overlapping the regulatory elements with high scores (good or excellent only) analyzed in figure 5.9. Chromosome 1 full sequence (NT079487) was searched in the OMIM database at the National Centre for Biotechnology Information (NCBI, USA, www.ncbi.nlm.nih.gov), and used to assign the actual position for each base in the genomic sequence of the LMNA gene analyzed (see Materials and Methods Chapter for methodology used).

A. LMNA gene genomic sequence from ATG to TAA only

B. Entire genomic sequence used for NIX analysis

C. Promoter region analyzed

D. 3' region analyzed

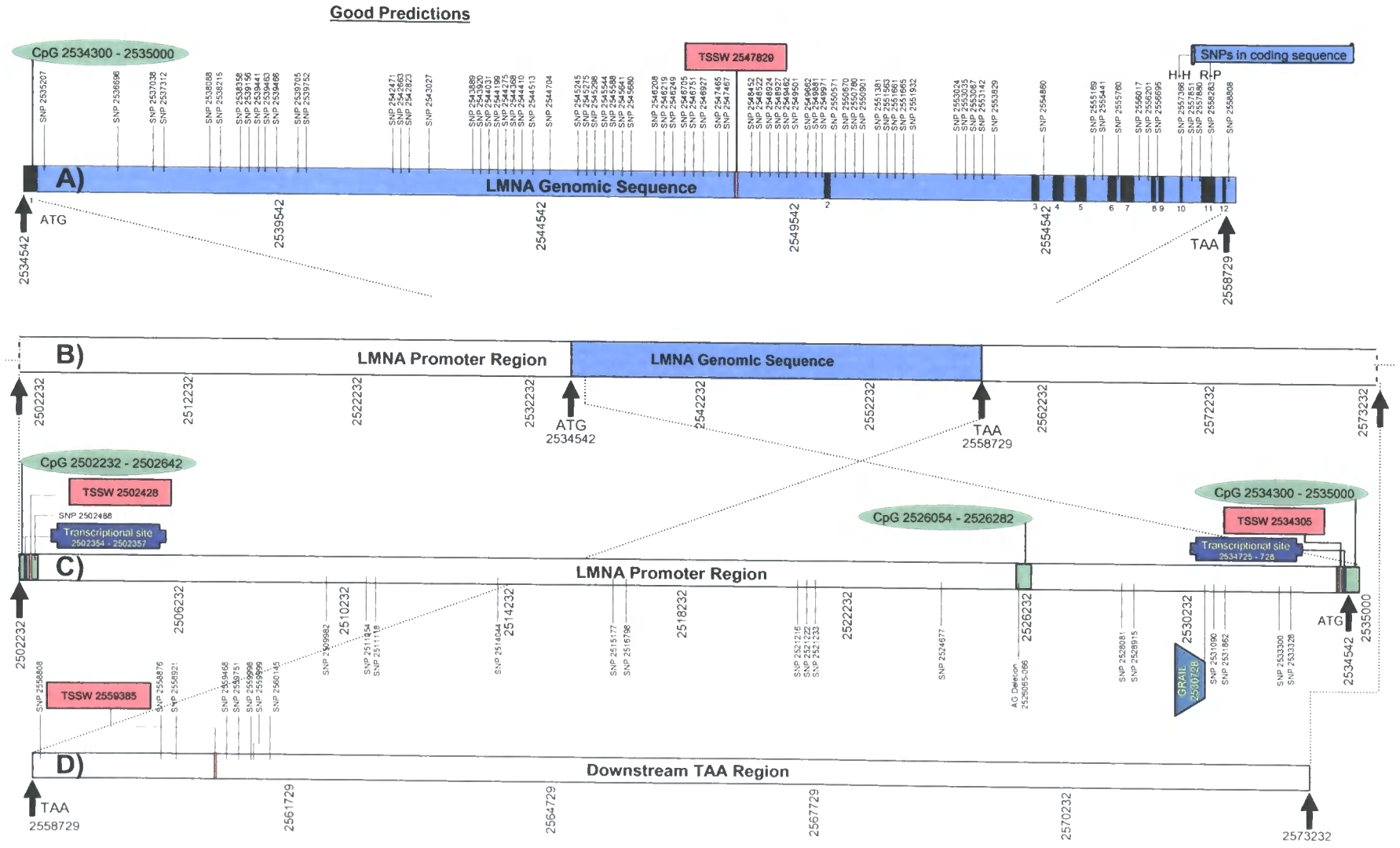
Good Predictions
CpG 2534300 - 2535000
TSSW 2547829
SNPs in coding sequence
H-H
R-P
A)
LMNA Genomic Sequence
ATG
TAA
2534542
2539542
2544542
2549542
2554542
2558729
B)
LMNA Promoter Region
LMNA Genomic Sequence
2502232
2512232
2522232
2532232
2542232
2552232
2562232
2572232
2573232
CpG 2502232 - 2502642
TSSW 2502428
SNP 2502488
Transcriptional site
2502354 - 2502357
CpG 2526054 - 2526282
TSSW 2534305
Transcriptional site
2534725 - 728
C)
LMNA Promoter Region
2506232
2510232
2514232
2518232
2522232
2526232
2530232
2535000
TSSW 2559385
GRAIL
2530728
D)
Downstream TAA Region
2561729
2564729
2567729
2570232
2573232

Figure 5.11

SNPs mapping in the genomic sequence for the human LMNA gene, overlapping the regulatory elements with high scores (marginal scores only) analyzed in figure 5.9. Chromosome 1 full sequence (NT079487) was searched in the OMIM database at the National Centre for Biotechnology Information (NCBI, USA, www.ncbi.nlm.nih.gov). and used to assign the actual position for each base in the genomic sequence of the LMNA gene analyzed (see Materials and Methods Chapter for methodology used).

A. LMNA gene genomic sequence from ATG to TAA only

B. Entire genomic sequence used for NIX analysis

C. Promoter region analyzed

D. 3' region analyzed

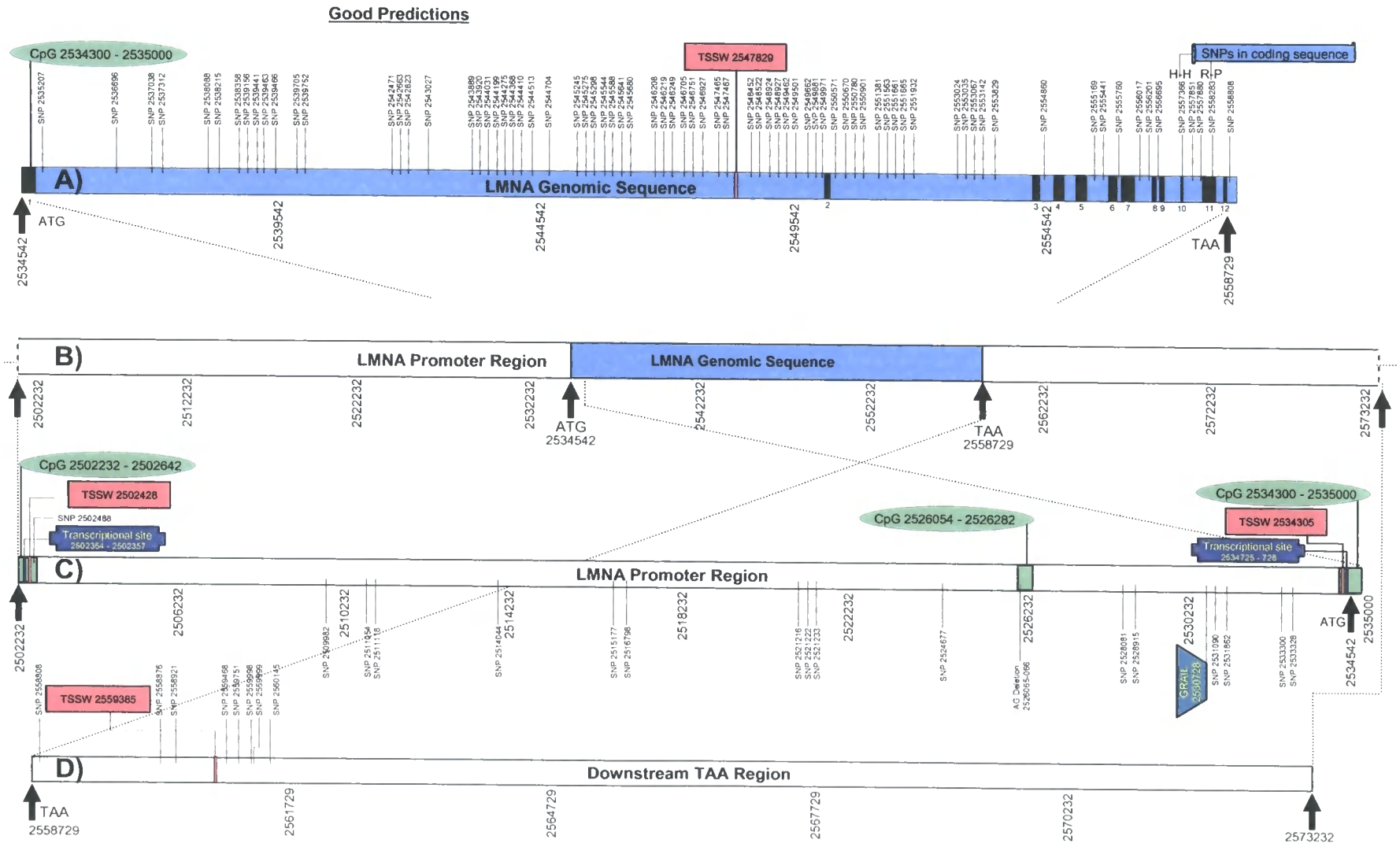
Good Predictions
CpG 2534300 - 2535000
TSSW 2547829
SNPs in coding sequence
A)
LMNA Genomic Sequence
ATG
TAA
2534542
2539542
2544542
2549542
2554542
2558729
B)
LMNA Promoter Region
LMNA Genomic Sequence
2502232
2512232
2522232
2532232
2542232
2552232
2562232
2572232
2573232
CpG 2502232 - 2502642
TSSW 2502428
SNP 2502488
Transcriptional site
2502354 - 2502357
CpG 2526054 - 2526282
CpG 2534300 - 2535000
TSSW 2534305
Transcriptional site
2534725 - 728
C)
LMNA Promoter Region
2506232
2510232
2514232
2518232
2522232
2526232
2530232
2535000
TSSW 2559365
GRAIL
2560728
D)
Downstream TAA Region
2561729
2564729
2567729
2570232
2573232

6. Chapter Six- General Discussion

6.1. Overview

The aims of this study were, first, to unravel the biochemical basis of the Emery-Dreifuss Muscular Dystrophy (EDMD), through the characterization of the interaction between emerin and lamins in vitro and in vivo, and secondly, to further investigate the functional consequences of the missense mutations in the LMNA gene and the loss of Emerin in Autosomal Dominant and XL-EDMD respectively.

The molecular interaction between Emerin and lamins became evident only after mutations in the LMNA gene were linked to Autosomal Dominant EDMD (**Bonne et al., 1999**). Previously, mutations in the STA gene were strongly linked to a genetically different but clinically close disorder: the XL–EDMD (**Bione et al., 1994**). The direct interaction between Emerin and lamins was initially demonstrated using in vitro biochemical assays like bio-molecular interaction analysis (BIA) combined with the use of monoclonal antibodies (**Clements et al., 2000**), overlay assays (**Vaughan et al., 2001**) and Yeast Two-Hybrid System (**Sakaki et al., 2001**).

To study the molecular basis of the clinically related EDMD phenotypes (AD and X-L), I used different approaches: first, a yeast two-hybrid assay and transfection experiments using fluorescent-tagged proteins (Emerin and A-type lamins) were used to further characterize the molecular interaction between Emerin and lamins, second, in vivo functional studies using established EDMD patient cell lines to analyze the structural weakness of the nuclear lamina and the possible involvement of other proteins/mechanisms in the disease phenotype, and third, a genomics-bioinformatics analysis of AD-EDMD cell lines and the LMNA gene to investigate the functional role of the

missense mutations in muscular dystrophies and/or other laminopathies.

6.2. Anchorage of Emerin to the nuclear envelope and its structural and functional role.

A classical yeast two-hybrid assay was set up using Emerin as a bait protein and a panel of lamin-deletion mutants (a kind gift from Dr. Howard Worman) that can be divided in different groups: Head-Coil, Coil-Tail or Tail. Head domain of lamins adopts a highly flexible conformation with low content of secondary structure and it is believed to play an important role in filament assembly (**Herrmann, 1996**). The rod domain forms a characteristic α-helix responsible for the coiled-coil associations (**Stuurman et al., 1998**) and the globular tail domain forms an Ig-like structure, where theoretical crystallographic data suggest it should be arranged in such a way that remains on the outside part of the core of the 10 -13 nm filament (**Strelkov et al., 2003**).

Two different approaches of the yeast two-hybrid system were used in the current study: a qualitative (β-galactosidase lift assay) and a semi-quantitative assay (liquid β-galactosidase assay). Although the interaction between Emerin and lamins was demonstrated by other in vitro assays (**Clements et al., 2000; Sakaki et al., 2001; Vaughan et al., 2001**), the interacting domain of lamins was not known and complementary methods were required to conclusively demonstrate the protein-protein interaction between these proteins. The in vitro approach of the two versions of the yeast two-hybrid system showed that Emerin interacts with all lamins, but more strongly with lamin B1, and that the region of interaction is the globular Tail domain. Transfection experiments using cell lines derived from XL-EDMD patients (lacking Emerin) showed that lamin B1 is stably localized with Emerin at the NE when A-type lamins are mislocalized to aggregates, which suggest that the retention of Emerin at the NE in fibroblasts may be due to its stable interaction with B-type lamins. This observation is different from what

happens in HeLa cells, where miss-localization of A-type lamins to aggregates causes retraction of Emerin to the ER (**Vaughan et al., 2001**). Previous studies suggested Emerin interacts preferentially with Lamin A (B-type lamins were not included in the study) (**Clements et al., 2000**) while interaction with lamin B1 is weaker (**Fairley et al., 1999**). Our previous study showed that lamin C interacts preferentially with Emerin in immuno-precipitation assays (**Vaughan et al., 2001**). Preferential interaction with Lamin A, specifically its globular tail domain, with Emerin was reported by (**Sakaki et al., 2001**), but they did not include B-type lamins in their study. Most probably, these results are a consequence of the biochemical nature of the assays used, and they represent a dynamic range of interactions between Emerin and lamins at different stages of the cell cycle and/or the presence of different multi-protein functional complexes between Emerin and A and B-type lamins during G1-S/G2 or quiescence.

6.3. Paradigm of the lamina assembly: Who goes first?

Previous studies showed that the presence of B-type lamins is obligatory for the correct alignment of A-type lamins at the lamina (**Dyer et al., 1999**). To our surprise, the AD-EDMD cell lines studied showed A-type lamins homo-filaments that segregated from B-type lamins, forming honeycomb-like structures, where Emerin, but not nuclear pores, co-localized. These structures were present in all cell lines studied, independently of the position of the mutation in the filament. These imply that mutations in the rod and tail domain abrogate the dependency for lamins A/C to form filaments through association with B-type lamins but do not disrupt A-type lamins-Emerin associations or probably with other lamin-associated proteins. It is possible that both types of mutation lead to weakened interactions between A-type and B-type lamins, which causes them to polymerize independently. Alternatively, the mutations alter A-type lamins interaction with chromatin, which may in turn promote the assembly of homotypic A-type lamin

filaments in areas of the nucleus depleted of chromatin. Another possibility might be influenced by the heterotypic nature of the interactions at the lamina between A and B-type lamins, where A-type lamin dimers/tetramers, with a random mixture of wild type and mutant monomers, fail to produce the precise conformational arrangement to associate with the pre-determined B-type lamina and/or with other inner nuclear membrane or nucleoplasmic components. This failure drives now the segregation of A-type lamin homo-filaments into one pole of the nuclei, deprived of heterochromatin. As demonstrated by my data, honeycombs appearance depends on the fixation method used. The stronger the fixation method, the higher the amount of honeycombs observed. Accordingly the methanol: acetone fixation method revealed the higher amount of honeycombs.

The most strikingly observation related to the weakness of the nuclear lamina in laminopathies is the fact that these abnormal structures (honeycombs) are only present in a subpopulation of cells, and they appear to be related to a certain nuclear checkpoint at the exit/re-entrance to the cell cycle, where A-type lamins and their associated partners fail to interact appropriately. It seems these structures occur naturally, as honeycombs were observed in normal human fibroblasts (Figure 4.2 A), and in XL-EDMD cell lines expressing ectopic wild type Lamin A (Figure 3.7 GFP-Lamin A v). But after growth inhibition by serum starvation, and back to a proliferative state, AD-EDMD cultures showed an increase in the amount of this nuclear abnormality, which is morphologically different from the bubbling structures observed in other studies in that honeycombs always appear depleted in heterochromatin.

Opposite to their cytoplasmic relatives, mutations in the nuclear intermediate filaments do not appear to disrupt drastically the structures of the filaments. Immuno-labelling experiments in biopsies and cell lines derived from X-L or AD-

EDMD patients have failed to show dramatic changes in the structure of the nuclear lamina as mutations in the cytoplasmic intermediate filaments does to the cytoskeleton. Maybe this is a direct consequence of the difference in length of the lamins rod and tail domain compared to the intermediate filaments type I, II III and IV, and the differential effect of the mutations in the thermodynamic properties of the different intermediate filament types, ultimately representing the different roles of each group of this family of proteins.

6.4. Direct evidence of other cellular events in EDMD.

Although conclusive linkage studies have demonstrated that missense mutations in A-type lamins are associated to different laminopathies (X-L, AD and AR-EDMD, LGMD1B, CMD-CD, MAD), it has been systematically reported the presence of all these clinical phenotypes with no mutation in the LMNA gene. This observation reveals the genetic diversity of these conditions, and has lead researchers to search for new candidate genes. In this effort, several genes have been studied using a functional candidate approach, and partially unique exonic DNA-variations causing amino acid exchanges have been found in FLPC (filamin C), LAP2, NRM (nurim) and DDX16 (DEAD/H-box polypeptide) (**Bonne G and al, 2003**).

Nesprins are a new family of spectrin-repeat proteins first reported in a search for markers of differentiation in vascular smooth muscle cells (VSMCs), and their pattern of distribution was revealed to be complex in the model cell lines studied (**Zhang et al., 2001**). In my study, dermal fibroblasts derived from AD-EDMD patient showed a high percentage of proliferating cells where Nesprin 1 (N-terminus) co-localized with α-S-Actin fibres, compared to the controls (normal human and rat fibroblasts) and XL-EDMD fibroblasts. Additionally, Nesprin 1 amino-terminal re-distributes during exit/re-entrance in normal cells towards the plasma membrane, but in AD-EDMD fibroblast, the Nesprin fibres are thicker than in control and XL-EDMD fibroblasts, while the latter ones resist redistribution

of Nesprin 1 amino-terminal in a significant sub-population of cells. In contrast, Nesprin 1 carboxy-terminal and Nesprin 2 (remained nucleoplasmic and absent in nucleoli) were never organized in any kind of fibre, but Nesprin 2 re-distributed to the perinuclear space in the same fashion than Heat Shock Protein 70 (HSP70) during metabolic stress. This observation was made on separate samples; hence I suggest that to establish co-localization of HSP70 and Nesprin 2 during quiescence and re-entrance to the cell cycle induced by serum deprivation, a double immuno-labelling experiment is needed. In addition, proliferating cultures of human fibroblasts harbouring mutations in the LMNA gene present a senescent phenotype compared to the controls, and an altered pattern of Nesprins expression, suggesting a possible implication of Nesprins in EDMD an revealing a possible involvement of an aging process in vitro.

Recent investigations have demonstrated that Nesprin 1α N-terminal binds Emerin and its C-terminal binds Lamin A in vitro (**Mislow et al., 2002**), and that they must interact in vivo (**Muchir et al., 2003**). Combining these published data, the re-arrangement of Nesprins at the exit/re-entrance of the cell cycle in my study (particularly in AD-EDMD) and previous studies of lamins interaction with other proteins, the role of nucleoplasmic intermediate filaments in the nuclear metabolism appear to be very dynamic. More experimental evidence are "drawing" the picture of tertiary or quaternary complexes involving lamins and their interacting partners, where a diverse range of molecular arrangements of lamin filaments (dimers/tetramers/filament units) can ultimately define key nuclear processes, and could explain better the complex genetic background in laminopathies (Figure 6.1). New experimental approaches could be used to test for tertiary complexes involving lamins, for example the yeast-three hybrid system.

6.5. Laminopathies: One disease and different mechanisms or different pathologies?

About 50% of mutations affecting membrane receptors and macromolecular complexes are dominant, which may result from the absence of substantial activity from one allele at a given locus and suggest that half of the normal amount of active product is insufficient to maintain a normal phenotype (**Jimenez-Sanchez et al., 2001**). This phenomenon is called haploinsufficiency (HI), where most of the known examples are compatible with survival of the individual. Dominant negative effect is a different phenomenon that refers to cases where a mutant protein interferes with the action of the normal one. Both, HI and dominant negative effect are direct consequence of heterozygosity and play a dominant role. As a consequence of heterozygosity, an imbalance in the concentration of the subcomponents of a protein-protein complex can be deleterious by different biochemical mechanisms, which is called the balance hypothesis (**Papp et al., 2003**).

Heterozygosity is the most common distribution pattern of mutations in the LMNA gene in laminopathies. ARMS-RT-PCR is able to detect imbalance in the relative amount of transcripts produced by the wild type and mutant alleles in AD-EDMD fibroblasts. Both cell lines studied show an overall transcript imbalance compared to the controls. In the case of the cell line with mutation R249Q, more transcripts from the wild type allele are present in proliferating cultures, while in the cell line harbouring the mutation R401C, the effect is the opposite. In both cases, lamina filament-units (dimers/tetramers) are assembled in such a way that for example, in the case of the dimers, at least 50% of the complexes will contain mutant monomers that could affect the higher assembly arrangements (tetramers, microfibrils, protofibrils, filaments) of the nuclear lamina. It is difficult to envision how missense mutations (leading to single point mutations) in the coding regions of any gene can give rise to the effect observed in the AD-EDMD cell lines. In the case of less mutant transcript, one could expect this can be due to mRNA degradation by

a process called nonsense-mediated decay (**Frischmeyer and Dietz, 1999**), like occurs in the intermediate filament associated protein Desmoplakin (OMIM125647) or collagens (OMIM120140). But in the other sample, where the mutant allele is expressed at a higher level compared to the wild type, mRNA stability can not be a possible explanation. However, both effects can be explained if unreported mutations affect the regulatory region/s of the LMNA gene. Before any further conclusions are drawn from these data, extended studies are needed. Firstly, more AD-EDMD and other laminopathies patients have to be tested to demonstrate that this is a dominant pattern produced by heterozygous conditions, and to support statistically any outcome. Secondly, a new primer design using LNA primers instead of the standard ARMS-primers, combined with a quantitative method would result in a more robust study. I propose that the fastest way to test clinical samples is isolating total RNA from blood after appropriate ethical approval.

Accordingly, bioinformatics analysis in parallel to the ARMS-RT-PCR data indicates that naturally occurring DNA variations in the LMNA gene (Single Nucleotide Polymorphisms, SNPs or di-nucleotide deletions occurring in more than 1% of the normal population) could affect its regulatory regions. The most surprising finding of this analysis is that, first, there are SNPs in or nearby the regulatory elements of the LMNA gene, which combined with intragenic variations can give rise to a defined haplotype (e.g. AD-EDMD, MAD, LGMD1B); second, 2% of the SNPs occurred in coding regions, where 50% were silent but affected the splicing region for lamin C, and the other 50% was missense, changing an arginine for a proline in exon 11 of the tail domain specific for Lamin A. While the ARMS-RT-PCR data was not conclusive, the bioinformatics approach is supporting the design of further experiments to first, determine whether an imbalance is a dominant pattern in laminopathies, secondly to search for mutations in the regulatory region of the LMNA gene, and third, to encourage new studies to unravel the

regulatory mechanisms that control transcription and translation of nuclear intermediate filaments.

6.6. Skin Dermal Fibroblast as experimental model to unravel the cell biology of muscular dystrophies.

Skin Dermal Fibroblasts have delivered a valuable model to study the cellular and molecular mechanisms underlying laminopathies, and became the first tool to study the effect of single point mutations in the biology of non-cytoplasmic intermediate filaments. But as any model has shown its own limitations, and has failed to explain the role of lamins in heart and skeletal muscle disorders. Not all laminopathies involve skin abnormalities from the pathological point of view (only MAD and the other progeria disorders), and sometimes it is difficult to extrapolate experimental data to the actual disease. New ethical approaches will need to be taken in order to investigate why A-type lamins, which are present in almost all known differentiated cells, are related to tissue-specific diseases, and whether they affect directly the patterns of gene expression, produce weakness of the nuclear envelope, or both.

Figures Chapter 6.

Figure 6.1.

Cartoon summarizing the general hypothesis that considers multi-complexes of proteins involving lamins, emerin, nesprins, actin and others in the regulation of several cell processes including gene regulation or chromating re-organization that influence the final commitment of certain cell types towards a normal differentiation process or to a disease phenotype.

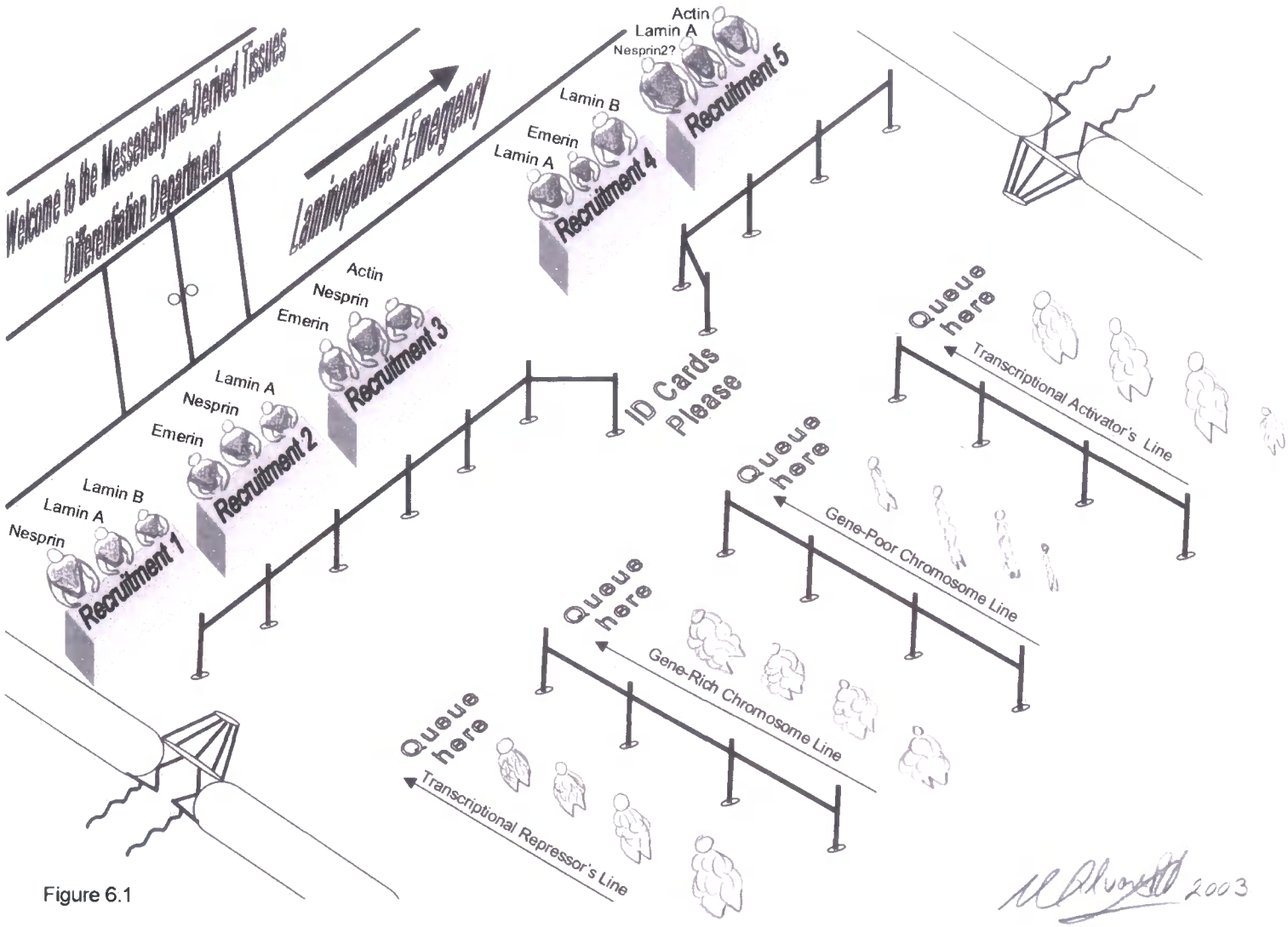
Welcome to the Messenchyme-Derived Tissues Differentiation Department
Laminopathies' Emergency
Recruitment 1
Lamin B
Lamin A
Nesprin
Recruitment 2
Lamin A
Nesprin
Emerin
Recruitment 3
Actin
Nesprin
Emerin
Recruitment 4
Lamin B
Emerin
Lamin A
Recruitment 5
Actin
Lamin A
Nesprin2?
ID Cards Please
Queue here
Transcriptional Activator's Line
Queue here
Gene-Poor Chromosome Line
Queue here
Gene-Rich Chromosome Line
Queue here
Transcriptional Repressor's Line
2003

Figure 6.1

Aaronson, R. P. and G. Blobel (1975). "Isolation of nuclear pore complexes in association with a lamina." Proc Natl Acad Sci U S A **72**(3): 1007-11.

Aebi, U., J. Cohn, et al. (1986). "The nuclear lamina is a meshwork of intermediate-type filaments." Nature **323**(6088): 560-4.

Agatep, R., Kirkpatrick, R.D., Parchaliuk, D.L., Woods, R.A., and Gietz, R.D. (1998). "Transformation of Saccaromyces cerevisiae by lithium acetate/single-stranded carrier DNA/Polyethylene glycol (LiAc/ss-DNA/PEG) protocol." Technical Tips Online (http://tto.trends.com).

Ahmadian, A., B. Gharizadeh, et al. (2001). "Genotyping by apyrase-mediated allele-specific extension." Nucleic Acids Res **29**(24): E121.

Al-Chalabi, A., P. M. Andersen, et al. (1999). "Deletions of the heavy neurofilament subunit tail in amyotrophic lateral sclerosis." Hum Mol Genet **8**(2): 157-64.

Alkema, M. J., M. Bronk, et al. (1997). "Identification of Bmi1-interacting proteins as constituents of a multimeric mammalian polycomb complex." Genes Dev **11**(2): 226-40.

Allen, N. P., L. Huang, et al. (2001). "Proteomic analysis of nucleoporin interacting proteins." J Biol Chem **276**(31): 29268-74.

Alsheimer, M., E. Fecher, et al. (1998). "Nuclear envelope remodelling during rat spermiogenesis: distribution and expression pattern of LAP2/thymopoietins." J Cell Sci **111 (Pt 15)**: 2227-34.

Alsheimer, M., E. von Glasenapp, et al. (2000). "Meiotic lamin C2: the unique amino-terminal hexapeptide GNAEGR is essential for nuclear envelope association." Proc Natl Acad Sci U S A **97**(24): 13120-5.

Altschul, S. F., T. L. Madden, et al. (1997). "Gapped BLAST and PSI-BLAST: a new generation of protein database search programs." Nucleic Acids Res **25**(17): 3389-402.

Ananthan J, Goldberg AL, et al. (1986). "Abnormal proteins serve as eukaryotic stress signal and trigger the activation of heat shock genes." Science **232**: 522 - 524.

Anderson, J. L., M. Khan, et al. (1999). "Confirmation of linkage of hereditary partial lipodystrophy to chromosome 1q21-22." Am J Med Genet **82**(2): 161-5.

Ano, T. and M. Shoda (1992). "Ultra-rapid transformation of Escherichia coli by an alkali cation." Biosci Biotechnol Biochem **56**(9): 1505.

Appelbaum, J., G. Blobel, et al. (1990). "In vivo phosphorylation of the lamin B receptor. Binding of lamin B to its nuclear membrane receptor is affected by phosphorylation." J Biol Chem **265**(8): 4181-4.

Arbustini, E., A. Pilotto, et al. (2002). "Autosomal dominant dilated cardiomyopathy with atrioventricular block: a lamin A/C defect-related disease." J Am Coll Cardiol **39**(6): 981-90.

Ayyadevara, S., J. J. Thaden, et al. (2000). "Anchor polymerase chain reaction display: a high-throughput method to resolve, score, and isolate dimorphic genetic markers based on interspersed repetitive DNA elements." Anal Biochem **284**(1): 19-28.

Ayyadevara, S., J. J. Thaden, et al. (2000). "Discrimination of primer 3'-nucleotide mismatch by taq DNA polymerase during polymerase chain reaction." Anal Biochem **284**(1): 11-8.

Bader, J. S. (2001). "The relative power of SNPs and haplotype as genetic markers for association tests." Pharmacogenomics **2**(1): 11-24.

Bailer, S. M., H. M. Eppenberger, et al. (1991). "Characterization of A 54-kD protein of the inner nuclear membrane: evidence for cell cycle-dependent interaction with the nuclear lamina." J Cell Biol **114**(3): 389-400.

Banwell, B. L. (2001). "Intermediate filament-related myopathies." Pediatr Neurol **24**(4): 257-63.

Barlow, S. B., M. L. Gonzalez-Garay, et al. (2002). "Paclitaxel-dependent mutants have severely reduced microtubule assembly and reduced tubulin synthesis." J Cell Sci **115**(Pt 17): 3469-78.

Barton, R. M. and H. J. Worman (1999). "Prenylated prelamin A interacts with Narf, a novel nuclear protein." J Biol Chem **274**(42): 30008-18.

Bechert, K., M. Lagos-Quintana, et al. (2003). "Effects of expressing lamin A mutant protein causing Emery-Dreifuss muscular dystrophy and familial partial lipodystrophy in HeLa cells." Exp Cell Res **286**(1): 75-86.

Beck, L. A., T. J. Hosick, et al. (1990). "Isoprenylation is required for the processing of the lamin A precursor." J Cell Biol **110**(5): 1489-99.

Becker, B., R. M. Bellin, et al. (1995). "Synemin contains the rod domain of intermediate filaments." Biochem Biophys Res Commun **213**(3): 796-802.

Becker, P. E. (1972). "[New data on the genetics and classification of muscular dystrophies]." Humangenetik **17**(1): 1-22.

Behrens, G. M., J. Genschel, et al. (2003). "Lack of mutations in LMNA, its promoter region, and the cellular retinoic acid binding protein II (CRABP II) in HIV associated lipodystrophy." Eur J Med Res **8**(5): 221-5.

Belmont, A. S., Y. Zhai, et al. (1993). "Lamin B distribution and association with peripheral chromatin revealed by optical sectioning and electron microscopy tomography." J Cell Biol **123**(6 Pt 2): 1671-85.

Benavente, R. and G. Krohne (1986). "Involvement of nuclear lamins in postmitotic reorganization of chromatin as demonstrated by microinjection of lamin antibodies." J Cell Biol **103**(5): 1847-54.

Benavente, R., G. Krohne, et al. (1985). "Cell type-specific expression of nuclear lamina proteins during development of Xenopus laevis." Cell **41**(1): 177-90.

Benham, A. M., A. Cabibbo, et al. (2000). "The CXXCXXC motif determines the folding, structure and stability of human Ero1-Lalpha." Embo J **19**(17): 4493-502.

Benjamin, I. and M. DR (1998). "Stress (Heat Shock) Proteins. Molecular chaperons in Cardiovascular Disease." Cir Res **83**: 117 - 132.

Bialer, M. G., N. L. McDaniel, et al. (1991). "Progression of cardiac disease in Emery-Dreifuss muscular dystrophy." Clin Cardiol **14**(5): 411-6.

Biamonti, G., M. Giacca, et al. (1992). "The gene for a novel human lamin maps at a highly transcribed locus of chromosome 19 which replicates at the onset of S-phase." Mol Cell Biol **12**(8): 3499-506.

Bione, S., E. Maestrini, et al. (1994). "Identification of a novel X-linked gene responsible for Emery-Dreifuss muscular dystrophy." Nat Genet **8**(4): 323-7.

Bione, S., K. Small, et al. (1995). "Identification of new mutations in the Emery-Dreifuss muscular dystrophy gene and evidence for genetic heterogeneity of the disease." Hum Mol Genet **4**(10): 1859-63.

Bione, S., F. Tamanini, et al. (1993). "Transcriptional organization of a 450-kb region of the human X chromosome in Xq28." Proc Natl Acad Sci U S A **90**(23): 10977-81.

Bird, A. P. (1986). "CpG-rich islands and the function of DNA methylation." Nature **321**(6067): 209-13.
Bloemendal, H., J. A. Lenstra, et al. (1980). "SV40-transformed hamster lens epithelial cells: a novel system for the isolation of cytoskeletal messenger RNAs and their translation products." Exp Eye Res **31**(5): 513-25.
Bochaton-Piallat, M. L., P. Ropraz, et al. (1996). "Phenotypic heterogeneity of rat arterial smooth muscle cell clones. Implications for the development of experimental intimal thickening." Arterioscler Thromb Vasc Biol **16**(6): 815-20.
Bonne, G., M. R. Di Barletta, et al. (1999). "Mutations in the gene encoding lamin A/C cause autosomal dominant Emery-Dreifuss muscular dystrophy." Nat Genet **21**(3): 285-8.
Bonne, G. and N. Levy (2003). "LMNA mutations in atypical Werner's syndrome." Lancet **362**(9395): 1585-6; author reply 1586.
Bonne, G., E. Mercuri, et al. (2000). "Clinical and molecular genetic spectrum of autosomal dominant Emery-Dreifuss muscular dystrophy due to mutations of the lamin A/C gene." Ann Neurol **48**(2): 170-80.
Bossie, C. A. and M. M. Sanders (1993). "A cDNA from Drosophila melanogaster encodes a lamin C-like intermediate filament protein." J Cell Sci **104 (Pt 4)**: 1263-72.
Bottema, C. D., G. Sarkar, et al. (1993). "Polymerase chain reaction amplification of specific alleles: a general method of detection of mutations, polymorphisms, and haplotypes." Methods Enzymol **218**: 388-402.
Bouhouche, A., A. Benomar, et al. (1999). "A locus for an axonal form of autosomal recessive Charcot-Marie-Tooth disease maps to chromosome 1q21.2-q21.3." Am J Hum Genet **65**(3): 722-7.
Boulton, S. J., A. Gartner, et al. (2002). "Combined functional genomic maps of the C. elegans DNA damage response." Science **295**(5552): 127-31.
Bowles, N. E., K. R. Bowles, et al. (2000). "The "final common pathway" hypothesis and inherited cardiovascular disease. The role of cytoskeletal proteins in dilated cardiomyopathy." Herz **25**(3): 168-75.
Boyd, D. L., M. E. Miskhin, et al. (1965). "Three Families with Familial Cardiomyopathy." Ann Intern Med **63**: 386-401.
Boyle, S., S. Gilchrist, et al. (2001). "The spatial organization of human chromosomes within the nuclei of normal and emerin-mutant cells." Hum Mol Genet **10**(3): 211-9.
Braasch, D. A. and D. R. Corey (2001). "Locked nucleic acid (LNA): fine-tuning the recognition of DNA and RNA." Chem Biol **8**(1): 1-7.
Brancolini, C. and C. Schneider (1994). "Phosphorylation of the growth arrest-specific protein Gas2 is coupled to actin rearrangements during Go-->G1 transition in NIH 3T3 cells." J Cell Biol **124**(5): 743-56.
Brenner, M., A. B. Johnson, et al. (2001). "Mutations in GFAP, encoding glial fibrillary acidic protein, are associated with Alexander disease." Nat Genet **27**(1): 117-20.
Brent, R. and R. L. Finley, Jr. (1997). "Understanding gene and allele function with two-hybrid methods." Annu Rev Genet **31**: 663-704.
Bridger, J. M., I. R. Kill, et al. (1993). "Internal lamin structures within G1 nuclei of human dermal fibroblasts." J Cell Sci **104 (Pt 2)**: 297-306.
Broder, Y. C., S. Katz, et al. (1998). "The ras recruitment system, a novel approach to the study of protein-protein interactions." Curr Biol **8**(20): 1121-4.

Brodsky, G. L., F. Muntoni, et al. (2000). "Lamin A/C gene mutation associated with dilated cardiomyopathy with variable skeletal muscle involvement." Circulation **101**(5): 473-6.
Broers, J. L., B. M. Machiels, et al. (1997). "A- and B-type lamins are differentially expressed in normal human tissues." Histochem Cell Biol **107**(6): 505-17.
Broers, J. L., B. M. Machiels, et al. (1999). "Dynamics of the nuclear lamina as monitored by GFP-tagged A-type lamins." J Cell Sci **112 (Pt 20)**: 3463-75.
Brown, W. T. (1990). "Genetic diseases of premature aging as models of senescence." Annu Rev Gerontol Geriatr **10**: 23-42.
Buckley, A. E., J. Dean, et al. (1999). "Cardiac involvement in Emery Dreifuss muscular dystrophy: a case series." Heart **82**(1): 105-8.
Burke, B. (2001). "Lamins and apoptosis: a two-way street?" J Cell Biol **153**(3): F5-7.
Burke, B. and L. Gerace (1986). "A cell free system to study reassembly of the nuclear envelope at the end of mitosis." Cell **44**(4): 639-52.
Burkhard P, S. J. a. S. S. (2001). "Coiled coils: a highly versatile veratileprotein folding motif." Trends Cell Biol **11**: 82 - 88.
Cai, M., Y. Huang, et al. (2001). "Solution structure of the constant region of nuclear envelope protein LAP2 reveals two LEM-domain structures: one binds BAF and the other binds DNA." Embo J **20**(16): 4399-407.
Canki-Klain, N., D. Recan, et al. (2000). "Clinical variability and molecular diagnosis in a four-generation family with X-linked Emery-Dreifuss muscular dystrophy." Croat Med J **41**(4): 389-95.
Cao, H. and R. A. Hegele (2000). "Nuclear lamin A/C R482Q mutation in canadian kindreds with Dunnigan-type familial partial lipodystrophy." Hum Mol Genet **9**(1): 109-12.
Cao, H. and R. A. Hegele (2003). "LMNA is mutated in Hutchinson-Gilford progeria (MIM 176670) but not in Wiedemann-Rautenstrauch progeroid syndrome (MIM 264090)." J Hum Genet **48**(5): 271-4.
Capanni, C., V. Cenni, et al. (2003). "Failure of lamin A/C to functionally assemble in R482L mutated familial partial lipodystrophy fibroblasts: altered intermolecular interaction with emerin and implications for gene transcription." Exp Cell Res **291**(1): 122-34.
Capco, D. G., K. M. Wan, et al. (1982). "The nuclear matrix: three-dimensional architecture and protein composition." Cell **29**(3): 847-58.
Capetanaki, Y., S. Starnes, et al. (1989). "Expression of the chicken vimentin gene in transgenic mice: efficient assembly of the avian protein into the cytoskeleton." Proc Natl Acad Sci U S A **86**(13): 4882-6.
Cardiff, T. H. G. M. D. (2003). "LMNA mutations." http://archive.uwcm.ac.uk/uwcm/mg/search/132146.html.
Carmo-Fonseca, M., L. Mendes-Soares, et al. (2000). "To be or not to be in the nucleolus." Nat Cell Biol **2**(6): E107-12.
Cartegni, L., M. R. di Barletta, et al. (1997). "Heart-specific localization of emerin: new insights into Emery-Dreifuss muscular dystrophy." Hum Mol Genet **6**(13): 2257-64.
Caux, F., E. Dubosclard, et al. (2003). "A new clinical condition linked to a novel mutation in lamins A and C with generalized lipoatrophy, insulin-resistant diabetes, disseminated leukomelanodermic papules, liver steatosis, and cardiomyopathy." J Clin Endocrinol Metab **88**(3): 1006-13.

Charniot, J. C., C. Pascal, et al. (2003). "Functional consequences of an LMNA mutation associated with a new cardiac and non-cardiac phenotype." Hum Mutat **21**(5): 473-81.
Chaudhary, N. and J. C. Courvalin (1993). "Stepwise reassembly of the nuclear envelope at the end of mitosis." J Cell Biol **122**(2): 295-306.
Chelsky, D., C. Sobotka, et al. (1989). "Lamin B methylation and assembly into the nuclear envelope." J Biol Chem **264**(13): 7637-43.
Chen, H. M., J. Zhou, et al. (2000). "Cleavage of lamin-like proteins in in vivo and in vitro apoptosis of tobacco protoplasts induced by heat shock." FEBS Lett **480**(2-3): 165-8.
Chen, L., L. Lee, et al. (2003). "LMNA mutations in atypical Werner's syndrome." Lancet **362**(9382): 440-5.
Chen, T., F. M. Boisvert, et al. (1999). "A role for the GSG domain in localizing Sam68 to novel nuclear structures in cancer cell lines." Mol Biol Cell **10**(9): 3015-33.
Chen, Y. H., S. J. Xu, et al. (2003). "KCNQ1 gain-of-function mutation in familial atrial fibrillation." Science **299**(5604): 251-4.
Chess, A., I. Simon, et al. (1994). "Allelic inactivation regulates olfactory receptor gene expression." Cell **78**(5): 823-34.
Chomczynski, P. (1993). "A reagent for the single-step simultaneous isolation of RNA, DNA and proteins from cell and tissue samples." Biotechniques **15**(3): 532-4, 536-7.
Chomczynski, P. and N. Sacchi (1987). "Single-step method of RNA isolation by acid guanidinium thiocyanate-phenol-chloroform extraction." Anal Biochem **162**(1): 156-9.
Coates, P. J., R. C. Hobbs, et al. (1996). "Identification of the antigen recognized by the monoclonal antibody BU31 as lamins A and C." J Pathol **178**(1): 21-9.
Cogulu, O. G., C.; Darcan, S.; Kadioglu, B.; Ozkinay, F.; Ozkinay, C.; Arkun, R. : (2003). "Mandibuloacral dysplasia with absent breast development. (Letter)." Am. J. Med. Genet. **119A**: 391 - 392.
Cohen, L. K., T. F. Thurmon, et al. (1973). "Werner's syndrome." Cutis **12**: 76 - 80.
Cohen, M., K. K. Lee, et al. (2001). "Transcriptional repression, apoptosis, human disease and the functional evolution of the nuclear lamina." Trends Biochem Sci **26**(1): 41-7.
Collard, J. F., J. L. Senecal, et al. (1992). "Redistribution of nuclear lamin A is an early event associated with differentiation of human promyelocytic leukemia HL-60 cells." J Cell Sci **101 (Pt 3)**: 657-70.
Collas, P. (1998). "Nuclear envelope disassembly in mitotic extract requires functional nuclear pores and a nuclear lamina." J Cell Sci **111 (Pt 9)**: 1293-303.
Collas, P., L. Thompson, et al. (1997). "Protein kinase C-mediated interphase lamin B phosphorylation and solubilization." J Biol Chem **272**(34): 21274-80.
Colomer, J., C. Iturriaga, et al. (2002). "Autosomal dominant Emery-Dreifuss muscular dystrophy: a new family with late diagnosis." Neuromuscul Disord **12**(1): 19-25.
Cornwell, T. L., J. Li, et al. (2001). "Reorganization of myofilament proteins and decreased cGMP-dependent protein kinase in the human uterus during pregnancy." J Clin Endocrinol Metab **86**(8): 3981-8.
Coulombe, P. A., and Funchs, E (1993). "Epidermolysis bullosa simplex." Semin. Dermatol **12**: 173 - 190.

Coulombe, P. A., O. Bousquet, et al. (2000). "The 'ins' and 'outs' of intermediate filament organization." Trends Cell Biol **10**(10): 420-8.
Coulombe, P. A., L. Ma, et al. (2001). "Intermediate filaments at a glance." J Cell Sci **114**(Pt 24): 4345-7.
Courvalin, J. C., N. Segil, et al. (1992). "The lamin B receptor of the inner nuclear membrane undergoes mitosis-specific phosphorylation and is a substrate for p34cdc2-type protein kinase." J Biol Chem **267**(27): 19035-8.
Crinelli, R., M. Bianchi, et al. (2002). "Design and characterization of decoy oligonucleotides containing locked nucleic acids." Nucleic Acids Res **30**(11): 2435-43.
Cronshaw, J. M., A. N. Krutchinsky, et al. (2002). "Proteomic analysis of the mammalian nuclear pore complex." J Cell Biol **158**(5): 915-27.
Cross, T., G. Griffiths, et al. (2000). "PKC-delta is an apoptotic lamin kinase." Oncogene **19**(19): 2331-7.
Csanady, M., M. Hogye, et al. (1995). "Familial dilated cardiomyopathy: a worse prognosis compared with sporadic forms." Br Heart J **74**(2): 171-3.
Cutler, D. A., T. Sullivan, et al. (2002). "Characterization of adiposity and metabolism in Lmna-deficient mice." Biochem Biophys Res Commun **291**(3): 522-7.
Cutler, D. L., S. Kaufmann, et al. (1991). "Insulin-resistant diabetes mellitus and hypermetabolism in mandibuloacral dysplasia: a newly recognized form of partial lipodystrophy." J. Clin. Endocr. Metab **73**: 1056 - 1061.
Dahl, D. and A. Bignami (1976). "Isolation from peripheral nerve of a protein similar to the glial fibrillary acidic protein." FEBS Lett **66**(2): 281-4.
Dahl, D., D. C. Rueger, et al. (1981). "Vimentin, the 57 000 molecular weight protein of fibroblast filaments, is the major cytoskeletal component in immature glia." Eur J Cell Biol **24**(2): 191-6.
Day, J. P., D. Bergstrom, et al. (1999). "Nucleotide analogs facilitate base conversion with 3' mismatch primers." Nucleic Acids Res **27**(8): 1810-8.
De Sandre-Giovannoli, A., R. Bernard, et al. (2003). "Lamin a truncation in Hutchinson-Gilford progeria." Science **300**(5628): 2055.
De Sandre-Giovannoli, A., M. Chaouch, et al. (2002). "Homozygous defects in LMNA, encoding lamin A/C nuclear-envelope proteins, cause autosomal recessive axonal neuropathy in human (Charcot-Marie-Tooth disorder type 2) and mouse." Am J Hum Genet **70**(3): 726-36.
de Stanchina, E., D. Gabellini, et al. (2000). "Selection of homeotic proteins for binding to a human DNA replication origin." J Mol Biol **299**(3): 667-80.
Dechat, T., B. Korbei, et al. (2000). "Lamina-associated polypeptide 2alpha binds intranuclear A-type lamins." J Cell Sci **113 Pt 19**: 3473-84.
Delgado Luengo, W., A. Rojas Martinez, et al. (2002). "Del(1)(q23) in a patient with Hutchinson-Gilford progeria." Am J Med Genet **113**(3): 298-301.
Dessev, G., C. Iovcheva, et al. (1988). "Protein kinase activity associated with the nuclear lamina." Proc Natl Acad Sci U S A **85**(9): 2994-8.
Dhe-Paganon, S., E. D. Werner, et al. (2002). "Structure of the globular tail of nuclear lamin." J Biol Chem **277**(20): 17381-4.
Diffley, J. F. and B. Stillman (1989). "Transcriptional silencing and lamins." Nature **342**(6245): 24.

Djabali, K., M. M. Portier, et al. (1991). "Network antibodies identify nuclear lamin B as a physiological attachment site for peripherin intermediate filaments." Cell **64**(1): 109-21.
Doring, V. and R. Stick (1990). "Gene structure of nuclear lamin LIII of Xenopus laevis; a model for the evolution of IF proteins from a lamin-like ancestor." Embo J **9**(12): 4073-81.
Dreger, M., L. Bengtsson, et al. (2001). "Nuclear envelope proteomics: novel integral membrane proteins of the inner nuclear membrane." Proc Natl Acad Sci U S A **98**(21): 11943-8.
Dreifuss, F. E. and G. R. Hogan (1961). "Survival in x-chromosomal muscular dystrophy." Neurology **11**: 734-7.
Dreuillet, C., J. Tillit, et al. (2002). "In vivo and in vitro interaction between human transcription factor MOK2 and nuclear lamin A/C." Nucleic Acids Res **30**(21): 4634-42.
Drysdale, C. M., D. W. McGraw, et al. (2000). "Complex promoter and coding region beta 2-adrenergic receptor haplotypes alter receptor expression and predict in vivo responsiveness." Proc Natl Acad Sci U S A **97**(19): 10483-8.
Duband-Goulet, I., J. C. Courvalin, et al. (1998). "LBR, a chromatin and lamin binding protein from the inner nuclear membrane, is proteolyzed at late stages of apoptosis." J Cell Sci **111 (Pt 10)**: 1441-51.
Dubowitz, V. (1973). "Rigid spine syndrome: a muscle syndrome in search of a name." Proc R Soc Med **66**(3): 219-20.
Dunnigan, M. G., M. A. Cochrane, et al. (1974). "Familial lipoatrophic diabetes with dominant transmission. A new syndrome." Q J Med **43**(169): 33-48.
Dyer, J. A., I. R. Kill, et al. (1997). "Cell cycle changes in A-type lamin associations detected in human dermal fibroblasts using monoclonal antibodies." Chromosome Res **5**(6): 383-94.
Dyer, J. A., B. E. Lane, et al. (1999). "Investigations of the pathway of incorporation and function of lamin A in the nuclear lamina." Microsc Res Tech **45**(1): 1-12.
Eckes, B., E. Colucci-Guyon, et al. (2000). "Impaired wound healing in embryonic and adult mice lacking vimentin." J Cell Sci **113 (Pt 13)**: 2455-62.
Ehrmann, J., Jr., Y. Collan, et al. (2001). "Apoptosis, analysed by means of lamin B detection, correlates with grade of astroglial tumours but not with p27Kip1/retinoblastoma protein expression." Virchows Arch **439**(4): 547-51.
Eliasson, C., C. Sahlgren, et al. (1999). "Intermediate filament protein partnership in astrocytes." J Biol Chem **274**(34): 23996-4006.
Ellenberg, J., E. D. Siggia, et al. (1997). "Nuclear membrane dynamics and reassembly in living cells: targeting of an inner nuclear membrane protein in interphase and mitosis." J Cell Biol **138**(6): 1193-206.
Ellis, D. J., H. Jenkins, et al. (1997). "GST-lamin fusion proteins act as dominant negative mutants in Xenopus egg extract and reveal the function of the lamina in DNA replication." J Cell Sci **110 (Pt 20)**: 2507-18.
Ellis, J. A., J. R. Yates, et al. (1999). "Changes at P183 of emerin weaken its protein-protein interactions resulting in X-linked Emery-Dreifuss muscular dystrophy." Hum Genet **104**(3): 262-8.
Emery, A. E. (1987). "X-linked muscular dystrophy with early contractures and cardiomyopathy (Emery-Dreifuss type)." Clin Genet **32**(5): 360-7.

Emery, A. E. (1989). "Emery-Dreifuss syndrome." J Med Genet **26**(10): 637-41.
Emery, A. E. and F. E. Dreifuss (1966). "Unusual type of benign x-linked muscular dystrophy." J Neurol Neurosurg Psychiatry **29**(4): 338-42.
Eng LF, Vanderhaeghen JJ, et al. (1971). "An acidic protein isolated from fibrous astrocytes." Brain Research **28**(2): 351-4.
Eriksson, M., W. T. Brown, et al. (2003). "Recurrent de novo point mutations in lamin A cause Hutchinson-Gilford progeria syndrome." Nature **423**(6937): 293-8.
Escurat, M., K. Djabali, et al. (1990). "Differential expression of two neuronal intermediate-filament proteins, peripherin and the low-molecular-mass neurofilament protein (NF-L), during the development of the rat." J Neurosci **10**(3): 764-84.
Evans, R. M. (1998). "Vimentin: the conundrum of the intermediate filament gene family." Bioessays **20**(1): 79-86.
Farnsworth, C. C., S. L. Wolda, et al. (1989). "Human lamin B contains a farnesylated cysteine residue." J Biol Chem **264**(34): 20422-9.
Fatkin, D., C. MacRae, et al. (1999). "Missense mutations in the rod domain of the lamin A/C gene as causes of dilated cardiomyopathy and conduction-system disease." N Engl J Med **341**(23): 1715-24.
Favreau, C., E. Dubosclard, et al. (2003). "Expression of lamin A mutated in the carboxyl-terminal tail generates an aberrant nuclear phenotype similar to that observed in cells from patients with Dunnigan-type partial lipodystrophy and Emery-Dreifuss muscular dystrophy." Exp Cell Res **282**(1): 14-23.
Felice, K. J., R. C. Schwartz, et al. (2000). "Autosomal dominant Emery-Dreifuss dystrophy due to mutations in rod domain of the lamin A/C gene." Neurology **55**(2): 275-80.
Fenichel, G. M., Y. C. Sul, et al. (1982). "An autosomal-dominant dystrophy with humeropelvic distribution and cardiomyopathy." Neurology **32**(12): 1399-401.
Fidzianska, A., D. Toniolo, et al. (1998). "Ultrastructural abnormality of sarcolemmal nuclei in Emery-Dreifuss muscular dystrophy (EDMD)." J Neurol Sci **159**(1): 88-93.
Firmbach-Kraft, I. and R. Stick (1993). "The role of CaaX-dependent modifications in membrane association of Xenopus nuclear lamin B3 during meiosis and the fate of B3 in transfected mitotic cells." J Cell Biol **123**(6 Pt 2): 1661-70.
Firmbach-Kraft, I. and R. Stick (1995). "Analysis of nuclear lamin isoprenylation in Xenopus oocytes: isoprenylation of lamin B3 precedes its uptake into the nucleus." J Cell Biol **129**(1): 17-24.
Fishbein, M. C., R. J. Siegel, et al. (1993). "Sudden death of a carrier of X-linked Emery-Dreifuss muscular dystrophy." Ann Intern Med **119**(9): 900-5.
Fisher, D. Z., N. Chaudhary, et al. (1986). "cDNA sequencing of nuclear lamins A and C reveals primary and secondary structural homology to intermediate filament proteins." Proc Natl Acad Sci U S A **83**(17): 6450-4.
Flick, M. J. and S. F. Konieczny (2000). "The muscle regulatory and structural protein MLP is a cytoskeletal binding partner of betaI-spectrin." J Cell Sci **113 (Pt 9)**: 1553-64.
Flier, J. S. (2000). "Pushing the envelope on lipodystrophy." Nat Genet **24**(2): 103-4.
Focus (1986). FOCUS. **8:** 9.

Foisner, R. and L. Gerace (1993). "Integral membrane proteins of the nuclear envelope interact with lamins and chromosomes, and binding is modulated by mitotic phosphorylation." Cell **73**(7): 1267-79.
Foisy, S. and V. Bibor-Hardy (1988). "Synthesis of nuclear lamins in BHK-21 cells synchronized with aphidicolin." Biochem Biophys Res Commun **156**(1): 205-10.
Frangioni, J. V. and B. G. Neel (1993). "Use of a general purpose mammalian expression vector for studying intracellular protein targeting: identification of critical residues in the nuclear lamin A/C nuclear localization signal." J Cell Sci **105 (Pt 2)**: 481-8.
Franke, W. W. (1987). "Nuclear lamins and cytoplasmic intermediate filament proteins: a growing multigene family." Cell **48**(1): 3-4.
Freidenberg, G. R., D. L. Cutler, et al. (1992). "Severe insulin resistance and diabetes mellitus in mandibuloacral dysplasia." Am. J. Dis. Child **146**: 93 - 99.
Frid, M. G., E. C. Dempsey, et al. (1997). "Smooth muscle cell heterogeneity in pulmonary and systemic vessels. Importance in vascular disease." Arterioscler Thromb Vasc Biol **17**(7): 1203-9.
Friedman, D. L. and R. Ken (1988). "Insulin stimulates incorporation of 32Pi into nuclear lamins A and C in quiescent BHK-21 cells." J Biol Chem **263**(3): 1103-6.
Fringer, J. and F. Grinnell (2001). "Fibroblast quiescence in floating or released collagen matrices: contribution of the ERK signaling pathway and actin cytoskeletal organization." J Biol Chem **276**(33): 31047-52.
Frischmeyer, P. A. and H. C. Dietz (1999). "Nonsense-mediated mRNA decay in health and disease." Hum Mol Genet **8**(10): 1893-900.
Fuchs, E. (1994). "Intermediate filaments and disease: mutations that cripple cell strength." J Cell Biol **125**(3): 511-6.
Fuchs, E. and H. Green (1980). "Changes in keratin gene expression during terminal differentiation of the keratinocyte." Cell **19**(4): 1033-42.
Fuchs, E. and K. Weber (1994). "Intermediate filaments: structure, dynamics, function, and disease." Annu Rev Biochem **63**: 345-82.
Fujimoto, S., T. Ishikawa, et al. (1999). "Early onset of X-linked Emery-Dreifuss muscular dystrophy in a boy with emerin gene deletion." Neuropediatrics **30**(3): 161-3.
Funakoshi, M., Y. Tsuchiya, et al. (1999). "Emerin and cardiomyopathy in Emery-Dreifuss muscular dystrophy." Neuromuscul Disord **9**(2): 108-14.
Furukawa, K. (1999). "LAP2 binding protein 1 (L2BP1/BAF) is a candidate mediator of LAP2-chromatin interaction." J Cell Sci **112 (Pt 15)**: 2485-92.
Furukawa, K., C. E. Fritze, et al. (1998). "The major nuclear envelope targeting domain of LAP2 coincides with its lamin binding region but is distinct from its chromatin interaction domain." J Biol Chem **273**(7): 4213-9.
Furukawa, K. and Y. Hotta (1993). "cDNA cloning of a germ cell specific lamin B3 from mouse spermatocytes and analysis of its function by ectopic expression in somatic cells." Embo J **12**(1): 97-106.
Furukawa, K., H. Inagaki, et al. (1994). "Identification and cloning of an mRNA coding for a germ cell-specific A-type lamin in mice." Exp Cell Res **212**(2): 426-30.
Furukawa, K. and T. Kondo (1998). "Identification of the lamina-associated-polypeptide-2-binding domain of B-type lamin." Eur J Biochem **251**(3): 729-33.

Furukawa, K., N. Pante, et al. (1995). "Cloning of a cDNA for lamina-associated polypeptide 2 (LAP2) and identification of regions that specify targeting to the nuclear envelope." Embo J **14**(8): 1626-36.
Gall, J. G. (2000). "Cajal bodies: the first 100 years." Annu Rev Cell Dev Biol **16**: 273-300.
Gallicano, G. I. (2001). "Composition, regulation, and function of the cytoskeleton in mammalian eggs and embryos." Front Biosci **6**: D1089-108.
Gant, T. M., C. A. Harris, et al. (1999). "Roles of LAP2 proteins in nuclear assembly and DNA replication: truncated LAP2beta proteins alter lamina assembly, envelope formation, nuclear size, and DNA replication efficiency in Xenopus laevis extracts." J Cell Biol **144**(6): 1083-96.
Gard, A. L., F. P. White, et al. (1985). "Extra-neural glial fibrillary acidic protein (GFAP) immunoreactivity in perisinusoidal stellate cells of rat liver." J Neuroimmunol **8**(4-6): 359-75.
Gard, D. L. and E. Lazarides (1980). "The synthesis and distribution of desmin and vimentin during myogenesis in vitro." Cell **19**(1): 263-75.
Gardner, E. E., D. Dahl, et al. (1984). "Formation of 10-nanometer filaments from the 150K-dalton neurofilament protein in vitro." J Neurosci Res **11**(2): 145-55.
Gardner, R. J. M., H. H. Ardinger, et al. (1985). "Dominantly inherited dilated cardiomyopathy with skeletal myopathy." Am. J. Hum. Genet **37**: A54.
Gardner, R. J. M., J. W. Hanson, et al. (1987). "Dominantly inherited dilated cardiomyopathy." Am. J. Med. Genet. **27**: 61 - 73.
Garg, A. (2000). "Gender differences in the prevalence of metabolic complications in familial partial lipodystrophy (Dunnigan variety)." J Clin Endocrinol Metab **85**(5): 1776-82.
Garg, A., R. M. Peshock, et al. (1999). "Adipose tissue distribution pattern in patients with familial partial lipodystrophy (Dunnigan variety)." J Clin Endocrinol Metab **84**(1): 170-4.
Garg, A., M. Vinaitheerthan, et al. (2001). "Phenotypic heterogeneity in patients with familial partial lipodystrophy (dunnigan variety) related to the site of missense mutations in lamin a/c gene." J Clin Endocrinol Metab **86**(1): 59-65.
Geisler, N. and K. Weber (1981). "Self-assembly in Vitro of the 68,000 molecular weight component of the mammalian neurofilament triplet proteins into intermediate-sized filaments." J Mol Biol **151**(3): 565-71.
Geisse, N. A., B. Wasle, et al. (2002). "Syncollin homo-oligomers associate with lipid bilayers in the form of doughnut-shaped structures." J Membr Biol **189**(2): 83-92.
Gelfant, S. (1981). "Cycling in equilibrium or formed from noncycling cell transitions in tissue aging, immunological surveillance, transformation, and tumor growth." Int Rev Cytol **70**: 1-25.
Genschel, J. and H. H. Schmidt (2000). "Mutations in the LMNA gene encoding lamin A/C." Hum Mutat **16**(6): 451-9.
Georgatos, S. D. and G. Blobel (1987). "Lamin B constitutes an intermediate filament attachment site at the nuclear envelope." J Cell Biol **105**(1): 117-25.
Georgatos, S. D., I. Maroulakou, et al. (1989). "Lamin A, lamin B, and lamin B receptor analogues in yeast." J Cell Biol **108**(6): 2069-82.

Georgatos, S. D., J. Meier, et al. (1994). "Lamins and lamin-associated proteins." Curr Opin Cell Biol **6**(3): 347-53.
Gerace, L. and G. Blobel (1980). "The nuclear envelope lamina is reversibly depolymerized during mitosis." Cell **19**(1): 277-87.
Gerace, L., A. Blum, et al. (1978). "Immunocytochemical localization of the major polypeptides of the nuclear pore complex-lamina fraction. Interphase and mitotic distribution." J Cell Biol **79**(2 Pt 1): 546-66.
Ghetti, A., S. Pinol-Roma, et al. (1992). "hnRNP I, the polypyrimidine tract-binding protein: distinct nuclear localization and association with hnRNAs." Nucleic Acids Res **20**(14): 3671-8.
Gieffers, C. and G. Krohne (1991). "In vitro reconstitution of recombinant lamin A and a lamin A mutant lacking the carboxy-terminal tail." Eur J Cell Biol **55**(2): 191-9.
Giglio, S., B. Pirola, et al. (2000). "Opposite deletions/duplications of the X chromosome: two novel reciprocal rearrangements." Eur J Hum Genet **8**(1): 63-70.
Gilford, H. (1904). "Ateleiosis and progeria: continuous youth and premature old age." Brit. Med. J. **2**: 914 - 918.
Gindullis, F., N. J. Peffer, et al. (1999). "MAF1, a novel plant protein interacting with matrix attachment region binding protein MFP1, is located at the nuclear envelope." Plant Cell **11**(9): 1755-68.
Gindullis, F., A. Rose, et al. (2002). "Four signature motifs define the first class of structurally related large coiled-coil proteins in plants." BMC Genomics **3**(1): 9.
Gittenberger-de Groot, A. C., M. C. DeRuiter, et al. (1999). "Smooth muscle cell origin and its relation to heterogeneity in development and disease." Arterioscler Thromb Vasc Biol **19**(7): 1589-94.
Glass, C. A., J. R. Glass, et al. (1993). "The alpha-helical rod domain of human lamins A and C contains a chromatin binding site." Embo J **12**(11): 4413-24.
Glass, J. R. and L. Gerace (1990). "Lamins A and C bind and assemble at the surface of mitotic chromosomes." J Cell Biol **111**(3): 1047-57.
Goldberg, M., A. Harel, et al. (1999). "The tail domain of lamin Dm0 binds histones H2A and H2B." Proc Natl Acad Sci U S A **96**(6): 2852-7.
Goldberg, M., H. Lu, et al. (1998). "Interactions among Drosophila nuclear envelope proteins lamin, otefin, and YA." Mol Cell Biol **18**(7): 4315-23.
Goldman, A. E., R. D. Moir, et al. (1992). "Pathway of incorporation of microinjected lamin A into the nuclear envelope." J Cell Biol **119**(4): 725-35.
Goldman, R. D., S. Khuon, et al. (1996). "The function of intermediate filaments in cell shape and cytoskeletal integrity." J Cell Biol **134**(4): 971-83.
Gomi, T., T. Ikeda, et al. (1995). "Protective effect of thromboxane synthetase inhibitor on hypertensive renal damage in Dahl salt-sensitive rats." Clin Exp Pharmacol Physiol Suppl **22**(1): S371-3.
Goudeau, B., A. Dagvadorj, et al. (2001). "Structural and functional analysis of a new desmin variant causing desmin-related myopathy." Hum Mutat **18**(5): 388-96.
Graham, R. M. and W. A. Owens (1999). "Pathogenesis of inherited forms of dilated cardiomyopathy." N Engl J Med **341**(23): 1759-62.
Grande, M. A., I. van der Kraan, et al. (1997). "Nuclear distribution of transcription factors in relation to sites of transcription and RNA polymerase II." J Cell Sci **110 (Pt 15)**: 1781-91.

Gruenbaum, Y., K. K. Lee, et al. (2002). "The expression, lamin-dependent localization and RNAi depletion phenotype for emerin in C. elegans." J Cell Sci **115**(Pt 5): 923-9.
Gruenbaum, Y., K. L. Wilson, et al. (2000). "Review: nuclear lamins--structural proteins with fundamental functions." J Struct Biol **129**(2-3): 313-23.
Guilly, M. N., A. Bensussan, et al. (1987). "A human T lymphoblastic cell line lacks lamins A and C." Embo J **6**(12): 3795-9.
Haas, M. and E. Jost (1993). "Functional analysis of phosphorylation sites in human lamin A controlling lamin disassembly, nuclear transport and assembly." Eur J Cell Biol **62**(2): 237-47.
Hall, T. A. (1999). "Bioedit: a user friendly biological sequence alignment editor and analysis program for Windows 95/98/NT." Nucl. Acids Symp. Ser. **41**: 95 - 98.
Hanahan, D. and M. Meselson (1983). "Plasmid screening at high colony density." Methods Enzymol **100**: 333-42.
Haraguchi, T., T. Koujin, et al. (2001). "BAF is required for emerin assembly into the reforming nuclear envelope." J Cell Sci **114**(Pt 24): 4575-85.
Harborth, J., S. M. Elbashir, et al. (2001). "Identification of essential genes in cultured mammalian cells using small interfering RNAs." J Cell Sci **114**(Pt 24): 4557-65.
Harendza, S., D. H. Lovett, et al. (2003). "Linked common polymorphisms in the gelatinase a promoter are associated with diminished transcriptional response to estrogen and genetic fitness." J Biol Chem **278**(23): 20490-9.
Hari, M., H. Yang, et al. (2003). "Expression of class III beta-tubulin reduces microtubule assembly and confers resistance to paclitaxel." Cell Motil Cytoskeleton **56**(1): 45-56.
Hartmann, K., T. G. Baier, et al. (1989). "Demonstration of type I insulin-like growth factor receptors on human platelets." J Recept Res **9**(2): 181-98.
Hasegawa, T., K. Kobayashi, et al. (1999). "[A novel splice-site mutation in the STA gene in a Japanese patient with Emery-Dreifuss muscular dystrophy]." Rinsho Shinkeigaku **39**(11): 1138-43.
Hass, R., M. Brach, et al. (1991). "Inhibition of phorbol ester-induced monocytic differentiation by dexamethasone is associated with down-regulation of c-fos and c-jun (AP-1)." J Cell Physiol **149**(1): 125-31.
Hatzfeld, M. and K. Weber (1992). "A synthetic peptide representing the consensus sequence motif at the carboxy-terminal end of the rod domain inhibits intermediate filament assembly and disassembles preformed filaments." J Cell Biol **116**(1): 157-66.
Hauptmann, A. T., S. J. (1941). "Muscular shortening and dystrophy: a heredofamilial disease." Arch. Neurol. Psychiat. **46**: 654-664, 1941.
Heald, R. and F. McKeon (1990). "Mutations of phosphorylation sites in lamin A that prevent nuclear lamina disassembly in mitosis." Cell **61**(4): 579-89.
Hebert, M. D., P. W. Szymczyk, et al. (2001). "Coilin forms the bridge between Cajal bodies and SMN, the spinal muscular atrophy protein." Genes Dev **15**(20): 2720-9.
Hegele, R. A. (2001). "Molecular basis of partial lipodystrophy and prospects for therapy." Trends Mol Med **7**(3): 121-6.
Hegele, R. A. (2003). "Drawing the line in progeria syndromes." Lancet **362**(9382): 416-7.

Hegele, R. A., C. M. Anderson, et al. (2000). "Lamin A/C mutation in a woman and her two daughters with Dunnigan-type partial lipodystrophy and insulin resistance." Diabetes Care **23**(2): 258-9.
Hegele, R. A., C. M. Anderson, et al. (2000). "Association between nuclear lamin A/C R482Q mutation and partial lipodystrophy with hyperinsulinemia, dyslipidemia, hypertension, and diabetes." Genome Res **10**(5): 652-8.
Hegele, R. A., H. Cao, et al. (2000). "Heterogeneity of nuclear lamin A mutations in Dunnigan-type familial partial lipodystrophy." J Clin Endocrinol Metab **85**(9): 3431-5.
Hegele, R. A., H. Cao, et al. (2002). "PPARG F388L, a transactivation-deficient mutant, in familial partial lipodystrophy." Diabetes **51**(12): 3586-90.
Hegele, R. A., H. Cao, et al. (2000). "Genetic variation in LMNA modulates plasma leptin and indices of obesity in aboriginal Canadians." Physiol Genomics **3**(1): 39-44.
Hegele, R. A., H. Cao, et al. (2000). "LMNA R482Q mutation in partial lipodystrophy associated with reduced plasma leptin concentration." J Clin Endocrinol Metab **85**(9): 3089-93.
Hegele, R. A., M. E. Kraw, et al. (2003). "Elevated serum C-reactive protein and free fatty acids among nondiabetic carriers of missense mutations in the gene encoding lamin A/C (LMNA) with partial lipodystrophy." Arterioscler Thromb Vasc Biol **23**(1): 111-6.
Hegele, R. A., J. Yuen, et al. (2001). "Single-nucleotide polymorphisms of the nuclear lamina proteome." J Hum Genet **46**: 351-354.
Heins, S. and U. Aebi (1994). "Making heads and tails of intermediate filament assembly, dynamics and networks." Curr Opin Cell Biol **6**(1): 25-33.
Heitlinger, E., M. Peter, et al. (1991). "Expression of chicken lamin B2 in Escherichia coli: characterization of its structure, assembly, and molecular interactions." J Cell Biol **113**(3): 485-95.
Helbling-Leclerc, A., G. Bonne, et al. (2002). "Emery-Dreifuss muscular dystrophy." Eur J Hum Genet **10**(3): 157-61.
Held, W., J. Roland, et al. (1995). "Allelic exclusion of Ly49-family genes encoding class I MHC-specific receptors on NK cells." Nature **376**(6538): 355-8.
Hennekes, H. and E. A. Nigg (1994). "The role of isoprenylation in membrane attachment of nuclear lamins. A single point mutation prevents proteolytic cleavage of the lamin A precursor and confers membrane binding properties." J Cell Sci **107 (Pt 4)**: 1019-29.
Hennekes, H., M. Peter, et al. (1993). "Phosphorylation on protein kinase C sites inhibits nuclear import of lamin B2." J Cell Biol **120**(6): 1293-304.
Henrion, D., F. Terzi, et al. (1997). "Impaired flow-induced dilation in mesenteric resistance arteries from mice lacking vimentin." J Clin Invest **100**(11): 2909-14.
Herrmann, H. and U. Aebi (1998). "Intermediate filament assembly: fibrillogenesis is driven by decisive dimer-dimer interactions." Curr Opin Struct Biol **8**: 177 -185.
Herrmann, H. and U. Aebi (2000). "Intermediate filaments and their associates: multi-talented structural elements specifying cytoarchitecture and cytodynamics." Curr Opin Cell Biol **12**(1): 79-90.
Herrmann, H., Haner M, Brettel M, Muller SA, Goldie KN, Fedtke B, Lustig A, Franke WW and Aedi U. (1996). "Structure and assembly properties

of the intermediate filament protein vimentin: the role of its head, rod and tail domains." J Mol Biol **264**: 933 - 953.
Hesse, M., T. M. Magin, et al. (2001). "Genes for intermediate filament proteins and the draft sequence of the human genome: novel keratin genes and a surprisingly high number of pseudogenes related to keratin genes 8 and 18." J Cell Sci **114**(Pt 14): 2569-75.
Hodel, A. E., M. R. Hodel, et al. (2002). "The three-dimensional structure of the autoproteolytic, nuclear pore-targeting domain of the human nucleoporin Nup98." Mol Cell **10**(2): 347-58.
Hoeltzenbein, M., T. Karow, et al. (1999). "Severe clinical expression in X-linked Emery-Dreifuss muscular dystrophy." Neuromuscul Disord **9**(3): 166-70.
Hofemeister, H., K. Weber, et al. (2000). "Association of prenylated proteins with the plasma membrane and the inner nuclear membrane is mediated by the same membrane-targeting motifs." Mol Biol Cell **11**(9): 3233-46.
Hoffman, P. N. and R. J. Lasek (1975). "The slow component of axonal transport. Identification of major structural polypeptides of the axon and their generality among mammalian neurons." J Cell Biol **66**(2): 351-66.
Hoger, T. H., G. Krohne, et al. (1988). "Amino acid sequence and molecular characterization of murine lamin B as deduced from cDNA clones." Eur J Cell Biol **47**(2): 283-90.
Hoger, T. H., G. Krohne, et al. (1991). "Interaction of Xenopus lamins A and LII with chromatin in vitro mediated by a sequence element in the carboxyterminal domain." Exp Cell Res **197**(2): 280-9.
Hoger, T. H., K. Zatloukal, et al. (1990). "Characterization of a second highly conserved B-type lamin present in cells previously thought to contain only a single B-type lamin." Chromosoma **99**(6): 379-90.
Holaska, J. M., K. K. Lee, et al. (2003). "Transcriptional repressor germ cell-less (GCL) and barrier to autointegration factor (BAF) compete for binding to emerin in vitro." J Biol Chem **278**(9): 6969-75.
Holt, I., L. Clements, et al. (2001). "The R482Q lamin A/C mutation that causes lipodystrophy does not prevent nuclear targeting of lamin A in adipocytes or its interaction with emerin." Eur J Hum Genet **9**(3): 204-8.
Holtz, D., R. A. Tanaka, et al. (1989). "The CaaX motif of lamin A functions in conjunction with the nuclear localization signal to target assembly to the nuclear envelope." Cell **59**(6): 969-77.
Hopkins, A. M., S. V. Walsh, et al. (2003). "Constitutive activation of Rho proteins by CNF-1 influences tight junction structure and epithelial barrier function." J Cell Sci **116**(Pt 4): 725-42.
Hornbeck, P., K. P. Huang, et al. (1988). "Lamin B is rapidly phosphorylated in lymphocytes after activation of protein kinase C." Proc Natl Acad Sci U S A **85**(7): 2279-83.
Horton, H., I. McMorrow, et al. (1992). "Independent expression and assembly properties of heterologous lamins A and C in murine embryonal carcinomas." Eur J Cell Biol **57**(2): 172-83.
Houseweart, M. K. and D. W. Cleveland (1998). "Intermediate filaments and their associated proteins: multiple dynamic personalities." Curr Opin Cell Biol **10**(1): 93-101.
Hozak, P., A. M. Sasseville, et al. (1995). "Lamin proteins form an internal nucleoskeleton as well as a peripheral lamina in human cells." J Cell Sci **108 (Pt 2)**: 635-44.

Huang, M. M., N. Arnheim, et al. (1992). "Extension of base mispairs by Taq DNA polymerase: implications for single nucleotide discrimination in PCR." Nucleic Acids Res **20**(17): 4567-73.
Huang, S. and D. E. Ingber (2000). "Shape-dependent control of cell growth, differentiation, and apoptosis: switching between attractors in cell regulatory networks." Exp Cell Res **261**(1): 91-103.
Hutchinson, J. (1886). "Case of congenital absence of hair, with atrophic condition of the skin and its appendages, in a boy whose mother had been almost wholly bald from alopecia areata from the age of six." Lancet **I**: 923.
Hutchison, C. J. (2002). "Lamins: building blocks or regulators of gene expression?" Nat Rev Mol Cell Biol **3**(11): 848-58.
Hutchison, C. J., M. Alvarez-Reyes, et al. (2001). "Lamins in disease: why do ubiquitously expressed nuclear envelope proteins give rise to tissue-specific disease phenotypes?" J Cell Sci **114**(Pt 1): 9-19.
Hutchison, C. J., J. M. Bridger, et al. (1994). "Weaving a pattern from disparate threads: lamin function in nuclear assembly and DNA replication." J Cell Sci **107 (Pt 12)**: 3259-69.
Iborra, F. J., A. Pombo, et al. (1996). "Active RNA polymerases are localized within discrete transcription "factories' in human nuclei." J Cell Sci **109 (Pt 6)**: 1427-36.
Ichikawa, Y., M. Watanabe, et al. (1997). "A Japanese family carrying a novel mutation in the Emery-Dreifuss muscular dystrophy gene." Ann Neurol **41**(3): 399-402.
Irons, S. L., D. E. Evans, et al. (2003). "The first 238 amino acids of the human lamin B receptor are targeted to the nuclear envelope in plants." J Exp Bot **54**(384): 943-50.
Irvine, A. D. and W. H. McLean (1999). "Human keratin diseases: the increasing spectrum of disease and subtlety of the phenotype-genotype correlation." Br J Dermatol **140**(5): 815-28.
Ito, H., Y. Fukuda, et al. (1983). "Transformation of intact yeast cells treated with alkali cations." J Bacteriol **153**(1): 163-8.
Ito, T., T. Chiba, et al. (2001). "A comprehensive two-hybrid analysis to explore the yeast protein interactome." Proc Natl Acad Sci U S A **98**(8): 4569-74.
Izumi, M., O. A. Vaughan, et al. (2000). "Head and/or CaaX domain deletions of lamin proteins disrupt preformed lamin A and C but not lamin B structure in mammalian cells." Mol Biol Cell **11**(12): 4323-37.
J. Sambrook, E. F. F., T. Maniatis. (1989). Molecular cloning : a laboratory manual, Cold Spring Harbor : Cold Spring Harbor Laboratory.
Jackson, S. N., T. A. Howlett, et al. (1997). "Dunnigan-Kobberling syndrome: an autosomal dominant form of partial lipodystrophy." Qjm **90**(1): 27-36.
Jackson, S. N., J. Pinkney, et al. (1998). "A defect in the regional deposition of adipose tissue (partial lipodystrophy) is encoded by a gene at chromosome 1q." Am J Hum Genet **63**(2): 534-40.
Jacobsen, N., J. Bentzen, et al. (2002). "LNA-enhanced detection of single nucleotide polymorphisms in the apolipoprotein E." Nucleic Acids Res **30**(19): e100.
Jacomy, H., Q. Zhu, et al. (1999). "Disruption of type IV intermediate filament network in mice lacking the neurofilament medium and heavy subunits." J Neurochem **73**(3): 972-84.

Jagatheesan, G., S. Thanumalayan, et al. (1999). "Colocalization of intranuclear lamin foci with RNA splicing factors." J Cell Sci **112 (Pt 24)**: 4651-61.
Jenkins, H., T. Holman, et al. (1993). "Nuclei that lack a lamina accumulate karyophilic proteins and assemble a nuclear matrix." J Cell Sci **106 (Pt 1)**: 275-85.
Jennekens, F. G., H. F. Busch, et al. (1975). "Inflammatory myopathy in scapulo-ilio-peroneal atrophy with cardiopathy. A study of two families." Brain **98**(4): 709-22.
Jimenez-Sanchez, G., B. Childs, et al. (2001). "Human disease genes." Nature **409**(6822): 853-5.
Johnsson, N. and A. Varshavsky (1994). "Split ubiquitin as a sensor of protein interactions in vivo." Proc Natl Acad Sci U S A **91**(22): 10340-4.
Jormsjo, S., S. Ye, et al. (2000). "Allele-specific regulation of matrix metalloproteinase-12 gene activity is associated with coronary artery luminal dimensions in diabetic patients with manifest coronary artery disease." Circ Res **86**(9): 998-1003.
Jost, E., K. Lepper, et al. (1986). "Redistribution of nuclear lamins in mitotic cells." Biol Cell **57**(2): 111-26.
Joung, J. K., E. I. Ramm, et al. (2000). "A bacterial two-hybrid selection system for studying protein-DNA and protein-protein interactions." Proc Natl Acad Sci U S A **97**(13): 7382-7.
Judson, R. and J. C. Stephens (2001). "Notes from the SNP vs. haplotype front." Pharmacogenomics **2**(1): 7-10.
Judson, R., J. C. Stephens, et al. (2000). "The predictive power of haplotypes in clinical response." Pharmacogenomics **1**(1): 15-26.
Kaltenbock, B. and R. Schneider (1998). "Differential amplification kinetics for point mutation analysis by PCR." Biotechniques **24**(2): 202-4, 206.
Kasahara, K., K. Chida, et al. (1991). "Identification of lamin B2 as a substrate of protein kinase C in BALB/MK-2 mouse keratinocytes." J Biol Chem **266**(30): 20018-23.
Kass, S., C. MacRae, et al. (1994). "A gene defect that causes conduction system disease and dilated cardiomyopathy maps to chromosome 1p1-1q1." Nat Genet **7**(4): 546-51.
Kettle, S., C. M. Card, et al. (2000). "Characterisation of fibrillin-1 cDNA clones in a human fibroblast cell line that assembles microfibrils." Int J Biochem Cell Biol **32**(2): 201-14.
Kihlmark, M., G. Imreh, et al. (2001). "Sequential degradation of proteins from the nuclear envelope during apoptosis." J Cell Sci **114**(Pt 20): 3643-53.
Kilic, F., D. A. Johnson, et al. (1999). "Subcellular localization and partial purification of prelamin A endoprotease: an enzyme which catalyzes the conversion of farnesylated prelamin A to mature lamin A." FEBS Lett **450**(1-2): 61-5.
Kill, I. R. and C. J. Hutchison (1995). "S-phase phosphorylation of lamin B2." FEBS Lett **377**(1): 26-30.
Kirk, B. W., M. Feinsod, et al. (2002). "Single nucleotide polymorphism seeking long term association with complex disease." Nucleic Acids Res **30**(15): 3295-311.
Kitten, G. T. and E. A. Nigg (1991). "The CaaX motif is required for isoprenylation, carboxyl methylation, and nuclear membrane association of lamin B2." J Cell Biol **113**(1): 13-23.

Klapper, M., K. Exner, et al. (1997). "Assembly of A- and B-type lamins studied in vivo with the baculovirus system." J Cell Sci **110 (Pt 20)**: 2519-32.
Klawitz, I., U. Preuss, et al. (2001). "Interaction of SV40 large T antigen with components of the nucleo/cytoskeleton." Int J Oncol **19**(6): 1325-32.
Knight, J. C., I. Udalova, et al. (1999). "A polymorphism that affects OCT-1 binding to the TNF promoter region is associated with severe malaria." Nat Genet **22**(2): 145-50.
Kobberling, J. and M. G. Dunnigan (1986). "Familial partial lipodystrophy: two types of an X linked dominant syndrome, lethal in the hemizygous state." J Med Genet **23**(2): 120-7.
Kobberling, J., B. Willms, et al. (1975). "Lipodystrophy of the extremities. A dominantly inherited syndrome associated with lipatrophic diabetes." Humangenetik **29**(2): 111-20.
Kouklis, P. D., A. Merdes, et al. (1993). "Transient arrest of 3T3 cells in mitosis and inhibition of nuclear lamin reassembly around chromatin induced by anti-vimentin antibodies." Eur J Cell Biol **62**(2): 224-36.
Kowluru, A. (2000). "Evidence for the carboxyl methylation of nuclear lamin-B in the pancreatic beta cell." Biochem Biophys Res Commun **268**(2): 249-54.
Krohne, G., M. C. Dabauvalle, et al. (1981). "Cell type-specific differences in protein composition of nuclear pore complex-lamina structures in oocytes and erythrocytes of Xenopus laevis." J Mol Biol **151**(1): 121-41.
Krohne, G., I. Waizenegger, et al. (1989). "The conserved carboxy-terminal cysteine of nuclear lamins is essential for lamin association with the nuclear envelope." J Cell Biol **109**(5): 2003-11.
Krohne, G., S. L. Wolin, et al. (1987). "Nuclear lamin LI of Xenopus laevis: cDNA cloning, amino acid sequence and binding specificity of a member of the lamin B subfamily." Embo J **6**(12): 3801-8.
Kumar, R., S. K. Singh, et al. (1998). "The first analogues of LNA (locked nucleic acids): phosphorothioate-LNA and 2'-thio-LNA." Bioorg Med Chem Lett **8**(16): 2219-22.
Laliberte, J. F., A. Dagenais, et al. (1984). "Identification of distinct messenger RNAs for nuclear lamin C and a putative precursor of nuclear lamin A." J Cell Biol **98**(3): 980-5.
Lane, E. B., E. L. Rugg, et al. (1992). "A mutation in the conserved helix termination peptide of keratin 5 in hereditary skin blistering." Nature **356**(6366): 244-6.
Lang, C., M. Paulin-Levasseur, et al. (1999). "Molecular characterization and developmentally regulated expression of Xenopus lamina-associated polypeptide 2 (XLAP2)." J Cell Sci **112 (Pt 5)**: 749-59.
Lang, S. and P. Loidl (1993). "Identification of proteins immunologically related to vertebrate lamins in the nuclear matrix of the myxomycete Physarum polycephalum." Eur J Cell Biol **61**(1): 177-83.
Lanoix, J., D. Skup, et al. (1992). "Regulation of the expression of lamins A and C is post-transcriptional in P19 embryonal carcinoma cells." Biochem Biophys Res Commun **189**(3): 1639-44.
Latorra, D., K. Arar, et al. (2003). "Design considerations and effects of LNA in PCR primers." Mol Cell Probes **17**(5): 253-9.
Latorra, D., K. Campbell, et al. (2003). "Enhanced allele-specific PCR discrimination in SNP genotyping using 3' locked nucleic acid (LNA) primers." Hum Mutat **22**(1): 79-85.

Latorra, D., D. Hopkins, et al. (2003). "Multiplex allele-specific PCR with optimized locked nucleic acid primers." Biotechniques **34**(6): 1150-2, 1154, 1158.

Lattanzi, G., V. Cenni, et al. (2003). "Association of emerin with nuclear and cytoplasmic actin is regulated in differentiating myoblasts." Biochem Biophys Res Commun **303**(3): 764-70.

Lawson, D., M. Harrison, et al. (1997). "Fibroblast transgelin and smooth muscle SM22alpha are the same protein, the expression of which is down-regulated in many cell lines." Cell Motil Cytoskeleton **38**(3): 250-7.

Lawyer, F. C., S. Stoffel, et al. (1993). "High-level expression, purification, and enzymatic characterization of full-length Thermus aquaticus DNA polymerase and a truncated form deficient in 5' to 3' exonuclease activity." PCR Methods Appl **2**(4): 275-87.

Lazarides, E. (1982). "Intermediate filaments: a chemically heterogeneous, developmentally regulated class of proteins." Annu Rev Biochem **51**: 219-50.

Lazebnik, Y. A., A. Takahashi, et al. (1995). "Studies of the lamin proteinase reveal multiple parallel biochemical pathways during apoptotic execution." Proc Natl Acad Sci U S A **92**(20): 9042-6.

Leal, A., B. Morera, et al. (2001). "A second locus for an axonal form of autosomal recessive Charcot-Marie-Tooth disease maps to chromosome 19q13.3." Am J Hum Genet **68**(1): 269-74.

Lebel, S., C. Lampron, et al. (1987). "Lamins A and C appear during retinoic acid-induced differentiation of mouse embryonal carcinoma cells." J Cell Biol **105**(3): 1099-104.

Lebel, S. and Y. Raymond (1987). "Lamin A is not synthesized as a larger precursor polypeptide." Biochem Biophys Res Commun **149**(2): 417-23.

Lebel, S. and Y. Raymond (1987). "Lamins A, B and C share an epitope with the common domain of intermediate filament proteins." Exp Cell Res **169**(2): 560-5.

Lee, K. K., T. Haraguchi, et al. (2001). "Distinct functional domains in emerin bind lamin A and DNA-bridging protein BAF." J Cell Sci **114**(Pt 24): 4567-73.

Lee, S. C., I. G. Kim, et al. (1993). "The structure of human trichohyalin. Potential multiple roles as a functional EF-hand-like calcium-binding protein, a cornified cell envelope precursor, and an intermediate filament-associated (cross-linking) protein." J Biol Chem **268**(16): 12164-76.

Lehner, C. F., V. Kurer, et al. (1986). "The nuclear lamin protein family in higher vertebrates. Identification of quantitatively minor lamin proteins by monoclonal antibodies." J Biol Chem **261**(28): 13293-301.

Lehner, C. F., R. Stick, et al. (1987). "Differential expression of nuclear lamin proteins during chicken development." J Cell Biol **105**(1): 577-87.

Leung, C. L., D. Sun, et al. (1999). "The intermediate filament protein peripherin is the specific interaction partner of mouse BPAG1-n (dystonin) in neurons." J Cell Biol **144**(3): 435-46.

Lewis, M. (2003). "PRELP, collagen, and a theory of Hutchinson-Gilford progeria." Ageing Res Rev **2**(1): 95-105.

Li, D., T. Tapscoft, et al. (1999). "Desmin mutation responsible for idiopathic dilated cardiomyopathy." Circulation **100**(5): 461-4.

Li, E., C. Beard, et al. (1993). "Role for DNA methylation in genomic imprinting." Nature **366**(6453): 362-5.
Li, Z., E. Colucci, et al. (1993). "The human desmin gene: a specific regulatory programme in skeletal muscle both in vitro and in transgenic mice." Neuromuscul Disord **3**(5-6): 423-7.
Li, Z., M. Mericskay, et al. (1997). "Desmin is essential for the tensile strength and integrity of myofibrils but not for myogenic commitment, differentiation, and fusion of skeletal muscle." J Cell Biol **139**(1): 129-44.
Liedtke, W., W. Edelmann, et al. (1996). "GFAP is necessary for the integrity of CNS white matter architecture and long-term maintenance of myelination." Neuron **17**(4): 607-15.
Liem, R. K. and S. B. Hutchison (1982). "Purification of individual components of the neurofilament triplet: filament assembly from the 70 000-dalton subunit." Biochemistry **21**(13): 3221-6.
Lin, F., D. L. Blake, et al. (2000). "MAN1, an inner nuclear membrane protein that shares the LEM domain with lamina-associated polypeptide 2 and emerin." J Biol Chem **275**(7): 4840-7.
Lin, F. and H. J. Worman (1993). "Structural organization of the human gene encoding nuclear lamin A and nuclear lamin C." J Biol Chem **268**(22): 16321-6.
Lin, F. and H. J. Worman (1997). "Expression of nuclear lamins in human tissues and cancer cell lines and transcription from the promoters of the lamin A/C and B1 genes." Exp Cell Res **236**(2): 378-84.
Lloyd, D. J., R. C. Trembath, et al. (2002). "A novel interaction between lamin A and SREBP1: implications for partial lipodystrophy and other laminopathies." Hum Mol Genet **11**(7): 769-77.
Lobov, I. B., K. Tsutsui, et al. (2001). "Specificity of SAF-A and lamin B binding in vitro correlates with the satellite DNA bending state." J Cell Biochem **83**(2): 218-29.
Lopez-Soler, R. I., R. D. Moir, et al. (2001). "A role for nuclear lamins in nuclear envelope assembly." J Cell Biol **154**(1): 61-70.
Lourim, D., A. Kempf, et al. (1996). "Characterization and quantitation of three B-type lamins in Xenopus oocytes and eggs: increase of lamin LI protein synthesis during meiotic maturation." J Cell Sci **109 (Pt 7)**: 1775-85.
Lourim, D. and G. Krohne (1993). "Membrane-associated lamins in Xenopus egg extracts: identification of two vesicle populations." J Cell Biol **123**(3): 501-12.
Lourim, D. and J. J. Lin (1992). "Expression of wild-type and nuclear localization-deficient human lamin A in chick myogenic cells." J Cell Sci **103 (Pt 3)**: 863-74.
Lu, J. Y., H. C. Chen, et al. (2003). "Establishment of red fluorescent protein-tagged HeLa tumor metastasis models: determination of DsRed2 insertion effects and comparison of metastatic patterns after subcutaneous, intraperitoneal, or intravenous injection." Clin Exp Metastasis **20**(2): 121-33.
Luderus, M. E., A. de Graaf, et al. (1992). "Binding of matrix attachment regions to lamin B1." Cell **70**(6): 949-59.
Luo, Y., A. Batalao, et al. (1997). "Mammalian two-hybrid system: a complementary approach to the yeast two-hybrid system." Biotechniques **22**(2): 350-2.

Luscher, B., L. Brizuela, et al. (1991). "A role for the p34cdc2 kinase and phosphatases in the regulation of phosphorylation and disassembly of lamin B2 during the cell cycle." Embo J **10**(4): 865-75.
Lutz, R. J., M. A. Trujillo, et al. (1992). "Nucleoplasmic localization of prelamin A: implications for prenylation-dependent lamin A assembly into the nuclear lamina." Proc Natl Acad Sci U S A **89**(7): 3000-4.
Lyman, S. K. and L. Gerace (2001). "Nuclear pore complexes: dynamics in unexpected places." J Cell Biol **154**(1): 17-20.
Ma, L., S. Yamada, et al. (2001). "A 'hot-spot' mutation alters the mechanical properties of keratin filament networks." Nat Cell Biol **3**(5): 503-6.
Machiels, B. M., F. C. Ramaekers, et al. (1997). "Nuclear lamin expression in normal testis and testicular germ cell tumours of adolescents and adults." J Pathol **182**(2): 197-204.
Machiels, B. M., A. H. Zorenc, et al. (1996). "An alternative splicing product of the lamin A/C gene lacks exon 10." J Biol Chem **271**(16): 9249-53.
Mack, J. W., A. C. Steven, et al. (1993). "The mechanism of interaction of filaggrin with intermediate filaments. The ionic zipper hypothesis." J Mol Biol **232**(1): 50-66.
MacLennan, B. A., E. Y. Tsoi, et al. (1987). "Familial idiopathic congestive cardiomyopathy in three generations: a family study with eight affected members." Q J Med **63**(240): 335-47.
MacLeod, H. M., M. R. Culley, et al. (2003). "Lamin A/C truncation in dilated cardiomyopathy with conduction disease." BMC Med Genet **4**(1): 4.
Maison, C., A. Pyrpasopoulou, et al. (1997). "The inner nuclear membrane protein LAP1 forms a native complex with B-type lamins and partitions with spindle-associated mitotic vesicles." Embo J **16**(16): 4839-50.
Manilal, S., T. M. Nguyen, et al. (1996). "The Emery-Dreifuss muscular dystrophy protein, emerin, is a nuclear membrane protein." Hum Mol Genet **5**(6): 801-8.
Manilal, S., D. Recan, et al. (1998). "Mutations in Emery-Dreifuss muscular dystrophy and their effects on emerin protein expression." Hum Mol Genet **7**(5): 855-64.
Manilal, S., C. A. Sewry, et al. (1999). "Distribution of emerin and lamins in the heart and implications for Emery-Dreifuss muscular dystrophy." Hum Mol Genet **8**(2): 353-9.
Maraldi, N. M., G. Lattanzi, et al. (2003). "Immunocytochemistry of nuclear domains and Emery-Dreifuss muscular dystrophy pathophysiology." Eur J Histochem **47**(1): 3-16.
Maraldi, N. M., G. Lattanzi, et al. (2002). "Functional domains of the nucleus: implications for Emery-Dreifuss muscular dystrophy." Neuromuscul Disord **12**(9): 815-23.
Markiewicz, E., T. Dechat, et al. (2002). "Lamin A/C Binding Protein LAP2alpha Is Required for Nuclear Anchorage of Retinoblastoma Protein." Mol Biol Cell **13**(12): 4401-13.
Markiewicz, E., R. Venables, et al. (2002). "Increased solubility of lamins and redistribution of lamin C in X-linked Emery-Dreifuss muscular dystrophy fibroblasts." J Struct Biol **140**(1): 241-53.
Martin, L., C. Crimaudo, et al. (1995). "cDNA cloning and characterization of lamina-associated polypeptide 1C (LAP1C), an integral protein of the inner nuclear membrane." J Biol Chem **270**(15): 8822-8.

Maul, G. G., F. A. Baglia, et al. (1984). "The major 67 000 molecular weight protein of the clam oocyte nuclear envelope is lamin-like." J Cell Sci **67**: 69-85.
Maul, G. G., D. Negorev, et al. (2000). "Review: properties and assembly mechanisms of ND10, PML bodies, or PODs." J Struct Biol **129**(2-3): 278-87.
Maus, N., N. Stuurman, et al. (1995). "Disassembly of the Drosophila nuclear lamina in a homologous cell-free system." J Cell Sci **108 (Pt 5)**: 2027-35.
Mawatari, S. and K. Katayama (1973). "Scapuloperoneal muscular atrophy with cardiopathy. An X-linked recessive trait." Arch Neurol **28**(1): 55-9.
McKeon, F. (1991). "Nuclear lamin proteins: domains required for nuclear targeting, assembly, and cell-cycle-regulated dynamics." Curr Opin Cell Biol **3**(1): 82-6.
McKeon, F. D., M. W. Kirschner, et al. (1986). "Homologies in both primary and secondary structure between nuclear envelope and intermediate filament proteins." Nature **319**(6053): 463-8.
McKusick, V. A. (1963). "Medical Genetics 1962." J Chronic Dis **16**: 457-634.
McLachlan, A. D. (1978). "Coiled coil formation and sequence regularities in the helical regions of alpha-keratin." J Mol Biol **124**: 297 - 304.
McLean, W. H. and E. B. Lane (1995). "Intermediate filaments in disease." Curr Opin Cell Biol **7**(1): 118-25.
McLean, W. H., L. Pulkkinen, et al. (1996). "Loss of plectin causes epidermolysis bullosa with muscular dystrophy: cDNA cloning and genomic organization." Genes Dev **10**(14): 1724-35.
McNulty, A. K. and M. J. Saunders (1992). "Purification and immunological detection of pea nuclear intermediate filaments: evidence for plant nuclear lamins." J Cell Sci **103 (Pt 2)**: 407-14.
Meier, J., K. H. Campbell, et al. (1991). "The role of lamin LIII in nuclear assembly and DNA replication, in cell-free extracts of Xenopus eggs." J Cell Sci **98 (Pt 3)**: 271-9.
Meier, J. and S. D. Georgatos (1994). "Type B lamins remain associated with the integral nuclear envelope protein p58 during mitosis: implications for nuclear reassembly." Embo J **13**(8): 1888-98.
Menache, C. C., C. A. Brown, et al. (2000). "Identification of a novel truncating mutation (S171X) in the Emerin gene in five members of a Caucasian American family with Emery-Dreifuss muscular dystrophy." Hum Mutat **16**(1): 94.
Mercuri, E., A. Y. Manzur, et al. (2000). "Early and severe presentation of autosomal dominant Emery-Dreifuss muscular dystrophy (EMD2)." Neurology **54**(8): 1704-5.
Merdes, A., M. Brunkener, et al. (1991). "Filensin: a new vimentin-binding, polymerization-competent, and membrane-associated protein of the lens fiber cell." J Cell Biol **115**(2): 397-410.
Merdes, A., F. Gounari, et al. (1993). "The 47-kD lens-specific protein phakinin is a tailless intermediate filament protein and an assembly partner of filensin." J Cell Biol **123**(6 Pt 1): 1507-16.
Merlini, L., C. Granata, et al. (1986). "Emery-Dreifuss muscular dystrophy: report of five cases in a family and review of the literature." Muscle Nerve **9**(6): 481-5.
Mical, T. I. and M. J. Monteiro (1998). "The role of sequences unique to nuclear intermediate filaments in the targeting and assembly of

human lamin B: evidence for lack of interaction of lamin B with its putative receptor." J Cell Sci **111 (Pt 23)**: 3471-85.
Michels, V. V. (1993). "Progress in defining the causes of idiopathic dilated cardiomyopathy." N Engl J Med **329**(13): 960-1.
Miller, R. G., R. B. Layzer, et al. (1985). "Emery-Dreifuss muscular dystrophy with autosomal dominant transmission." Neurology **35**(8): 1230-3.
Minguez, A. and S. Moreno Diaz de la Espina (1993). "Immunological characterization of lamins in the nuclear matrix of onion cells." J Cell Sci **106 (Pt 1)**: 431-9.
Moir, R. D., A. D. Donaldson, et al. (1991). "Expression in Escherichia coli of human lamins A and C: influence of head and tail domains on assembly properties and paracrystal formation." J Cell Sci **99 (Pt 2)**: 363-72.
Moir, R. D. and R. D. Goldman (1993). "Lamin dynamics." Curr Opin Cell Biol **5**(3): 408-11.
Moir, R. D., M. Montag-Lowy, et al. (1994). "Dynamic properties of nuclear lamins: lamin B is associated with sites of DNA replication." J Cell Biol **125**(6): 1201-12.
Moir, R. D., R. A. Quinlan, et al. (1990). "Expression and characterization of human lamin C." FEBS Lett **268**(1): 301-5.
Moir, R. D., T. P. Spann, et al. (1995). "The dynamic properties and possible functions of nuclear lamins." Int Rev Cytol **162B**: 141-82.
Moir, R. D., T. P. Spann, et al. (2000). "Disruption of nuclear lamin organization blocks the elongation phase of DNA replication." J Cell Biol **149**(6): 1179-92.
Moir, R. D., T. P. Spann, et al. (2000). "Review: the dynamics of the nuclear lamins during the cell cycle-- relationship between structure and function." J Struct Biol **129**(2-3): 324-34.
Moir, R. D., M. Yoon, et al. (2000). "Nuclear lamins A and B1: different pathways of assembly during nuclear envelope formation in living cells." J Cell Biol **151**(6): 1155-68.
Monneron, A. and W. Bernhard (1969). "Fine structural organization of the interphase nucleus in some mammalian cells." J Ultrastruct Res **27**(3): 266-88.
Monteiro, M. J. and D. W. Cleveland (1989). "Expression of NF-L and NF-M in fibroblasts reveals coassembly of neurofilament and vimentin subunits." J Cell Biol **108**(2): 579-93.
Moore, S. (1981). Pancreatic DNase In: The Enzymes.
Mora, M., L. Cartegni, et al. (1997). "X-linked Emery-Dreifuss muscular dystrophy can be diagnosed from skin biopsy or blood sample." Ann Neurol **42**(2): 249-53.
Moss, S. F., V. Krivosheyev, et al. (1999). "Decreased and aberrant nuclear lamin expression in gastrointestinal tract neoplasms." Gut **45**(5): 723-9.
Mostoslavsky, R. and Y. Bergman (1997). "DNA methylation: regulation of gene expression and role in the immune system." Biochim Biophys Acta **1333**(1): F29-50.
Muchir, A., G. Bonne, et al. (2000). "Identification of mutations in the gene encoding lamins A/C in autosomal dominant limb girdle muscular dystrophy with atrioventricular conduction disturbances (LGMD1B)." Hum Mol Genet **9**(9): 1453-9.
Muchir A, M. J., van der Kooi A, Mayer M, Ferrer X, Briault S, Hirano M, Worman HJ, Manilal S, Mallet A, Wehnerr M, Schwartz K and Bonne G

(2002). "Alterations of the nuclear envelope in fibroblats from patients with muscular dystrophy, cardiomyopathy and partial lipodystrophy carring mutations of the lamin A/C gene and emerin gene." Personal communication.
Muchir, A., B. G. van Engelen, et al. (2003). "Nuclear envelope alterations in fibroblasts from LGMD1B patients carrying nonsense Y259X heterozygous or homozygous mutation in lamin A/C gene." Exp Cell Res **291**(2): 352-362.
Muller, P. R., R. Meier, et al. (1994). "Nuclear lamin expression reveals a surprisingly high growth fraction in childhood acute lymphoblastic leukemia cells." Leukemia **8**(6): 940-5.
Muntoni, F., E. J. Lichtarowicz-Krynska, et al. (1998). "Early presentation of X-linked Emery-Dreifuss muscular dystrophy resembling limb-girdle muscular dystrophy." Neuromuscul Disord **8**(2): 72-6.
Muralikrishna, B., J. Dhawan, et al. (2001). "Distinct changes in intranuclear lamin A/C organization during myoblast differentiation." J Cell Sci **114**(Pt 22): 4001-11.
Muralikrishna, B. and V. K. Parnaik (2001). "SP3 and AP-1 mediate transcriptional activation of the lamin A proximal promoter." Eur J Biochem **268**(13): 3736-43.
Nagano, A., R. Koga, et al. (1996). "Emerin deficiency at the nuclear membrane in patients with Emery-Dreifuss muscular dystrophy." Nat Genet **12**(3): 254-9.
Nakajima, N. and K. Abe (1995). "Genomic structure of the mouse A-type lamin gene locus encoding somatic and germ cell-specific lamins." FEBS Lett **365**(2-3): 108-14.
Nakamachi, K. and N. Nakajima (2000). "DNase I hypersensitive sites and transcriptional activation of the lamin A/C gene." Eur J Biochem **267**(5): 1416-22.
Nakielny, S. and G. Dreyfuss (1999). "Transport of proteins and RNAs in and out of the nucleus." Cell **99**(7): 677-90.
Nevo, Y., M. Al-Lozi, et al. (1999). "Mutation analysis in Emery-Dreifuss muscular dystrophy." Pediatr Neurol **21**(1): 456-9.
Newey, S. E., E. V. Howman, et al. (2001). "Syncoilin, a novel member of the intermediate filament superfamily that interacts with alpha-dystrobrevin in skeletal muscle." J Biol Chem **276**(9): 6645-55.
Newport, J. (1987). "Nuclear reconstitution in vitro: stages of assembly around protein-free DNA." Cell **48**(2): 205-17.
Newport, J. and W. Dunphy (1992). "Characterization of the membrane binding and fusion events during nuclear envelope assembly using purified components." J Cell Biol **116**(2): 295-306.
Newport, J. and T. Spann (1987). "Disassembly of the nucleus in mitotic extracts: membrane vesicularization, lamin disassembly, and chromosome condensation are independent processes." Cell **48**(2): 219-30.
Newport, J. W., K. L. Wilson, et al. (1990). "A lamin-independent pathway for nuclear envelope assembly." J Cell Biol **111**(6 Pt 1): 2247-59.
Newton, C. R., A. Graham, et al. (1989). "Analysis of any point mutation in DNA. The amplification refractory mutation system (ARMS)." Nucleic Acids Res **17**(7): 2503-16.
Nielsen, C. B., S. K. Singh, et al. (1999). "The solution structure of a locked nucleic acid (LNA) hybridized to DNA." J Biomol Struct Dyn **17**(2): 175-91.

Nigg, E. A. (1992). "Assembly-disassembly of the nuclear lamina." Curr Opin Cell Biol **4**(1): 105-9.
Nigro, V., P. Bruni, et al. (1995). "SSCP detection of novel mutations in patients with Emery-Dreifuss muscular dystrophy: definition of a small C-terminal region required for emerin function." Hum Mol Genet **4**(10): 2003-4.
Niki, T., M. Pekny, et al. (1999). "Class VI intermediate filament protein nestin is induced during activation of rat hepatic stellate cells." Hepatology **29**(2): 520-7.
Nikolakaki, E., J. Meier, et al. (1997). "Mitotic phosphorylation of the lamin B receptor by a serine/arginine kinase and p34(cdc2)." J Biol Chem **272**(10): 6208-13.
Nikolakaki, E., G. Simos, et al. (1996). "A nuclear envelope-associated kinase phosphorylates arginine-serine motifs and modulates interactions between the lamin B receptor and other nuclear proteins." J Biol Chem **271**(14): 8365-72.
Nilausen, K. and H. Green (1965). "Reversible arrest of growth in G1 of an established fibroblast line (3T3)." Exp Cell Res **40**(1): 166-8.
Nili, E., G. S. Cojocaru, et al. (2001). "Nuclear membrane protein LAP2beta mediates transcriptional repression alone and together with its binding partner GCL (germ-cell-less)." J Cell Sci **114**(Pt 18): 3297-307.
Novelli, G., A. Muchir, et al. (2002). "Mandibuloacral dysplasia is caused by a mutation in LMNA-encoding lamin A/C." Am J Hum Genet **71**(2): 426-31.
Nutt, S. L., S. Vambrie, et al. (1999). "Independent regulation of the two Pax5 alleles during B-cell development." Nat Genet **21**(4): 390-5.
Ogihara, T., T. Hata, et al. (1986). "Hutchinson-Gilford progeria syndrome in a 45-year-old man." Am J Med **81**(1): 135-8.
Ognibene, A., P. Sabatelli, et al. (1999). "Nuclear changes in a case of X-linked Emery-Dreifuss muscular dystrophy." Muscle Nerve **22**(7): 864-9.
Oguchi, M., J. Sagara, et al. (2002). "Expression of lamins depends on epidermal differentiation and transformation." Br J Dermatol **147**(5): 853-8.
Ohlsson, R., B. Tycko, et al. (1998). "Monoallelic expression: 'there can only be one'." Trends Genet **14**(11): 435-8.
Okumura, K., K. Nakamachi, et al. (2000). "Identification of a novel retinoic acid-responsive element within the lamin A/C promoter." Biochem Biophys Res Commun **269**(1): 197-202.
Olson, T. M. and M. T. Keating (1996). "Mapping a cardiomyopathy locus to chromosome 3p22-p25." J Clin Invest **97**(2): 528-32.
Olson, T. M., S. N. Thibodeau, et al. (1995). "Exclusion of a primary gene defect at the HLA locus in familial idiopathic dilated cardiomyopathy." J Med Genet **32**(11): 876-80.
Orphanides, G. and D. Reinberg (2002). "A unified theory of gene expression." Cell **108**(4): 439-51.
Orum, H., M. H. Jakobsen, et al. (1999). "Detection of the factor V Leiden mutation by direct allele-specific hybridization of PCR amplicons to photoimmobilized locked nucleic acids." Clin Chem **45**(11): 1898-905.
Osborn, M., J. Caselitz, et al. (1981). "Heterogeneity of intermediate filament expression in vascular smooth muscle: a gradient in desmin positive cells from the rat aortic arch to the level of the arteria iliaca communis." Differentiation **20**(3): 196-202.

Osborn, M., M. Ludwig-Festl, et al. (1981). "Expression of glial and vimentin type intermediate filaments in cultures derived from human glial material." Differentiation **19**(3): 161-7.
Oshima, J., A. Garg, et al. (2003). "LMNA mutations in atypical Werner's syndrome." Lancet **362**(9395): 1586.
Ostlund, C., G. Bonne, et al. (2001). "Properties of lamin A mutants found in Emery-Dreifuss muscular dystrophy, cardiomyopathy and Dunnigan-type partial lipodystrophy." J Cell Sci **114**(Pt 24): 4435-45.
Ottaviano, Y. and L. Gerace (1985). "Phosphorylation of the nuclear lamins during interphase and mitosis." J Biol Chem **260**(1): 624-32.
Owens, G. K. (1998). "Molecular control of vascular smooth muscle cell differentiation." Acta Physiol Scand **164**(4): 623-35.
Pachter, J. S. and R. K. Liem (1985). "alpha-Internexin, a 66-kD intermediate filament-binding protein from mammalian central nervous tissues." J Cell Biol **101**(4): 1316-22.
Paddy, M. R., A. S. Belmont, et al. (1990). "Interphase nuclear envelope lamins form a discontinuous network that interacts with only a fraction of the chromatin in the nuclear periphery." Cell **62**(1): 89-106.
Papp, B., C. Pal, et al. (2003). "Dosage sensitivity and the evolution of gene families in yeast." Nature **424**(6945): 194-7.
Parchaliuk, D. L., Kirkpatrick, R.D., Simon, S.L., Agatep, R., Gietz, R.D (1999b). "Technical Tips Online (http://www.biomedet.com/db/tto). P01714."
Parchaliuk, D. L., Kirkpatrick, R.D., Simon, S.L., Agatep, R., Gietz, R.D. (1999a). "Technical Tips Online (http://www.biomedet.com/db/tto). P01713."
Pardee, A. B. (1974). "A restriction point for control of normal animal cell proliferation." Proc Natl Acad Sci U S A **71**(4): 1286-90.
Parry, D. A., J. F. Conway, et al. (1986). "Structural studies on lamin. Similarities and differences between lamin and intermediate-filament proteins." Biochem J **238**(1): 305-8.
Parry, D. A. and P. M. Steinert (1999). "Intermediate filaments: molecular architecture, assembly, dynamics and polymorphism." Q Rev Biophys **32**(2): 99-187.
Paterson, D. (1922). "Case of progeria. Proc. Roy. Soc. Med." **16**: 42.
Paulin-Levasseur, M., G. Giese, et al. (1989). "Expression of vimentin and nuclear lamins during the in vitro differentiation of human promyelocytic leukemia cells HL-60." Eur J Cell Biol **50**(2): 453-61.
Paulin-Levasseur, M., A. Scherbarth, et al. (1988). "Lack of lamins A and C in mammalian hemopoietic cell lines devoid of intermediate filament proteins." Eur J Cell Biol **47**(1): 121-31.
Pellissier, J. F., J. Pouget, et al. (1989). "Myopathy associated with desmin type intermediate filaments. An immunoelectron microscopic study." J Neurol Sci **89**(1): 49-61.
Perez-Olle, R., C. L. Leung, et al. (2002). "Effects of Charcot-Marie-Tooth-linked mutations of the neurofilament light subunit on intermediate filament formation." J Cell Sci **115**(Pt 24): 4937-46.
Peter, M., E. Heitlinger, et al. (1991). "Disassembly of in vitro formed lamin head-to-tail polymers by CDC2 kinase." Embo J **10**(6): 1535-44.
Peter, M., J. Nakagawa, et al. (1990). "In vitro disassembly of the nuclear lamina and M phase-specific phosphorylation of lamins by cdc2 kinase." Cell **61**(4): 591-602.

Peter, M., J. S. Sanghera, et al. (1992). "Mitogen-activated protein kinases phosphorylate nuclear lamins and display sequence specificity overlapping that of mitotic protein kinase p34cdc2." Eur J Biochem **205**(1): 287-94.
Peters, J. M., R. Barnes, et al. (1998). "Localization of the gene for familial partial lipodystrophy (Dunnigan variety) to chromosome 1q21-22." Nat Genet **18**(3): 292-5.
Pinelli, G., P. Dominici, et al. (1987). "[Cardiologic evaluation in a family with Emery-Dreifuss muscular dystrophy]." G Ital Cardiol **17**(7): 589-93.
Pollard, K. M., E. K. Chan, et al. (1990). "In vitro posttranslational modification of lamin B cloned from a human T-cell line." Mol Cell Biol **10**(5): 2164-75.
Porter, K. R. and R. D. Machado (1960). "Studies on the endoplasmic reticulum. IV. Its form and distribution during mitosis in cells of onion root tip." J Biophys Biochem Cytol **7**: 167-80.
Portier, M. M., B. de Nechaud, et al. (1983). "Peripherin, a new member of the intermediate filament protein family." Dev Neurosci **6**(6): 335-44.
Prather, R. S., M. M. Sims, et al. (1989). "Nuclear lamin antigens are developmentally regulated during porcine and bovine embryogenesis." Biol Reprod **41**(1): 123-32.
Prescott, D. M. (1976). Reproduction of eukaryote cells. New York, Academic Press.
Promega (2002). Access RT-PCR System and Access RT-PCR System Introductory System Technical Bulletin # TB220.
Pugh, G. E., P. J. Coates, et al. (1997). "Distinct nuclear assembly pathways for lamins A and C lead to their increase during quiescence in Swiss 3T3 cells." J Cell Sci **110 (Pt 19)**: 2483-93.
Quinlan, R., C. Hutchison, et al. (1995). "Intermediate filament proteins." Protein Profile **2**(8): 795-952.
Quinlan, R. A., J. A. Cohlberg, et al. (1984). "Heterotypic tetramer (A2D2) complexes of non-epidermal keratins isolated from cytoskeletons of rat hepatocytes and hepatoma cells." J Mol Biol **178**(2): 365-88.
Raffaele Di Barletta, M., E. Ricci, et al. (2000). "Different mutations in the LMNA gene cause autosomal dominant and autosomal recessive Emery-Dreifuss muscular dystrophy." Am J Hum Genet **66**(4): 1407-12.
Raharjo, W. H., P. Enarson, et al. (2001). "Nuclear envelope defects associated with LMNA mutations cause dilated cardiomyopathy and Emery-Dreifuss muscular dystrophy." J Cell Sci **114**(Pt 24): 4447-57.
Ramaekers, F. C., D. Haag, et al. (1983). "Coexpression of keratin- and vimentin-type intermediate filaments in human metastatic carcinoma cells." Proc Natl Acad Sci U S A **80**(9): 2618-22.
Ramaekers, F. C., M. W. Hukkelhoven, et al. (1984). "Changing protein patterns during lens cell aging in vitro." Biochim Biophys Acta **799**(3): 221-9.
Rao, L., D. Perez, et al. (1996). "Lamin proteolysis facilitates nuclear events during apoptosis." J Cell Biol **135**(6 Pt 1): 1441-55.
Rao, M. V., M. K. Houseweart, et al. (1998). "Neurofilament-dependent radial growth of motor axons and axonal organization of neurofilaments does not require the neurofilament heavy subunit (NF-H) or its phosphorylation." J Cell Biol **143**(1): 171-81.

Riemer, D., H. Dodemont, et al. (1993). "A nuclear lamin of the nematode Caenorhabditis elegans with unusual structural features; cDNA cloning and gene organization." Eur J Cell Biol **62**(2): 214-23.
Riemer, D., N. Stuurman, et al. (1995). "Expression of Drosophila lamin C is developmentally regulated: analogies with vertebrate A-type lamins." J Cell Sci **108 (Pt 10)**: 3189-98.
Riemer, D., J. Wang, et al. (2000). "Tunicates have unusual nuclear lamins with a large deletion in the carboxyterminal tail domain." Gene **255**(2): 317-25.
Robbins, D. C., E. S. Horton, et al. (1982). "Familial partial lipodystrophy: complications of obesity in the non-obese?" Metabolism **31**(5): 445-52.
Robbins, E. and N. K. Gonatas (1964). "The Ultrastructure of a Mammalian Cell During the Mitotic Cycle." J Cell Biol **21**: 429-63.
Rober, R. A., K. Weber, et al. (1989). "Differential timing of nuclear lamin A/C expression in the various organs of the mouse embryo and the young animal: a developmental study." Development **105**(2): 365-78.
Rosenblum, B. B., L. G. Lee, et al. (1997). "New dye-labeled terminators for improved DNA sequencing patterns." Nucleic Acids Res **25**(22): 4500-4.
Rothenburg, S., F. Koch-Nolte, et al. (2001). "DNA methylation and Z-DNA formation as mediators of quantitative differences in the expression of alleles." Immunol Rev **184**: 286-98.
Rothenburg, S., F. Koch-Nolte, et al. (2001). "A polymorphic dinucleotide repeat in the rat nucleolin gene forms Z-DNA and inhibits promoter activity." Proc Natl Acad Sci U S A **98**(16): 8985-90.
Rothenburg, S., F. Koch-Nolte, et al. (2001). "DNA methylation contributes to tissue- and allele-specific expression of the T-cell differentiation marker RT6." Immunogenetics **52**(3-4): 231-41.
Rotthauwe, H. W., W. Mortier, et al. (1972). "[New type of recessive X-linked muscular dystrophy: scapulo-humeral-distal muscular dystrophy with early contractures and cardiac arrhythmias]." Humangenetik **16**(3): 181-200.
Rowland, L. P., M. Fetell, et al. (1979). "Emery-Dreifuss muscular dystrophy." Ann Neurol **5**(2): 111-7.
Ruchaud, S., N. Korfali, et al. (2002). "Caspase-6 gene disruption reveals a requirement for lamin A cleavage in apoptotic chromatin condensation." Embo J **21**(8): 1967-77.
Ruiz, P., V. Brinkmann, et al. (1996). "Targeted mutation of plakoglobin in mice reveals essential functions of desmosomes in the embryonic heart." J Cell Biol **135**(1): 215-25.
Rutter, J. L., T. I. Mitchell, et al. (1998). "A single nucleotide polymorphism in the matrix metalloproteinase-1 promoter creates an Ets binding site and augments transcription." Cancer Res **58**(23): 5321-5.
Ryynanen, M., R. G. Knowlton, et al. (1991). "Mapping of epidermolysis bullosa simplex mutation to chromosome 12." Am J Hum Genet **49**(5): 978-84.
Rzepecki, R. (2002). "The nuclear lamins and the nuclear envelope." Cell Mol Biol Lett **7**(4): 1019-35.
Sakaki, M., H. Koike, et al. (2001). "Interaction between emerin and nuclear lamins." J Biochem (Tokyo) **129**(2): 321-7.
Salamon, T. (1993). "Regression and disappearance of clinical symptoms in some cases of genodermatoses." Dermatology **186**(4): 245-7.

Sarria, A. J., J. G. Lieber, et al. (1994). "The presence or absence of a vimentin-type intermediate filament network affects the shape of the nucleus in human SW-13 cells." J Cell Sci **107 (Pt 6)**: 1593-607.
Sasseville, A. M. and Y. Langelier (1998). "In vitro interaction of the carboxy-terminal domain of lamin A with actin." FEBS Lett **425**(3): 485-9.
Sasseville, A. M. and Y. Raymond (1995). "Lamin A precursor is localized to intranuclear foci." J Cell Sci **108 (Pt 1)**: 273-85.
Schirmer, E. C., T. Guan, et al. (2001). "Involvement of the lamin rod domain in heterotypic lamin interactions important for nuclear organization." J Cell Biol **153**(3): 479-89.
Schmidt, M., M. Tschodrich-Rotter, et al. (1994). "Properties of fluorescently labeled Xenopus lamin A in vivo." Eur J Cell Biol **65**(1): 70-81.
Schrader, W. H., G. A. Pankey, et al. (1961). "Familial idiopathic cardiomegaly." Circulation **24**: 599-606.
Schwacke, R., A. Schneider, et al. (2003). "ARAMEMNON, a novel database for Arabidopsis integral membrane proteins." Plant Physiol **131**(1): 16-26.
Schwartz, S. M., D. deBlois, et al. (1995). "The intima. Soil for atherosclerosis and restenosis." Circ Res **77**(3): 445-65.
Schwartz, T., M. A. Rould, et al. (1999). "Crystal structure of the Zalpha domain of the human editing enzyme ADAR1 bound to left-handed Z-DNA." Science **284**(5421): 1841-5.
Schweitzer, S. C., M. W. Klymkowsky, et al. (2001). "Paranemin and the organization of desmin filament networks." J Cell Sci **114**(Pt 6): 1079-89.
Schwikowski, B., P. Uetz, et al. (2000). "A network of protein-protein interactions in yeast." Nat Biotechnol **18**(12): 1257-61.
Scott, E. S. and P. O'Hare (2001). "Fate of the inner nuclear membrane protein lamin B receptor and nuclear lamins in herpes simplex virus type 1 infection." J Virol **75**(18): 8818-30.
Sebillon, P., C. Bouchier, et al. (2003). "Expanding the phenotype of LMNA mutations in dilated cardiomyopathy and functional consequences of these mutations." J Med Genet **40**(8): 560-7.
SEB-Symposia (2003). Communication and Gene Regulation at the Nuclear Envelope, 16 - 19, July, Durham.
Semsarian, C. and C. E. Seidman (2001). "Molecular medicine in the 21st century." Intern Med J **31**(1): 53-9.
Senior, A. and L. Gerace (1988). "Integral membrane proteins specific to the inner nuclear membrane and associated with the nuclear lamina." J Cell Biol **107**(6 Pt 1): 2029-36.
Serebriiskii, I., V. Khazak, et al. (1999). "A two-hybrid dual bait system to discriminate specificity of protein interactions." J Biol Chem **274**(24): 17080-7.
Sewry, C. A. (2000). "Immunocytochemical analysis of human muscular dystrophy." Microsc Res Tech **48**(3-4): 142-54.
Sewry, C. A., S. C. Brown, et al. (2001). "Skeletal muscle pathology in autosomal dominant Emery-Dreifuss muscular dystrophy with lamin A/C mutations." Neuropathol Appl Neurobiol **27**(4): 281-90.
Shackleton, S., D. J. Lloyd, et al. (2000). "LMNA, encoding lamin A/C, is mutated in partial lipodystrophy." Nat Genet **24**(2): 153-6.
Shalev, A. (2000). "Discovery of a lipodystrophy gene: one answer, one hundred questions." Eur J Endocrinol **143**(5): 565-7.

Shanahan, C. M. and P. L. Weissberg (1998). "Smooth muscle cell heterogeneity: patterns of gene expression in vascular smooth muscle cells in vitro and in vivo." Arterioscler Thromb Vasc Biol **18**(3): 333-8.
Shimanuki, M., M. Goebl, et al. (1992). "Fission yeast sts1+ gene encodes a protein similar to the chicken lamin B receptor and is implicated in pleiotropic drug-sensitivity, divalent cation-sensitivity, and osmoregulation." Mol Biol Cell **3**(3): 263-73.
Shimizu, T., C. X. Cao, et al. (1998). "Lamin B phosphorylation by protein kinase calpha and proteolysis during apoptosis in human leukemia HL60 cells." J Biol Chem **273**(15): 8669-74.
Shoeman, R. L. and P. Traub (1993). "Assembly of intermediate filaments." Bioessays **15**(9): 605-11.
Shumaker, D. K., K. K. Lee, et al. (2001). "LAP2 binds to BAF.DNA complexes: requirement for the LEM domain and modulation by variable regions." Embo J **20**(7): 1754-64.
Simha, V., A. K. Agarwal, et al. (2003). "Genetic and phenotypic heterogeneity in patients with mandibuloacral dysplasia-associated lipodystrophy." J. Clin. Endocr. Metab. **88**: 2821 - 2824.
Simha, V. and A. Garg (2002). "Body fat distribution and metabolic derangements in patients with familial partial lipodystrophy associated with mandibuloacral dysplasia." J. Clin. Endocr. Metab. **87**: 776 - 785.
Simos, G., C. Maison, et al. (1996). "Characterization of p18, a component of the lamin B receptor complex and a new integral membrane protein of the avian erythrocyte nuclear envelope." J Biol Chem **271**(21): 12617-25.
Sinensky, M., K. Fantle, et al. (1994). "The processing pathway of prelamin A." J Cell Sci **107 (Pt 1)**: 61-7.
Sinensky, M., T. McLain, et al. (1994). "Expression of prelamin A but not mature lamin A confers sensitivity of DNA biosynthesis to lovastatin on F9 teratocarcinoma cells." J Cell Sci **107 (Pt 8)**: 2215-8.
Siu, B. L., H. Niimura, et al. (1999). "Familial dilated cardiomyopathy locus maps to chromosome 2q31." Circulation **99**(8): 1022-6.
Skalli, O., Y. H. Chou, et al. (1992). "Cell cycle-dependent changes in the organization of an intermediate filament-associated protein: correlation with phosphorylation by p34cdc2." Proc Natl Acad Sci U S A **89**(24): 11959-63.
Small, K., J. Iber, et al. (1997). "Emerin deletion reveals a common X-chromosome inversion mediated by inverted repeats." Nat Genet **16**(1): 96-9.
Small, K., M. Wagener, et al. (1997). "Isolation and characterization of the complete mouse emerin gene." Mamm Genome **8**(5): 337-41.
Small, K. and S. T. Warren (1998). "Emerin deletions occurring on both Xq28 inversion backgrounds." Hum Mol Genet **7**(1): 135-9.
Smith, S. and G. Blobel (1993). "The first membrane spanning region of the lamin B receptor is sufficient for sorting to the inner nuclear membrane." J Cell Biol **120**(3): 631-7.
Smith, S. and G. Blobel (1994). "Colocalization of vertebrate lamin B and lamin B receptor (LBR) in nuclear envelopes and in LBR-induced membrane stacks of the yeast Saccharomyces cerevisiae." Proc Natl Acad Sci U S A **91**(21): 10124-8.
Smythe, C., H. E. Jenkins, et al. (2000). "Incorporation of the nuclear pore basket protein nup153 into nuclear pore structures is dependent upon

lamina assembly: evidence from cell-free extracts of Xenopus eggs." Embo J **19**(15): 3918-31.
Soellner, P., R. A. Quinlan, et al. (1985). "Identification of a distinct soluble subunit of an intermediate filament protein: tetrameric vimentin from living cells." Proc Natl Acad Sci U S A **82**(23): 7929-33.
Soling, A., A. Simm, et al. (2002). "Intracellular localization of Herpes simplex virus type 1 thymidine kinase fused to different fluorescent proteins depends on choice of fluorescent tag." FEBS Lett **527**(1-3): 153-8.
Sommer, S. S., J. D. Cassady, et al. (1989). "A novel method for detecting point mutations or polymorphisms and its application to population screening for carriers of phenylketonuria." Mayo Clin Proc **64**(11): 1361-72.
Soullam, B. and H. J. Worman (1993). "The amino-terminal domain of the lamin B receptor is a nuclear envelope targeting signal." J Cell Biol **120**(5): 1093-100.
Spann, T. P., R. D. Moir, et al. (1997). "Disruption of nuclear lamin organization alters the distribution of replication factors and inhibits DNA synthesis." J Cell Biol **136**(6): 1201-12.
Speckman, R. A., A. Garg, et al. (2000). "Mutational and haplotype analyses of families with familial partial lipodystrophy (Dunnigan variety) reveal recurrent missense mutations in the globular C-terminal domain of lamin A/C." Am J Hum Genet **66**(4): 1192-8.
Spector, D. L. (2001). "Nuclear domains." J Cell Sci **114**(Pt 16): 2891-3.
Squarzoni, S., P. Sabatelli, et al. (2000). "Emerin presence in platelets." Acta Neuropathol (Berl) **100**(3): 291-8.
Squarzoni, S., P. Sabatelli, et al. (1998). "Immunocytochemical detection of emerin within the nuclear matrix." Neuromuscul Disord **8**(5): 338-44.
Stagljar, I., C. Korostensky, et al. (1998). "A genetic system based on split-ubiquitin for the analysis of interactions between membrane proteins in vivo." Proc Natl Acad Sci U S A **95**(9): 5187-92.
Steinert, P. M. and S. J. Bale (1993). "Genetic skin diseases caused by mutations in keratin intermediate filaments." Trends Genet **9**(8): 280-4.
Steinert, P. M., Y. H. Chou, et al. (1999). "A high molecular weight intermediate filament-associated protein in BHK-21 cells is nestin, a type VI intermediate filament protein. Limited co-assembly in vitro to form heteropolymers with type III vimentin and type IV alpha-internexin." J Biol Chem **274**(14): 9881-90.
Steinert, P. M. and M. I. Gullino (1976). "Bovine epidermal keratin filament assembly in vitro." Biochem Biophys Res Commun **70**(1): 221-7.
Steinert, P. M., W. W. Idler, et al. (1981). "In vitro assembly of homopolymer and copolymer filaments from intermediate filament subunits of muscle and fibroblastic cells." Proc Natl Acad Sci U S A **78**(6): 3692-6.
Steinert, P. M., W. W. Idler, et al. (1976). "Self-assembly of bovine epidermal keratin filaments in vitro." J Mol Biol **108**(3): 547-67.
Steinert, P. M., M. L.N., et al. (1993). "Diversity of intermediate filament structure. Evidence that the aligment of coiled-coil molecules in vimentin is different from that in keratin intermediate filaments." J Biol Chem **268**(24916 - 24925).
Steinert, P. M., L. N. Marekov, et al. (1999). "Molecular parameters of type IV alpha-internexin and type IV-type III alpha-internexin-vimentin copolymer intermediate filaments." J Biol Chem **274**(3): 1657-66.

Steinert, P. M. and D. R. Roop (1988). "Molecular and cellular biology of intermediate filaments." Annu Rev Biochem **57**: 593-625.
Steinert, P. M., A. C. Steven, et al. (1985). "The molecular biology of intermediate filaments." Cell **42**(2): 411-20.
Stewart, C. and B. Burke (1987). "Teratocarcinoma stem cells and early mouse embryos contain only a single major lamin polypeptide closely resembling lamin B." Cell **51**(3): 383-92.
Stewart, M. (1990). "Intermediate filaments: structure, assembly and molecular interactions." Curr Opin Cell Biol **2**(1): 91-100.
Stick, R. (1988). "cDNA cloning of the developmentally regulated lamin LIII of Xenopus laevis." Embo J **7**(10): 3189-97.
Stick, R. (1992). "The gene structure of Xenopus nuclear lamin A: a model for the evolution of A-type from B-type lamins by exon shuffling." Chromosoma **101**(9): 566-74.
Stick, R., B. Angres, et al. (1988). "The fates of chicken nuclear lamin proteins during mitosis: evidence for a reversible redistribution of lamin B2 between inner nuclear membrane and elements of the endoplasmic reticulum." J Cell Biol **107**(2): 397-406.
Stick, R. and P. Hausen (1985). "Changes in the nuclear lamina composition during early development of Xenopus laevis." Cell **41**(1): 191-200.
Stoffler, D., B. Fahrenkrog, et al. (1999). "The nuclear pore complex: from molecular architecture to functional dynamics." Curr Opin Cell Biol **11**(3): 391-401.
Stoppin, V., M. Vantard, et al. (1994). "Isolated Plant Nuclei Nucleate Microtubule Assembly: The Nuclear Surface in Higher Plants Has Centrosome-like Activity." Plant Cell **6**(8): 1099-1106.
Strelkov SV, Herrmann H, et al. (2002). "Conserved segments 1A and 2B of the intermediate filament dimer: their atomic structures and role in filament assembly." EMBO J **21**: 1255 -1266.
Strelkov, S. V., H. Herrmann, et al. (2003). "Molecular architecture of intermediate filaments." Bioessays **25**(3): 243-51.
Stuurman, N., M. Haner, et al. (1999). "Interactions between coiled-coil proteins: Drosophila lamin Dm0 binds to the bicaudal-D protein." Eur J Cell Biol **78**(4): 278-87.
Stuurman, N., S. Heins, et al. (1998). "Nuclear lamins: their structure, assembly, and interactions." J Struct Biol **122**(1-2): 42-66.
Stuurman, N., N. Maus, et al. (1995). "Interphase phosphorylation of the Drosophila nuclear lamin: site-mapping using a monoclonal antibody." J Cell Sci **108 (Pt 9)**: 3137-44.
Sulaiman, A. R., M. P. McQuillen, et al. (1981). "Scapuloperoneal syndrome. Report on two families with neurogenic muscular atrophy." J Neurol Sci **52**(2-3): 305-25.
Sullivan, K. M., W. B. Busa, et al. (1993). "Calcium mobilization is required for nuclear vesicle fusion in vitro: implications for membrane traffic and IP3 receptor function." Cell **73**(7): 1411-22.
Sullivan, T., D. Escalante-Alcalde, et al. (1999). "Loss of A-type lamin expression compromises nuclear envelope integrity leading to muscular dystrophy." J Cell Biol **147**(5): 913-20.
Sultana, S., S. W. Sernett, et al. (2000). "Intermediate filament protein synemin is transiently expressed in a subset of astrocytes during development." Glia **30**(2): 143-53.
Suprynowicz, F. A. and L. Gerace (1986). "A fractionated cell-free system for analysis of prophase nuclear disassembly." J Cell Biol **103**(6 Pt 1): 2073-81.

Sutherland, B. W., G. B. Spiegelman, et al. (2001). "A Ras subfamily GTPase shows cell cycle-dependent nuclear localization." EMBO Rep **2**(11): 1024-8.
Sutherland, H. G., G. K. Mumford, et al. (2001). "Large-scale identification of mammalian proteins localized to nuclear sub-compartments." Hum Mol Genet **10**(18): 1995-2011.
Takamoto, K., K. Hirose, et al. (1984). "A genetic variant of Emery-Dreifuss disease. Muscular dystrophy with humeropelvic distribution, early joint contracture, and permanent atrial paralysis." Arch Neurol **41**(12): 1292-3.
Takano, M., M. Takeuchi, et al. (2002). "The binding of lamin B receptor to chromatin is regulated by phosphorylation in the RS region." Eur J Biochem **269**(3): 943-53.
Talkop, U. A., I. Talvik, et al. (2002). "Early onset of cardiomyopathy in two brothers with X-linked Emery-Dreifuss muscular dystrophy." Neuromuscul Disord **12**(9): 878-81.
Tang, K., R. L. Finley, Jr., et al. (2000). "Identification of 12-lipoxygenase interaction with cellular proteins by yeast two-hybrid screening." Biochemistry **39**(12): 3185-91.
Taniura, H., C. Glass, et al. (1995). "A chromatin binding site in the tail domain of nuclear lamins that interacts with core histones." J Cell Biol **131**(1): 33-44.
Taylor, J., C. A. Sewry, et al. (1998). "Early onset, autosomal recessive muscular dystrophy with Emery-Dreifuss phenotype and normal emerin expression." Neurology **51**(4): 1116-20.
Temin, H. M. (1971). "Stimulation by serum of multiplication of stationary chicken cells." J Cell Physiol **78**(2): 161-70.
Terzi, F., D. Henrion, et al. (1997). "Reduction of renal mass is lethal in mice lacking vimentin. Role of endothelin-nitric oxide imbalance." J Clin Invest **100**(6): 1520-8.
Tews, D. S. (1999). "Emerin." Int J Biochem Cell Biol **31**(9): 891-4.
Thomas, P. K., D. B. Calne, et al. (1972). "X-linked scapuloperoneal syndrome." J Neurol Neurosurg Psychiatry **35**(2): 208-15.
Thomas, P. K. P., R. K. H. (1985). "Emery-Dreifuss muscular dystrophy." J. Med. Genet. **22**: 138-139.
Thompson, L. J., M. Bollen, et al. (1997). "Identification of protein phosphatase 1 as a mitotic lamin phosphatase." J Biol Chem **272**(47): 29693-7.
Tiwari, B. and V. K. Parnaik (1999). "Identification of altered DNA-protein interactions at the lamin A proximal promoter in quiescent hepatocytes." Cell Mol Biol (Noisy-le-grand) **45**(6): 865-75.
Tohyama, T., V. M. Lee, et al. (1992). "Nestin expression in embryonic human neuroepithelium and in human neuroepithelial tumor cells." Lab Invest **66**(3): 303-13.
Toivola, D. M., R. D. Goldman, et al. (1997). "Protein phosphatases maintain the organization and structural interactions of hepatic keratin intermediate filaments." J Cell Sci **110 (Pt 1)**: 23-33.
Tournamille, C., Y. Colin, et al. (1995). "Disruption of a GATA motif in the Duffy gene promoter abolishes erythroid gene expression in Duffy-negative individuals." Nat Genet **10**(2): 224-8.
Traub, P. and R. L. Shoeman (1994). "Intermediate filament and related proteins: potential activators of nucleosomes during transcription initiation and elongation?" Bioessays **16**(5): 349-55.

Tsuchiya, Y., A. Hase, et al. (1999). "Distinct regions specify the nuclear membrane targeting of emerin, the responsible protein for Emery-Dreifuss muscular dystrophy." Eur J Biochem **259**(3): 859-65.
Udalova, I. A., A. Richardson, et al. (2000). "Functional consequences of a polymorphism affecting NF-kappaB p50-p50 binding to the TNF promoter region." Mol Cell Biol **20**(24): 9113-9.
Uetz, P., L. Giot, et al. (2000). "A comprehensive analysis of protein-protein interactions in Saccharomyces cerevisiae." Nature **403**(6770): 623-7.
Ulitzur, N., A. Harel, et al. (1992). "Lamin activity is essential for nuclear envelope assembly in a Drosophila embryo cell-free extract." J Cell Biol **119**(1): 17-25.
van der Kooi, A. J., T. M. Ledderhof, et al. (1996). "A newly recognized autosomal dominant limb girdle muscular dystrophy with cardiac involvement." Ann Neurol **39**(5): 636-42.
van der Kooi, A. J., M. van Meegen, et al. (1997). "Genetic localization of a newly recognized autosomal dominant limb-girdle muscular dystrophy with cardiac involvement (LGMD1B) to chromosome 1q11-21." Am J Hum Genet **60**(4): 891-5.
Vaughan, A., M. Alvarez-Reyes, et al. (2001). "Both emerin and lamin C depend on lamin A for localization at the nuclear envelope." J Cell Sci **114**(Pt 14): 2577-90.
Veitia, R. A. (2002). "Exploring the etiology of haploinsufficiency." Bioessays **24**(2): 175-84.
Venables, R. S., S. McLean, et al. (2001). "Expression of individual lamins in basal cell carcinomas of the skin." Br J Cancer **84**(4): 512-9.
Vidal, M., P. Braun, et al. (1996). "Genetic characterization of a mammalian protein-protein interaction domain by using a yeast reverse two-hybrid system." Proc Natl Acad Sci U S A **93**(19): 10321-6.
Vigouroux, C., M. Auclair, et al. (2001). "Nuclear envelope disorganization in fibroblasts from lipodystrophic patients with heterozygous R482Q/W mutations in the lamin A/C gene." J Cell Sci **114**(Pt 24): 4459-68.
Vigouroux, C., F. Caux, et al. (2003). "LMNA mutations in atypical Werner's syndrome." Lancet **362**(9395): 1585; author reply 1586.
Vigouroux, C., J. Magre, et al. (2000). "Lamin A/C gene: sex-determined expression of mutations in Dunnigan-type familial partial lipodystrophy and absence of coding mutations in congenital and acquired generalized lipoatrophy." Diabetes **49**(11): 1958-62.
Villard, L., V. des Portes, et al. (2000). "Linkage of X-linked myopathy with excessive autophagy (XMEA) to Xq28." Eur J Hum Genet **8**(2): 125-9.
Virtanen, I., H. von Koskull, et al. (1981). "Cultured human amniotic fluid cells characterized with antibodies against intermediate filaments in indirect immunofluorescence microscopy." J Clin Invest **68**(5): 1348-55.
Vlcek, S., H. Just, et al. (1999). "Functional diversity of LAP2alpha and LAP2beta in postmitotic chromosome association is caused by an alpha-specific nuclear targeting domain." Embo J **18**(22): 6370-84.
von Mering, C., R. Krause, et al. (2002). "Comparative assessment of large-scale data sets of protein-protein interactions." Nature **417**(6887): 399-403.
Vytopil, M., E. Ricci, et al. (2002). "Frequent low penetrance mutations in the Lamin A/C gene, causing Emery Dreifuss muscular dystrophy." Neuromuscul Disord **12**(10): 958-63.

Wahlestedt, C., P. Salmi, et al. (2000). "Potent and nontoxic antisense oligonucleotides containing locked nucleic acids." Proc Natl Acad Sci U S A **97**(10): 5633-8.
Walhout, A. J., R. Sordella, et al. (2000). "Protein interaction mapping in C. elegans using proteins involved in vulval development." Science **287**(5450): 116-22.
Walikonis, R. S., O. N. Jensen, et al. (2000). "Identification of proteins in the postsynaptic density fraction by mass spectrometry." J Neurosci **20**(11): 4069-80.
Ward, G. E. and M. W. Kirschner (1990). "Identification of cell cycle-regulated phosphorylation sites on nuclear lamin C." Cell **61**(4): 561-77.
Warren, G. and W. Wickner (1996). "Organelle inheritance." Cell **84**(3): 395-400.
Watanabe, D. and D. P. Barlow (1996). "Random and imprinted monoallelic expression." Genes Cells **1**(9): 795-802.
Waterfall, C. M. and B. D. Cobb (2002). "SNP genotyping using single-tube fluorescent bidirectional PCR." Biotechniques **33**(1): 80, 82-4, 86 passim.
Weber, K., U. Plessmann, et al. (1989). "Maturation of nuclear lamin A involves a specific carboxy-terminal trimming, which removes the polyisoprenylation site from the precursor; implications for the structure of the nuclear lamina." FEBS Lett **257**(2): 411-4.
Weilbach, F. X., W. Kress, et al. (1999). "[Current diagnosis in muscular dystrophies. New developments, methods of examination and case examples]." Nervenarzt **70**(2): 89-100.
Wettstein, A. H., H. R.; Janzer, R. C.; Jerusalem, F.; Steinmann, B. (1983). "Rigid spine-syndrom." Verh. Dtsch. Ges. Neurol **2**: 812 - 814.
Whitfield, A. G. (1961). "Familial cardiomyopathy." Q J Med **30**: 119-34.
Wilkinson, F. L., J. M. Holaska, et al. (2003). "Emerin interacts in vitro with the splicing-associated factor, YT521-B." Eur J Biochem **270**(11): 2459-66.
Witt, T. N., C. G. Garner, et al. (1988). "Autosomal dominant Emery-Dreifuss syndrome: evidence of a neurogenic variant of the disease." Eur Arch Psychiatry Neurol Sci **237**(4): 230-6.
Wolfner, M. F. and K. L. Wilson (2001). "The nuclear envelope: emerging roles in development and disease." Cell Mol Life Sci **58**(12-13): 1737-40.
Wolin, S. L., G. Krohne, et al. (1987). "A new lamin in Xenopus somatic tissues displays strong homology to human lamin A." Embo J **6**(12): 3809-18.
Worman, H. J. (1990). "Cellular intermediate filament networks and their derangement in alcoholic hepatitis." Alcohol Clin Exp Res **14**(6): 789-804.
Worman, H. J., C. D. Evans, et al. (1990). "The lamin B receptor of the nuclear envelope inner membrane: a polytopic protein with eight potential transmembrane domains." J Cell Biol **111**(4): 1535-42.
Wu, D. Y., L. Ugozzoli, et al. (1989). "Allele-specific enzymatic amplification of beta-globin genomic DNA for diagnosis of sickle cell anemia." Proc Natl Acad Sci U S A **86**(8): 2757-60.
Wulff, K., U. Ebener, et al. (1997). "Direct molecular genetic diagnosis and heterozygote identification in X-linked Emery-Dreifuss muscular dystrophy by heteroduplex analysis." Dis Markers **13**(2): 77-86.

Wulff, K., J. E. Parrish, et al. (1997). "Six novel mutations in the emerin gene causing X-linked Emery-Dreifuss muscular dystrophy." Hum Mutat **9**(6): 526-30.
Wydner, K. L., J. A. McNeil, et al. (1996). "Chromosomal assignment of human nuclear envelope protein genes LMNA, LMNB1, and LBR by fluorescence in situ hybridization." Genomics **32**(3): 474-8.
Xu, Z., L. C. Cork, et al. (1993). "Increased expression of neurofilament subunit NF-L produces morphological alterations that resemble the pathology of human motor neuron disease." Cell **73**(1): 23-33.
Yamada, T. and T. Kobayashi (1996). "A novel emerin mutation in a Japanese patient with Emery-Dreifuss muscular dystrophy." Hum Genet **97**(5): 693-4.
Yang, L., T. Guan, et al. (1997). "Integral membrane proteins of the nuclear envelope are dispersed throughout the endoplasmic reticulum during mitosis." J Cell Biol **137**(6): 1199-210.
Yang, L., T. Guan, et al. (1997). "Lamin-binding fragment of LAP2 inhibits increase in nuclear volume during the cell cycle and progression into S phase." J Cell Biol **139**(5): 1077-87.
Yanisch-Perron, C., J. Vieira, et al. (1985). "Improved M13 phage cloning vectors and host strains: nucleotide sequences of the M13mp18 and pUC19 vectors." Gene **33**(1): 103-19.
Yates, J. (1998). EDM Online Database.
Yates, J. R. and M. Wehnert (1999). "The Emery-Dreifuss Muscular Dystrophy Mutation Database." Neuromuscul Disord **9**(3): 199.
Ye, Q. and H. J. Worman (1994). "Primary structure analysis and lamin B and DNA binding of human LBR, an integral protein of the nuclear envelope inner membrane." J Biol Chem **269**(15): 11306-11.
Ye, Q. and H. J. Worman (1995). "Protein-protein interactions between human nuclear lamins expressed in yeast." Exp Cell Res **219**(1): 292-8.
Ye, Q. and H. J. Worman (1996). "Interaction between an integral protein of the nuclear envelope inner membrane and human chromodomain proteins homologous to Drosophila HP1." J Biol Chem **271**(25): 14653-6.
Yoon, M., R. D. Moir, et al. (1998). "Motile properties of vimentin intermediate filament networks in living cells." J Cell Biol **143**(1): 147-57.
Yorifuji, H., Y. Tadano, et al. (1997). "Emerin, deficiency of which causes Emery-Dreifuss muscular dystrophy, is localized at the inner nuclear membrane." Neurogenetics **1**(2): 135-40.
Yoshioka, M., K. Saida, et al. (1989). "Follow up study of cardiac involvement in Emery-Dreifuss muscular dystrophy." Arch Dis Child **64**(5): 713-5.
Young, L. W., J. F. Radebaugh, et al. (1971). "New syndrome manifested by mandibular hypoplasia, acroosteolysis, stiff joints and cutaneous atrophy (mandibuloacral dysplasia) in two unrelated boys." Birth Defects Orig Artic Ser **7**(7): 291-7.
Yuan, J., G. Simos, et al. (1991). "Binding of lamin A to polynucleosomes." J Biol Chem **266**(14): 9211-5.
Zeligs, J. D. and S. H. Wollman (1979). "Mitosis in rat thyroid epithelial cells in vivo. I. Ultrastructural changes in cytoplasmic organelles during the mitotic cycle." J Ultrastruct Res **66**(1): 53-77.

Zetterberg, A. and G. Auer (1970). "Proliferative activity and cytochemical properties of nuclear chromatin related to local cell density of epithelial cells." Exp Cell Res **62**(1): 262-70.
Zhang, B., S. Ye, et al. (1999). "Functional polymorphism in the regulatory region of gelatinase B gene in relation to severity of coronary atherosclerosis." Circulation **99**(14): 1788-94.
Zhang, C., H. Jenkins, et al. (1996). "Nuclear lamina and nuclear matrix organization in sperm pronuclei assembled in Xenopus egg extract." J Cell Sci **109 (Pt 9)**: 2275-86.
Zhang, J. and S. Lautar (1996). "A yeast three-hybrid method to clone ternary protein complex components." Anal Biochem **242**(1): 68-72.
Zhang, L. P., J. Stroud, et al. (1999). "Multiple elements influence transcriptional regulation from the human testis-specific PGK2 promoter in transgenic mice." Biol Reprod **60**(6): 1329-37.
Zhang, M., R. R. Pan, et al. (2003). "[Assessment of the Escherichia coli Tat Protein Translocation System with Fluorescent Proteins]." Sheng Wu Hua Xue Yu Sheng Wu Wu Li Xue Bao (Shanghai) **35**(8): 702-6.
Zhao, K., A. Harel, et al. (1996). "Binding of matrix attachment regions to nuclear lamin is mediated by the rod domain and depends on the lamin polymerization state." FEBS Lett **380**(1-2): 161-4.
Zhen, Y. Y., T. Libotte, et al. (2002). "NUANCE, a giant protein connecting the nucleus and actin cytoskeleton." J Cell Sci **115**(Pt 15): 3207-22.